UNIVERSIDADE FEDERAL DO CEARÁ
CENTRO DE CIÊNCIAS
DEPARTAMENTO DE BIOQUÍMICA
PROGRAMA DE PÓS-GRADUAÇÃO EM BIOQUÍMICA

RAFAEL XAVIER MARTINS

HEPATOTOXICIDADE INDUZIDA PELO HERBICIDA 2,4-D E SEU METABÓLITO 2,4-DCP: UMA INVESTIGAÇÃO MECANISTICA INTEGRANDO TOXICOLOGIA DE REDES E ANÁLISES EM PEIXE-ZEBRA

FORTALEZA
2025

RAFAEL XAVIER MARTINS

HEPATOTOXICIDADE INDUZIDA PELO HERBICIDA 2,4-D E SEU METABÓLITO 2,4-DCP: UMA INVESTIGAÇÃO MECANISTICA INTEGRANDO TOXICOLOGIA DE REDES E ANÁLISES EM PEIXE-ZEBRA

Tese apresentada ao Programa de Pós-Graduação em Bioquímica da Universidade Federal do Ceará, como parte dos requisitos para obtenção do título de Doutor em Bioquímica. Área de concentração: Bioquímica Vegetal.

Orientador: Prof. Dr. Davi Felipe Farias

Coorientadora: Dra. Terezinha Maria de Souza

FORTALEZA

2025

Dados Internacionais de Catalogação na Publicação
Universidade Federal do Ceará
Sistema de Bibliotecas
Gerada automaticamente pelo módulo Catalog, mediante os dados fornecidos pelo(a) autor(a)

M345h Martins, Rafael Xavier.
Hepatotoxicidade induzida pelo herbicida 2,4-De seu metabólito 2,4-DCP: : uma investigação mecanistica integrando toxicologia de redes e análises em peixe-zebra / Rafael Xavier Martins. – 2025.
252 f. : il. color.

Tese (doutorado) – Universidade Federal do Ceará, Centro de Ciências, Programa de Pós-Graduação em Bioquímica , Fortaleza, 2025.
Orientação: Prof. Dr. Davi Felipe Farias.
Coorientação: Prof. Dr. Terezinha Maria de Souza.

1. Agrotóxicos. 2. Contaminação aquática. 3. Danos ao fígado. I. Título.

CDD 572

RAFAEL XAVIER MARTINS

HEPATOTOXICIDADE INDUZIDA PELO HERBICIDA 2,4-D E SEU METABÓLITO 2,4-DCP: UMA INVESTIGAÇÃO MECANISTICA INTEGRANDO TOXICOLOGIA DE REDES E ANÁLISES EM PEIXE-ZEBRA

Tese apresentada ao Programa de Pós-Graduação em Bioquímica da Universidade Federal do Ceará, como parte dos requisitos para obtenção do título de Doutor em Bioquímica. Área de concentração: Bioquímica Vegetal.

Aprovada em: 31/10/2025

BANCA EXAMINADORA

_____

Prof. Dr. Davi Felipe Farias
Universidade Federal da Paraíba (UFC)

_____

Prof.ª Dra. Margareth de Fátima Formiga Melo Diniz
Universidade Federal da Paraíba (UFPB)

_____

Prof. Dr. Ian Porto Gurgel do Amaral
Universidade Federal da Paraíba (UFPB)

_____

Prof ª. Dra. Glaucia Veríssimo Faheina Martins
Universidade Federal da Paraíba (UFPB)

_____

Prof. Dr. Sócrates Golzio dos Santos
Universidade Federal da Paraíba (UFPB)

Aos meus pais, Antônia e Joseildo, e à minha irmã, Ana Clara.

AGRADECIMENTOS

O presente trabalho foi realizado com apoio (Bolsa) do Conselho Nacional de Desenvolvimento Científico e Tecnológico (CNPq) - Chamada GD Processo 160431/2021-2, bem como com suporte financeiro da Fundação de Apoio à Pesquisa do Estado da Paraíba (FAPESQ).

À Universidade Federal do Ceará (UFC) e à Universidade Federal da Paraíba (UFPB), pela infraestrutura e vivências academicas que permitiram o desenvolvimento desta tese e a minha formação profissional.

Ao Laboratório de Avaliação de Risco de Novas Tecnologias (LabRisco) e a Unidade de Produção de Organismos Modelo Não Convencionais (UniPOM) pelo suporte técnico científico e acolhimento durante todos esses anos de formação acadêmica.

Ao Prof. Dr. Davi Farias, pela orientação, confiança e amizade nutrida ao longo desses anos. Para mim, você é uma inspiração enquanto pessoa e profissional. Obrigado por tantas trocas!

À Dra. Terezinha Souza, pela coorientação e pelos valiosos conselhos que acrescentaram significativamente à tese e à minha formação.

Aos meus amigos e colegas de trabalho Me. Maria Eduarda de Souza, Me. Juliana Souza, Dr. Leonardo Vieira, Matheus Alves, Cleyton Gomes, Milena Arruda, Thaís Feitosa, Ana Júlia Guimarães, Marcos Porto, Micaelle Barros, Wellington Sobrinho e Kathia Beatriz. Agradeço pelo apoio científico na execução da tese, pela companhia e pelas boas risadas. Vocês ajudaram a tornar essa trajetória mais leve.

Ao Laboratório de Biologia Celular e do Desenvolvimento (LABID), ao Prof. Dr. Luís Fernando Marques, à Me. Catarina Serrão e à Bianca Mataribu, pela infraestrutura disponibilizada e pelo apoio na realização de parte dos experimentos desta tese, bem como pelo intercâmbio científico e amizade.

Ao Laboratório de Peixes (FishLab) da Universidade Federal do Rio Grande do Norte (UFRN), ao Me. Romério Filho, à Profª. Dra. Ana Carolina Luchiari e à Profª. Drª. Silvia Batistuzzo, pela infraestrutura e pelo apoio na realização das análises de expressão gênica.

Ao Laboratório de Imunologia e Patologia de Invertebrados Marinhos (LABIPI) e à Profª. Dra. Patrícia Mirella Scardua, pela infraestrutura e pelo apoio na realização das análises histopatológicas.

Ao Laboratório de Metabolismo Mitocondrial do Zebrafish (MitoFish) da Universidade de Pernambuco (UPE) e ao Prof. Dr. Rafael de Azevedo, pela infraestrutura e pelo apoio na realização de ensaios bioquímicos.

À equipe de técnicos e servidores administrativos da UFC e da UFPB, em especial a Dione, César, Alexandra e ao Sr. Bosco.

À minha família, Antônia (mãe), Joseildo (pai), Ana Clara (irmã) e Maria José (avó), pelo apoio imensurável durante todos os anos de trajetória acadêmica. Amo vocês!

Eu sou o sonho dos meus pais, que eram sonhos dos avós que eram sonhos dos meus ancestrais. Vitória é sonho dos olhares, que nos aguardam nos lares, crendo que na volta somos mais. (Emicida, 2020).

RESUMO

O herbicida ácido 2,4-Diclorofenoxiacético (2,4-D) e seu principal metabólito ambiental, o 2,4-Diclorofenol (2,4-DCP), são contaminantes emergentes frequentemente detectados em ecossistemas aquáticos. Embora sua hepatotoxicidade em vertebrados já tenha sido reportada, os mecanismos moleculares subjacentes permanecem pouco conhecidos. Além disso, a maior parte dos estudos utiliza concentrações elevadas e exposições agudas, o que limita a compreensão dos efeitos sob condições ambientalmente realistas, caracterizadas por exposições prolongadas a baixas concentrações. Neste estudo, adotamos uma abordagem integrada combinando toxicologia computacional e experimentos *in vivo* com peixe-zebra (*Danio rerio*) para investigar os mecanismos de toxicidade hepática induzidos por 2,4-D e 2,4-DCP, bem como seus efeitos agudos e crônicos em concentrações ambientalmente relevantes. As análises de toxicologia de rede e docking molecular revelaram interação potencial de ambos os compostos com proteínas-chave associadas à hepatotoxicidade, como SRC, AKT1, RXRA, HSP90AA1 e MDM2. O enriquecimento funcional (Gene Ontology e Reactome) indicou a participação de vias de sinalização críticas, incluindo receptores nucleares e PI3K/AKT, além de processos biológicos associados à toxicidade hepática, como estresse oxidativo, acúmulo lipídico, disfunção mitocondrial e morte celular. Ensaios *in vivo* demonstraram que concentrações ambientalmente relevantes (3, 30 e 300 µg/L) induzem hepatotoxicidade aguda em larvas de peixe-zebra, corroborando os mecanismos preditos *in silico*. Em adultos, a exposição crônica resultou em alterações histopatológicas, incluindo acúmulo lipídico, morte celular e desorganização tecidual, inclusive na concentração de 30 µg/L de 2,4-D, equivalente ao valor máximo permitido (VMP) em água potável no Brasil. Este estudo descreve pela primeira vez alvos biológicos e vias moleculares associados à hepatotoxicidade induzida por 2,4-D e 2,4-DCP e demonstra que concentrações ambientalmente relevantes são capazes de perturbar processos celulares essenciais, que culminam em dano hepático. Esses achados questionam a segurança do VMP de 2,4-D adotado pela legislação brasileira para organismos não alvo e destacam a necessidade urgente de inclusão do 2,4-DCP em programas de monitoramento ambiental, além da reavaliação de limites seguros de exposição a esses contaminantes.

Palavras-chave: contaminantes orgânicos; organoclorados; toxicologia preditiva.

ABSTRACT

The herbicide 2,4-dichlorophenoxyacetic acid (2,4-D) and its main environmental metabolite, 2,4-dichlorophenol (2,4-DCP), are emerging contaminants frequently detected in aquatic ecosystems. Although their hepatotoxicity in vertebrates is already recognized, the underlying molecular mechanisms remain poorly understood. Moreover, most studies employ high concentrations and acute exposures, limiting the understanding of effects under environmentally relevant conditions characterized by prolonged exposure to low concentrations. In this study, we adopted an integrated approach combining computational toxicology and *in vivo* experiments using zebrafish (*Danio rerio*) to investigate the mechanisms of liver toxicity induced by 2,4-D and 2,4-DCP, as well as their acute and chronic effects at environmentally relevant concentrations. Network toxicology and molecular docking analyses revealed potential interactions of both compounds with key proteins associated with liver toxicity, including SRC, AKT1, RXRA, HSP90AA1, and MDM2. Functional enrichment analyses (Gene Ontology and Reactome) indicated the involvement of critical signaling pathways, including nuclear receptors and PI3K/AKT, as well as biological processes associated with liver toxicity, such as oxidative stress, lipid accumulation, mitochondrial dysfunction, and cell death. *In vivo* assays demonstrated that environmentally relevant concentrations (3, 30, and 300 µg/L) induced acute liver toxicity in zebrafish larvae, corroborating the *in silico* predicted mechanismse. In adult fish, chronic exposure resulted in histopathological alterations, including lipid accumulation, cell death, and tissue disorganization, even at 30 µg/L of 2,4-D, corresponding to the maximum allowed value (MAV) for drinking water in Brazil. This study describes, for the first time, biological targets and molecular pathways associated with 2,4-D and 2,4-DCP-induced hepatotoxicity and demonstrates that environmentally relevant concentrations can disrupt essential cellular processes, leading to liver damage. These findings question the safety of the MAV of 2,4-D established by Brazilian legislation for non-target organisms and highlight the urgent need to include 2,4-DCP in environmental monitoring programs, as well as to reassess safe exposure limits for these contaminants.

Keywords: organic contaminants; organochlorines; predictive toxicology

LISTA DE ABREVIATURAS E SIGLAS

2,4-D	Ácido 2,4-diclorofenoxiacético
2,4-DCP	2,4-diclorofenol
ALP	Fosfatase Alcalina
ALT	Alanina Aminotransferase
AST	Aspartato Aminotransferase
ATP	Trifosfato de Adenosina
ANVISA	Agência Nacional de Vigilância Sanitária
ATSDR	Agency for Toxic Substances and Disease Registry
CAT	Catalase
CETESB	Companhia Ambiental do Estado de São Paulo
CTD	Comparative Toxicogenomics Database
CYP450	Citocromo P450
DILI	Drug-Induced Liver Injury
USEPA	United States Environmental Protection Agency
GO	Gene Ontology
GPx	Glutationa Peroxidase
GST	Glutationa S-Transferase
hpf	Horas Pós-Fertilização
IL-8	Interleucina-8
KEGG	Kyoto Encyclopedia of Genes and Genomes
MDA	Malondialdeído
NAFLD	Non-Alcoholic Fatty Liver Disease
NRC	National Research Council
NT	Network Toxicology
OECD	Organização para a Cooperação e Desenvolvimento Econômico
ROS	Reactive Oxygen Species
SOD	Superóxido Dismutase
TNF-α	Tumor Necrosis Factor Alpha
USDA	United States Department of Agriculture
VMP	Valor Máximo Permitido

SUMÁRIO

1. FUNDAMENTAÇÃO TEÓRICA

1.1. Fígado como centro metabólico dos vertebrados

O fígado é um órgão metabolicamente ativo e funcionalmente conservado entre os vertebrados, desempenhando papel central em diversos processos fisiológicos essenciais à manutenção da vida (Delgado-Coello, 2021). Entre esses processos destacam-se o metabolismo de macronutrientes, a regulação do volume sanguíneo, o suporte a diferentes sistemas do organismo (*e.g.*, imunológico e o endócrino) e a neutralização e excreção de metabólitos tóxicos e xenobióticos (Cheng *et al.*, 2021; Delgado-Coello, 2021).

Em humanos, as células hepáticas se organizam para formar a unidade estrutural e funcional do fígado, o lóbulo hepático (Figura 1A). Cada lóbulo apresenta formato hexagonal, composto por cordões de hepatócitos dispostos ao redor de uma veia central. Nas extremidades, encontra-se a tríade portal formada pela artéria hepática, veia porta e ductos biliares (Trefts *et al.*, 2017). O sangue oxigenado proveniente da artéria hepática mistura-se ao sangue rico em nutrientes trazido pela veia porta (proveniente do intestino) nos sinusoides hepáticos, uma rede de capilares que percorre os hepatócitos até ser coletada pela veia central (Wilkins e Pack, 2013). Essa organização cria gradientes de oxigênio e nutrientes ao longo do lóbulo, originando três zonas metabolicamente distintas, cada uma com funções específicas no metabolismo hepático (Trefts *et al.*, 2017).

As principais populações celulares do fígado humano incluem hepatócitos, células epiteliais biliares (colangiócitos), células estreladas, células de Kupffer e células endoteliais sinusoidais hepáticas (Figura 1B) (Wilkins e Pack, 2013). Dentre elas, os hepatócitos representam cerca de 70% das células hepáticas e são responsáveis pela maior parte das funções metabólicas do órgão, incluindo o metabolismo de lipídios, carboidratos e proteínas (Trefts *et al.*, 2017).

Figura 1. Organização estrutural do fígado humano. (A) Representação esquemática do lóbulo hepático, destacando sua disposição geométrica. (B) Esquema ilustrativo das principais células e vasos que compõem o tecido hepático, bem como das principais funções metabólicas desempenhadas pelo fígado.

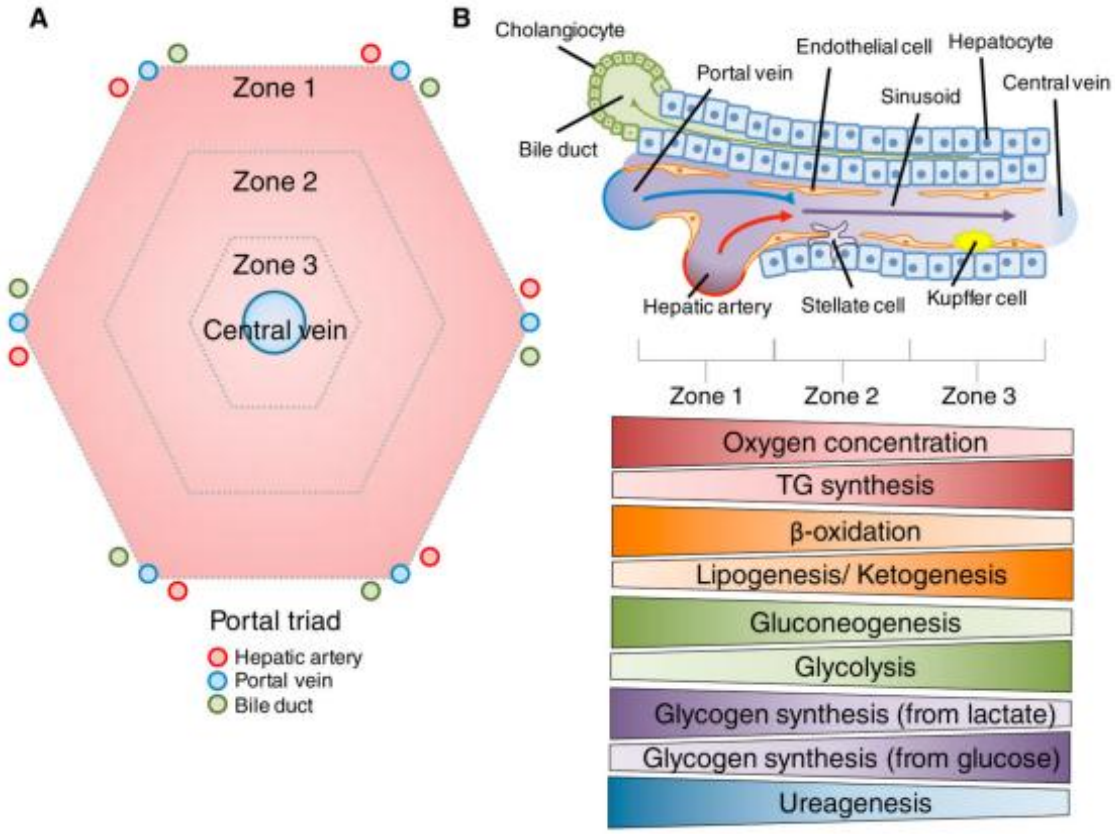

Fonte: Trefts *et al.* (2017)

O fígado é um órgão estrategicamente localizado entre o trato digestivo e a circulação geral, o que facilita a metabolização, o armazenamento e a distribuição de nutrientes (Chiang *et al.*, 2014). Nesse órgão, a glicose é oxidada para gerar energia na forma de ATP (glicólise). O fígado também regula o metabolismo da glicose por meio da glicogênese (síntese de glicogênio), glicogenólise (degradação do glicogênio) e gliconeogênese (formação de glicose) (Jones, 2016).

Além disso, é no fígado que ocorre a síntese de ácidos graxos e colesterol, precursor de hormônios, vitaminas e sais biliares (Chiang *et al.*, 2014). O tecido hepático também realiza a β-oxidação de ácidos graxos para obtenção de energia e converte parte deles em triglicerídeos, que são transportados a outros tecidos ou armazenados em adipócitos (Ding *et al.*, 2018).

O fígado exerce um papel essencial no metabolismo de aminoácidos e proteínas. Ele capta alanina e glutamina provenientes de músculos, rins e outros tecidos e converte o nitrogênio dos aminoácidos em ureia, que é excretada na urina. Além disso, é responsável pela síntese de 85 a 90% das proteínas circulantes, incluindo a albumina, que ajuda a regular o volume sanguíneo e atua como carreadora de ácidos graxos, esteroides, aminoácidos e vitaminas (Trefts *et al.*, 2017).

Além de seu papel central no metabolismo de macronutrientes, o fígado exerce função primordial na depuração do organismo, participando ativamente da metabolização e eliminação de compostos tóxicos, fármacos e xenobióticos ambientais (Chiang *et al.*, 2014). O metabolismo de detoxificação ocorre em duas etapas: fases I e II. Na fase I, ocorrem reações como oxidação, redução e hidrólise, catalisadas principalmente pelo sistema citocromo P450 (CYP450), um conjunto de enzimas localizadas no retículo endoplasmático que converte compostos químicos em moléculas mais polares, que podem ou não ser tóxicas (Gulati *et al.*, 2018). Na fase II, essas substâncias são conjugadas a compostos hidrofílicos, como glicuronídeos, sulfatos ou aminoácidos, formando metabólitos mais solúveis em água e facilmente excretáveis. Essa fase também pode envolver a glutationa, que se liga covalentemente a intermediários tóxicos com auxílio da glutationa-S-transferase (GST) (Gulati *et al.*, 2018).

1.2. Agentes agressores hepáticos e seus mecanismos de indução de dano

O fígado desempenha um papel central em processos essenciais à vida dos vertebrados. Fatores que comprometam sua fisiologia podem causar danos severos, uma vez que nenhum outro órgão consegue compensar integralmente todas as suas funções vitais (Chiang *et al.*, 2014). Entre os principais fatores que afetam a saúde hepática estão a nutrição inadequada, infecções virais e o uso excessivo de álcool e medicamentos (Elufioye e Habtemariam, 2019). Devido ao seu papel crucial no metabolismo e na eliminação de xenobióticos, o fígado é particularmente suscetível a danos causados por drogas e outros compostos químicos.

Um fato que ilustra bem essa vulnerabilidade é que a hepatotoxicidade induzida por medicamentos é um dos principais gargalos enfrentados pela indústria farmacêutica no desenvolvimento de novas drogas (Gulati *et al.*, 2018). Entre os fármacos conhecidos por induzir hepatotoxicidade estão o paracetamol (analgésico); os anti-inflamatórios não

esteroidais nimesulida, diclofenaco e ibuprofeno; e os medicamentos anti-tuberculose rifampicina, isoniazida e pirazinamida (Gulati *et al.*, 2018).

As doenças hepáticas representam um importante problema de saúde pública, sendo responsáveis por cerca de 2 milhões de mortes por ano, correspondendo a 4% da mortalidade global (Gan *et al.*, 2025). As formas agudas dessas doenças estão frequentemente associadas a infecções por vírus hepatotrópicos e a lesão hepática induzida por fármacos ("drug-induced liver injury, DILI"). Já as doenças hepáticas crônicas estão mais relacionadas ao consumo excessivo de álcool, às infecções pelos vírus da hepatite B e C, e às disfunções metabólicas associadas à esteatose hepática (Gan *et al.*, 2025).

Substâncias hepatotóxicas podem induzir danos por diferentes mecanismos. Inicialmente, o químico ou seus metabólitos ativos podem causar estresse celular ao depletar os níveis de glutationa ou ao se ligar covalentemente a proteínas, enzimas, lipídios, ácidos nucleicos e outras estruturas celulares (Jaeschke *et al.*, 2012). A interação de agentes tóxicos com proteínas intracelulares pode levar à redução dos níveis de ATP, resultando no enfraquecimento dos filamentos de actina, componentes essenciais do citoesqueleto. A ruptura desses filamentos no hepatócito pode comprometer a integridade da membrana plasmática, provocando o extravasamento de conteúdo celular (Gulati *et al.*, 2018).

A falha na produção ou no fluxo de sais biliares pode causar danos ao fígado, resultando em uma doença chamada colestase (Mawardi *et al.*, 2021). A retenção de constituintes biliares provoca apoptose de hepatócitos, frequentemente associada à inibição de bombas de transporte. Além disso, substâncias tóxicas excretadas na bile podem interagir com estruturas celulares e induzir lesões no epitélio dos ductos biliares (Elufioye e Habtemariam, 2019; Mawardi *et al.*, 2021).

Alguns compostos, como fármacos anfifílicos catiônicos, acumulam-se nas mitocôndrias e comprometem a β-oxidação de ácidos graxos e a respiração celular (Elufioye e Habtemariam, 2019; Fromenty e Roden, 2023). A inibição da β-oxidação reduz a produção de energia durante o jejum e provoca acúmulo de gordura nos hepatócitos, podendo evoluir para esteatose hepática, a doença crônica de fígado mais comum, que afetou 38% da população global entre 2016 e 2019 (Fromenty e Roden, 2023; Gan *et al.*, 2025).

A inibição da respiração mitocondrial causa depleção de ATP e aumento de espécies reativas de oxigênio (ROS), resultando em peroxidação lipídica e danos às

membranas celulares (Gulati *et al.*, 2018). ROS e peroxidação lipídica estimulam a liberação de citocinas pró-inflamatórias, como TNF-α e IL-8, promovendo respostas inflamatórias hepáticas (Elufioye e Habtemariam, 2019). A inflamação hepática ou sistêmica, com recrutamento de macrófagos e neutrófilos, pode potencializar o dano inicial. Embora essas células participem da remoção de células mortas e detritos, células saudáveis também podem ser afetadas, agravando a lesão (Del Campo *et al.*, 2018; Elufioye e Habtemariam, 2019).

Apesar estar sujeito a múltiplos agressores, o fígado possui elevada capacidade regenerativa (Forbes e Newsome, 2016). Tanto fatores extrínsecos, como sais biliares e fatores de crescimento circulantes, quanto fatores intrínsecos ao próprio fígado contribuem para a regeneração. No entanto, danos extensos podem comprometer esses mecanismos e levar à insuficiência hepática, tornando necessário, em alguns casos, o transplante (Forbes e Newsome, 2016; Vieira *et al.*, 2023). Portanto, torna-se cada vez mais importante compreender o potencial hepatotóxico de diferentes substâncias. Além de medicamentos, compostos químicos como agrotóxicos podem causar efeitos deletérios ao fígado de vertebrados. Esses produtos são amplamente utilizados na agricultura e têm sido alvo de estudos em diversas regiões, devido ao seu uso em larga escala, à detecção frequente em amostras ambientais e a dados prévios de toxicidade (EPA e OITA, 2014).

1.3. Herbicida 2,4-D e seu metabólito 2,4-DCP como contaminantes ambientais

O ácido 2,4-diclorofenoxiacético (2,4-D) (Figura 2) é um herbicida da classe dos derivados do ácido fenoxiacético, utilizado mundialmente na agricultura desde 1946 (Li *et al.*, 2017). Este hidrocarboneto aromático clorado foi um dos primeiros herbicidas sintéticos a serem comercializados e atualmente é o principal ingrediente de mais de 1.500 produtos disponíveis no mercado (Islam *et al.*, 2018). O 2,4-D figura entre os herbicidas mais empregados no mundo e, no Brasil, seu uso é autorizado para culturas de arroz, aveia, café, centeio, cevada, milho, milheto, soja, sorgo e trigo (Anvisa, 2021).

Este composto foi desenvolvido para mimetizar as auxinas, hormônios que regulam o crescimento das plantas (Tiwari *et al.*, 2018). Em baixas concentrações (20–50 mg/L), ele estimula a divisão celular, acelera o desenvolvimento das plantas e melhora a aparência e a durabilidade dos frutos (Li *et al.*, 2017). Entretanto, em altas concentrações (≥ 500 mg/L), apresenta efeito herbicida, eliminando seletivamente plantas

dicotiledôneas ao induzir crescimento anormal dos tecidos, entre outros efeitos prejudiciais que levam à morte (Li *et al.*, 2017; Tiwari *et al.*, 2018).

Figura 2. Fórmula estrutural 2D do 2,4-D

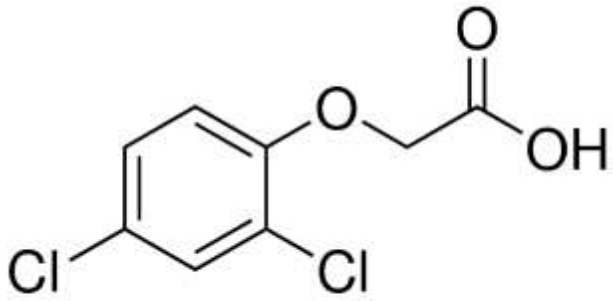

Fonte: Sigma aldrich, S/D.

Este herbicida é amplamente utilizado em todo o mundo. Segundo o Departamento de Agricultura dos Estados Unidos (USDA), os principais mercados e produtores de 2,4-D incluem os EUA, a América do Sul, a Europa e a Rússia, e seu consumo aumentou aproximadamente 40% na última década (USDA, 2014; Magnoli *et al.*, 2020). Nos Estados Unidos, cerca de 600 produtos agrícolas e residenciais contêm 2,4-D como ingrediente ativo e, em 2012, ele foi o quinto herbicida mais aplicado no setor agrícola do país (Freisthler *et al.*, 2014; Peterson *et al.*, 2016; ATSDR, 2020).

Na Argentina, mais de 2.000 toneladas de 2,4-D são empregadas em diferentes culturas, especialmente em milho e soja tolerantes ao glifosato (Kennepohl e Munro, 2001; Magnoli *et al.*, 2020). O 2,4-D também apresenta elevado consumo em países asiáticos: na Tailândia, foi o herbicida mais importado em 2021, totalizando 11.781 toneladas (Casimero *et al.*, 2022), enquanto na China a produção atingiu um marco de 40.000 toneladas em 2010 (Liu *et al.*, 2013). No Brasil, o herbicida é o segundo mais comercializado desde 2013, com 51.872,24 toneladas vendidas em 2023 (IBAMA, 2024).

A ampla comercialização do 2,4-D reflete-se no ambiente, sendo ele um contaminante frequentemente detectado em corpos d'água. No Brasil, dados do Ministério da Saúde, por meio do Sistema de Informação de Vigilância da Qualidade da Água para Consumo Humano (SISAGUA), indicam que um coquetel complexo de

agrotóxicos foi identificado na água de mais de 2.300 cidades entre 2014 e 2017, com o 2,4-D presente em 92% das amostras (SISAGUA, 2018). Em apenas duas cidades, os níveis ultrapassaram o Valor Máximo Permitido (VMP) para água potável, estabelecido em 30 µg/L, valor cerca de 300 vezes superior ao limite de 0,1 µg/L adotado pela União Europeia (SISAGUA, 2018; Zuanazzi *et al.*, 2020).

Entretanto, concentrações mais altas também foram registradas em rios de regiões produtoras de cana-de-açúcar no estado de São Paulo, chegando a 366,6 µg/L (CETESB, 2018). O 2,4-D ainda foi detectado em corpos d'água de outros países, incluindo Estados Unidos (0,1–12 µg/L), Espanha (62–207 ng/L), Austrália (3,5 ng/L), Irã (16,6 µg/L) e Grécia (1,16 µg/L) (Rodil *et al.*, 2012; Yamini e Saleh, 2013; Tsaboula *et al.*, 2016; Peterson *et al.*, 2016; ATSDR, 2020; Meftaul *et al.*, 2020).

O 2,4-D é um contaminante ambiental persistente, com meia-vida na água variando de 15 a 300 dias, dependendo das condições ambientais (EPA, 2005; Nault *et al.*, 2014; Dehnert *et al.*, 2019; Gaaied *et al.*, 2019;). No ambiente, ele pode sofrer degradação química e/ou biológica, formando metabólitos que podem ser mais tóxicos para organismos não-alvo do que o composto original (Magnoli *et al.*, 2020). O principal produto de degradação do 2,4-D é o 2,4-diclorofenol (2,4-DCP) (Figura 3), resultante da quebra da cadeia lateral e posterior hidroxilação do anel aromático (Magnoli *et al.*, 2020). Esse processo ocorre principalmente por degradação bacteriana aeróbia, embora certas espécies de fungos também possam gerar 2,4-DCP ao clivar a ligação éter do 2,4-D (Ferreira-Guedes *et al.*, 2012; Itoh *et al.*, 2016; Magnoli *et al.*, 2020).

Além disso, o 2,4-DCP também é produzido a partir de outros contaminantes organoclorados, como o triclosan, o que aumenta sua presença no ambiente (Liu *et al.*, 2018). Classificado como um composto tóxico e resistente, é considerado um contaminante prioritário na China e nos Estados Unidos (USEPA, 1979; Liu *et al.*, 2018; Magnoli *et al.*, 2020; Zhang *et al.*, 2020).

Na China, o 2,4-DCP foi detectado em 51,3% das amostras de água superficial de mais de 600 locais, com concentrações variando de 0,01 a 19,96 µg/L (Gao *et al.*, 2008). Também foi identificado em águas de rios na França (0–4,89 µg/L), na África do Sul (0,1–10 µg/L) e em águas residuais na Austrália (0,1–6,72 µg/L) (Farounbi e Ngqwala, 2020; Pan *et al.*, 2021). No Brasil, no principal sistema de abastecimento de água potável de Minas Gerais foram detectadas concentrações de 2,4-DCP entre 0,42 e 10,03 µg/L na água não tratada e de 2,94 a 3,33 µg/L na água tratada (Ramos *et al.*, 2021).

Figura 3. Fórmula estrutural 2D do 2,4-DCP

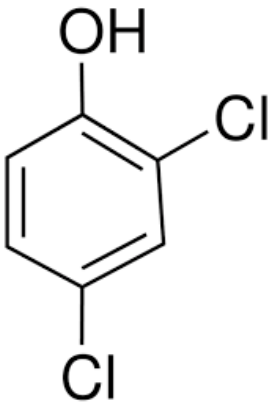

Fonte: Sigma aldrich, S/D.

1.4. Hepatotoxicidade induzida pelo 2,4-D e 2,4-DCP

A presença de 2,4-D e 2,4-DCP no ambiente é preocupante devido aos seus efeitos tóxicos, especialmente sobre a função hepática relatada em diferentes modelos biológicos, incluindo roedores, peixes e células hepáticas (Troudi *et al.*, 2012; Tichati *et al.*, 2020; Martins *et al.*, 2021; Tichati *et al.*, 2021;). Tichati *et al.* (2020) mostraram que ratos tratados com 5 mg/kg de 2,4-D apresentaram aumento do peso do fígado, danos teciduais, elevação da atividade de aminotransferases (AST - aspartato aminotransferase e ALT – alanina aminotransferase) e fosfatase alcalina (ALP), além de redução na atividade das enzimas antioxidantes hepáticas GST, CAT (catalase), SOD (superóxido dismutase) e GPx (glutationa peroxidase). O 2,4-D também aumentou os níveis de proteínas carboniladas e malondialdeído (MDA), indicando estresse oxidativo e peroxidação lipídica (Tichati *et al.*, 2021).

Em larvas de peixe-zebra, exposições a 2,4-D (5 e 10 mg/L) causaram graves alterações hepáticas, como vacuolização do citosol, deslocamento nuclear excêntrico e perda da arquitetura tecidual e dos limites celulares (Martins *et al.*, 2021). Além disso, um estudo em camundongos realizado por Romualdo *et al.* (2023) mostrou que a exposição crônica a 2 mg/kg/dia de 2,4-D agravou a esteatose hepática não alcoólica (NAFLD) induzida por uma alimentação rica em gorduras e açúcares, aumentando parâmetros pró-inflamatórios e a fibrose.

Por sua vez, estudos *in vitro* com 2,4-DCP demonstraram redução da viabilidade celular e inibição da formação de colônias em células hepáticas humanas (HL7702), além de colapso do potencial de membrana mitocondrial e indução de apoptose após 24 horas de exposição (Fu *et al.*, 2016). Em modelos *in vivo*, o 2,4-DCP aumentou o peso do fígado, provocou danos histopatológicos e elevou os níveis de AST e ALT em camundongos, com estresse significativo do retículo endoplasmático contribuindo para a hepatotoxicidade (Fu *et al.*, 2016). Além disso, o 2,4-DCP induziu apoptose em hepatócitos primários de *Ctenopharyngodon idella* por meio de uma via mitocondrial dependente (Li *et al.*, 2013).

Apesar do conhecimento sobre a hepatotoxicidade do 2,4-D e do 2,4-DCP, ainda existem lacunas significativas na literatura. A maioria dos estudos concentra-se em ensaios de toxicidade aguda, envolvendo exposições a altas concentrações por curtos períodos. Embora relevantes, essas abordagens raramente refletem cenários realistas, em que organismos não-alvo são expostos a baixas concentrações de contaminantes por períodos prolongados. Assim, estudos crônicos com concentrações ambientalmente relevantes são essenciais para fornecer subsídios aos órgãos regulatórios na definição de limites seguros para o 2,4-D e o 2,4-DCP no ambiente.

Além disso, os alvos e vias moleculares afetados por esses compostos ainda não são totalmente conhecidos, o que limita o entendimento de seus mecanismos tóxicos. A elucidação desses processos pode auxiliar no desenvolvimento de estratégias de mitigação de danos e servir de base para a identificação de biomarcadores de intoxicação, inclusive em populações humanas mais vulneráveis, como trabalhadores rurais (Dalmolin *et al.*, 2020; Venugopal *et al.*, 2022). Nesse contexto, abordagens computacionais têm se mostrado ferramentas promissoras para investigar os mecanismos de toxicidade induzidos por compostos químicos.

1.5. Uso de abordagens computacionais para elucidar mecanismos de toxicidade

A avaliação de risco de substâncias químicas, incluindo agrotóxicos, baseia-se principalmente em estudos *in vivo* que investigam efeitos patofisiológicos em exposições agudas, subcrônicas e crônicas (Rebelo e Caldas, 2014). Contudo, o uso de animais vertebrados vem sendo amplamente questionado pela comunidade cientifica sobre o ponto de vista ético, o que estimulou o desenvolvimento de tecnologias alternativas

alinhadas ao princípio dos 3Rs (“reduction, refinement, replacement”) na experimentação animal (Liebsch *et al.*, 2011).

Um marco nessa transição foi o relatório do Conselho Nacional de Pesquisa dos Estados Unidos (NRC), publicado em 2007 e intitulado “Toxicity Testing in the 21st Century: A Vision and a Strategy”. O documento propõe a substituição gradual dos testes tradicionais por abordagens baseadas em ensaios *in vitro* e *ex vivo*, dados ômicos, biologia de sistemas, bioinformática e toxicologia computacional (Gibb, 2008; Vinken *et al.*, 2017).

Organizações como a “U.S. Environmental Protection Agency (US EPA)” e a “Organization for Economic Co-operation and Development (OECD)” também têm promovido o uso de ferramentas computacionais para a avaliação de risco e compreensão dos mecanismos de toxicidade de compostos químicos (Krewski *et al.*, 2020). Esses avanços refletem o aprofundamento do conhecimento sobre a biologia de diferentes organismos e o aprimoramento contínuo das metodologias empregadas na avaliação dos efeitos de substâncias químicas em sistemas biológicos.

O grande volume de dados toxicológicos gerado nas últimas décadas está disponível em bases públicas, como o “Comparative Toxicogenomics Database, CTD” (https://www.ctdbase.org/), permitindo estudos *in silico* voltados à identificação de mecanismos moleculares de ação de compostos tóxicos. Entre as abordagens emergentes, destaca-se a “Network Toxicology (NT)”, que integra dados biológicos e computacionais para investigar redes moleculares associadas aos efeitos tóxicos das substâncias (Gong *et al.*, 2021; Souza *et al.*, 2023).

Compostos bioativos geralmente interagem com múltiplos alvos moleculares, o que dificulta a elucidação de seus mecanismos de ação por abordagens farmacológicas ou toxicológicas tradicionais (Chandran *et al.*, 2017). A NT utiliza dados de múltiplas fontes para construir redes de interação entre os compostos e seus potenciais alvos, fornecendo modelos gráficos que permitem a análise sistemática dos mecanismos moleculares de múltiplos alvos (Chandran *et al.*, 2017; Gong *et al.*, 2021; Souza *et al.*, 2023).

Também é possível realizar análises de enriquecimento funcional, como as oferecidas pelo “Reactome Pathway” e “Kyoto Encyclopedia of Genes and Genomes (KEGG)”, que identificam vias moleculares relacionadas aos efeitos tóxicos, e pelo “Gene Ontology (GO)”, que indica os processos biológicos, funções moleculares e componentes celulares aos quais os conjuntos de alvos potenciais estão associados (Gaudet *et al.*, 2017; Milacic *et al.*, 2024). Além disso, ferramentas de análise de

interações moleculares, como docking e dinâmica molecular, podem avaliar a afinidade de uma substância tóxica por diferentes alvos, contribuindo para a elucidação das proteínas com as quais o composto pode interagir (Santos *et al.*, 2019).

Essa metodologia tem sido aplicada em diferentes estudos. Por exemplo, Souza *et al.* (2023) identificaram com sucesso alvos e vias potenciais compartilhados relacionados à neurotoxicidade de organofosforados, enquanto Huang (2023) utilizou a abordagem para esclarecer os mecanismos neurotóxicos do acetil tributil citrato. No campo da hepatotoxicidade, a estratégia tem sido empregada para investigar potenciais mecanismos de ação de poluentes ambientais, como diisononil ciclohexano-1,2-dicarboxilato, aflatoxina B1 e benzo[a]pireno (Ge *et al.*, 2024; Yang *et al.*, 2024; Xin *et al.*, 2025).

Embora esses estudos forneçam informações valiosas sobre potenciais mecanismos de toxicidade, ensaios *in vitro* e *in vivo* continuam sendo necessários para confirmar se esses alvos e vias são realmente modulados. Nesse contexto, o peixe-zebra (*Danio rerio*) é amplamente reconhecido como modelo de referência para estudos de hepatotoxicidade (Shimizu *et al.*, 2023).

1.6. Peixe-zebra como organismo modelo para estudo de doenças hepáticas

O peixe-zebra (*D. rerio*) é um pequeno teleósteo pertencente à família Cyprinidae que, quando adulto, apresenta comprimento de 3 a 4 cm. É nativo do sul da Ásia, principalmente de países como Índia, Bangladesh, Nepal e Mianmar. Habita rios, córregos e lagoas rasas, geralmente com vegetação abundante e água de corrente lenta, em regiões tropicais e subtropicais (Parichy, 2015). Esse modelo apresenta dimorfismo sexual evidente: as fêmeas podem ser diferenciadas dos machos pelo ventre mais arredondado e pela ausência da coloração avermelhada ao longo das linhas longitudinais prateadas (Figura 4) (Braunbeck e Lammer; 2005; Chua *et al.*, 2025).

Figura 4. Dimorfismo sexual em peixe-zebra. Acima, fêmea; abaixo, macho

Fonte: Braunbeck e Lammer (2005)

Atualmente, o peixe-zebra é um organismo modelo amplamente utilizado em toxicologia, inclusive na investigação dos efeitos hepatotóxicos de substâncias químicas e na modelagem de doenças hepáticas humanas (Shimizu *et al.*, 2023). Esse potencial decorre de características biológicas e genéticas intrínsecas à espécie.

Uma das principais vantagens desse modelo é o acesso a um conjunto de biomarcadores de toxicidade hepática relevantes para a saúde humana. Um exemplo clássico é a quantificação da atividade de ALT e AST no soro sanguíneo, marcador amplamente utilizado para avaliar lesões hepáticas (Zhang *et al.*, 2017 Zhao *et al.*, 2019; Shimizu *et al.*, 2023). Em peixe-zebra, a quantificação desses biomarcadores pode ser realizada ainda no estágio larval, às 120 horas pós-fertilização (hpf), quando o fígado já está funcional e perfundido por sangue (Zhang *et al.*, 2017; Zhao *et al.*, 2019; Martins *et al.*, 2021). Estudos comparativos demonstram que modelos *in vitro* de células humanas, de roedores e de peixe-zebra apresentam perfis semelhantes de expressão gênica após exposição a substâncias hepatotóxicas (Cassar *et al.*, 2019). Essa correspondência é explicada pela elevada homologia genética entre o peixe-zebra e seres humanos (aproximadamente 70%), o que resulta na conservação de vias moleculares envolvidas em respostas tóxicas (Howe *et al.*, 2013).

Além disso, a hepatogênese e os aspectos morfofisiológicos do fígado do peixe-zebra são semelhantes aos dos humanos (Wilkins e Pack, 2013). Embora apresente uma arquitetura menos organizada, sem lóbulos bem definidos, o fígado do peixe-zebra conserva os principais tipos celulares hepáticos (Figura 5). Em humanos, o fígado exibe uma organização lobular clássica centrada na veia central e na tríade portal (veia porta, artéria hepática e ducto biliar), enquanto no peixe-zebra a morfologia é mais simples (Goessling e Sadler, 2015; Shimizu *et al.*, 2023). Ainda assim, os aspectos funcionais são bem preservados, incluindo secreção de bile, armazenamento de glicogênio e lipídios, metabolismo de xenobióticos e síntese de proteínas séricas (Wilkins e Pack, 2013).

Figura 5. Representação da arquitetura e anatomia celular do fígado de humanos e de peixes-zebra

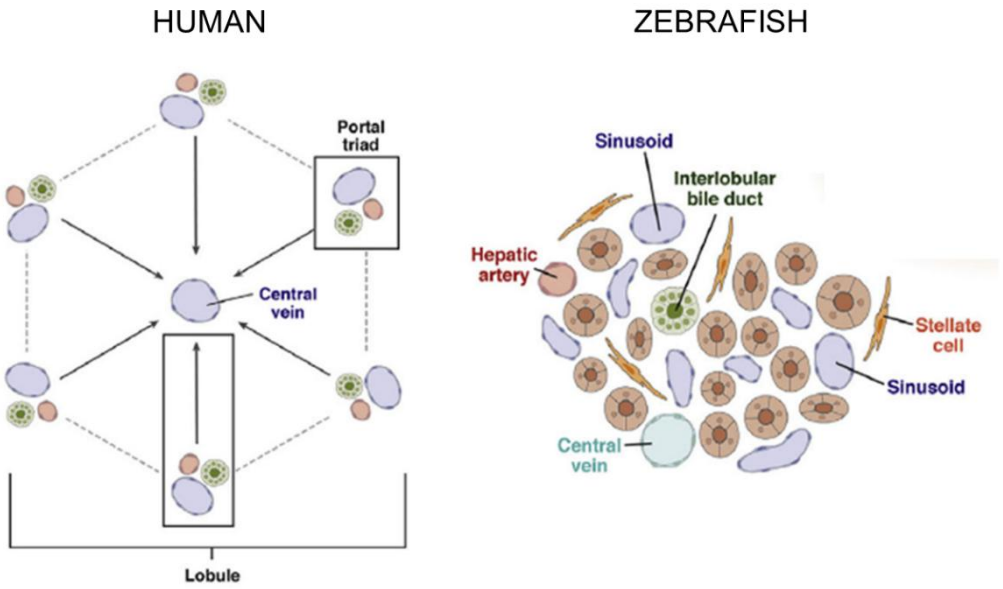

Fonte: Adaptado de Goessling e Sadler (2015)

Outra vantagem importante do peixe-zebra é a translucidez nas fases iniciais de vida, que permite observar diretamente alterações morfológicas no fígado sem necessidade de dissecação, a partir de 120 hpf (Zhang *et al.*, 2017 Zhao *et al.*, 2019; Martins *et al.*, 2021**)**. Essa característica possibilita o uso de sondas fluorescentes e corantes para avaliar diferentes aspectos da progressão de doenças hepáticas, como espécies reativas de oxigênio (H_2DCFDA), morte celular (laranja de acridina e iodeto de propídeo) e acúmulo lipídico (“Nile Red” e “Oil Red”) (Smirnova *et al.*, 2021; Balamurugan *et al.*, 2022; Maia *et al.*, 2025). Também é possível desenvolver linhagens

transgênicas que expressam proteínas fluorescentes em tecidos hepáticos, permitindo a marcação de células específicas como hepatócitos, células epiteliais biliares, células endoteliais e células estreladas (Goessling e Sadler, 2015).

O rápido desenvolvimento do peixe-zebra é uma vantagem para estudos de toxicidade prolongada. Entre 48 e 72 hpf, o organismo passa do estágio embrionário ao larval e atinge a maturidade sexual em cerca de três meses (Meyers, 2018). Assim, ensaios crônicos que exigem até dois anos em roedores podem ser realizados em poucos meses no peixe-zebra (Peng *et al.*, 2019).

2. HIPÓTESES

O herbicida 2,4-D e seu principal metabólito ambiental, 2,4-DCP, são reconhecidamente hepatotóxicos para vertebrados. Apesar de amplamente utilizados e detectados em diversos ecossistemas aquáticos, os mecanismos moleculares subjacentes à sua toxicidade hepática ainda não estão completamente elucidados. Ademais, faltam evidências sobre os efeitos decorrentes de exposições a concentrações ambientalmente relevantes e toxicidade crônica dessas substâncias.

Diante dessas lacunas, o presente estudo propõe investigar potenciais mecanismos de ação hepatotóxicos do 2,4-D e do 2,4-DCP por meio de abordagens *in silico* e *in vivo*, a partir das seguintes hipóteses:

- A integração de abordagens de "network toxicology" e docking molecular permitirá identificar um conjunto convergente de potenciais alvos proteicos e vias moleculares implicadas na hepatotoxicidade induzida por 2,4-D e 2,4-DCP.
- Exposições a concentrações ambientalmente relevantes de 2,4-D e 2,4-DCP provocarão perturbações em vias moleculares associadas à hepatotoxicidade em peixe-zebra.
- A concentração máxima permitida de 2,4-D em água potável no Brasil (30 µg/L) induz hepatotoxicidade em peixe-zebra, refletindo o potencial risco de exposição para vertebrados aquáticos e outros organismos não-alvo.

3. OBJETIVOS

3.1. Objetivo geral

Identificar potenciais alvos e vias moleculares associadas à hepatotoxicidade induzida pelo 2,4-D e 2,4-DCP, e validar *in vivo* se esses mecanismos são perturbados por concentrações ambientalmente relevantes em peixe-zebra.

3.2. Objetivos específicos

- Realizar levantamento bibliográfico sobre a hepatotoxicidade induzida pelo 2,4-D e pelo 2,4-DCP, destacando os modelos biológicos utilizados, os principais biomarcadores de toxicidade e as alterações em sistemas hepáticos.

- Empregar as abordagens "network toxicology" e docking molecular para identificar potenciais alvos e vias moleculares associadas à hepatotoxicidade induzida pelo 2,4-D e 2,4-DCP.

- Caracterizar a toxicidade aguda do 2,4-DCP em embriões e larvas de peixe-zebra, correlacionando alterações morfológicas e bioquímicas com a disrupção de alvos e vias moleculares relacionadas à toxicidade do desenvolvimento.

- Validar *in vivo* os mecanismos associados à hepatotoxicidade identificados *in silico*, por meio da exposição de larvas de peixe-zebra a concentrações ambientalmente relevantes, avaliando marcadores bioquímicos e moleculares.

- Avaliar se a exposição crônica ao 2,4-D e ao 2,4-DCP provoca hepatotoxicidade em peixes-zebra adultos, utilizando concentrações baseadas no valor máximo permitido (VMP) em água potável no Brasil para o 2,4-D (30 μg/L).

- Contribuir para o avanço do conhecimento sobre a toxicidade do 2,4-D e do 2,4-DCP em organismos não alvo e para a definição de limites seguros desses compostos no ambiente.

4. RESULTADOS E DISCUSSÃO

Os resultados obtidos durante o desenvolvimento desta tese são apresentados em formato de artigo científico, seguindo as orientações do Regimento Interno do Programa de Pós-Graduação em Bioquímca da Universidade Federal do Ceará, Art. 60º, Parágrafo único). Os referidos artigos foram produzidos ao longo do desenvolvimento desta tese e correspondem a um artigo de revisão, quatro artigos originais e um capítulo de livro, este último apresentado na seção de Anexos. Os materiais suplementares dos artigos também serão apresentados como anexos.

Artigo 1: o artigo de revisão intitulado "2,4-D herbicide-induced hepatotoxicity: unveiling disrupted liver functions and associated biomarkers" foi publicado na revista **Toxics** (fator de impacto: 4,1) (DOI: 10.3390/toxics12010035; https://www.mdpi.com/2305-6304/12/1/35) e traz um panorama do que se sabe sobre a hepatotoxicidade causada pelo 2,4-D. No período em que o trabalho foi elaborado, nosso grupo de pesquisa ainda não havia investigado o 2,4-DCP, o que explica a sua ausência na revisão.

Artigo 2: o artigo intitulado "A network toxicology and molecular docking-based approach revealed shared hepatotoxic mechanisms and targets between the herbicide 2,4-D and its metabolite 2,4-DCP*"* foi publicado na revista **Toxicology** (fator de impacto: 4,6) (DOI: 10.1016/j.tox.2025.154086; https://www.sciencedirect.com/science/article/abs/pii/S0300483X25000423). Neste trabalho conseguimos identificar potenciais alvos e vias moleculares associadas a hepatotoxicidade induzida pelo 2,4-D e 2,4-DCP.

Artigo 3: o artigo intitulado "Nuclear receptor disruption mediates 2,4-Dichlorophenol-induced developmental toxicity: Evidence from network toxicology and zebrafish analysis" está em processo de revisão por pares (segunda rodada, após correções sugeridas pelos revisores) na revista **Science of Total Environment** (fator de impacto: 8,0). Neste artigo, caracterizamos a toxicidade aguda do 2,4-DCP em embriões e larvas de peixe-zebra, abordando também mecanismos moleculares associados a toxicidade do desenvolvimento.

Artigo 4: O artigo intitulado "Environmental levels of 2,4-D herbicide and its 2,4-DCP metabolite disrupt hepatotoxicity-related mechanisms in zebrafish larvae" será submetido ao periódico **Environmental Pollution** (fator de impacto: 7.3) após as considerações da banca avaliadora. Neste estudo, identificamos que concentrações

ambientalmente relevantes de 2,4-D e 2,4-DCP induzem hepatotoxicidade em larvas de peixe-zebra. Além disso, observamos que vias moleculares identificadas no Capítulo 2 foram perturbadas, corroborando sua participação nos mecanismos de toxicidade hepática desencadeados por esses compostos.

Artigo 5: O artigo intitulado "Long-term exposure to the herbicide 2,4-D and its metabolite 2,4-DCP promotes hepatic morphological alterations in adult zebrafish" será submetido ao periódico **Comparative Biochemistry and Physiology Part C** (fator de impacto: 4,3) após as considerações da banca avaliadora. Verificou-se que a exposição crônica ao 2,4-D e 2,4-DCP promove alterações histopatológicas hepáticas em peixes-zebra adultos, inclusive na concentração correspondente ao VMP para o 2,4-D em água potável no Brasil (30 µg/L).

Anexo: o capítulo de livro intitulado "Biochemical markers for liver injury in zebrafish larvae" foi publicado no livro **Teratogenicity Testing**, 2nd edition, como parte da coleção de livros **Methods in Molecular Biology**, editora Humana (DOI: 10.1007/978-1-0716-3625-1_29; https://link.springer.com/protocol/10.1007/978-1-0716-3625-1_29). Neste trabalho, apresentamos protocolos para a determinação de cinco biomarcadores enzimáticos por espectrofotometria, úteis para a avaliação de hepatotoxicidade em larvas de peixe-zebra. Este trabalho está incluído como anexo pois forneceu uma base metodológica importante para os ensaios conduzidos no Artigo 4.

4.1. Artigo 1

2,4-D herbicide-induced liver injury: unveiling disrupted liver functions and associated biomarkers

Rafael Xavier Martins[1,2], Matheus Carvalho[2], Maria Eduarda Maia[1,2], Bruno flor[2], Terezinha Souza[2], Thiago Lopes Rocha[3], Luís M. Félix[4,5], Davi Farias[1,2,*]

[1]Post-Graduation Program in Biochemistry, Department of Biochemistry and Molecular Biology, Building 907, Campus Pici, Federal University of Ceará, 60455-970 Fortaleza, Brazil

[2]Laboratory for Risk Assessment of Novel Technologies, Department of Molecular Biology, Federal University of Paraiba, João Pessoa, 58050-085, Brazil

[3]Laboratory of Environmental Biotechnology and Ecotoxicology, Institute of Tropical Pathology and Public Health, Federal University of Goiás, Goiânia, Brazil

[4]Centre for the Research and Technology of Agro-Environment and Biological Sciences (CITAB), University of Trás-os-Montes and Alto Douro (UTAD), 5000-801 Vila Real, Portugal

[5]Inov4Agro, Institute for Innovation, Capacity Building and Sustainability of Agri-food Production, University of Trás-os Montes and Alto Douro (UTAD), 5000-801 Vila Real, Portugal

[*]Correspondence:

E-mail: davi@dbm.ufpb.br.

Phone: +55-83-32167633

Graphical Abstract

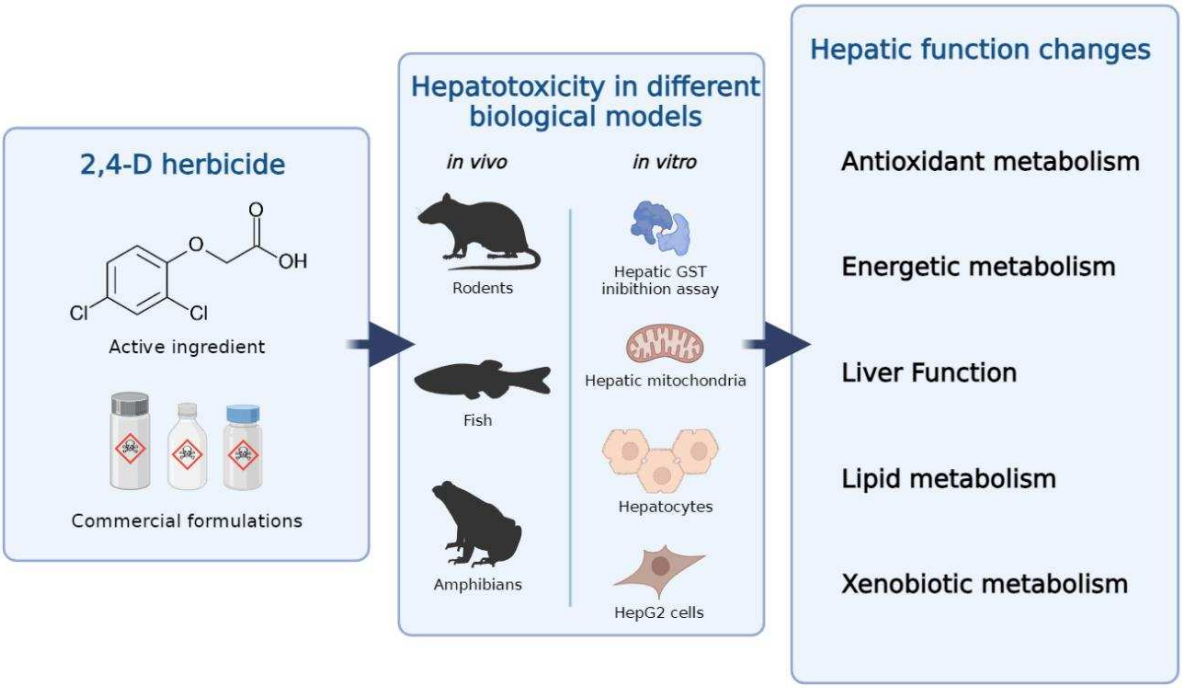

Abstract

2,4-dichlorophenoxyacetic acid (2,4-D) is a herbicide widely used worldwide and is frequently found in water samples. This knowledge has prompted studies on its effects in non-target organisms, revealing significant alterations on liver structure and function. In this review, we evaluated the literature on the hepatotoxicity of 2,4-D, focusing on morphological damages, toxicity biomarkers and affected liver functions. Searches were conducted on PubMed, Web of Science and Scopus and 83 articles were selected after curation. Among these studies, 72% used *in vivo* models and 30% used *in vitro* models. Additionally, 48% used the active ingredient, and 35% used commercial formulations in exposure experiments. The most affected biomarkers were related to a decrease in antioxidant capacity, through alterations in the activities of catalase, superoxide dismutase and in the levels of malondialdehyde. Changes in energy metabolism, lipids, liver function, and xenobiotic metabolism were also identified. Furthermore, studies about the effects of 2,4-D in mixtures with other pesticides were found, as well as hepatoprotection trials. The reviewed data indicate the essential role of reduction in antioxidant capacity and oxidative stress in 2,4-D-induced hepatotoxicity. However, the mechanism of action of the herbicide is still not fully understood and further research in this area is necessary.

Keywords: emerging contaminant, oxidative stress, water pollution, agrochemical.

1. Introduction

2,4-Dichlorophenoxyacetic acid (2,4-D) is an herbicide derived from phenoxyacetic acid. It has been widely used in agriculture since 1946 for weed control[1,2]. This chlorinated aromatic hydrocarbon was one of the first synthetic herbicides to enter the market and is currently the main ingredient in over 1,500 products available in the market, such as Weedestroy® AM40 and DMA® 4 IVM[3,4].

The 2,4-D herbicide mimics the effects of auxins, hormones that regulate plant growth[5]. Due to its high water solubility, the herbicide is able to reach conducting vessels through plants leaves and roots, thus spreading throughout the plant, causing abnormal tissue growth and other deleterious effects that ultimately lead to plant death[5–8]. Due to its high efficiency and low-cost, 2,4-D is globally used as a pre- and post-emergence herbicide in crops such as rice, coffee, sugarcane, corn, and soybeans[6,9,10].

Countries with greater agricultural activity exhibit a prominent use of the herbicide. According to the United States Department of Agriculture, the USA, South America, Europe, and Russia are the primary markets and producers of 2,4-D, with their consumption experiencing a significant 40% increase over the last decade[11,12]. In the United States, approximately 600 agricultural and residential products contain 2,4-D as the active ingredient. Furthermore, in 2012, it was the fifth most widely applied herbicide in the agricultural sector of the country[13–15]. In Argentina, over 2000 tons of 2,4-D are employed in various crop types, particularly in glyphosate-tolerant corn and soybean cultivation[11,16]. In Brazil, a total of 62,165.70 tons of 2,4-D were sold in 2021, making it the second best-selling agrochemical in the country, a prominent position maintained since 2013[17]. 2,4-D is also highly consumed in Asian countries. In Thailand, 2,4-D emerged as the most imported herbicide in 2021, totaling 11,781 tons[18]. In China, the production of 2,4-D reached a significant milestone of 40,000 tons in 2010[19].

Considering that products applied in crops undergo leaching and have access to water bodies, the high level of commercialization of 2,4-D is evident in its frequent detection in surface, groundwater, and drinking water samples[5]. Furthermore, 2,4-D is environmentally persistent, with a half-life in water ranging from 15 to 300 days depending on environmental parameters[20–23]. Concentrations of 2,4-D detected in aquatic environments usually range from 4 to 24 μg/L[3,24]. In surface water, 2,4-D has been detected at varying concentrations around the world. In Spain, the detection in drinking and surface water ranged from 62 to 207 ng/L while in the United States, it was

found to be between 0.1-12 µg/L in urban surface water and sediments[25,26]. Likewise, in Australia, 2,4-D was identified in urban waterways at a concentration of 3.5 ng/L[27]. In northern Iran, 2,4-D was detected in river water at 16.6 µg/L[28]. In Greece, similarly in river water, the herbicide was detected at 1.16 µg/L[29]. Furthermore, values ranging from 359 to 656 µg/L have already been detected in surface waters shortly after herbicide spraying in plantations[3,23].

In Brazil, according to data obtained by the Ministry of Health through the Water Quality Surveillance Information System for Human Consumption (SISAGUA), 2,4-D was detected in 92% of water samples that supplied more than 2300 cities in Brazil between 2014 and 2017[30]. Despite only two detections showing concentrations above the permissible limit in Brazil (30 µg/L), 4270 detections exhibited values exceeding the limit set by the European Union, which adopts a more conservative stance (0.1 µg/L) [30,31]. The concern about the presence of 2,4-D in water lies in its toxic effects on non-target organisms. Among these effects, there is a growing number of studies in the literature that highlight its hepatotoxicity in different biological models (e.g., rodents and fish). The effects include liver cellular and tissue damage, inhibition of hepatic antioxidant enzymes, lipid peroxidation (LPO), and increased seric levels of transaminases[32–34].

The liver plays vital functions in vertebrates, including nutrient metabolism and detoxification processes[35]. Hepatic damage can have negative impacts on these processes and lead to the development of several diseases such as fibrosis, cirrhosis, steatosis, and hepatocellular carcinoma[35]. Therefore, the current study aimed to summarize and analyze, from a critical standpoint, the available literature on the hepatotoxicity induced by pure 2,4-D or commercial formulations containing it as the active ingredient. To do so, we address markers of toxicity and affected liver functions, as well as biological models, chemical compounds, effects in mixtures, and hepatoprotection assays. Research gaps and recommendations for future studies were also addressed.

2. Material and methods

The articles used in the literature review were obtained from the PubMed, Web of Science and Scopus databases, and the search covered all papers published until July 2023. Two keyword combinations were used: (i) "2,4-D" and "liver"; (ii) "2,4-D" and

"hepatotoxicity". The decision to utilize the abbreviation 2,4-D rather than its full nomenclature in the database queries was motivated by the higher volume of located articles and the consistency in outcomes across various keyword combinations. The articles found were curated according to the following inclusion and exclusion criteria:

(i) Inclusion criteria: Articles written and published in English; original and experimental articles; articles that used pure 2,4-D or commercial formulations containing it as the active ingredient; articles that used vertebrates or derivatives (e.g., cells, organelles, enzymes) as biological models; articles that used biological samples derived from hepatic tissue.

(ii) Exclusion criteria: Articles that were not written and published in English; articles that studied other chemical compounds but not 2,4-D; articles that did not use vertebrates or derivatives as biological models; review articles; clinical cases, efficacy studies, protocols, technical reports, and studies that did not meet the research aims.

Subsequently, the selected articles were examined for relevant information on the theme of the review. The extracted information included: DOI, year of publication, geographic location of the study identified by the corresponding author's address, nature of the chemical compound (active ingredient or commercial formulation), biological model used, route of administration/exposure, exposure period, evaluated concentrations, morphological liver damages and toxicity biomarkers.

2.1 Overview

The searches in PubMed using the keyword combinations resulted in a total of 232 findings. After applying the inclusion and exclusion criteria, 64 articles remained. In Web of Science, a total of 193 findings were identified, and 46 articles remained after applying the eligibility criteria. In Scopus, a total of 869 articles were identified, from which 62 were selected. At the end of the curation process and removal of duplicates, a total of 83 articles remained, with 31 of them being present in all three databases (Figure 1a and 1b). These articles are summarized in Table 1 (*in vivo* studies) and Table 2 (*in vitro* studies).

a

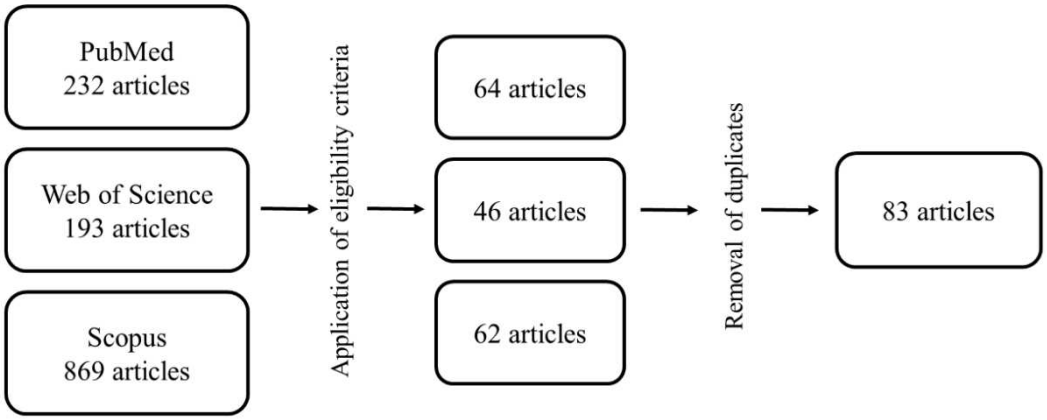

b

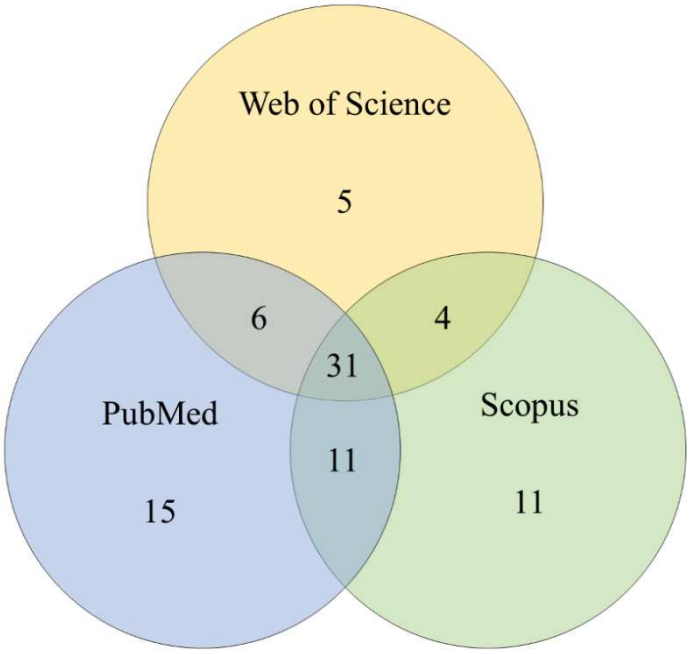

Figure 1. (a) methodological approach to the systematic review of 2,4-D herbicide-induced hepatotoxicity and (b) degree of overlap across the databases queried in this study.

Table 1 Studies of the hepatotoxicity of 2,4-dichlorophenoxiacetic acid (2,4-D) in *in vivo* biological models.

Biological model	Exposure compounds	Exposure conditions	Cellular and tissues damage	Impaired biochemical markers	References
Chinese Hamsters	Commercial formulation (550 g/L)	AR: oral gavage T: 9 days C: 100 mg/kg of body weight	NA	ND: Peroxissomes plorifaration	Vainio *et al.* (1982)[36]
Rattus novergicus	Commercial formulation (550 mg/kg)	AR: oral gavage T: 2 weeks C: 100-200 mg/kg of body weight	NA	LM: peroxissome proliferation, CrAT, protein lipases AM: CAT	Vainio *et al.* (1983)[37]
Rattus novergicus	Commercial formulation (550 g/L)	AR.: intragastrically gavage T: 2 weeks C: 100, 150 and 200 mg/kg of body weight	NA	XM: EH, UDPglucuronosyltransferase , GST AM: GST	Hietanen *et al.* (1983)[38]
Rattus novergicus	Active ingredient	AR: feeding T: 14 h C: 0.25% w/w	NA	LM: CrAT, palmitoyl-CoA, triglycerides AM: CAT	Kawashima *et al.* (1984)[39]

Biological model	Exposure compounds	Exposure conditions	Cellular and tissues damage	Impaired biochemical markers	References
Rattus novergicus	not specified	AR.: feeding T: 14 days C: 0.5 % of diet	NA	LM: stearoyl-CoA	Kawashima *et al.* (1984)[40]
Rattus novergicus	Active ingredient	AR: feeding and subcutaneously T: 1 or 2 weeks C: 0.25% of diet or 0.93 mmole or 1.86 mmole per kg of body weight	NA	LM: acyl-CoA hydrolase II; β oxidation	Katoh *et al.* (1984)[41]
Rattus novergicus	Commercial formulation (550 g/L)	AR: intragastrically ET: 14 days CT: 1 mmol/kg of body weight	NA	LM: peroxissome proliferation, β-oxidation AM: GR	Hietanen *et al.* (1985)[42]
Mus musculus	not specified	AR: diet T: 4 days C: ---	Increase liver somatic index	LM: palmitoil-CoA, CrAT EM: cytochrome oxidase	Lundgren *et al.* (1987)[43]

Biological model	Exposure compounds	Exposure conditions	Cellular and tissues damage	Impaired biochemical markers	References
Rattus novergicus	Active ingredient	AR: gavage and feeding T: single dose and 13 days C: 553 mg/kg and 1090 mg/kg (single dose); 0, 15, 60, 100, or 150 mg/kg/day (13 days)	Dose levels of 100 or 150 mg/kg/day produced minimal swelling and increased staining homogeneity in the liver cells and were associated with a slight elevation of liver weight	LF: ALT, ALP EM: glucose	Gorzinskj *et al.* (1987)[44]
Mus musculus	not specified	AR: feeding T: 4 days C: 100 mg/kg/bw	NA	XM: EH, CYP450, GST, peroxissome proliferation AM: GST	Lundgren *et al.* (1987)[45]
Rattus novergicus	Active ingredient (>99%)	AR.: intragastrically gavage T: 2 weeks C: 100 mg/kg of body weight	NA	XM: peroxisome proliferation, CYP450, UDP-glucunorosyl transferase, NADPH diaphorase	Mustonen *et al.* (1989)[46]
Rattus novergicus	Active ingredient	AR.: feeding T: 7 months C: 0.05% of diet	NA	LM: peroxissome proliferation, acyl Coa oxidase, dicarboxylyl CoA oxidase	Abdellatif *et al.*. (1990)[47]

Biological model	Exposure compounds	Exposure conditions	Cellular and tissues damage	Impaired biochemical markers	References
Mus musculus	Active ingredient (97- 99%)	AR.: oral intubathion T: 14 days exposure + 7 days recovery C: 50 mg/kg	Increase liver/ body weight ratio	LF: ALT	Kuntz *et al.* (1990)[48]
Rattus novergicus	Active ingredient	AR: feeding T: 6 days C: 1.680 ppm	NA	LM: CrAT; carnitine palmitoyltransferase fatty acyl-CoA dehydrogenase cyanide-insensitive fatty acyl-CoA, peroxissome proliferation AM: CAT	Kozuka (1991)[49]
Rattus novergicus	not specified	AR.: oral T: 2 weeks C: 200 mg/kg/day	NA	XM: NADPH cytocrome C reductase, aniline hydroxylase, Cytocrome B, NADPH ferricicyanide reductase, aminopyrine N-demethylase	N Inomata *et al.* (1991)[50]
Mus musculus	Active ingredient (>97%)	AR: oral intubation T: 7 days C: 50 mg/kg of body weight	NA	XM: amidopyrine N-demethylas, Benzo[a]pyrene hydroxilase	Chaturvedi *et al.* (1991)[51]

Biological model	Exposure compounds	Exposure conditions	Cellular and tissues damage	Impaired biochemical markers	References
Rattus novergicus	Commercial formulation	AR: oral and middorsal skin applications T: single dose C: 1.9 and 2.6 mg/kg of body weight	NA	XM: CYP450, ethylmorphine N-demethylase, ethoxyresorufin O-deethylase	Knopp and Schiller (1992)[52]
Rattus novergicus	not specified	AR: oral T: single dose; 30 days and 180 days C: 600 mg/kg (single dose) and 200 ppm (30 and 180 days)	NA	LF: AST, ALT, ALP EM: LDH, amylase, glucose ND: Creatinine	Paulino *et al.* (1996)[53]
Mus musculus	Active ingredient	AR.: feeding T: 4 days C: 0.125% of diet	NA	LF: mdr2 gene	Miranda *et al.* (1997)[54]
Rattus novergicus	Active ingredient	AR: oral gavage T: single dose C: 375 mg/L	NA	XM: CYP1A1, CYP1A2, CYP1B1	Badawi *et al.* (2000)[55]

Biological model	Exposure compounds	Exposure conditions	Cellular and tissues damage	Impaired biochemical markers	References
Rattus novergicus	Active ingredient (>98%)	AR: injections T: 30 days C: 70 mg/kg of body weight	NA	EM: mitochondrial dysfunction	Di Paolo *et al.* (2001)[56]
Rattus novergicus; *Mus musculus* and Syrian hamsters	Active ingredient	AR: feeding T: 3 months C: 0, 12, 28, 83, 250, 700, and 1,680 ppm (*M. musculus*); 0, 17, 83, 250, 750, 1,250, and 2,500 ppm (*R. novergicus*); 0, 12, 100, 500, 1,000, and 5,000 ppm (*Syrian hamsters*)	Increase of mice liver weith	XM: CYP450; peroxissome proliferation AM: CAT	Ozaki *et al.* (2001)[57]
Mus musculus	Active ingredient	AR: feeding T: 6 days C: 1.680 ppm	NA	ND: c-myc gene	Ge *et al.* (2002)[58]
Mus musculus	Active ingredient	AR: Intraperitoneally T: 55 days C: 3.8 mg/kg bw	NA	EM: LDH, MDH	Yilmaz and Yuksel (2005)[59]

Biological model	Exposure compounds	Exposure conditions	Cellular and tissues damage	Impaired biochemical markers	References
Rattus novergicus	not specified	AR: drink water T: 25 day C: 50 and 100 ppm	NA	AM: SOD, GSH, GR, MDA EM: LDH, creatine kinase LF: AST XM: GSH	Celik *et al.* (2006)[60]
Rattus novergicus	Active ingredient	AR: Feed and drink water T: 30 days C: 25 ppm and 50 ppm (water) and 50 ppm and 100 ppm (food)	No hepatic damage was observed, but the level of 2,4-D in the liver was found to be significantly higher in both the feed and water groups compared to the control group.	NA	Aydin *et al.* (2006)[61]
Rattus novergicus	Active ingredient	AR: drink water T: 21 days C: 600 ppm or 126 mg/kg	Vascular congestion, cytoplasmic vacuolization, and mononuclear cells' infiltration	AM: SOD, CAT, GPx, MDA LF: AST, ALT, ALP, γ-glutamyl transpeptidase EM: LDH	Troudi *et al.* (2012)[34]

Biological model	Exposure compounds	Exposure conditions	Cellular and tissues damage	Impaired biochemical markers	References
Rattus novergicus	Commercial formulation (600 g/L)	AR: oral gavage T: 4 weeks C: 5 mg/ kg/ bw	NA	AM: SOD, CAT, GPx, GR, MDA LF: AST, ALT, ALP, γ-GGT, total bilirubin. LM: change of fatty acid composition	Nakbi. et al (2010)[62]
Rattus novergicus	Commercial formulation (600 g/L)	AR: oral gavage T: 4 weeks C: 15, 75 and 150 mg/kg of body weight	Body weight decreased and the liver weight increased significantly .2,4-D induced hepatic cord disruption, focal necrosis, vessel dilation and pycnotic nucleus	LF: AST, ALT, ALP, γ-GGT AM: CAT, GR	Tayeb *et al.* (2010)[63]
Rattus novergicus	Commercial formulation (600 g/L)	AR: oral gavage T: 4 weeks C: 5 mg/kg of body weight/ day	Vascular congestion and wide sinusoidal spaces and a necrotic	AM: SOD, CAT, GPx, MDA LF: AST, ALT LM: low density lipoprotein, cholesterol	Nakbi *et al.* (2012)[64]

Biological model	Exposure compounds	Exposure conditions	Cellular and tissues damage	Impaired biochemical markers	References
Rattus novergicus	Commercial formulation (600 g/L)	AR: oral gavage T: 28 days C: 15, 75 and 150 mg/kg/bw/day	NA	AM: SOD, CAT, GPx, GR, MDA LM: change of fatty acid composition	Tayeb *et al.* (2013)[65]
Rattus novergicus	not specified	AR: feeding T: 16 weeks C: 200 mg/kg/day	2,4-D acid iso-octylester caused the formation of atypical cell foci (ACF) in the pancreata and livers of rats.	NA	Kalipici *et al.* (2013)[66]
Rattus novergicus	Active ingredient (≥ 90%)	AR: oral gavage T: 19 days C: 100 mg/kg of body weight	NA	AM: CAT, MDA, total antioxidant capacity	Mazhar. *et al.* (2014)[67]

Biological model	Exposure compounds	Exposure conditions	Cellular and tissues damage	Impaired biochemical markers	References
Rattus novergicus	Commercial formulation	AR: oral T: 28 days C: 75 or 150 mg/kg of body weight	2,4-D. increased liver weight and induced nuclear changes in liver cells, including alterations in size and shape, irregularity, and slight distention of nuclear envelope, Hepatic nuclei exhibited varying degrees of pyknosis, disaggregation and apoptosis.	LF: AST, ALT, ALP, total bilirubin AM: GR, SOD EM: LDH	Al-Baroudi *et al.* (2014)[68]
Rattus novergicus	Commercial formulation	AR: oral gavage T: 24 h (single dose) C: 639 mg/kg of body weight	NA	AM: hydroperoxyl and carbonyl lipids EM: glycogen	Dakhakhni *et al.* (2016)[69]
Mus musculus	Active ingredient	AR: oral T: 45 days C: 30, 60, 90 mg/kg/day	Vascular and hepatocellular lesions with necrotic changes and focal areas of necrosis in the liver	AM: GSH, SOD, CAT, GPx, GR, GST and total –SH EM: ATP and SDH XM: GSH and GST	Satapathy and Rao (2018)[70]

Biological model	Exposure compounds	Exposure conditions	Cellular and tissues damage	Impaired biochemical markers	References
Rattus novergicus	Active ingredient	AR: oral gavage T: 4 weeks C: 150 mg/Kg/day	NA	AM: SOD, CAT, GSH, MDA LF: AST, ALT XM: GSH ND: Urea and creatinine	Shafeeq and Mahboob (2020)[71]
Rattus novergicus	Commercial formulation (806 g/L)	AR: inhalation and feed T: 6 months C: 3.71/6.19 and 9.28×10^{-3} g a.i./ha	The groups exposed to oral 2,4-D had a higher incidence of steatosis, and exposed to high doses had increased liver inflammation.	LF: ALT	Bonfim et al (2020)[72]
Rattus novergicus	Commercial formulation (600 g/L)	AR: oral gavage T: 4 weeks C: 5 mg/kg/b.w./day	Rat livers shown perivascular inflammatory infiltration around the vessel, sinusoidal dilatation and vacuolization of hepatocytes	AM: SOD, CAT, GSH, GPx, GST, MDA LF: AST, ALT, ALP, total bilirubin EM: LDH XM: GST, GSH	Tichati *et al.* (2020)[32]

Biological model	Exposure compounds	Exposure conditions	Cellular and tissues damage	Impaired biochemical markers	References
Rattus novergicus	Active ingredient (> 98%)	AR: cannulation of portal and cava veins liver T: 20 min. C: 10 – 400 µM	Membrane lipid bilayer deformity	EM: NADH, NAD^+ , lactate, glycolisis, gluconeogenesis	Salla *et al.* (2019)[73]
Rattus novergicus	Active ingredient	AR: oral gavage T: 4 weeks C: 150 mg/Kg/day	NA	AM: SOD, CAT, GSH, MDA LF: AST, ALT, ALP XM: GSH ND: urea and creatinine	Shafeeq and Mahboob (2021)[74]
Rattus novergicus	Commercial formulation (600 g/L)	AR: oral gavage T: 30 days C: 5 mg/kg/b.w	2,4-D increases relative and absolute liver weights. Furthermore, 2,4-D induces severe infiltration of mononuclear inflammatory cells with vacuolar degeneration around a dilated central lobular vein, congestion of the hepatic sinusoids, and degenerative hepatocytes with largely vacuolated cytoplasm and a large number of lipid droplets.	AM: SOD, CAT, GPx, GST, MDA, carbonyl proteins LF: AST, ALT, ALP, γ-GGT EM: LDH XM: GST, GSH	Tichati *et al.* (2021)[33]

Biological model	Exposure compounds	Exposure conditions	Cellular and tissues damage	Impaired biochemical markers	References
Rattus novergicus	Commercial formulation (480 g/L)	AR: oral T: 60 days C: 5 mg/kg of body weight	In the liver tissue of rats, focal areas of mononuclear cell infiltration in the pericentral and periacinal region, sinusoidal dilatation, and hyperemia in the vessels and areas of pyknosis and parenchymal degeneration in the nuclei of hepatocytes were determined	LF: AST, ALT, ALP AM: SOD, GSH, CAT, MDA XM: GSH ND: NF-κB, COX-2, TNF-α, MCP-I, TGFβI, and CYP2E P53, Bax/Bcl-2, caspase-3, caspase-8, caspase-9, and PARP	Sinan Ince *et al.* (2022)[75]
Rattus novergicus	2,4-D, gliphosate and dicamba (not specified)	AR: drink water T: 90 days C: gliphosate (0.5 mg/kg bw/day) + 2,4-D (0.3 mg/kg bw/day) + dicamba (0.02 mg/kg bw/ day)	NA	AM: GSH and MDA	Nechalioti *et al.* (2023)[76]
Ictalurus punctatus	Active ingredient 2,4-D (>99%) Picloram (>99%)	AR: water expossure T: 10 days C: 22.5, 7.5, and 2.25 mg/L	NA	XM: ethoxyresorufin 0-deethylase	Gallagher and Digiulio (1991)[77]

Biological model	Exposure compounds	Exposure conditions	Cellular and tissues damage	Impaired biochemical markers	References
Cyprinus carpio	Active ingredient (>98%)	AR: water exposure T: 96 h and 14 days C: 310, 295 and 270 mg/L (96 h) 150, 200, and 250 mg/L (14 days)	Hepatocycites shown slight vacuolar degeneration and pycnotic nuclei (some of them displaced)	LF: AST, ALT	Neskovic *et al.* (1994)[78]
Oreochromis niloticus	Commercial formulation (500 g/L)	AR: water exposure T: 96 h C: 27 ppm	NA	AM: SOD, GPx, GR EM: *glucose-6-phosphate dehydrogenase*	Oruç. and Uner (2000)[79]
Fundulus heteroclitus	not specified	AR: water expossure T: 21 days C: 0.04, 0.41, and 4.1 μM	NA	ND: peroxissome proliferation	Ackers *et al.* (2000)[80]
Cyprinus carpio	Commercial formulation (500 g/L)	AR: water exposure T: 96 h C: 87 ppm	NA	AM: GST, SOD EM: G6PD XM*:* GST	Oruç and Uner (2002)[81]

Biological model	Exposure compounds	Exposure conditions	Cellular and tissues damage	Impaired biochemical markers	References
Leporinus obtusidens	Commercial formulation (868 g/L)	AR: water exposure T: 96 h C: 1 and 10 mg/L	NA	EM: glycogen, lactate, glucose	Fonseca *et al.* (2008)[82]
Rhamdia quelen	Commercial formulation (720 g/L)	AR: water exposure T: 96 h C: 0, 400, 600 and 700 mg/L	Hepatocytes vacualization and changes in its arrangement cords	EM: glycogen,lactate, glucose	Cattaneo *et al.* (2008)[83]
Carassius auratus	Active ingredient	AR: water exposure T: 90 h C: 1, 10 and 100 mg/L	NA	AM: carbonyl proteins, lipid peroxidases LM: lipid peroxidases	Matviishyn *et al.* (2014)[84]

Biological model	Exposure compounds	Exposure conditions	Cellular and tissues damage	Impaired biochemical markers	References
Poecilia vivipara	Commercial formulation (868g/L)	AR: water exposure T: 48 h C: 10,20 and 40µl	Swollen nuclei and cytoplasmic vacuolization. Finally, the 40 µl/L group presented blood vessel alterations indicating vasodilatation, hepatocytes with swollen nuclei, Ito cells, and micronuclei.	NA	Vigário and Sabóia-Morais (2014)[85]
Rhamdia quelen	Commercial formulation (720 g/L)	AR: water exposure T: 90 days C: 0.5 and 2 mg/L	NA	AM: CAT, MDA EM: glycogen; lactate, glucose	Menezes. *et al.* (2015)[86]
Cyprinus carpio L	not specified	A.R.: water exposure T: --- C: 0.2 mg/dm^3	NA	EM: ICDH, LDH, G6PD	Yakovenko *et al.* (2018)[87]
Capoeta capoeta	not specified	AR: water expossure T: 7 days C: 10 and 20 mg/L	NA	AM: plasma oxidative status index LF: AST	Kaya *et al.* (2018)[88]

Biological model	Exposure compounds	Exposure conditions	Cellular and tissues damage	Impaired biochemical markers	References
Danio rerio	Active ingredient (> 97%)	AR: water exposure T: 48 h C: 2.5, 5 and 10 mg/L	Hepatocytes had heterogeneous eosiniphilic, cytosol vacualization and cell nucleus were eccentric, Loss of cell boundaries and liver with necrotic appearence, Release of cytosolic content among adjacent cells	LF: AST, ALT, ALP AM: CAT, GST XM: GST EM: LDH	Martins *et al.* (2021)[4]
Triturus cristatus carnifex	Commercial formulation (37% of 2,4-D as iso-octylic ester)	AR: water exposure T: 3 months C: 25, 50, 75, 100, 125, and 150 ppm	Vacuolar degeneration of liver parenchyma and necrosis of kidney tubules	NA	Zaffaroni *et al.* (1986)[89]
Lithobates clamitans	Active ingredient (>98%)	AR: soil exposition T: 2 days C: 14.3 µg/cm²	NA	NA	Van Meter *et al.* (2018)[90]

Biological model	Exposure compounds	Exposure conditions	Cellular and tissues damage	Impaired biochemical markers	References
Physalaemus albonotatus	Commercial formulation) (48.5% w/v of active ingredient)	AR: water exposure T: 96 h (acute) and 49 days (chronic) C: 350, 700, 1400, and 2400 mg/L(acute); 43.7, 87.5, 175 or 262.5 mg/L (chronic)	The liver of treated tadpoles showed enlargement of hepatic sinu- soids , hypervascularization, dilation of blood vessels, and vacuolization of hepatocytes	NA	Curi *et al.* (2019)[91]

Abbreviations. (AR) administration route; (T) time; (C) concentrations; (AM) antioxidant metabolism; (EM) energetic metabolism; (LF) liver function; (LM) lipid metabolism; (XM) xenobiotic metabolism; (ND) Not determined; (NA) no analysed; (NS) not specified; (---) information not informed by the authors. Abbreviations. (AR) administration route; (T) time; (C) concentrations; (AM) antioxidant metabolism; (EM) energetic metabolism; (LF) liver function; (LM) lipid metabolism; (XM) xenobiotic metabolism; (ND) Not determined; (NA) no analysed; (NS) not specified; (CAT) catalase; (GST) glutathione S-transferase; (GPx) glutathione peroxidase; (CrAT) carnitine acetyltransferase; (EH) epoxide hydrolases; (GR) glutathione reductase; (ALT) alanine aminotransferase; (AST) aspartate aminotransferase; (ALP) alcaline phosphatase; (CYP450) cytochrome P450; (LDH) lactate dehydrogenase; (MDH) malate dehydrogenase; (SOD) superoxide dismutase; (GSH) reduced glutathione; (MDA) malondialdehyde; (γ-GGT) gamma-glutamyltransferase; (SDH) succinate dehydrogenase; (G6PD) glicose-6-fosfato desidrogenase; (IDH) isocitrate dehydrogenase.

Table 2 Studies of the hepatotoxicity of 2,4-dichlorophenoxiacetic acid (2,4-D) in *in vitro* biological models.

Biological model	**Exposure compounds**	**Exposure conditions**	**Impaired biochemical markers**	**References**
Liver GST of *Rattus novergicus*	Active ingredient	AR.: enzyme kinetics T: --- C:---	AM: GST XM: GST	Dierickx (1983)[92]
Liver GST of *Rattus novergicus*	Active ingredient (>99%)	AR: enzyme kinetics T: --- C: 2 -12 mM	XM: GST AM: GST	Vessey and Boyer (1984)[93]
Liver GST of *Salmo gairdneri*	Active ingredient	AR: enzyme kinetics T: --- C: 2 mM	AM: GST XM: GST	Dierick (1985)[94]
Liver GST of *Homo sapiens* (autopsy)	Active ingredient (>97%)	AR: --- T: --- C: ---	AM: GST XM: GST	Singh (1985)[95]
Liver GST of *Cyprinus carpio*	not specified	AR: cell culture T: --- C: ---	AM: GST XM: GST	Elia *et al.* (2000)[96]
Liver GST of *Rattus novergicus*	not specified	AR: --- T: --- C: ---	AM: GST XM: GST	Dierickx (1988)[97]

Biological model	Exposure compounds	Exposure conditions	Impaired biochemical markers	References
Liver GST of *Chalcalburnus tarichii Pallas*	Active ingredient	AR.: --- T: --- C: 0.6, 0.23 and 0.57 mM	AM: GST XM: GST	Özaslan *et al.* (2018)[98]
Liver mitochondria of *Rattus novergicus*	Active ingredient	AR.: cell culture T: --- C: 0, 0.2, 0.5, 1.0, and 2 mM.	LM: palmitoyl CoA hydrolase , fatty acyl CoA EM: mitochondrial dysfunction	Dixon *et al.* (1990)[99]
Liver mitochondria of *Rattus novergicus*	not specified	AR: cell culture T: --- C: 0.1 - 4.0 mM	EM: mitochondrial dysfunction	Zychlinski and Zolnierowicz (1990)[100]
Liver mitochondria of *Rattus novergicus*	Active ingredient	AR: cell culture T: --- C: 100, 200, 300, 400, 500, 600, 700 and 800 µM	EM: SDH, cytochrome c reductase, mitochondrial dysfunction	Palmeira *et al.* (1994)[101]
Liver mitochondria of *Rattus novergicus*	Commercial formulation (2,4-D 1.08 M + Picloram 0.265 M)	AR: cell culture T: --- C: 66.2 nmol picloram + 270 nmol 2,4-D mg^{-1} protein	EM: NADH oxidase, NADH cytochrome c reductase, ATP, mitochondrial dysfunction	Pereira *et al.* (1994)[102]
Liver mitochondria of *Rattus novergicus*	Commercial formulation. Tordon (2,4-D 300 g/L + picloram 75 g/L)	AR.: cell culture T: --- C: ---	EM: mitochondrial dysfunction	Oakes and Pollak (1999)[103]

Biological model	Exposure compounds	Exposure conditions	Impaired biochemical markers	References
Liver *Rattus novergicus* mitochondria	Active ingredient (>98%)	AR: injections T: 30 days C: 70 mg/kg of body weight	EM: mitochondrial dysfunction	Di Paolo *et al.* (2001)[56]
Hepatocytes of *Rattus novergicus*	Active ingredient	AR: cell culture T: --- C: 1-10 mM	EM: LDH, ATP, ADP, AMP, NADH, NAD^+ AM: GSH, GSSG XM: GSH, GSSG	Palmeira *et al.* (1994)[104]
Hepatocytes of *Rattus novergicus*	Active ingredient (> 98%)	AR: cell culture T: 200 min C: 1, 5 and 10 mM	AM: MDA, proteins thiol, GSH XM: GSH	Palmeira *et al.* (1995)[105]
Hepatocytes of *Rattus novergicus*	Active ingredient	AR: cell culture ET: 3 months C.T: 1 mM	NA	Li *et al.* (2003)[106]
Hepatocytes of *Metynnis roosevelti*	Active ingredient	AR: cell culture T: --- C: 0.275, 2.75 and 27.5 mg/L	EM: mitochondrial dysfunction	Salvo *et al.* (2015)[107]
HepG2 cells	Active ingredient	AR: cell culture T: 48 h C: 4, 8 and 16 mM	EM: mitochondrial dysfunction ND: Cell cicle alterations, apoptose, DNA damage	Tuschl and Schwab (2003)[108]
HepG2 cells	Active ingredient	AR: cell culture T: 48 h C: 8, 14 and 16 mM	ND: Cell cycle alterations, apoptosis, DNA damage	Tuschl and Schwab (2004)[109]

Biological model	Exposure compounds	Exposure conditions	Impaired biochemical markers	References
HepG2 cells	Commercial formulation	AR: cell culture T: --- C: 0.1 nM to 4 mM	ND: Genes involved to stress response, cell cycle control, immunological and DNA repair genes. (FTH1, FTL, PCNA, DCLRE1C, TCLK1, JM11, VEGF, USP19, DDB2, IL1RL1, PTGER3 and GTF2A.	Bharadwaj *et al.* (2005)[110]
HepG2 cell	Active ingredient (>90%)	AR.: cell culture T: --- C: 0.001 - 0.1 mM	NA	Barrón Cuenca *et al.* (2022)[111]
Liver homogenates of *Rattus novergicus*	Active ingredient	AR: cell culture T: --- C: ---	LM: cholesterol	Olson *et al.* (1974)[112]
Chicken embryo	Commercial formulation (37%)	AR.: injected into the air cell of the eggs T: 19 days C: 1, 2 and 4 mg/egg	XM: ethoxycoumarin O-deethylase, GST AM: GST	Santagostino *et al.* (1991)[113]
Chicken Liver	Commercial formulation (31.6% w/v)	AR: Fertilized eggs were externally treated T: 21 days C: 3.1 mg	EM: G6Pase LM: total lipids AM: CAT	Duffard *et al.* (1993)[114]

Abbreviations. (AR) administration route; (T) time; (C) concentrations; (AM) antioxidant metabolism; (EM) energetic metabolism; (LF) liver function; (LM) lipid metabolism; (XM) xenobiotic metabolism; (ND) Not determined; (NA) no analysed; (NS) not

specified; (---) information not informed by the authors. Abbreviations. (AR) administration route; (T) time; (C) concentrations; (AM) antioxidant metabolism; (EM) energetic metabolism; (LF) liver function; (LM) lipid metabolism; (XM) xenobiotic metabolism; (ND) Not determined; (NA) no analysed; (NS) not specified; (CAT) catalase; (GST) glutathione S-transferase; (G6Pase) glucose 6-phosphatase; (LDH) lactate dehydrogenase; (GSH) reduced glutathione; (MDA) malondialdehyde; (SDH) succinate dehydrogenase

The toxicity biomarkers identified were grouped based on their relationship to different aspects of liver physiology[115–117]. The categories were: antioxidant metabolism (AM), energetic metabolism (EM), lipid metabolism (LM), liver function (LF), and xenobiotic metabolism (XM). The biomarkers grouped in the LF category are utilized in both clinical diagnosis and research to investigate liver damage and function, including AST, ALT, and ALP[118]. Effects that were not directly related to any specific category were allocated to "not determined" (ND). Markers related to more than one category were placed in both groups (e.g., glutathione S-transferase and glutathione were allocated in both AM and XM). After this classification, it was possible to determine which categories were evaluated by each article in the review and identify the toxicity markers that appeared most frequently in the studies. Additionally, eight studies were identified containing information on the hepatotoxic effects of 2,4-D in association with other agrochemicals, and eight studies focused on hepatoprotection against damage induced by the herbicide.

3. Results and discussion

3.1. Historical review and geographic distribution

The article published by Olson *et al.* (1974) was the oldest study on the hepatotoxicity of 2,4-D[112]. Since then, a significant number of studies have been published (Figure 2a). It is noteworthy that approximately 55% (n=46) of the articles in this review were published prior to the year 2000. In part, the high number of older studies can be explained by the fact that 2,4-D was the first synthetic herbicide to be developed (in the 1940s) and its worldwide use in agriculture, which sparked the interest of research groups in studying its effects on non-target organisms[1]. In addition to its use in agriculture, the fact that 2,4-D is one of the components of Agent Orange, a defoliant

widely used during the Vietnam War, may have also contributed to the significant number of studies conducted during that period[3].

The studies identified in the review were conducted by research groups from 23 countries, most notably the USA (n=17; 20%), Brazil (n=11; 13%) and Turkey (n=9; 11%) (Figure 2b). In both countries, agriculture plays a significant economic role, and 2,4-D is widely commercialized[14,17].

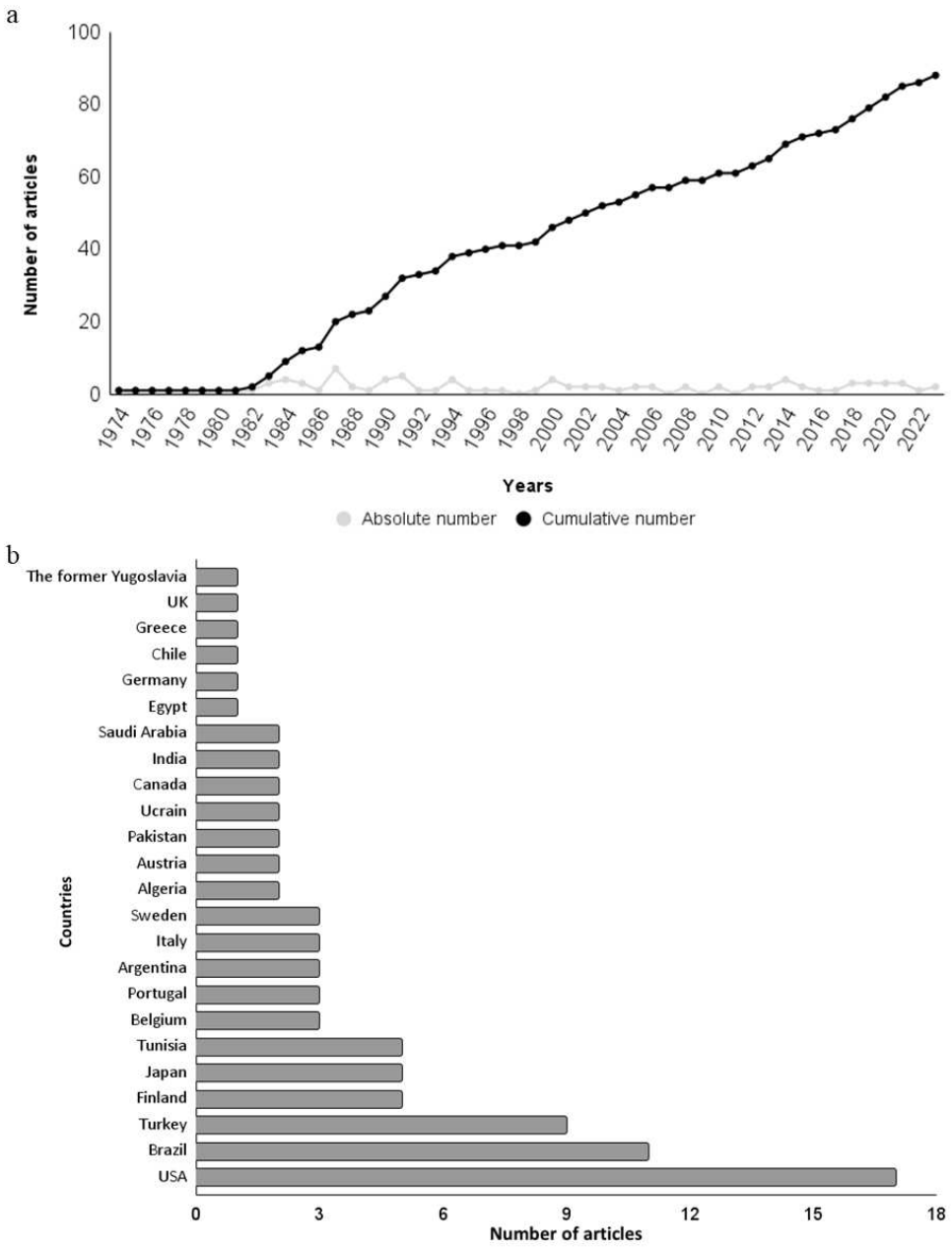

Figure 2. Bibliometric data of articles on the 2,4-D herbicide induced hepatotoxicity. a Absolute and cumulative number of articles over the years. b Number of articles per Country.

3.2. Chemical compounds

In the toxicity assays of the selected studies, 2,4-D was used either in its pure form (n=40; 48%) or as a commercial formulation containing it as the active ingredient (n=29; 35%). Articles that did not specify the origin of the substance used in the exposure assays were classified as "not specified" (n=14; 17%) (Figure 3a).

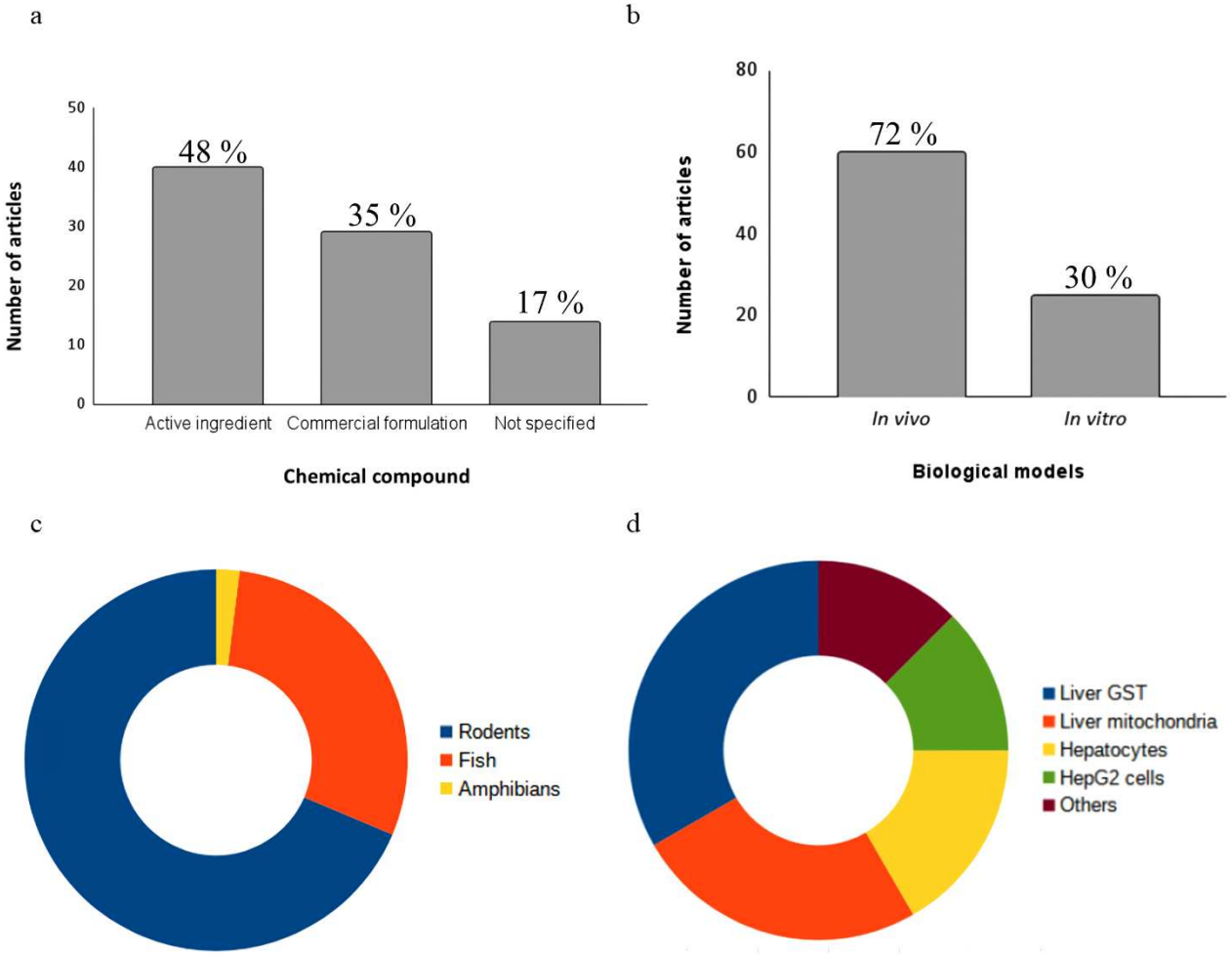

Figure 3. (a) Types of 2,4-D formulation used in hepatotoxicity studies (b) across in vivo and in vitro models. (c) types of in vivo models used and (d) types of in vitro models used.

Désormone Lourd (600 g/L), U46D-Fluid (868 g/L), Vesakontuho tasku (500 g/kg), and Tordon 75D® (300g/L 2,4-D + 75 g/L picloram) are examples of 2,4-D-based commercial formulations used in the studies of this review. Commercial formulations are cocktails containing one or more active ingredients and other substances known as inert or adjuvant ingredients (e.g., surfactants, solvents, and preservatives). These substances serve to improve the dissolution, stability, absorption, and pesticidal action of the active

ingredient[119]. However, adjuvants can have biological activity and influence the toxicity of the active ingredient[120]. This makes it difficult to compare experimental data since different formulations vary in the composition and concentration of these compounds[119]. Furthermore, among the analyzed studies, only one conducted a comparative analysis of the hepatotoxic effects of the active ingredients of the herbicide (Tordon 75D®) and its inert ingredients[103]. Comparative studies are essential for evaluating differences in toxicity among different 2,4-D formulations, including the pure herbicide, and identifying variations in toxic effects due to adjuvants[120]. This highlights the lack of such studies in the literature, which could provide important information for establishing safe limits for these compounds in the environment.

3.3.Biological models

Approximately 72% (n=60) of studies used *in vivo* biological models, while around 30% (n=25) used *in vitro* models (Figure 3b). Only the study by Di Paolo *et al.* (2001) employed both approaches[56]. *In vivo* models have advantages in hepatotoxicity studies compared to in vitro models because they consider the interactions between different liver cell types, as well as the influence of systemic factors[121]. Revised results showed that further studies using Organs-on-chips (OoCs) and Body-on-a-chip (BoC) platforms are needed, since these methodologies create the environments that recapitulate one or more tissue-specific functions[122].

Regarding the *in vivo* models, 68% (n=41) were rodents, 27% (n=16) were fish, and 5% (n=3) were amphibians (Figure 3c). Among these, 18 different species were identified, with *Rattus norvegicus* and *Mus musculus* being the notable ones (Table 1). Rodents are widely used in hepatotoxicity studies due to their high morphophysiological, biochemical, and genetic homology with humans, including liver metabolism[123]. Fish, such as *Poecilia vivipara*, *Cyprinus carpio* and *Rhandia quelen* are organisms sensitive to changes in environmental parameters and directly affected by the presence of agrochemicals in aquatic bodies[124]. Figure 3d depicts in vitro biological models. Among them, the most commonly used were the inibithion assay of isolated hepatic glutathione S-transferase (GST) (n=7, 28%). Isolated liver mitochondria from R. norvegicus were also used as a model (n=6, 24%), along with hepatocyte cultures (n=4, 16%) and HepG2 cells (n=4, 16%). The remaining studies utilized liver and chicken

embryo and were categorized as "other" (n=2, 8%). More information about the in vitro biological models can be found in Table 2.

3.4. Morphological markers

The liver is composed of different cell types, such as hepatocytes, Kupffer cells, stellate cells, and hepatic sinusoidal endothelial cells[125]. The composition and organization of these cells in the organ vary according to the species, but in general, hepatocytes are more abundant and perform many of the hepatic functions[126].

Data collected in this review show that 2,4-D causes various impacts on liver tissue. Macroscopically, exposure to 2,4-D induces hepatomegaly in rodents. Male rats treated with 150 mg/kg of Désormone Lourd (600 g/L 2,4-D) for 4 weeks showed approximately a 43% increase in absolute organ weight compared to the negative control[63]. At the cellular and tissue level, histopathological analyses were predominant in identifying damages in the reviewed articles. Rats treated with 15 mg/kg of Désormone Lourd (600 g/L 2,4-D) for 4 weeks exhibited cellular death indicated by the formation of pyknotic nuclei and focal necrosis[63]. Additionally, 5 mg/kg of the same commercial formulation induced perivascular inflammatory infiltration in the liver of rats, indicating the presence of immune system cells and other components involved in the inflammatory response[32]. In addition to inflammatory effects, dietary exposure to 2,4-D has been previously associated with a high incidence of hepatic steatosis in rats[72]. It is important to emphasize that the mentioned morphological changes are associated with a decrease in hepatic antioxidant function, indicated by the reduced activity of antioxidant enzymes such as superoxide dismutase (SOD), catalase (CAT), glutathione S-transferase (GST), glutathione peroxidase (GPx), and hepatic GSH levels[32,63]. Morphological damages can also contribute to hepatobiliary disorders. Tichati *et al.* (2020) shown an increase in alkaline phosphatase (ALP) activity and total bilirubin levels, which are used as indicators of biliary flow dysfunction[32]. Furthermore, obstruction of the bile ducts can lead to the accumulation of bile salts in the liver, exposing hepatocytes to toxic concentrations of bile acids and enhancing hepatic injuries[127].

Other histopathological changes frequently observed after exposure to 2,4-D include hepatocyte vacuolization and deterioration of liver tissue structure. Cattaneo *et al.* (2008) identified these effects in the liver of *R. quelen* after exposure to 700 mg/L of U46D-Fluid (868 g/L 2,4-D) for 96 hours[83]. Similar effects were found in the liver of

zebrafish larvae at 120 hours post-fertilization (hpf) exposed to pure 2,4-D (> 97%) at 2.5, 5, and 10 mg/L[4].

The morphological changes founded by Cattaneo *et al.* (2008) were accompanied by an impairment in liver energetic function, as evidenced by blood glucose alterations and a decrease in hepatic glycogen level[83]. These effects are commonly associated with disruptions in gluconeogenesis and glycogenolysis pathways, which play a crucial role in maintaining blood glucose levels [63,128]. Moreover, an increase in hepatic lactate dehydrogenase (LDH) activity was observed, suggesting enhanced anaerobic glucose metabolism, possibly attributed to tissue damage and reduced oxygen availability[83].

3.5. Toxicity biomarkers

3.5.1. Antioxidant metabolism

Toxicity biomarkers associated with antioxidant metabolism and oxidative stress were the most frequent, reported in 49% (n=41) of the reviewed articles (Figure 4a). Free radicals, such as reactive oxygen species (ROS) and reactive nitrogen species (RNS), are natural byproducts of cellular aerobic metabolism[129]. However, when the production of free radicals exceeds the antioxidant capacity of the organism and reaches high concentrations, oxidative stress occurs, resulting in oxidative damage to cellular macromolecules, such as proteins, lipids, and nucleic acids[35,130].

The decrease in antioxidant capacity was mainly shown by the reduction in the activity of hepatic antioxidant enzymes, such as superoxide dismutase (SOD), catalase (CAT), glutathione S-transferase (GST), glutathione peroxidase (GPx), and glutathione reductase (GR)[62,64,75]. Among them, CAT (n=19, 46%), GST (n=16, 39%), and SOD (n= 13, 31%) were the most frequently reported in the articles that investigated markers related to the antioxidant response. (Figure 4b). SOD is responsible for converting the superoxide radical (O_2-) into a less reactive form, hydrogen peroxide (H_2O_2), while CAT decomposes H_2O_2 into water and oxygen[131]. GST, GPx, and GR are involved in the regulation and metabolism of glutathione (GSH), a crucial non-enzymatic antioxidant involved in neutralizing free radicals and eliminating endogenous and exogenous toxic compounds from the body[132].

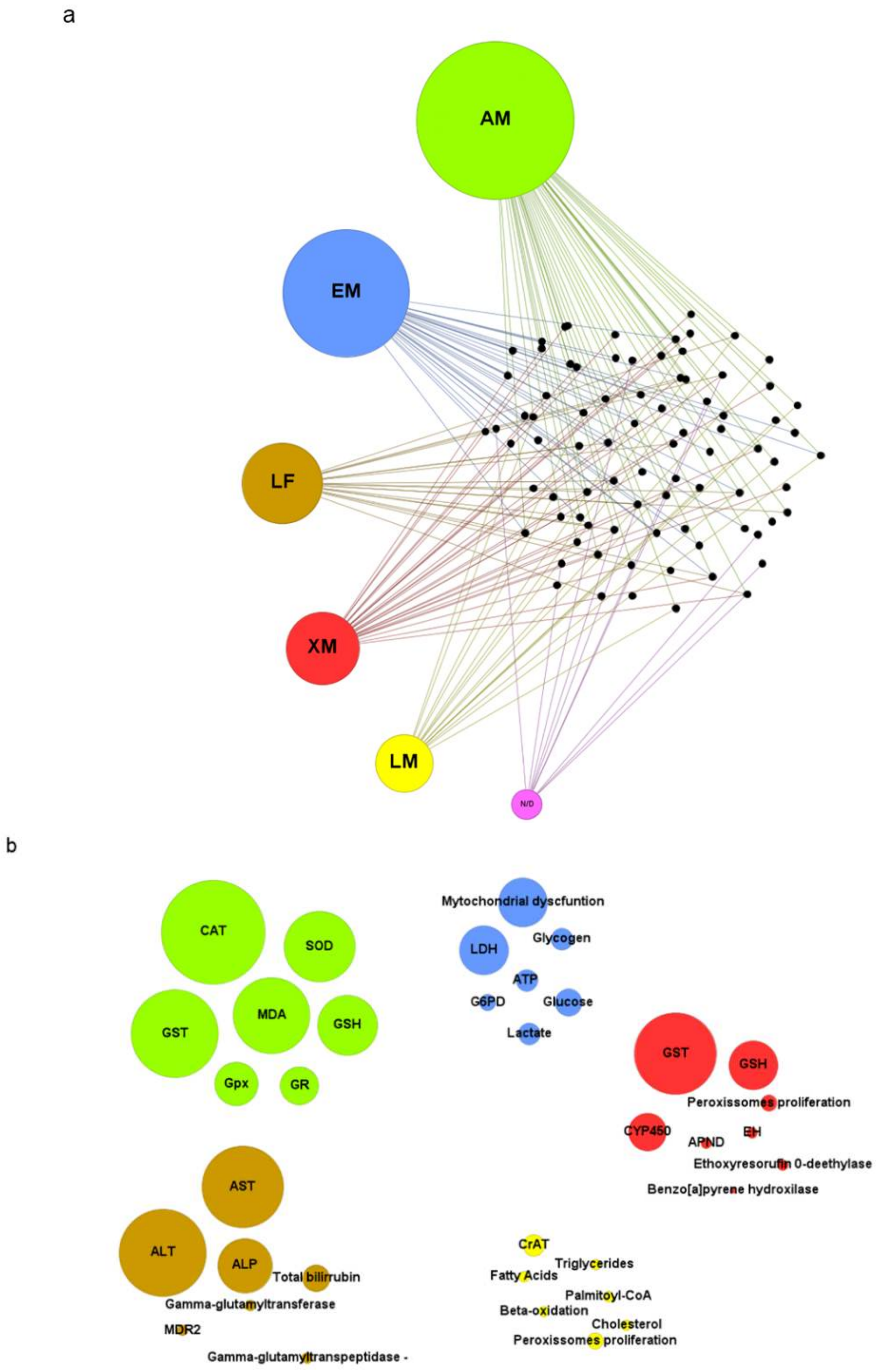

Figure 4. (a)Selected articles in the review (small black dots) and the hepatic functions that were affected: antioxidant metabolism (AM), energetic metabolism (EM), liver function (LF), lipid metabolism (LM), xenobiotic metabolism (XM) and not determined (ND). (b) The top-seven disturbed biochemical markers for each hepatic function. Size circles correspond to the number of occurrences in the articles. Abbreviations: catalase (CAT), Superoxide dismutase (SOD), glutathione S-transferase (GST), malondialdeíde (MDA), glutathione peroxidase (GPx), reduced glutathione (GSH), glutathione reductase (GR). Lactate dehydrogenase (LDH), glucose 6 phosphate dehydrogenase (G6PD). alanine aminotransferase (ALT), aspartate aminotransferase (AST), alkaline phosphatase (ALP), multidrug resistance protein 2 gene (MDR2). GST, cytochrome p450 enzymes (CYP450), epoxide hydrolases (EH), amidopyrine N-demethylase (APND). Carnitine acetyltransferase (CrAT).

Exposure to 2,4-D also leads to depletion of GSH levels in the liver, contributing to the decrease in antioxidant capacity[71,119]. This effect was observed in rats receiving doses of 5 mg/kg of Désormone Lourd (600 g/L 2,4-D) for 4 weeks, resulting in a decrease in hepatic GSH levels and the activity of SOD, CAT, GPx, and GST[33]. Toxicity studies conducted with the active ingredient in rats identified similar results, further supporting that this effect is attributed to the active ingredient[71,74].

The decrease in antioxidant response and induction of an oxidative stress state lead to cellular and tissue damage. This is evidenced by the increase in MDA levels, an effect frequently reported in the articles (n=14, 34%)[34,60]. This alteration indicates the oxidative degradation of lipids (LPO) induced by 2,4-D. MDA is a product of lipid peroxidation, especially of polyunsaturated fatty acids, and is considered a common marker of oxidative stress and oxidative damage to lipids and cell membranes[34]. Hepatic cells are particularly vulnerable to oxidative stress from various toxic agents as the liver serves as the primary site for drug metabolism[35]. Furthermore, oxidative stress plays a crucial role in the progression of liver diseases induced by toxic chemical compounds, such as Nonalcoholic Fatty Liver Disease (NAFLD)[129]. These data suggest that oxidative stress plays an important role in the progression of 2,4-D-induced hepatotoxicity.

3.5.2. Energetic metabolism

The analyzed articles demonstrate that markers associated with energetic metabolism are disrupted following exposure to 2,4-D and were reported in 36% (n=30) of the studies (Figure 4a). Among them, alterations associated with mitochondrial dysfunction were frequent (n=9, 30%) (Figure 4b). 2,4-D can inhibit the activity of mitochondrial enzymes and cause a depletion in cellular ATP levels, compromising the availability of energy required for proper functioning of the hepatic cells[102,104]. Isolated liver mitochondria treated with 600 μM of 2,4-D showed inhibition of complex III (cytochrome c reductase)[104]. Additionally, complex I (NADH cytochrome c reductase) was also inhibited in liver mitochondria exposed to 13.2 nmol/mg of the herbicide Tordon 2,4-D 64/240 triethanolamine BR[102]. This compromises the proton gradient across the mitochondrial inner membrane and impairs electron transfer necessary for ATP production during oxidative phosphorylation[133]. Furthermore, various studies in the literature report that the uncoupling of oxidative phosphorylation is a common mechanism of toxicity for chlorophenols[134–136]. The mitochondrial respiratory chain

represents the major source of intracellular ROS formation, with complexes I and III being the major sites of O_2- production[137,138]. Inhibition of these complexes results in an accumulation of superoxide-generating electron transport intermediates, enhances electron transfer to oxygen, and triggers excessive O_2- production[137,138]. This contributed to oxidative stress, depletion of antioxidant systems, and damage at cellular and tissue levels[137,138].

Lactate dehydrogenase (LDH) was a frequently disrupted biomarker (n=9, 30%) in articles related to energy metabolism (Figure 4b). LDH participates in energy production through anaerobic metabolism, and the increase in its activity may be associated with low oxygen availability and/or tissue injury[139,140]. Although LDH is not a specific marker of hepatotoxicity, the increase in its levels is related to liver disorders. Rats treated with 126 mg/kg of 2,4-D for approximately 21 days exhibited histopathological damage in the liver and a significant increase in LDH activity[34]. Two days of treatment with 2.5 mg/L of 2,4-D also caused this effect in zebrafish larvae at 120 hpf[4]. Furthermore, different analyzed articles reported that the increase in LDH activity is accompanied by a reduction in antioxidant enzyme activity and hepatic tissue damage[4,32–34]. This reinforces that oxidative stress plays a crucial role in the progression of 2,4-D-induced hepatotoxicity.

3.5.3. Lipid metabolism

2,4-D also has negative impacts on lipid metabolism, as reported in 18% (n=15) of the reviewed articles. The analyzed biomarkers indicate that 2,4-D induces an increase in fatty acid oxidation in the liver, as evidenced by the elevation in the activity of mitochondrial enzymes involved in the β-oxidation process[37,39,43]. Rats fed a diet containing 0.25% (w/w) of 2,4-D for seven days showed an increase in the activity of carnitine acetyltransferase (CrAT) and an elevation in the oxidation of palmitoyl-CoA[39]. CrAT catalyzes the reversible transfer of acetyl groups between acyl-coenzyme A and L-carnitine, a fundamental process for transporting short and medium-chain fatty acids into the mitochondria, where they are oxidized to generate energy[115,141]. Carnitine palmitoyltransferase, fatty acyl-CoA dehydrogenase, and acyl-CoA hydrolase II are also crucial mitochondrial enzymes for fatty acid oxidation, and their activity is increased by the herbicide[41,49]. 2,4-D also enhances peroxisomal β-oxidation of fatty acids[42,49]. Peroxisomes are organelles that house vital enzymes for a range of metabolic process, including fatty acid oxidation, phospholipid synthesis, and the

maintenance of cellular redox balance[142]. Fatty acid β-oxidation represents a pivotal peroxisomal function, being crucial for shortening the chains of very long-chain fatty acids that cannot be oxidized in mitochondria[142].

Peroxisomes and mitochondria are significant sources of ROS generation and maintain a close relationship with redox balance[143]. Peroxisomes serve as a major source of H_2O_2, generated through the activities of various FAD-dependent oxidoreductases involved in peroxisomal metabolic processes, including β-oxidation[144]. Although peroxisomes contain antioxidant enzymes such as catalase, imbalances in H_2O_2 levels can compromise antioxidant systems and contribute to oxidative stress[143,144]. Furthermore, disruptions in antioxidant mechanisms and peroxisomal β-oxidation can lead to mitochondrial oxidative stress in different organs, including the liver[144]. This underscores that the increase in fatty acid oxidation may be a significant factor in the generation of oxidative damage induced by exposure to 2,4-D.

3.5.4. Liver function

Liver markers are used to evaluate liver function and are particularly useful in detecting and monitoring injuries caused by various factors, including toxic chemical compounds. 2,4-D increased the levels of different liver markers, with aspartate aminotransferase (AST) and alanine aminotransferase (ALT) being the most recurrent among the analyzed articles (Figure 4b). The widespread usage of AST and ALT is due to the fact that the AST/ALT ratio is a well-established markers of liver damage[145]. The AST/ALT ratio is relevant because it is a parameter frequently used to assess liver health in both clinical diagnosis and research. Furthermore, its disturbance can indicate different hepatic conditions such as hepatitis, cirrhosis, or hepatic steatosis[118,146]. AST and ALT are enzymes involved in amino acid metabolism, catalyzing the conversion of aspartate and alanine to pyruvate, respectively[146]. Both enzymes are primarily found inside hepatocytes. When liver damage occurs, hepatocyte membranes are compromised, resulting in the release of these enzymes into the bloodstream[145,146]. This leads to an increase in AST and ALT activity and levels in the blood, making them sensitive markers of liver damage[145]. Shafeeq and Mahboob (2021) demonstrated that rats receiving 150 mg/kg/day of 2,4-D for 4 weeks showed increased levels of AST, ALT, and alkaline phosphatase (ALP)[74]. The increase in enzymatic activity of these three markers was also observed in zebrafish larvae at 120 hpf treated with 2.5 mg/L of 2,4-D for two days[4].

Alkaline phosphatase (ALP) was the third most mentioned marker of liver function in the analyzed studies. This enzyme is located in the membranes of the biliary canaliculi, structures responsible for bile transport in the liver. An increase in ALP levels indicates dysfunction or obstruction of the biliary flow, a condition that can be caused by liver damage and hepatobiliary disorders[145,147]. Additionally, an increase in total bilirubin levels was also induced by 2,4-D[32,62]. Bilirubin is metabolized by the liver and excreted in the bile, implying that any abnormality in this process can result in its accumulation in the blood[145].

3.5.5. Xenobiotic metabolism

Exposure to 2,4-D alters the activity of enzymes related to xenobiotic metabolism (Figure 4a). Among them, the most frequent marker are GST and GSH. GST plays an important role in the conjugation of xenobiotics with GSH molecules, resulting in the formation of water-soluble conjugates, facilitating their excretion from the body[132]. Additionally, 2,4-D also affects enzymes related to cytochrome P450 (CYP450)[45,57]. CYP450 is a family of enzymes, primarily present in the liver, responsible for the metabolism of a wide range of substances, including xenobiotics[116]. Different isoforms of CYP450 are involved in the metabolism of 2,4-D. Badawi *et al.* (2000) demonstrated that rats treated with a single dose of 2,4-D (375 mg/L) showed an increase in the expression of CYP1A1, CYP1A2, and CYP1B1 isoforms in the liver[55]. Furthermore, rats receiving doses of 1.6 and 2.9 mg/kg/bw of 2,4-D exhibited changes in the activity of CYP450 and the enzymes ethylmorphine N-demethylase and ethoxyresorufin O-deethylase, which are also part of the cytochrome P450 family[52]. Furthermore, the CYP-mediated metabolism can also produce ROS, in addition to bioactivated intermediates, leading to oxidative stress, particularly in the liver, and contributing to liver pathologys[148].

Exposure to 2,4-D also induces the proliferation of peroxisomes, organelles that contain a variety of oxidative enzymes important in xenobiotic metabolism[45,57]. Epoxide hydrolases are enzymes present in peroxisomes that are increased in activity by exposure to 2,4-D[38,45]. These enzymes function to convert epoxides, intermediates formed during oxidative metabolism by CYP450, into more stable and less reactive metabolites, contributing to the detoxification and elimination of the compound in the body[149]. Figure 5 depicts a schematic representation of the mechanisms underlying the 2,4-D-induced hepatotoxicity reported in section 3.6 of this study.

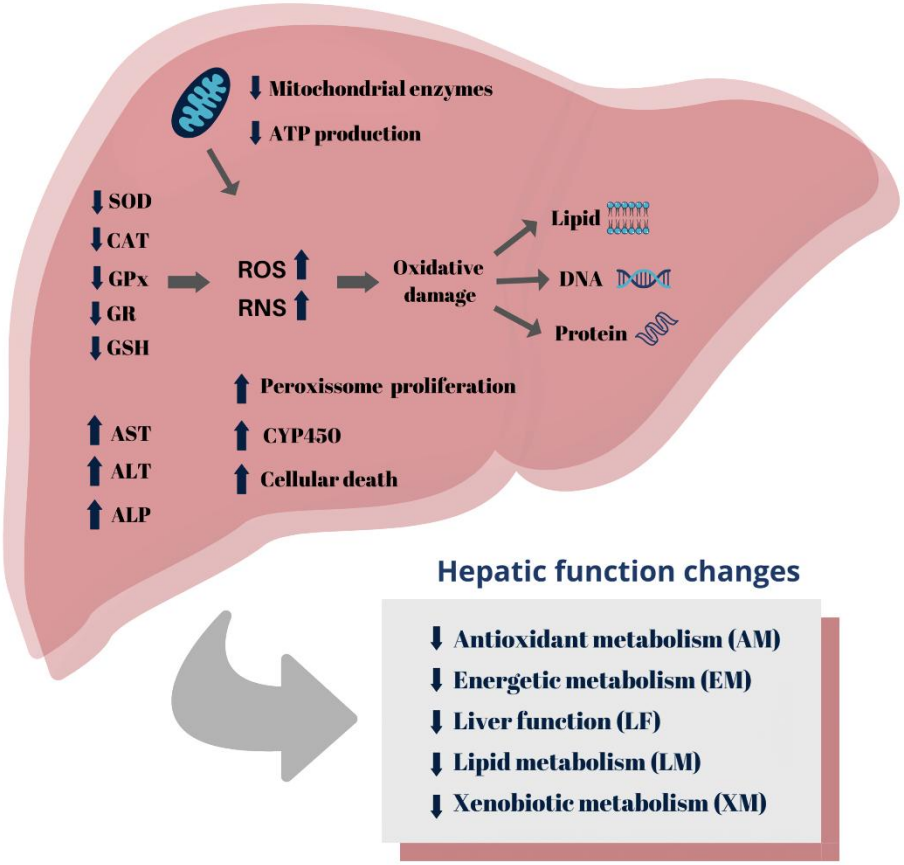

Figure 5. Summary of 2,4-D herbicide induced-hepatotoxicity mechanisms.

3.6. Hepatoprotective assessments

Oxidative stress plays a significant role in the hepatotoxicity induced by 2,4-D[32,33,74]. Therefore, chemical compounds with antioxidant properties are being tested in hepatoprotection assays, aiming to reduce the damages caused by the herbicide (Table 3). Studies in rats have demonstrated that supplementation with selenium (Se) attenuates the 2,4-D-induced hepatotoxicity. This protection is indicated by the reduction in markers

of liver function (AST, ALT, ALP), levels of MDA, reduction in histopathological liver damage, and improvement in the activity of hepatic antioxidant enzymes (CAT, GR, SOD, and GPx)[32,74]. Similar results were also found in rats supplemented with magnesium (Mg)[71]. Se and Mg play essential roles as enzymatic cofactors in antioxidant systems (e.g., for GPx activation and activity), contributing to cell protection against oxidative damage[71,74].

Olive oil and its hydrophilic fraction have also shown promising results against oxidative damage in the livers of 2,4-D-induced rats. The promoted outcomes include the recovery of antioxidant enzyme activity, reduction in the AST/ALT ratio and MDA levels, and preservation of hepatic histoarchitecture[62,64]. These benefits are attributed to the presence of phenolic compounds (e.g., flavonoids, terpenoids) known for their antioxidant properties, as they have the ability to donate electrons to neutralize free radicals and stimulate antioxidant enzyme activity[33]. The aqueous extract of Thymus munbyanus, a plant also rich in phenolic compounds, was also effective against herbicide-induced oxidative damage[33].

Table 3. Hepatoprotection studies against 2,4-D herbicide induced-hepatotoxicity

Biological model	Hepatoprotective agent	Concentrations and time of exposure	Hepatoprotective effects	References
Rattus novergicus	Extra virgin olive oil (EVOO) and its hydrophilic fraction (OOHF)	C: 2,4-D (5 mg/kg body weight) + EVOO (300 µl/day) or OOHF (1 mL/day) T: 4 weeks	EVOO and OOHF suplementation induced a significant increase in the antioxidant enzyme activities (SOD, CAT, GPx and GR), liver marker (AST, ALT and total bilirubin) and a decrease in the conjugated dienes (CD) and thiobarbituric acid-reactive substances (TBARs) levels in the liver.	Nakbi, A. *et al.* (2010)[62]
Rattus novergicus	Extra virgin olive oil (EVOO) and its hydrophilic fraction (OOHF)	C: 2,4-D (5 mg/kg body weight) + EVOO (300 µl/day) or OOHF (1 mL/day) T: 4 weeks	EVOO and OOHF suplementation induced a significant increase in the antioxidant enzyme activities (SOD, CAT, GPx), liver marker (AST, ALT and total bilirubin), and decreased MDA levels in the liver.	Nakbi, A. *et al.* (2012)[64]

Biological model	Hepatoprotective agent	Concentrations and time of exposure	Hepatoprotective effects	References
Rattus novergicus	Chamomile capitula extract	C: 2,4-D (75 or 150 mg/kg body weight) + Chamomile capitula extract- (500 mg/kg body weight) T: 28 days	Chamomile capitula extract presented antioxidant effects, improving the levels of SOD and GR. The levels of hepatic enzymes AST, ALT, ALP, and LDH decreased, as well as total bilirubin. Additionally, the degenerative damages in the hepatic tissue caused by 2,4-D were also alleviated.	Al-Baroudi *et al.* (2014)[68]
Mus musculus	Curcumin	C: 2,4-D (30, 60, 90 mg/kg/day) + Curcumin (10 mg/kg/day) T: 45 days	Curcumin supplementation exhibited antioxidant effects, mainly normalizing the levels of GSH, GR, and lipid peroxidation. Furthermore, curcumin supplementation reduced hepatic tissue damage.	Satapathy and Rao (2018)[70]

Biological model	Hepatoprotective agent	Concentrations and time of exposure	Hepatoprotective effects	References
Rattus novergicus	Magnesium (Mg)	C: 2,4-D (150 mg/kg body weight/day) + Mg supplement (50 mg/kg body weight/day) T: 4 weeks	Mg supplementation exhibited its antioxidant properties by significantly improving urea, creatinine SOD, MDA, CAT, GSH and MDA levels and antioxidant enzyme activities. Hepatic markers were also improved: AST, ALT and ALP and absolute liver weight.	Shafeeq and Mahboob (2020)[71]
Rattus novergicus	Selenium (Se)	C: 2,4-D (5 mg/kg body weight/day) + Se supplement (1 mg/kg body weight/day) T: 4 weeks	Se supplementation in 2,4- D-treated rats elicited a reduction in the toxic effects of the pesticide by improving the studied parameters (absolute liver weight, total bilirubin, AST, ALP, LDH, MDA and carbonyl proteins) which was confirmed by the histological study of the liver.	Tichati, L. *et al.* (2020)[32]
Rattus novergicus	Selenium (Se)	C: 2,4-D (150 mg/kg body weight/day) + Se supplement (1 mg/kg body weight/day) T: 4 weeks	Se supplementation exhibited its antioxidant properties by significantly improving urea, creatinine, ALP, AST, and ALT, and MDA levels and antioxidant enzyme activities. Hepatic and renal toxicities were attenuated by Se supplementation.	Shafeeq and Mahboob (2021)[74]

Biological model	Hepatoprotective agent	Concentrations and time of exposure	Hepatoprotective effects	References
Rattus novergicus	*Thymus munbyanus* extract (AETM)	C: 2,4-D (5 mg/kg body weight) + AETM (10 ml/kg body weight) T: 30 days	AETM supplementation showed a marked enhancement in the above altered hepatic functional and antioxidant parameters (CAT, GST, total bilirubin, AST, ALP, MDA, carbonyl proteins) and liver histopathology.	Tichati, L. *et al.* (2021)[33]

Abbreviations. (C): concentration, (T): time of exposure.

3.7. Pesticide mixtures containing 2,4-D

This review identified studies that evaluated the toxic effects of 2,4-D when combined with other pesticide products. This approach is important as it reflects a more realistic scenario of exposure for non-target organisms. After all, these products are often applied in combination in target crops[150]. Additionally, the mixtures can influence the absorption, distribution, and metabolism of pesticides in non-target organisms, resulting in potential alterations in the toxicity of the individual active ingredients[150,151].

Exposure with commercial formulations of 2,4-D (27 ppm) and azinphosmethyl (0.3 ppm) individually and in combination for 96 hours produced different results in altering the levels of hepatic antioxidant enzymes in Oreochromis niloticus[79]. A synergistic effect between the pesticides was observed in SOD activity, while an antagonistic effect was seen in GPx and GR activity[79]. Chaturvedi *et al.* (1991) tested the effects of 2,4-D alone and in combination with the insecticides toxaphene (TOX) and parathion (PA) in mice and observed different effects on hepatic xenobiotic metabolism enzymes[51]. When administered alone at 50 mg/kg, 2,4-D altered the activities of Amidopyrine N-demethylase and Benzo[a]pyrene hydroxylase. However, when combined with TOX (50 mg/kg) or TOX (50 mg/kg) + PA (5 mg/kg), it induced the activity of other enzymes such as aniline hydroxylase, phenacetin O-dealkylase, and increased CYP450 activity[51].

2,4-D was also evaluated in combination with the herbicide picloram, both of which are components of the commercial herbicide formulation Tordon[77]. The mixture of 5.5 mg/L 2,4-D + 0.5 mg/L picloram increased the hepatic ethoxyresorufin 0-deethylase activity in Ictalurus punctatus, as well as decreased the liver-to-body weight ratio. These effects were not observed in treatments with the individual herbicides, indicating a synergistic effect[77]. These findings highlight the importance of conducting studies that investigate the toxicity of pesticide mixtures, given the scarcity of research in this field of literature.

3.8. Conclusions and perspectives

In conclusion, 2,4-D has a negative impact on various hepatic biochemical parameters, particularly components of the antioxidant system. This indicates that oxidative damage may play a significant role in the progression of 2,4-D-induced hepatotoxicity. However, despite the advancements made in this field, the mechanism of action, targets, and molecular pathways involved in the herbicide's hepatotoxicity are not

yet fully understood. Comprehending the mechanism of action of herbicides is of paramount importance in the development of more efficient agricultural strategies that minimize risks to the environment and non-target organisms[152,153].

In this context, the use of in silico and in chemico tools has emerged as a viable and efficient alternative for predicting toxicity mechanisms of contaminants (Cotterill *et al.*, 2019). Examples include network analyses (e.g., protein-protein interaction networks) that provide a comprehensive understanding of the interactions between molecular targets and the toxic substance of interest[154,155]. In chemico approaches, such as docking and molecular dynamics, can also be employed to assess the affinity between a chemical compound and different targets, thereby increasing the reliability of the obtained results[156]. Moreover, these approaches make use of toxicological data available in freely accessible databases, such as GeneCards (https://www.genecards.org/) and DisGeNET (https://www.disgenet.org/), and are aligned with the principles of the 3 R's of animal experimentation (Replacement, Reduction, and Refinement)[157]. Therefore, the use of predictive methodologies in investigating the mechanism of action of 2,4-D offers a promising perspective for advancing our knowledge of its toxicity and contributes to the development of more effective strategies for environmental safety and public health.

Author contributions: Rafael Xavier Martins: Methodology, Data curation, Formal analysis, Writing – review & editing. Matheus Carvalho, Maria Eduarda Maia and Bruno Flor: Data curation, Methodology, Formal analysis. Terezinha Souza, Thiago Lopes Rocha and Luís M. Félix: Methodology, Supervision, Writing – review & editing. Davi Farias: Conceptualization, Supervision, Writing – review & editing. All authors approved the submitted version.

Funding: This research was funded by Public Call n. 03 Produtividade em Pesquisa PROPESQ/PRPG/UFPB, grant number PVA13245-2020, Public Call Demanda Universal FAPESQ, grant number 3045/2021, and CNPq Productivity Scholarship for T.LR., grant number 306329/2020–4.

Acknowledgements: We thank the Universidade Federal do Ceará (UFC, Brazil), Universidade Federal da Paraíba (UFPB, Brazil), Fundação de Apoio à Pesquisa do Estado da Paraíba (FAPESQ, Brazil), Coordenação de Aperfeiçoamento de Pessoal de

Nível Superior (CAPES, Brazil), and Conselho Nacional de Desenvolvimento Científco e Tecnológico (CNPq, Brazil) for supporting this research with grants and scholarships.

Declaration of competing interest: The authors declare that they have no known competing financial interests or personal relationships that could have appeared to influence the work reported in this paper.

4.2. Artigo 2

A network toxicology and molecular docking-based approach revealed shared hepatotoxic mechanisms and targets between the herbicide 2,4-D and its metabolite 2,4-DCP

Rafael Xavier Martins[1,2], Cleyton Gomes[2], Matheus Carvalho[2], Juliana Alves da Costa Ribeiro Souza[2], Terezinha Souza[2], Davi Farias[1,2,*]

[1]Post-Graduation Program in Biochemistry, Department of Biochemistry and Molecular Biology, Building 907, Campus Pici, Federal University of Ceará, 60455-970 Fortaleza, Brazil

[2]Laboratory for Risk Assessment of Novel Technologies, Department of Molecular Biology, Federal University of Paraiba, João Pessoa, 58050-085, Brazil

[*]Corresponding author:

Professor Davi F. Farias

E-mail: davi@dbm.ufpb.br

Phone: +55-83-32167633

Graphical abstract

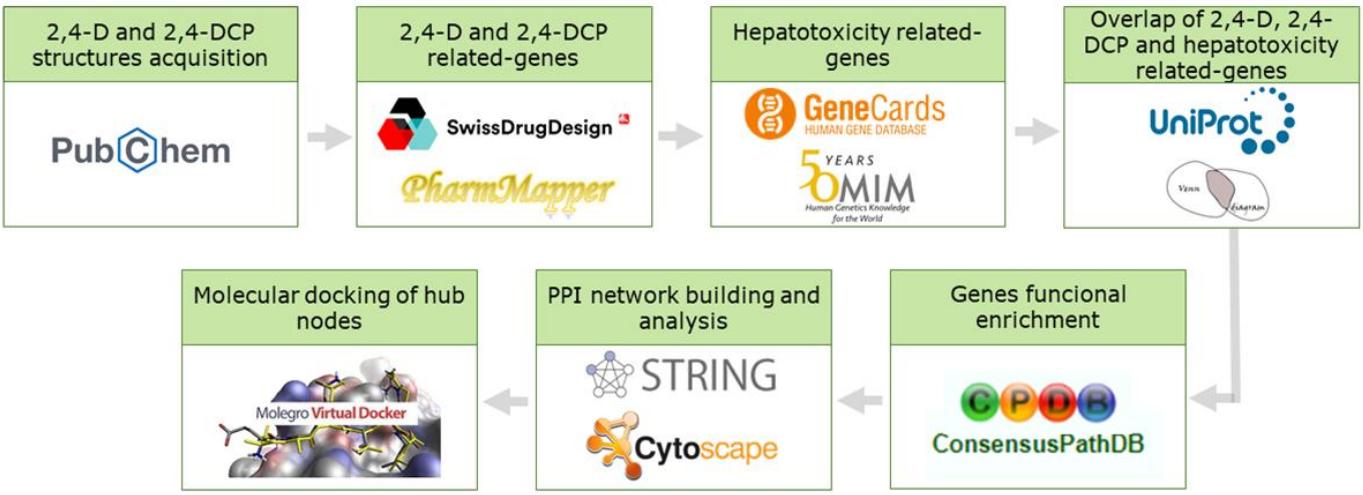

Abstract

The herbicide 2,4-dichlorophenoxyacetic acid (2,4-D) and its major environmental metabolite 2,4-dichlorophenol (2,4-DCP) are pollutants associated with hepatotoxicity, whose molecular mechanisms remain poorly understood. This study investigated the molecular pathways and targets involved in 2,4-D and 2,4-DCP-induced hepatotoxicity using protein-protein interaction (PPI) network analyses and molecular docking. Target genes were identified using PharmMapper and SwissTargetPrediction, and cross-referenced with hepatotoxicity-related genes from GeneCards and OMIM databases. The PPI network, constructed via STRING and visualized in Cytoscape, revealed 12 critical hub nodes, including HSP90AA1, RXRA, EGFR, SRC, CREBBP, PIK3R1, ESR1, AKT1, RAF1, IGF1R, MDM2, and MAPK14. Gene Ontology (GO) analysis indicated processes such as apoptosis, oxidative stress, mitochondrial dysfunction, and lipid metabolism impairment, while Reactome pathway analysis highlighted disruptions in PI3K/AKT and nuclear receptors signaling. Molecular docking confirmed significant interactions of 2,4-D and 2,4-DCP with key proteins, including SRC, AKT, RXRA, MDM2, and HSP90AA1. These results suggest that 2,4-D and 2,4-DCP share similar toxic mechanisms, providing new insights into their hepatotoxicity pathways for the first time.

Keywords: Environmental toxicity; Pesticide exposure; Cellular stress response; Liver dysfunction.

1. Introduction

Pesticides are toxic substances widely used in agriculture to combat pests that damage crops, such as insects (insecticides), fungi (fungicides), and weeds (herbicides) (Kim *et al.*, 2016). Among these, herbicides hold a significant position, accounting for approximately 47.5% of the pesticides applied to crops worldwide (Sharma *et al.*, 2019). 2,4-Dichlorophenoxyacetic acid (2,4-D) is a synthetic compound belonging to the phenoxyacetic acid class and was the first herbicide commercially introduced to the market in 1946. It is used to control broadleaf weeds (pre- and post-emergence) in various crops, including rice, wheat, sorghum, sugarcane, and corn (Islam *et al.*, 2017; Martins *et al.*, 2024). Additionally, 2,4-D is one of the most widely used herbicides globally due to its low cost, selectivity, efficacy, and water solubility (Islam *et al.*, 2017).

According to the United States Department of Agriculture (USDA), the main markets and producers of 2,4-D include the U.S., South America, Europe, and Russia, with its consumption increasing by approximately 40% over the past decade (USDA, 2014; Magnoli *et al.*, 2020). In Brazil, it has been the second most-used herbicide since 2013, with 62,165 tonnes sold in 2021 (IBAMA, 2022). Due to its extensive use, 2,4-D has become a major environmental contaminant, commonly found in both drinking water and environmental samples.

Data from the Brazilian Ministry of Health indicate that 2,4-D was detected in 92% of water samples collected for public supply across more than 2,300 municipalities between 2014 and 2017. Although only two samples exceeded the permissible limit in Brazil (30 µg/L), 4,270 detections surpassed the European Union limit of 0.1 µg/L (SISAGUA, 2018; Zuanazzi *et al.*, 2020). In the U.S., 2,4-D was the fifth most-used herbicide in agriculture in 2012, with concentrations ranging from 0.1 to 12 µg/L detected in urban surface waters (Peterson *et al.*, 2016, ATSDR, 2020). It has also been detected in water bodies in Spain (62-207 ng/L), Australia (3.5 ng/L), Iran (16.6 µg/L), and Greece (1.16 µg/L) (Rodil *et al.*, 2012; Yamini *et al.*, 2013; Tsaboula *et al.*, 2016; Meftaul *et al.*, 2020).

2,4-D is a persistent environmental contaminant with a water half-life ranging from 15 to 300 days, depending on environmental conditions (EPA, 2005; Dehnert *et al.*, 2019; Gaaied *et al.*, 2019; Nault *et al.*, 2014). It undergoes chemical or biological degradation and forms metabolites that can be more toxic to non-target organisms than the original compound (Magnoli *et al.*, 2020). 2,4-D primary degradation product is 2,4-

dichlorophenol (2,4-DCP), produced from the breakdown of the side chain and subsequent hydroxylation of the aromatic ring (Magnoli *et al.*, 2020). This process generally occurs via aerobic bacterial degradation, however certain fungal strains can also produce 2,4-DCP by cleaving the 2,4-D ether linkage (Ferreira-Guedes *et al.*, 2012; Itoh *et al.*, 2016; Magnoli *et al.*, 2020).

Additionally, 2,4-DCP is a metabolite of other organochlorine contaminants, such as triclosan, which increases its presence in the environment (Liu *et al.*, 2018). Classified as a toxic and resistant compound, 2,4-DCP is considered a priority contaminant in China and the U.S. (USEPA, 1979; Liu *et al.*, 2018; Magnoli *et al.*, 2020; Zhang *et al.*, 2020). 2,4-DCP was found in 51.3% of surface water samples from over 600 sites in China, with concentrations ranging from 0.01 to 19.96 µg/L (Gao *et al.*, 2008). Furthermore, 2,4-DCP has been detected in river waters in France (0–4.89 µg/L), South Africa (0.1–10 µg/L), and wastewater in Australia (0.1–6.72 µg/L) (Farounbi and Ngqwala, 2020; Pan *et al.*, 2021).

The presence of 2,4-D and 2,4-DCP in the environment raises concerns due to their toxic effects, particularly on liver function across various biological models, including rodents, fish, and liver cells (Troudi *et al.*, 2012; Tichati *et al.*, 2020; Tichati *et al.*, 2021). Tichati *et al.* (2020) showed that rats treated with 5 mg/kg of 2,4-D exhibited increased liver weight, tissue damage, elevated aminotransferases (AST and ALT) and alkaline phosphatase, and reduced activity of antioxidant enzymes GST, CAT, SOD, and GPx. Additionally, 2,4-D raised carbonyl protein and malondialdehyde (MDA) levels, indicating oxidative stress (Tichati *et al.*, 2021). In zebrafish larvae, 2,4-D (2.5 – 10 mg/L) caused severe liver damage, including cytosol vacuolization, eccentric nuclear positioning, loss of tissue architecture and cell boundaries (Martins *et al.*, 2021). 2,4-DCP, *in vitro*, decreased cell viability and inhibited colony formation in human liver cells (HL7702). Furthermore, the mitochondrial membrane potential collapsed and apoptosis was triggered after 2,4-DCP exposure for 24h (Fu *et al.*, 2016). *In vivo*, 2,4-DCP increased liver weight, caused histopathological damage, and elevated AST and ALT levels in mice, with significant endoplasmic reticulum stress contributing to hepatotoxicity (Fu *et al.*, 2016). Additionally, 2,4-DCP induced apoptosis in primary hepatocytes of *Ctenopharyngodon idella* through a mitochondrial-dependent pathway (Li *et al.*, 2013).

Despite the knowledge of 2,4-D and 2,4-DCP's toxic effects on liver function in various vertebrates, the mechanisms, targets, and molecular pathways involved are not

fully understood. In this context, network toxicology and molecular docking emerge as promising strategies for investigating toxic mechanisms (Souza *et al.*, 2023). Network toxicology uses data from multiple sources to create interaction networks between chemicals and their potential targets, providing graphical models for systematic analysis of multi-target molecular mechanisms (Huang, 2023). Molecular docking, in turn, evaluates the affinity between compounds and target proteins (Huang, 2023). Souza *et al.* (2023) successfully identified shared potential targets and pathways associated with organophosphate neurotoxicity using these methodologies. Similarly, this approach has been applied to clarify the neurotoxic mechanisms of acetyl tributyl citrate (Huang, 2023). Therefore, this study aims to use network toxicology and molecular docking to investigate the hepatotoxic mechanisms of 2,4-D and 2,4-DCP.

2. Material and methods

The methodology employed in this study was adapted from the work of Souza *et al.* (2023).

2.1. Prediction of 2,4-D and 2,4-DCP potential targets

The Canonical SMILES of 2,4-D and 2,4-DCP were obtained from PubChem (https://pubchem.ncbi.nlm.nih.gov) and subsequently subjected to the PharmMapper (http://www.lilab-ecust.cn/pharmmapper/) and Swiss Target Prediction (http://www.swisstargetprediction.ch) software tools with the aim of identifying potential target genes. In PharmMapper, we used the default settings without customizing any advanced options. GA match was enabled, and the maximum number of hits allowed by the system was returned. All targets identified by both software tools were considered and converted into the standard gene names through the UniProt database (https://www.uniprot.org/). Subsequently, the predicted genes were grouped and redundant entries were removed to identify the 2,4-D and 2,4-DCP potential targets.

2.2. Identification of 2,4-D and 2,4-DCP hepatotoxicity related targets

For the identification of hepatotoxicity-related genes, we consulted the GeneCards database (https://www.genecards.org/) and the Online Mendelian Inheritance in Man (OMIM, http://omim.org/) in October 2023 using five distinct keywords: "hepatotoxicity," "drug-induced liver injury," "liver injury," "liver failure," and "liver damage." The searches were limited to *Homo sapiens* species. After standardizing gene

names using UniProt, all predicted targets from both databases were merged, and duplicate entries were subsequently removed.

After that, the hepatotoxicity-related genes and predicted targets for 2,4-D and 2,4-DCP were overlapped using the Draw Venn Diagram tool (http://bioinformatics.psb.ugent.be/webtools/Venn/) to identify potential targets of these chemical compounds associated with hepatotoxic effects. The intersections among hepatotoxicity-related genes, 2,4-D and 2,4-DCP targets were used for further analysis in this study.

2.3. Construction and analysis of a protein-protein interaction (PPI) network

The protein-protein interaction (PPI) network was constructed using the String database (https://string-db.org) for the *Homo sapiens* species. For this, the intersections between the potential targets of 2,4-D and 2,4-DCP and the hepatotoxicity-related genes obtained from the Venn diagram were employed. The type of network constructed was a full string network, indicating that the edges represent both functional and physical protein associations. For network construction, only experimentally derived data were used and with a minimum required interaction score of 0.7 (high confidence). Disconnected nodes were removed from the network.

Subsequently, the PPI network was imported for visualization and analysis in Cytoscape 3.10.0. To identify the central nodes in the network, the analyze network tool was used to perform topological analyses, based on the metrics degree and betweenness centrality (BC). The degree represents the number of connections a node has with other nodes in the network, quantifying the number of edges connected to it. Nodes with a high degree value are important for information transmission in the network, as they have more control over the flow of information (Souza *et al.*, 2023). On the other hand, BC is a measure that indicates a node's ability to connect other nodes in the network. A high BC value indicates that the node is important for communication between different parts of the network (Souza *et al.*, 2023). Then, the cytoHubba plugin (v 0.1) was used to identify the central nodes of PPI network, computing the top 10 hub nodes in terms of degree and BC, respectively.

2.4. Functional Enrichment Analysis

The potential targets of 2,4-D and 2,4-DCP related to hepatotoxicity were separately subjected to functional enrichment analysis using the ConsensusPathDB

database (http://cpdb.molgen.mpg.de), restricting the species to *Homo sapiens*. We utilized Gene Ontology (GO) and Reactome Pathway databases to identify the biological processes (BP) and pathways associated with the selected targets, respectively. The default settings of ConsensusPathDB were applied, with a p-value cutoff of 0.01 for both databases and a minimum input list overlap of 2 for Reactome. GO terms and Reactome Pathways with a p-value < 0.01 were considered statistically significant. Through manual curation, we selected BP directly associated with cell injury/death (CID), increased reactive oxygen species (IROS), mitochondrial dysfunction (MD), and fatty acid metabolic process (FAMP). The rationale for focusing on these processes is that they are central and highly interconnected key event signatures (KES) in the Adverse Outcome Pathway (AOP) hepatotoxicity network for humans, as highlighted by Arnesdotter *et al.* (2021). This means they are very common perturbations in the development of hepatotoxicity by different types of stressors. Regarding the Reactome Pathway analysis, the top 15 pathways for 2,4-D and 2,4-DCP based on the lowest p-value were selected. All enrichment graphs were constructed using specific Python (v. 3.11.1) libraries: matplotlib (v 3.8.2; https://matplotlib.org/stable/project/citing.html), pandas (v 1.5.2; https://pandas.pydata.org/about/citing.html), scipy (v, 1.13.0; https://scipy.org/citing-scipy/), and numpy (v 1.24.0; https://numpy.org/citing-numpy/).

2.5. Molecular docking

Molecular docking analysis were performed to evaluate the potential interactions of 2,4-D and 2,4-DCP with the main hubs of the network, based on degree and betweenness centrality (BC) criteria. The 3D structures of 2,4-D and 2,4-DCP were obtained from the PubChem database (https://pubchem.ncbi.nlm.nih.gov), both in SDF format. The crystal structures of the proteins were sourced from the RCSB Protein Data Bank (https://www.rcsb.org). Only *Homo sapiens* proteins were used. The PDB IDs and their resolutions are listed in Supplementary Table 1.

For each target, a positive control was assigned. In most cases, these were the ligands co-crystallized in the PDB structures. For EGFR (2M0B) and IGF1R (7V3P), well-characterized inhibitors (PD168393 and PubChem ID 59442083, respectively) were used as positive controls instead of the co-crystallized ligands. Information about positive controls is provided in Supplementary Table 2.

The Discovery Studio 2021 software was used to remove water molecules, potential cofactors, unwanted ligands, and to add polar hydrogen bonds. Subsequently,

Swiss-PdbViewer 4.1.0 (https://spdbv.unil.ch/) was employed for global energy minimization of the structures. Molecular docking simulations were carried out using Molegro Virtual Docker (MVD) 6.0. The grid box in the docking simulations was defined based on the binding site of the co-crystalized ligand, with dimensions of 20x20x20 Å, and poses with the lowest binding energy were selected to represent the results. The grid box xyz coordinates are presented in Supplementary Table 3. Finally, Discovery Studio 2021 was used for the analysis and visualization of the obtained results.

3. Results

3.1. Screening of 2,4-D, 2,4-DCP and hepatotoxicity common targets

Using the PharmMapper and SwissTargetPrediction databases, we identified a total of 408 targets for 2,4-D and 187 targets for 2,4-DCP. We also determined 3.191 targets related to hepatotoxicity from the OMIM and GeneCards databases. Figure 1 (A, B, and C) shows the 2D structures of 2,4-D and 2,4-DCP, along with a Venn diagram of their overlapping targets related to hepatotoxicity. The intersections regions reveal that 216 targets for 2,4-D (126 unique + 90 shared) and 113 targets for 2,4-DCP (23 unique + 90 shared) are related to hepatotoxicity. Additionally, there are 90 targets common to both compounds and linked to liver damage. The 216 targets for 2,4-D and 113 targets for 2,4-DCP (Supplementary table 4) served as the basis for the subsequent analyses in this study.

Figure 1. (a) 2D structure of 2,4-D (CAS: 94-75-7). (b) 2D structure of 2,4-DCP (CAS: 120-83-2). (c) Venn diagram showing the overlap of target proteins related to 2,4-D, 2,4-DCP, and hepatotoxicity.

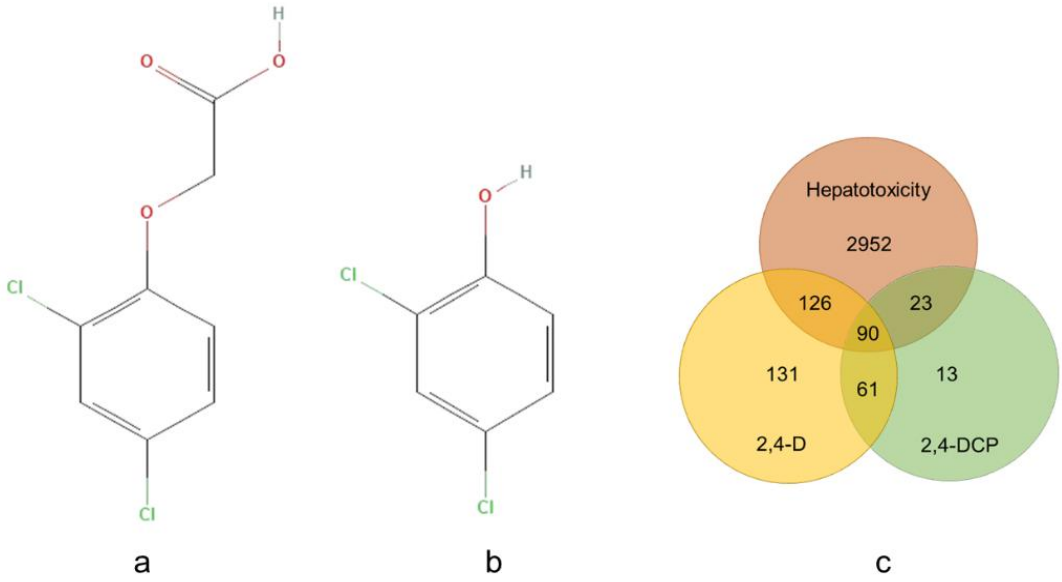

3.2. Protein-protein interaction (PPI) network

We combined all targets of 2,4-D and 2,4-DCP associated with hepatotoxicity to construct a single protein-protein interaction (PPI) network using the STRING database. This resulted in a network with 238 nodes and 132 edges. After importing the network into Cytoscape and removing disconnected nodes, the final network comprised 82 nodes and 132 edges. Of these nodes, 24 (29.3%) are exclusive to 2,4-D, 8 (9.7%) are exclusive to 2,4-DCP, and 50 (70%) are shared between the herbicide and its metabolite, indicating similar mechanisms of hepatotoxicity.

In Cytoscape, we created an optimized visual representation of the PPI network (Figure 2a) and analyzed the topological measures using the Network Analyzer tool. The protein names and topological measures for the entire PPI network are listed in Supplementary Table 5. We identified the top 10 hub nodes with the highest degree (Figure 2b) and BC (Figure 2c), and compiled a table of 12 nodes considered most relevant to the network (Table 1). Most targets were common between the compounds, with AKT1, RAF1, and IGF1R specific to 2,4-D, and CREBBP specific to 2,4-DCP. It is important to emphasize that the applied filter criteria directly influence the results, and additional connections might emerge with less stringent filters. For instance, CREBBP

links ESR1 and RXRA in the 2,4-DCP network, suggesting a potential direct connection between ESR1 and RXRA in 2,4-D as well.

Figure 2. (A) PPI network of targets related to 2,4-D and 2,4-DCP-induced hepatotoxicity. Nodes represent genes, and edges show interactions. Node size reflects degree, and color intensity indicates BC. (B) Top 10 hub nodes by degree. (C) Top 10 hub nodes by BC. Color intensity indicates high degree or BC. Shapes denote targets: 2,4-D (triangle), 2,4-DCP (diamond), or both (circle).

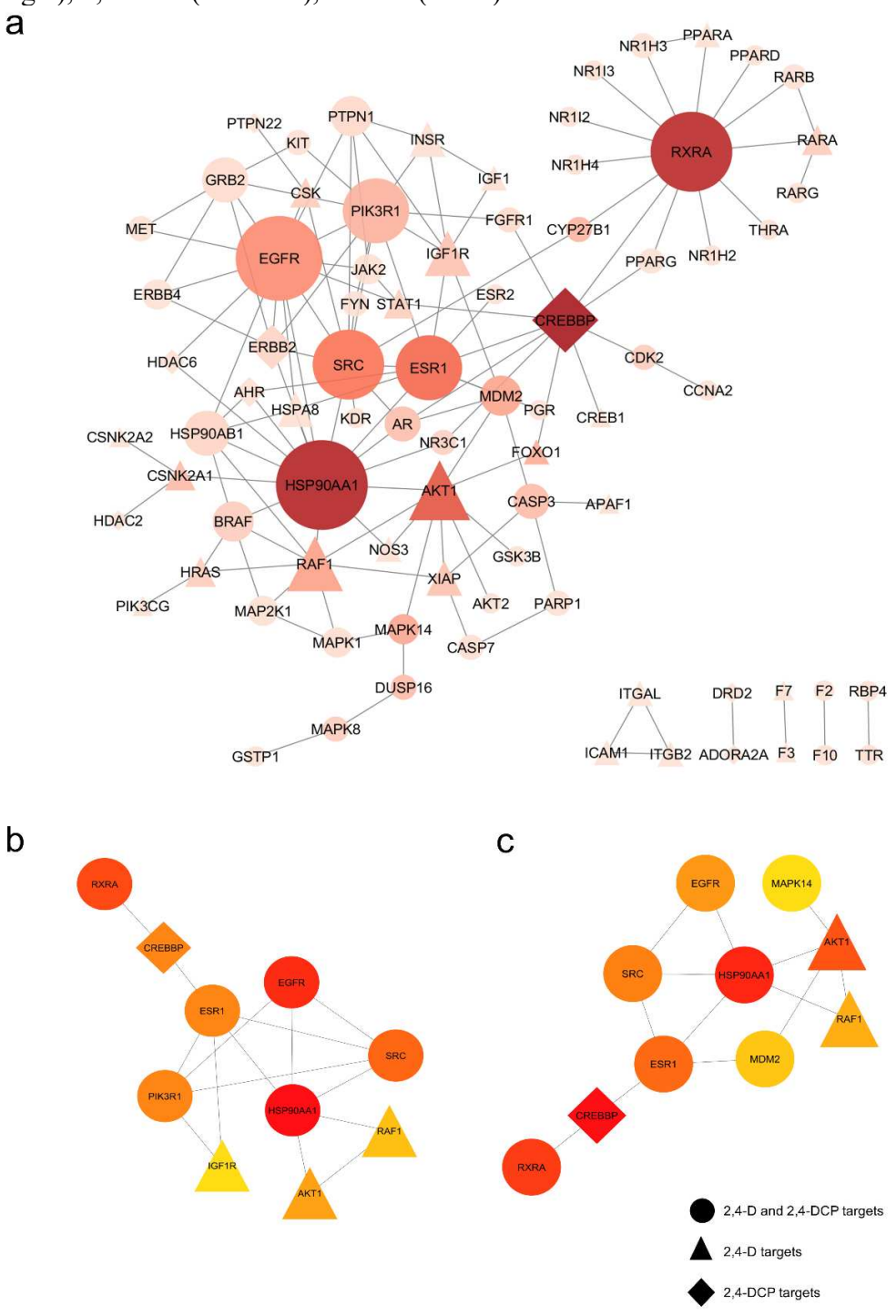

Table 1. Topological measurements of core nodes in the PPI networks identified by degree and betweenness centrality (BC).

Compound Target	Node	Protein	Degree	BC
Both	HSP90AA1	Heat Shock Protein 90 Alpha Family Class A Member 1	15	0.308
Both	RXRA	Retinoid X Receptor Alpha	13	0.293
Both	EGFR	Epidermal growth factor receptor	14	0.126
Both	SRC	Proto-oncogene tyrosine kinase SRC	11	0.158
2,4-DCP	CREBBP	CREB Binding Protein	10	0.328
2,4-D	AKT1	AKT Serine/Threonine Kinase 1	9	0.214
Both	PIK3R1	Phosphatidylinositol 3-kinase regulatory subunit alpha	10	0.069
Both	ESR1	Estrogen Receptor 1	10	0.180
2,4-D	RAF1	Raf-1 Proto-Oncogene, Serine/Threonine Kinase	8	0.095
2,4-D	IGF1R	Insulin Like Growth Factor 1 Receptor	6	0.045
Both	MDM2	E3 ubiquitin-protein ligase Mdm2	5	0.087
Both	MAPK14	Mitogen-activated protein kinase 14	3	0.086

3.3. Genes functional enrichment

3.3.1 Biological process (BP)

We performed a Gene Ontology (GO) analysis using 216 targets for 2,4-D and 113 targets for 2,4-DCP. A total of 535 statistically significant biological processes (BP) were identified for 2,4-D, and 451 for 2,4-DCP (p-value < 0.01). To minimize redundancy, the analysis was restricted to GO categories at level 4. Following manual curation, we identified 38 BPs for 2,4-D and 31 for 2,4-DCP, as shown in Figure 3 (a and b). The results indicate that enriched target genes are involved in various BPs associated with hepatotoxicity, with a high degree of similarity between the herbicide and its metabolite. Common BPs include apoptotic processes and regulation of cell death (CID), cellular response to oxidative stress, response to oxygen species (IROS), lipid response, fatty acid metabolic processes (FAMP), and regulation of mitochondrial membrane potential (MD).

3.3.2 Reactome pathway analysis

We identified 379 statistically significant pathways (p-value < 0.01) for 2,4-D and 314 for 2,4-DCP. The top 15 Reactome pathways with the lowest p-values for both compounds are presented in Figure 4 (a and b). There was a strong overlap between the hepatotoxicity-related pathways of both compounds. Nuclear receptor transcription pathways had the lowest p-values for both, highlighting nuclear receptor disruption as a key toxicity mechanism. Both compounds also shared the Signaling by nuclear receptors pathway, reinforcing its role in their toxicity.

Additionally, pathways related to PI3K/AKT signaling were identified for both: three for 2,4-D and five for 2,4-DCP, including PI3K/AKT signaling in cancer, Negative regulation of the PI3K/AKT network, and PIP3 activates AKT signaling, underscoring the PI3K/AKT pathway's relevance in their toxicity mechanisms. Other identified pathways involved growth factor signaling, second messengers, and receptor tyrosine kinase signaling. For 2,4-D, Metabolism was the second most significant pathway, which is crucial for understanding its hepatotoxic effects due to its role in liver function.

Figure 3. Gene Ontology (GO) analysis of genes associated with hepatotoxicity induced by 2,4-D and 2,4-DCP. The x-axis showing the number of genes involved in each process and BPs are color-coded to reflect their association with specific hepatotoxic effects: cell death (blue), reactive oxygen species (ROS) generation (yellow), mitochondrial dysfunction (green), and lipid metabolism (red).

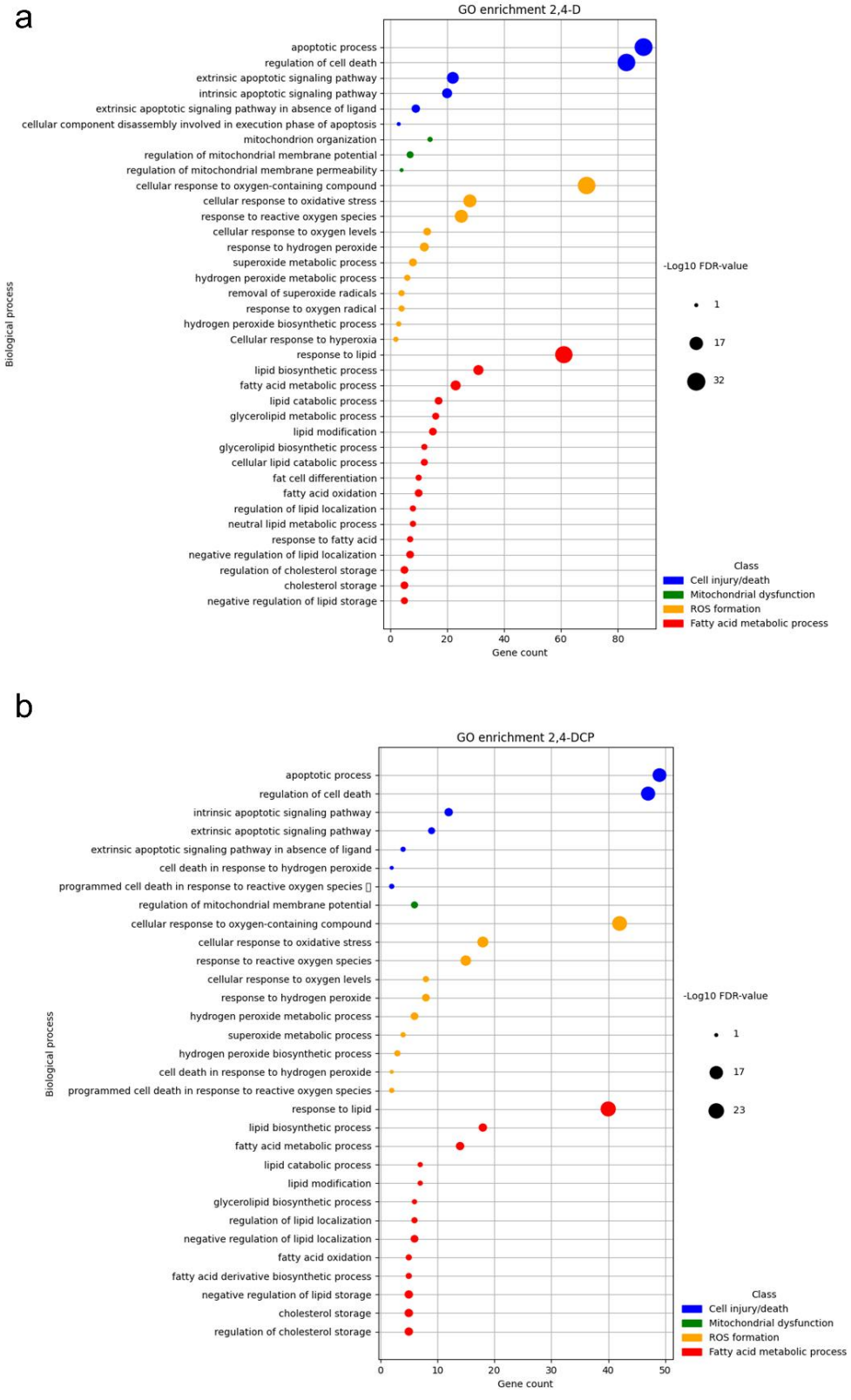

Figure 4. Reactome pathway analysis results for genes associated with hepatotoxicity induced by 2,4-D and 2,4-DCP. The top 15 pathways are displayed based on p-value significance, with the x-axis representing the number of genes associated with each pathway. Colors transition from yellow to blue to indicate a decrease in p-value, with yellow representing higher significance and blue representing lower significance.

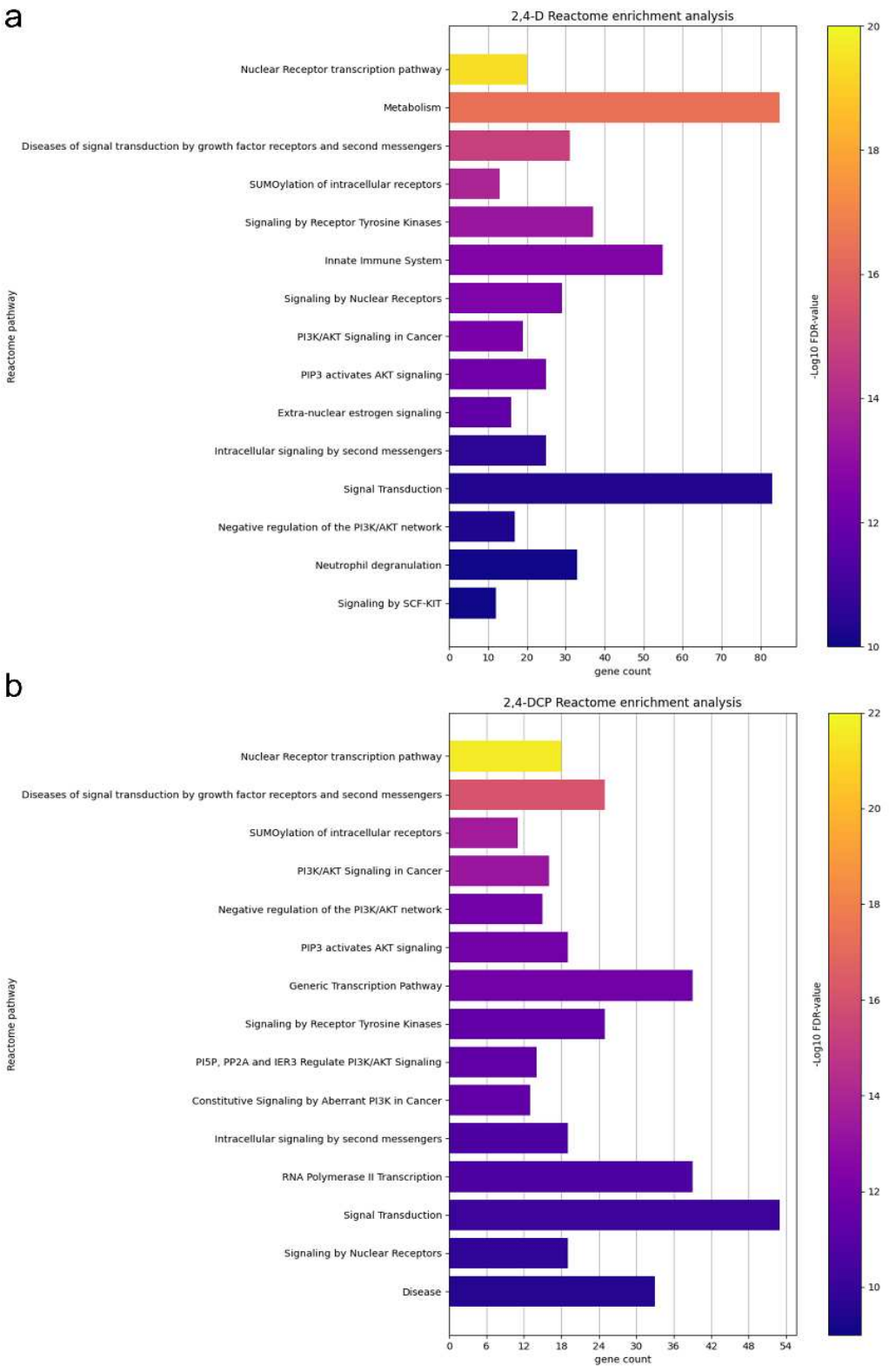

3.4. Molecular docking

Figure 5 shows that 2,4-D has more favorable binding energies compared to 2,4-DCP across all tested proteins. The binding energy values are provided in Supplementary Table 6. We conducted a literature review to identify potential targets and assess the relevance of these interactions, focusing on binding energy, residue importance, binding distances, and overlap with positive controls and known inhibitors. Five proteins stood out: HSP90AA1, RXRA, SRC, MDM2, and AKT1. For HSP90AA1, both 2,4-D and 2,4-DCP interact with residues at the ATP-binding site (Asn 51, Met 98, Val 186, and Ala 55), which are also targeted by the inhibitor PU3 (Wright *et al.*, 2004). In SRC, 2,4-D bound to Glu 178, Thr 179, and Lys 203, while 2,4-DCP bound to His 201, Cys 185, and Lys 203, matching the targets of the inhibitor Scaranitib, used as a positive control in our docking simulations (Hennequin *et al.*, 2006; Tou and Shen, 2012). In MDM2, both substances interact with Val 93, Ile 61, and His 96, which are part of the active site and targeted by the inhibitor WY-5 (Vassilev *et al.*, 2004; Zhang *et al.*, 2022). Additionally, 2,4-D interacts with Val 164 in AKT1, which is part of the nucleotide phosphate-binding region, as annotated in the UniProt database (entry: P31749). This region is defined based on curated data and patterns identified by PROSITE-ProRule (PRU00159). Notably, our docking results indicate that this residue is also targeted by the pyrrolopyrimidine inhibitor of AKT kinase described by Lippa *et al.* (2008), which was used as a positive control. The overlap with known inhibitors suggests a potential mechanism of protein inhibition by 2,4-D and its metabolite.

Finally, for RXRA, both 2,4-D and 2,4-DCP interact with crucial amino acids for binding to 9-cis-retinoic acid, a metabolite of retinoic acid and RXRA agonist (Egea *et al.*, 2000). Residues such as Ala 271 and Ala 272 are essential for forming a hydrophobic pocket crucial for stabilizing the ligand-binding domain (LBD). The interactions between 2,4-D, 2,4-DCP, and the amino acid residues are illustrated in Figure 6. The 2D representations of all docking analyses performed are provided in Supplementary Figures 1, 2, and 3.

Furthermore, the positive controls exhibited stronger binding energies than 2,4-D and 2,4-DCP, as expected, given their well-characterized high affinity for the target proteins. Comparing binding energies with positive controls is essential, as it provides a reference for interaction strength and identifies shared amino acids involved in binding. It is important to note that binding energies can vary depending on experimental

conditions. For example, 2,4-D showed a higher Rerank score (an additional MDV analysis) with RXRA than the positive control, highlighting the complexity of these interactions. Although the binding energies of 2,4-D and 2,4-DCP were less favorable than those of the positive controls, their interactions with key amino acids in the target proteins suggest potential modulatory effects, making them promising candidates for further investigation through molecular dynamics simulations and experimental validation

Figure 5. Heatmap of molecular docking interactions of 2,4-D and 2,4-DCP with core targets. The y-axis lists the hub nodes, and the x-axis shows the herbicide, its metabolite, and the positive control for each protein. The color scale represents the predicted binding energy for each interaction. Gap indicates that the protein was not identified as a target of 2,4-D or 2,4-DCP in the SwissTargetPrediction and PharmMapper analyses.

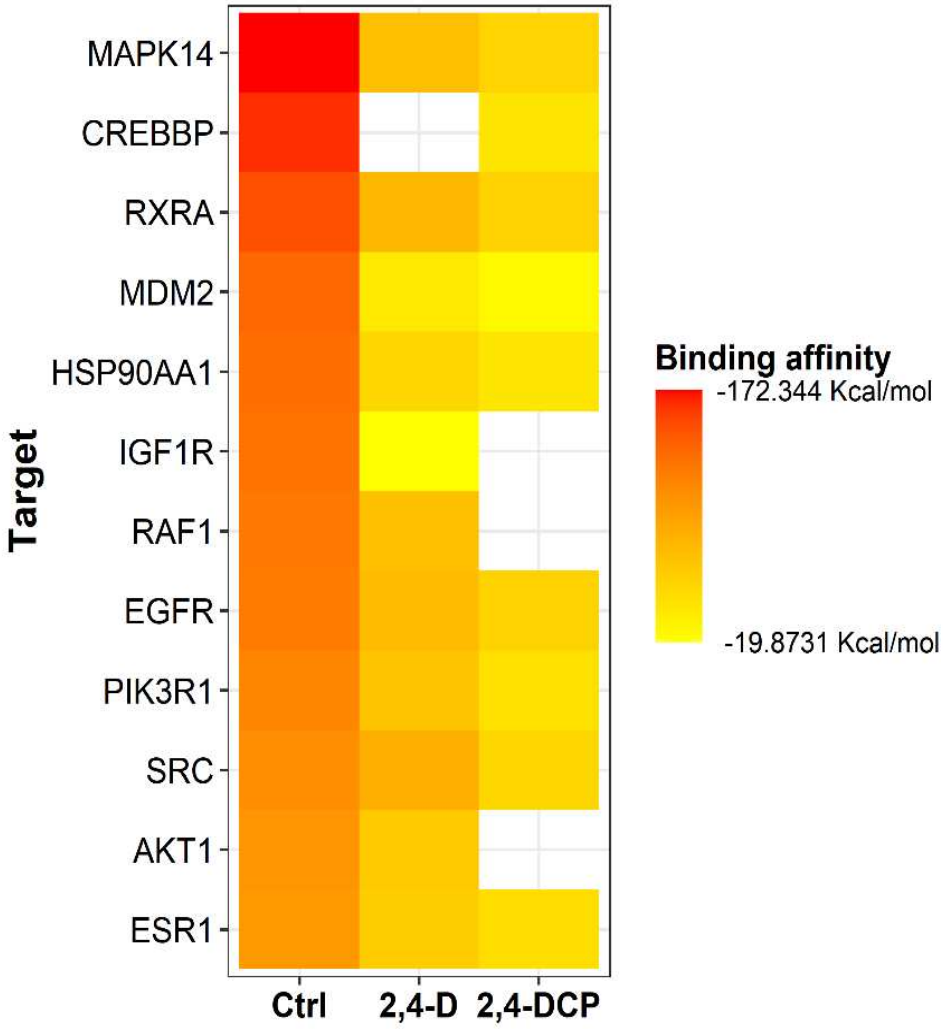

Figure 6. Interactions of 2,4-D and 2,4-DCP with potential target proteins. Panels (a–e) show the interactions of 2,4-D with five target proteins: SRC, RXRA, MDM2, HSP90AA1, and AKT1. Panels (g–i) display the interactions of 2,4-DCP with SRC, RXRA, MDM2, HSP90AA1. Each panel includes both 2D and 3D representations, highlighting the binding sites and interactions between the herbicide/metabolite and the respective protein targets.

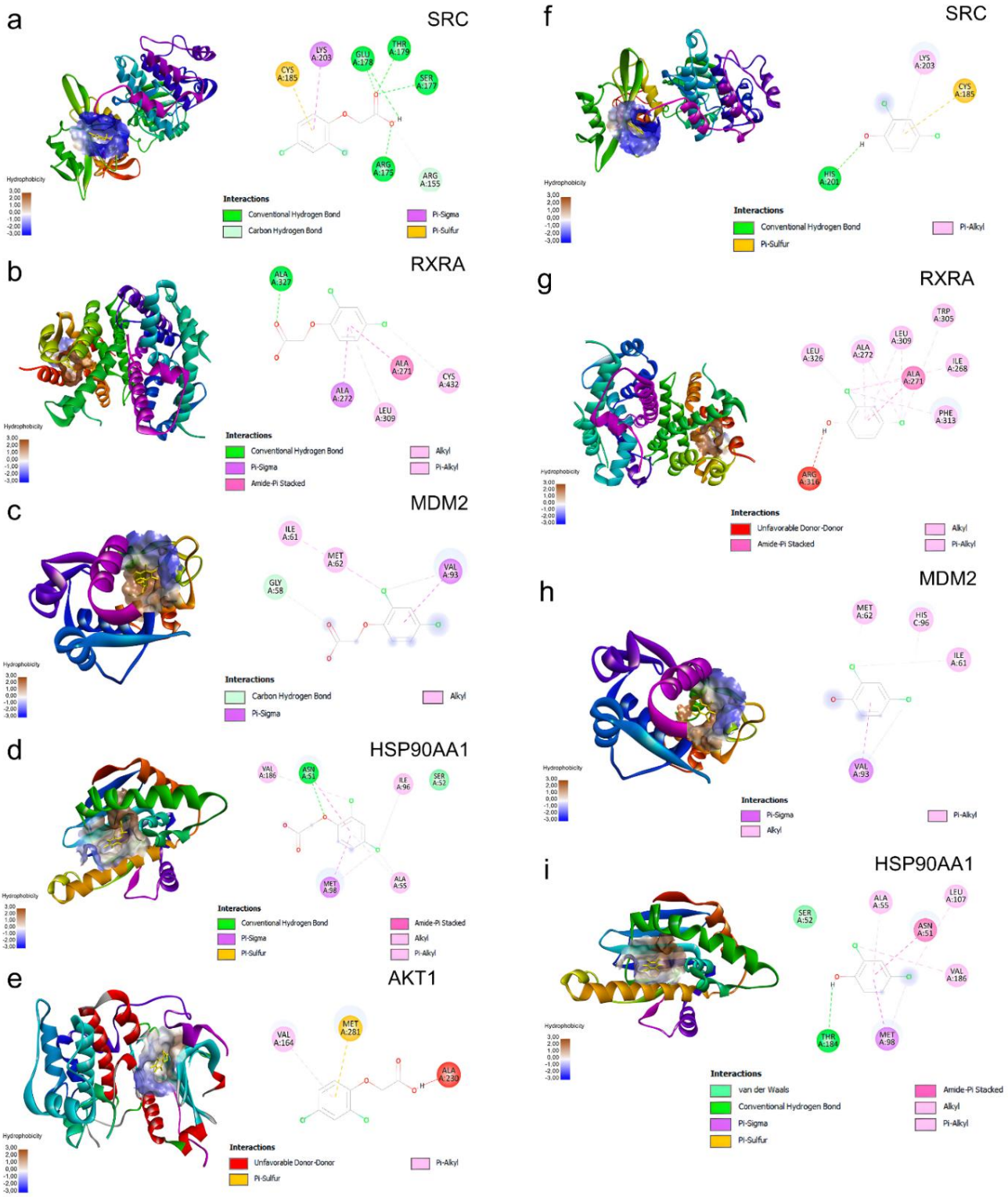

4. Discussion

The results indicate that both 2,4-D and 2,4-DCP interact with key proteins essential for hepatic health, such as SRC, RXRA, MDM2, and HSP90AA1, with only 2,4-D additionally interacting with AKT1. Gene Ontology (GO) and Reactome pathway analyses reveal notable similarities in the hepatotoxic mechanisms of these compounds. For instance, inhibition of SRC and AKT1 can suppress the PI3K/AKT pathway, a key signaling cascade (Fortner *et al.*, 2022). This inhibition may reduce anti-apoptotic signaling and increase apoptosis through mitochondrial dysfunction and oxidative stress (Wang and Joule, 2009; Fortner *et al.*, 2022;). Furthermore, as the PI3K/AKT pathway is crucial for hepatic lipid and glucose metabolism, its suppression may also impair energy metabolism (Liu *et al.*, 2016; Huang *et al.*, 2018).

Additionally, both 2,4-D and 2,4-DCP may disrupt lipid metabolism by modulating nuclear receptor signaling through interactions with RXRA, subsequently affecting PPAR pathways. (Li *et al.*, 2021; Valdez *et al.*, 2023). Inhibition of MDM2 and HSP90AA1 by both compounds could also exacerbate cellular stress and proteotoxicity (Nag *et al.*, 2013; Murshid *et al.*, 2013). Collectively, these findings underscore potential hepatotoxic mechanisms of 2,4-D and 2,4-DCP, highlighting their role in driving oxidative stress, mitochondrial dysfunction, impaired lipid metabolism, and apoptosis, as discussed below.

4.1 Perturbation of PI3K/AKT signaling network

SRC is a non-receptor tyrosine kinase crucial for signal transduction, regulating processes like growth, differentiation, and survival. It activates the PI3K/AKT pathway by phosphorylating tyrosine residues on other proteins, triggering downstream signaling cascades (Fortner *et al.*, 2022). Docking analysis suggests that 2,4-D and 2,4-DCP may interact with SRC, which could potentially affect PI3K/AKT pathway activation. In addition to SRC, AKT itself is also a target of 2,4-D, which may further compromise its activity. A decrease in AKT activity could induce a pro-apoptotic effect, as AKT normally phosphorylates transcription factors that promote anti-apoptotic genes (e.g., Bcl-2) and suppresses pro-apoptotic proteins (e.g., Bax and p53) (Fortner *et al.*, 2022; Wang and Joule, 2009).

Studies have shown that 2,4-D triggers apoptosis in rat liver, marked by an increased Bax/Bcl-2 ratio, elevated p53 and TNF-α levels, caspase activation, and heightened oxidative stress (Sinan Ince *et al.*, 2023). Similarly, 2,4-DCP induces

apoptosis in grass carp hepatocytes, as indicated by changes in the Bax/Bcl-2 ratio, increased caspase activity, and elevated levels of TNF-α and reactive oxygen species (ROS) (Li *et al.*, 2013). The elevated Bax/Bcl-2 ratio points to apoptosis via the intrinsic (mitochondrial) pathway, and these molecular events may be associated with the suppression of the PI3K/AKT pathway, as highlighted by Reactome analyses.

Inhibition of the PI3K/AKT pathway leads to increased Bax and decreased Bcl-2 levels, which result in mitochondrial membrane permeabilization. This permeabilization allows for the release of cytochrome c, apoptosome formation, caspase activation, and ultimately, programmed cell death (Wang and Youle, 2009). Thus, PI3K/AKT pathway inhibition not only decreases anti-apoptotic signaling mediated by AKT but also contributes to mitochondrial dysfunction, facilitating intrinsic apoptosis. Furthermore, the elevated levels of TNF-α suggest that apoptosis may also proceed through the extrinsic pathway, amplifying the apoptotic response (Jan and Chaudhry, 2019).

Moreover, 2,4-D has a significant impact on mitochondrial function, reinforcing the role of mitochondrial dysfunction in the hepatotoxicity of these compounds. In HepG2 cells treated with 16 mM of 2,4-D, apoptosis was linked to the disruption of mitochondrial membrane potential (Tuschl and Schwab, 2003). In rat (*Rattus norvegicus*) hepatocytes, 2,4-D inhibited mitochondrial complexes II and III, uncoupled oxidative phosphorylation, disrupted mitochondrial membrane potential, and reduced ATP production (Palmeira *et al.*, 1994; Pereira *et al.*, 1994). Similarly, 2,4-DCP caused comparable effects in HL7702 cells, leading to mitochondrial membrane potential collapse and apoptosis after 24 hours of exposure (Fu *et al.*, 2016).

These findings underscore the interconnectedness of PI3K/AKT pathway inhibition and mitochondrial dysfunction in the induction of apoptosis, with significant implications for the hepatotoxicity induced by 2,4-D and 2,4-DCP. Mitochondria are a primary source of reactive oxygen species (ROS), and their dysfunction significantly increases ROS production, contributing to oxidative stress (Wieckowska *et al.*, 2021). This dysfunction results in excessive generation of superoxide and hydrogen peroxide, particularly at complexes I and III of the electron transport chain. The resulting oxidative stress can damage lipids, proteins, and DNA, ultimately triggering apoptosis and necrosis (Wieckowska *et al.*, 2021).

Oxidative stress plays a central role in the hepatotoxicity induced by 2,4-D and 2,4-DCP (Zhang *et al.*, 2004; Fu *et al.*, 2016; Martins *et al.*, 2024). Hepatic damage is often accompanied by reduced activity of key antioxidant enzymes, such as superoxide

dismutase (SOD), catalase (CAT), and glutathione peroxidase (GPx), alongside increased levels of malondialdehyde (MDA), a marker of lipid peroxidation (Nakbi *et al.*, 2012; Sinan Ince *et al.*, 2023; Zhang *et al.*, 2004; Luo *et al.*, 2005).

The inhibition of the PI3K/AKT pathway can heighten hepatic cell susceptibility to oxidative stress from 2,4-D and 2,4-DCP, as AKT is critical for antioxidant protection. It regulates the transcription factor Nrf2, facilitating its movement to the nucleus where it activates antioxidant genes such as GST and catalases (Kondouros and Poulogiannis, 2018). Furthermore, AKT is essential for producing NADPH, which is vital for synthesizing glutathione, a key molecule for neutralizing free radicals (Kondouros and Poulogiannis, 2018). The PI3K/AKT pathway thus maintains adequate NADPH levels, crucial for glutathione metabolism and ROS reduction. Consequently, inhibition of this pathway compromises the antioxidant response and glutathione regeneration, exacerbating oxidative stress and contributing to hepatotoxicity (Kondouros and Poulogiannis, 2018). Furthermore, oxidative stress further exacerbates pro-apoptotic signaling, resulting in a compounded apoptotic response that significantly impacts liver health (Allameh *et al.*, 2023).

The PI3K/AKT pathway is crucial for hepatic lipid and glucose metabolism. It promotes lipogenesis by activating genes like SREBP-1c and inhibits lipolysis (Huang *et al.*, 2018). When this pathway is inhibited, lipid accumulation decreases, lipogenic gene expression is reduced, and fatty acid oxidation is enhanced, as shown by Liu *et al.* (2016) in primary hepatocytes. In terms of glucose metabolism, the PI3K/AKT pathway inhibits gluconeogenesis and is vital for insulin signaling, facilitating glucose uptake by promoting GLUT4 translocation to the cell membrane (Świderska *et al.*, 2018). Inhibition of this pathway is associated with insulin resistance, increased gluconeogenesis, and reliance on fatty acid oxidation for energy (Świderska *et al.*, 2018; Savova *et al.*, 2023).

Toxicity data on 2,4-D suggests it inhibits the PI3K/AKT pathway, leading to hepatotoxic effects. In rodents, 2,4-D has been shown to increase mitochondrial and peroxisomal β-oxidation (Lundgren *et al.*, 1987; Kozuka *et al.*, 1991; Hietanen *et al.*, 1985). For instance, rats fed 0.25% 2,4-D for seven days exhibited increased carnitine acetyltransferase (CrAT) activity and enhanced palmitoyl-CoA oxidation (Kawashima *et al.*, 1984). Similarly, South American catfish (*Rhamdia quelen*) exposed to 2,4-D showed reduced hepatic glycogen and glucose levels alongside increased plasma glucose, reflecting possible compensatory mechanisms in response to insulin resistance and highlighting alterations in hepatic energy metabolism (Caetano *et al.*, 2008).

The impact of 2,4-DCP on energy metabolism is less studied. However, zebrafish exposed to 2.5 mg/L of 2,4-DCP exhibited lipid accumulation and increased ROS production (Tsukazawa *et al.*, 2022). This difference compared to 2,4-D may arise from distinct targets and mechanisms of action, with AKT being a specific target of 2,4-D. Reactome analysis ranks the metabolism pathway as the second most significant for 2,4-D, indicating substantial interference in metabolic pathways, including PI3K/AKT. Furthermore, docking results show stronger interactions of 2,4-D with all analyzed targets, suggesting a greater potential for metabolic disruption. These differences underscore the need for further research into the hepatotoxic mechanisms of these compounds. Notably, disruptions in lipid metabolism can lead to increased ROS generation and oxidative stress, which are central mechanisms in the development of liver diseases such as non-alcoholic fatty liver disease (NAFLD) (Arroyave-Ospina *et al.*, 2021).

4.2. Perturbation of nuclear receptors signaling pathways

Reactome results indicate that disruptions in pathways involving nuclear receptors (NRs) are associated with the hepatotoxicity induced by 2,4-D and its metabolite, 2,4-DCP. NRs are transcription factors activated by ligands, regulating gene expression in response to lipid molecules like steroid hormones and fatty acids (Li *et al.*, 2021). Upon activation, NRs form dimers and bind to regulatory regions of target genes, modulating their transcription (Li *et al.*, 2021; Valdez *et al.*, 2023). Our docking results suggest that 2,4-D and 2,4-DCP interact with residues critical for stabilizing RXRA with 9-cis-retinoic acid, potentially interfering with its function. RXRA forms heterodimers with other NRs, such as peroxisome proliferator-activated receptors (PPARs), which regulate vital processes like lipid metabolism (Valdez *et al.*, 2023; Li *et al.*, 2021).

Harada *et al.* (2016) showed that the toxic effects of 2,4-D on testicular function and testosterone metabolism are mediated by the PPARα receptor. Additionally, 2,4-D is recognized as a weak peroxisome proliferator (Hietanen *et al.*, 1985). PPARα is the main regulator of peroxisome proliferation in the liver, crucial for fatty acid oxidation by regulating genes involved in mitochondrial and peroxisomal β-oxidation (Tahri-Joutey *et al.*, 2021; Qiu *et al.*, 2023).

In male rats treated with 2,4-D for 14 days, increases in peroxisome proliferation and fatty acid β-oxidation were observed, along with a roughly 40% rise in hepatic glutathione reductase (GR) activity, indicating an antioxidant response (Hietanen *et al.*,

1985). This heightened peroxisomal activity may lead to excessive reactive oxygen species (ROS) generation, contributing to oxidative stress and liver damage (Qiu *et al.*, 2023).

In HepG2 cells, 2,4-D increased PPARβ expression, glucose consumption, and the expression of gluconeogenesis-related genes like FOXO1 and CREB (Sun *et al.*, 2018). Silencing PPARβ reversed these effects, suggesting that 2,4-D disrupts glucose metabolism through PPARβ dysregulation (Sun *et al.*, 2018). Other mechanisms may be involved, such as inhibition of the PI3K/AKT pathway and potential insulin resistance, which could increase gluconeogenesis (Świderska *et al.*, 2018; Savova *et al.*, 2023). Elevated PPARβ expression may enhance fatty acid β-oxidation, contributing to glucose production via gluconeogenesis from glycerol (Qiu *et al.*, 2023). These combined effects suggest that 2,4-D may act as an agonist for nuclear receptors like RXRA, PPARα, and PPARβ.

In contrast, while studies on 2,4-DCP are limited, it has been associated with decreased PPARα expression, lipid accumulation, and increased ROS in zebrafish embryos, indicating a possible inhibitory effect on RXRA (Tsukazawa *et al.*, 2022). These differences compared to 2,4-D may reflect 2,4-DCP's lower potential to interfere with metabolic pathways. Therefore, further studies using various biological models are needed to better understand the differing toxicity mechanisms of 2,4-D and 2,4-DCP.

4.3. Inhibition of MDM2 and HSP90AA1 can potentiates cellular stress and death

Docking results suggest that both 2,4-D and 2,4-DCP inhibit MDM2, a critical negative regulator of p53. Inhibition of MDM2 can lead to increased p53 activity, which promotes the expression of pro-apoptotic genes such as Bax and Puma, thereby enhancing apoptosis induction (Nag *et al.*, 2013). Additionally, both 2,4-D and 2,4-DCP appear to inhibit HSP90AA1, a molecular chaperone essential for maintaining protein homeostasis, particularly under cellular stress conditions like oxidative stress (Murshid *et al.*, 2013). Inhibition of HSP90AA1 may result in the accumulation of misfolded proteins, which increases apoptosis and proteotoxicity. These combined effects elevate susceptibility to cellular stress and contribute to the hepatotoxicity induced by these compounds (Murshid *et al.*, 2013; Peng *et al.*, 2022).

4.4. Proposed mechanism of 2,4-D and 2,4-DCP- induced hepatotoxicity

Based on our findings and the available literature, we propose a mechanism for the hepatotoxicity of 2,4-D and 2,4-DCP shown in Figure 7. It is highlighted proteins, pathways, and cellular processes potentially inhibited by both compounds. The inhibition of the PI3K/AKT pathway is likely responsible for the reduced antioxidant capacity, mitochondrial damage, and cell death observed in the literature following exposure to these substances. Additionally, the inhibition of HSP90AA1 and MDM2 activity further exacerbates the molecular stress and pro-apoptotic environment. The PI3K/AKT pathway inhibition may also contribute to metabolic effects, including the increased need for lipid oxidation to generate energy. However, due to a lack of data on 2,4-DCP toxicity, these effects are primarily supported by findings for 2,4-D.

Additionally, proteins and processes related to nuclear receptors that are shown to be affected by both 2,4-D and 2,4-DCP. However, the available toxicity data is insufficient to determine whether these pathways are inhibited or activated. While 2,4-D enhances the expression of PPARs and peroxisomes, 2,4-DCP seems to have the opposite effect, reducing PPAR expression and promoting lipid accumulation. More research is needed to clarify the role of these pathways in the hepatotoxicity induced by both compounds.

Figure 7. Proposed mechanism of 2,4-D and 2,4-DCP- induced hepatotoxicity. Targets, biological processes, and pathways inhibited by these chemicals are shown in red. Perturbed processes are highlighted in yellow. Events related to key events (KE) crucial for hepatotoxicity development are in purple. Triangles denote proteins and processes supported by literature only for 2,4-D, while diamonds indicate those specific to 2,4-DCP.

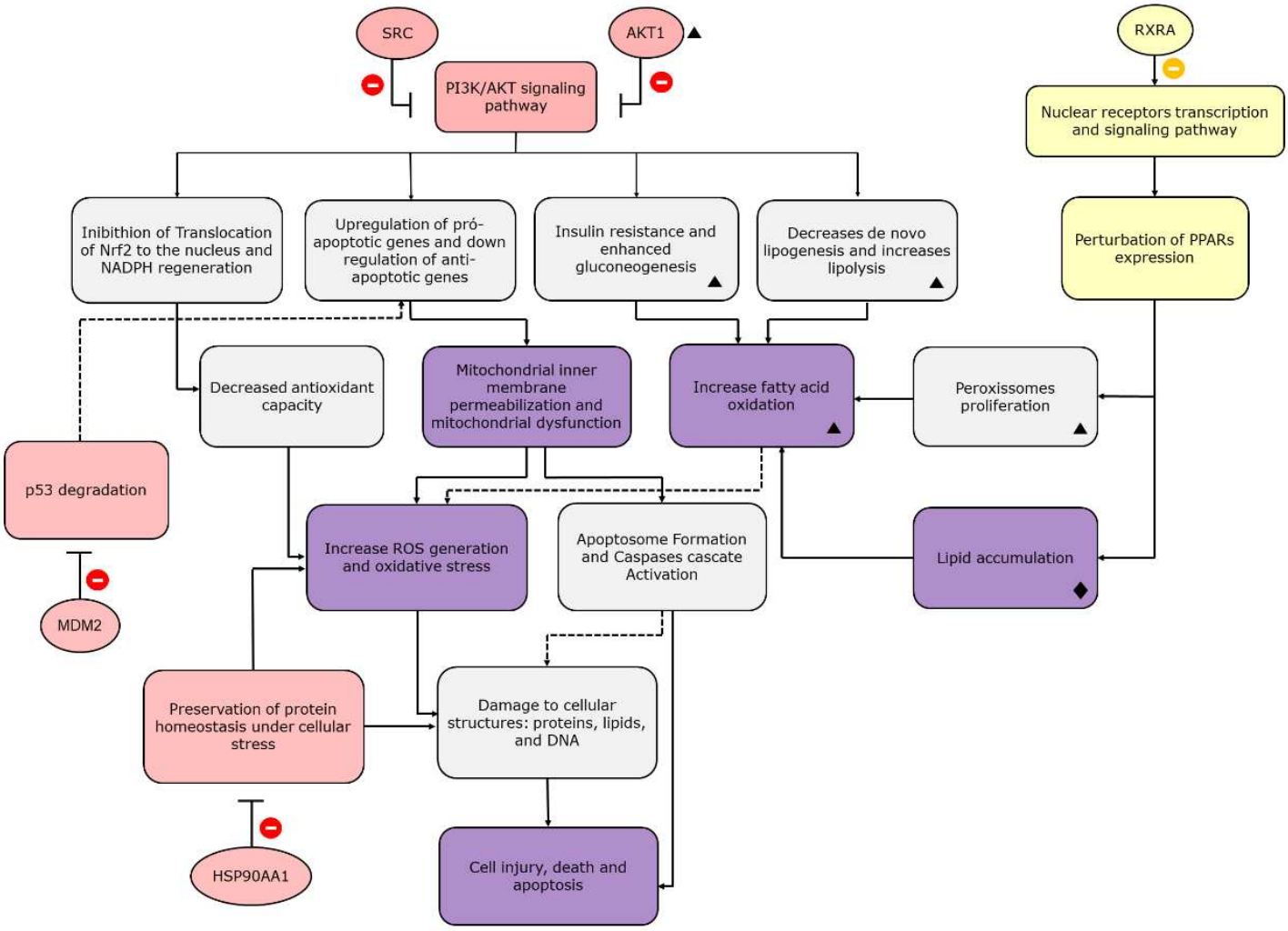

4.5. Considerations and future perspectives

This study offers valuable insights into the toxicity mechanisms of 2,4-D and 2,4-DCP, identifying, for the first time, specific molecular targets associated with their toxic effects. Key proteins, including SRC, AKT1, RXRA, HSP90AA1, and MDM2, were identified as critical regulators of pathways involved in hepatotoxicity. For example, HSP90AA1 is associated with stress resistance, while MDM2 plays a role in regulating cell death (Murshid *et al.*, 2013; Nag *et al.*, 2013). Additionally, SRC and AKT1 are integral to the PI3K/AKT signaling pathway, and RXRA serves as a central modulator of nuclear receptor activity (Li *et al.*, 2021; Fortner *et al.*, 2022; Valdez *et al.*, 2023).

These findings fill gaps in the literature by elucidating the molecular targets and pathways disrupted by these compounds. Moreover, the implications extend beyond hepatotoxicity, as the identified pathways are involved in other toxicological outcomes. For instance, 2,4-D has been linked to neurotoxicity, and disruptions in the PI3K/AKT pathway are associated with neurodegenerative diseases (Ueda *et al.*, 2021; Rai *et al.*, 2019).

From a clinical perspective, these findings could inform the management of intoxication cases. Regarding hepatotoxicity, studies have reported significant alterations in hepatic biomarkers, such as AST, ALT, ALP, and bilirubin, in models relevant to human health, including rodents and zebrafish (Fu *et al.*, 2016; Tichati *et al.*, 2020; Martins *et al.*, 2021). Furthermore, a notable human case known as the "Golf Ball Liver" highlighted the development of hepatitis following repeated exposure to 2,4-D from contaminated golf balls, with elevated levels of bilirubin, AST, ALT, γ-GT, and ALP (Leonard *et al.*, 1997). Oxidative stress, widely recognized as a key effect of 2,4-D and 2,4-DCP intoxication, has been a key focus in efforts to mitigate toxicity (Tichati *et al.*, 2020, Shafeeq and Mahboob, 2020; Shafeeq and Mahboob, 2021, Martins *et al.*, 2024). Previous studies have demonstrated success with antioxidant-enhancing compounds (such as magnesium, selenium, extra virgin olive oil and curcumin) to reduce oxidative damage and alleviate hepatotoxicity (Nakbi *et al.*, 2010; Nakbi *et al.*, 2012; Satapathy and Rao, 2018; Tichati *et al.*, 2020; Shafeeq and Mahboob, 2020; Shafeeq and Mahboob, 2021). Our findings suggest that targeted therapeutic approaches could be developed by modulating the disrupted pathways and targets, especially within the PI3K/AKT axis and nuclear receptor signaling pathways. These pathways are already being explored as potential therapeutic targets for liver diseases such as fibrosis and Non-alcoholic Fatty

Liver Disease (NAFLD) (Yang *et al.*, 2020; Shamsan *et al.*, 2024), and may offer a promising strategy for mitigating hepatotoxicity induced by 2,4-D and 2,4-DCP exposure.

The integration of network toxicology and molecular docking methodologies offers an efficient approach to identifying key targets and toxicity pathways (Huang, 2023). This in silico strategy not only reduces costs and time but also aligns with the ethical principles of the 3Rs by minimizing animal use in research (Huang, 2023). Nevertheless, certain limitations must be considered, including the need for experimental validation to confirm the biological relevance of the predicted interactions and the lack of specific information regarding concentrations and doses, which are essential to understanding the compounds effects under physiological conditions (He *et al.*, 2024). Furthermore, since different tools can yield varying results, it is essential to carefully document the methodology to ensure reproducibility and integrate multiple approaches for a more comprehensive and reliable understanding (Valls-Margarit *et al.*, 2023).

Despite these limitations, the findings of this study provide valuable direction for future research, enabling more targeted investigations into the toxicity of 2,4-D and 2,4-DCP and supporting the development of precise and effective therapeutic strategies.

5. Conclusions

This study highlights the shared molecular mechanisms of hepatotoxicity induced by the herbicide 2,4-D and its metabolite 2,4-DCP. Using an integrated approach with PPI network analysis, GO and Reactome pathway enrichment, and molecular docking, we identified key proteins and pathways disrupted by both compounds. The findings show that 2,4-D and 2,4-DCP target similar biological processes, including apoptosis, oxidative stress, mitochondrial dysfunction, and lipid metabolism impairment. Notably, the "metabolism" pathway was only identified for 2,4-D, suggesting differences in their toxic mechanisms. Key pathways like PI3K/AKT signaling and nuclear receptor-mediated transcription were central to both compounds. Molecular docking indicated direct interactions with proteins such as SRC, AKT1, RXRA, HSP90AA1 and MDM2. This is the first study to investigate pathways and targets of these compounds, providing insights into their environmental and health risks and potential therapeutic targets. Further experimental validation is needed to confirm these findings and their implications in vivo.

Acknowledgments

We thank the Universidade Federal do Ceará (UFC, Brazil), Universidade Federal da Paraíba (UFPB, Brazil), Fundação de Apoio à Pesquisa do Estado da Paraíba (FAPESQ, Brazil), Coordenação de Aperfeiçoamento de Pessoal de Nível Superior (CAPES, Brazil), and Conselho Nacional de Desenvolvimento Científco e Tecnológico (CNPq, Brazil) for supporting this research with grants and scholarships.

Author Contributions

Rafael Xavier Martins.: Conceptualization, Data curation, Formal analysis, Investigation, Methodology, Data curation, Visualization, Writing— original draft, review & editing and Projetc administration. Cleyton Gomes and Matheus Carvalho: Data curation, Methodology, Formal analysis. Juliana Alves da Costa Ribeiro Souza and Terezinha Souza: Methodology, Supervision, Writing—review & editing. Davi Farias: Conceptualization, Writing—review & editing, Supervision, Writing—review & editing, Resources, Funding acquisition and Projetc administration. All authors have read and agreed to the published version of the manuscript.

Conflicts of Interest

The authors declare that they have no known competing financial interests or personal relationships that could have appeared to influence the work reported in this paper.

Funding

This research was funded by Public Call n. 03 Produtividade em Pesquisa PROPESQ/PRPG/ UFPB, grant number PVA13245-2020, Public Call Demanda Universal FAPESQ, grant number 3045/2021.

4.3. Artigo 3

Nuclear receptor disruption mediates 2,4-Dichlorophenol-induced developmental toxicity: Evidence from network toxicology and zebrafish analysis

Rafael Xavier Martins[1,2], Romério de Oliveira Lima Filho[3], Cleyton de Sousa Gomes[2], Matheus Carvalho[2], Maria Eduarda de Souza Maia[1,2], Bianca Mataribu[4,5], Catarina Serrão[4,5], Marcos Vinicius Porto Medeiros[2], Milena Pereira Arruda[2], Ana Julia Antunes de Magalhães[2], Juliana Alves da Costa Ribeiro Souza[2], Thaís Feitosa Guimarães[2], Luis Fernando Marques-Santos[4,5], Ana Carolina Luchiari[3], Sílvia Regina Batistuzzo de Medeiros[6], Terezinha Souza[2], Davi Farias[1,2,*]

[1]Post-Graduation Program in Biochemistry, Department of Biochemistry and Molecular Biology, Building 907, Campus Pici, Federal University of Ceará, 60455-970 Fortaleza, Brazil

[2]Laboratory for Risk Assessment of Novel Technologies, Department of Molecular Biology, Federal University of Paraiba, João Pessoa, 58050-085, Brazil

[3]FishLab, Department of Physiology & Behavior, Federal University of Rio Grande do Norte, Natal, RN, Brazil

[4]Post-Graduation Program in Biological Sciences, Center for Exact and Natural Sciences, Federal University of Paraiba, João Pessoa, 58050-085, Brazil

[5]Laboratory of Cell and Developmental Biology, Department of Molecular Biology, Federal University of Paraiba, João Pessoa, 58050-085, Brazil

[6]Department of Cell Biology and Genetics, Biosciences Center, Federal University of Rio Grande do Norte, Natal, RN, Brazil

[*]Corresponding author:

Professor Davi F. Farias

E-mail: davi@dbm.ufpb.br

Phone: +55-83-32167633

Graphical abstract

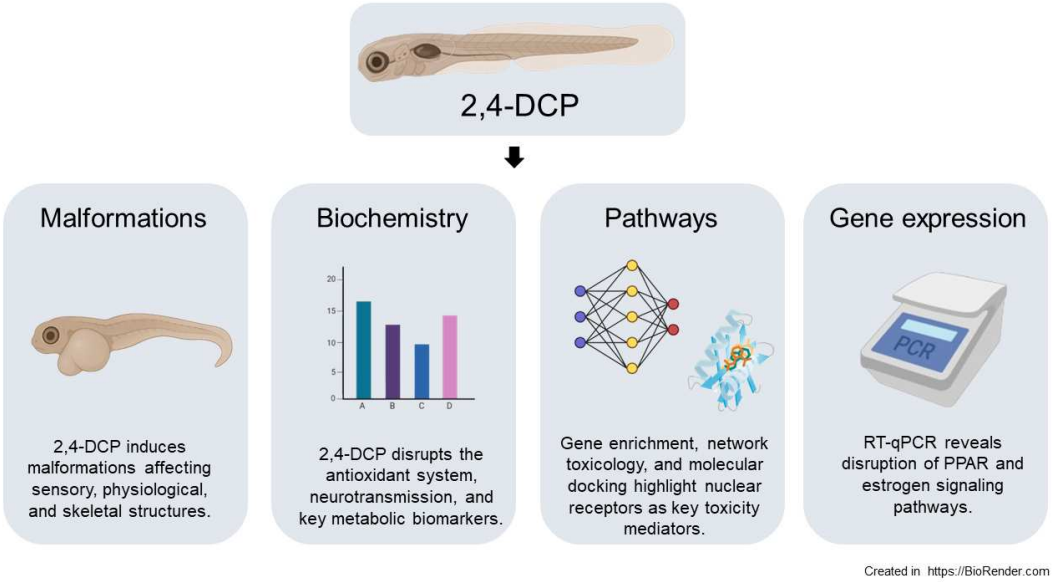

Abstract

2,4-Dichlorophenol (2,4-DCP) is an environmental pollutant associated with developmental toxicity in zebrafish (*Danio rerio*) embryos and larvae, though its underlying mechanisms remain poorly understood. This study investigated 2,4-DCP-induced toxicity through integrated morphological, biochemical, computational and molecular analyses. Acute exposure (2.5–20 mg/L) yielded a 144-h LC_{50} of 13.94 mg/L. Intermediate concentrations (10–15 mg/L) induced severe malformations, including yolk sac retention, pericardial and yolk sac edemas, and craniofacial, spinal, and tail deformities. In contrast, lower concentrations (2.5–5 mg/L) elicited subtle morphological alterations alongside disruptions in defense antioxidant system (CAT, GST, GPx, MDA), neurotransmission (AChE), and metabolic activity (LDH). Network toxicology, gene ontology, and pathway analyses identified nuclear receptors (NCOA1, RXRA, PPARG, ESR1) as key mediators of 2,4-DCP toxicity, influencing energy metabolism, skeletal development, antioxidant responses, and neurotransmission. Molecular docking confirmed stable interactions between 2,4-DCP and these targets, while gene expression analysis revealed perturbations in PPAR (*ppara*, *pparb*, *pparg*) and estrogen (*esr1*) signaling pathways. These findings highlight nuclear receptor signaling as a critical mechanism in 2,4-DCP-induced developmental toxicity, providing a foundation for future environmental risk assessments.

Keywords: Developmental malformations; organic contaminant; emerging contaminant; computational toxicology.

1. Introduction

Chlorophenols and their derivatives are widely used in agricultural and industrial applications, resulting in their pervasive presence as environmental contaminants in water, soil, and air (Igbinosa *et al.*, 2013; Dai *et al.*, 2021). Prominent examples include 2,4-dichlorophenoxyacetic acid (2,4-D), a globally applied herbicide, and triclosan (TCS), an antimicrobial agent frequently incorporated into personal care products (Zhang *et al.*, 2018; Magnoli *et al.*, 2020; Martins *et al.*, 2025).

Upon environmental release, chlorophenols undergo degradation through biotic (e.g., bacteria and/or fungal metabolism) and abiotic processes (e.g., photolysis, thermal breakdown), generating metabolites that often exhibit distinct physicochemical and toxicological properties compared to their parent compounds (Canosa *et al.*, 2005; Magnoli *et al.*, 2020).

Among these, 2,4-dichlorophenol (2,4-DCP) is recognized as one of the most abundant chlorophenols (CPs) in aquatic ecosystems and can originate from 2,4-D and triclosan degradation (Ma *et al.*, 2012; Park & Kim, 2018; Hu *et al.*, 2022). Due to its toxicity and persistence, 2,4-DCP is classified as a priority pollutant by regulatory agencies in China and the United States (USEPA, 1979; Liu *et al.*, 2018; Magnoli *et al.*, 2020; Zhang *et al.*, 2020).

In China, monitoring studies have reported 2,4-DCP in 51.3% of surface water samples collected from over 600 sites, with concentrations ranging from 0.01 to 19.96 μg/L (Gao *et al.*, 2008; Zhong *et al.*, 2010). Its presence has also been documented in French (0–4.89 μg/L), South Africa (0.1–10 μg/L), and Australia (0.1–6.72 μg/L) (Farounbi & Ngqwala, 2020; Pan *et al.*, 2021).

The environmental concern surrounding 2,4-DCP stems from its toxic effects on non-target organisms. In zebrafish (*Danio rerio*) embryos and larvae, exposure to 2,4-DCP has been linked to developmental toxicity (Zhang *et al.*, 2018; Dai *et al.*, 2021; Tsukazawa *et al.*, 2022).

Tsukazawa *et al.* (2022) demonstrated that 2,4-DCP induces malformations in zebrafish embryos, along with oxidative stress, lipid accumulation, and reduced expression of key genes such as *pparα*, *aco*, and *gpx*. Furthermore, Zhang *et al.* (2018) reported that 2,4-DCP increases embryo mortality and delays hatching. Additionally, Hu *et al.* (2022) revealed that 2,4-DCP acts as an endocrine disruptor, interfering with estrogenic responses,

increasing the number of primordial germ cells (PGCs) in zebrafish larvae, and leading to feminization.

Despite existing research, significant gaps remain in understanding the specific mechanisms underlying the developmental toxicity of 2,4-dichlorophenol (2,4-DCP). Zebrafish early stages serve as valuable models for toxicological studies due to their ability to link morphological and biochemical abnormalities with disruptions in physiological systems (Von Hellfeld *et al.*, 2020; Juan-Garcia *et al.*, 2020; De Oliveira *et al.*, 2023). For instance, impaired yolk sac absorption and altered lactate dehydrogenase (LDH) activity are indicative of metabolic disruption (Miyares *et al.*, 2014; Yang *et al.*, 2017; Martins *et al.*, 2021), while changes in spontaneous tail motility and acetylcholinesterase activity suggest neurotoxicity and compromised neurotransmission (Ton *et al.*, 2006; Gonzáles-Fraga *et al.*, 2019; Gaaied *et al.*, 2020). Furthermore, changes in ROS levels and antioxidant systems provide valuable insights into redox balance (Tsukazawa *et al.*, 2022).

Therefore, a detailed characterization of the malformations and associated biochemical changes induced by 2,4-DCP is crucial for advancing our understanding of its developmental toxicity. This study seeks to address this literature gap, as previous research has not specifically focused on these aspects (Zhang *et al.*, 2018; Tsukazawa *et al.*, 2022; Hu *et al.*, 2022).

Furthermore, despite previous studies demonstrating various effects of 2,4-DCP toxicity in zebrafish, the specific developmental targets and pathways remain poorly understood. Network toxicology and molecular docking offer valuable tools for elucidating these mechanisms (Souza *et al.*, 2023; Huang, 2023). Network toxicology integrates diverse data sources to construct interaction networks between chemicals and their biological targets, allowing for a systematic exploration of multi-target molecular mechanisms (Huang, 2023). Molecular docking complements this by predicting the binding affinities of compounds with target proteins, providing detailed insights into their interactions (Souza *et al.*, 2023; Huang, 2023; Martins *et al.*, 2025).

This study aims to enhance the understanding of 2,4-DCP's developmental toxicity by examining morphological and biochemical perturbation in zebrafish embryos and larvae and identifying key molecular targets and pathways through network toxicology and molecular docking approaches. We hypothesize that this mechanistic investigation will correlate with the observed *in vivo* effects, offering a comprehensive explanation of the molecular mechanisms underlying 2,4-DCP-induced developmental toxicity.

2. Material and Methods

2.1. Chemicals

2,4-dichlorophenol (2,4-DCP, CAS 120-83-2, Sigma-105953) was purchased from Sigma-Aldrich Co. (St. Louis, MO, USA) with a purity of 99%. For each exposure, 2,4-DCP was dissolved in E3 embryo medium to prepare a stock solution at 100 mg/L, which was subsequently diluted to obtain the desired concentrations (2.5, 5, 10, 15, and 20 mg/L). E3 medium was employed as the negative control and vehicle in the exposures, given the high water solubility of 2,4-DCP. All other reagents used in the study were of analytical grade.

2.2. Animals

Zebrafish embryos (AB strain) at 1 h post-fertilization (hpf) were obtained from the Production Unit for Alternative Model Organisms (UniPOM), Federal University of Paraíba, João Pessoa, Brazil. Six-month-old parental fish were maintained in a recirculating aquaculture system with monitored water quality (pH, ammonia, nitrite), temperature (26 ± 1 °C), and photoperiod (14:10 h light/dark). One day before the experiment, adults were placed in breeding tanks (male-to-female ratio: 2:1). Embryos were collected on the next day, incubated in E3 medium (5.0 mM NaCl, 0.17 mM KCl, 0.33 mM $CaCl_2$, 0.33 mM $MgSO_4$), and screened for viability (normal cleavage, no deformities) under a light microscope (Televal 31, Zeiss, Germany; 50× magnification). All procedures were approved by the Ethics Committee on Animal Use, Federal University of Paraíba (protocol No. 7468180624).

2.3. Acute exposure to 2,4-DCP

Acute toxicity tests were conducted following the Fish Embryo Acute Toxicity Test (FET test), OECD Protocol No. 236 (2013), with adaptations. Zebrafish embryos at 3 hpf were exposed to five concentrations of 2,4-DCP (2.5, 5, 10, 15, and 20 mg/L) over six days. The tested concentrations were based on Tsukazawa *et al.* (2022), which previously evaluated the acute toxicity of 2,4-DCP in zebrafish embryos. Experiments were repeated to account for strain-specific variation in zebrafish responses (Parichy, 2015) and to determine the susceptibility of our strain.

Exposures were conducted in 96-well plates, with each well containing a single embryo in 300 µL of exposure solution, using 20 embryos per concentration. A separate plate with 20 embryos exposed only to E3 medium was used as the negative control (and also solvent control), totaling 120 embryos per biological replicate. Well plates were sealed with plastic wrap to prevent evaporation. The plates were maintained in an incubator under a controlled photoperiod (14 h light / 10 h dark) and temperature (26 ± 1 °C). The pH of the exposure solutions was measured both before and after the assay to ensure stability throughout the experiment. Exposures were performed in triplicate.

Lethal and non-lethal effects were recorded daily over the six-day exposure period. Embryos exhibiting lethal effects (egg coagulation, failure to form somites, tail detachment, and absence of heartbeat) were considered dead. Non-lethal effects were identified following the guidelines of Von Hellfeld *et al.* (2020), which provide a detailed overview of developmental malformations in zebrafish embryos and larvae. The data were used to determine: (1) survival rate (% alive organisms/total organisms x 100) per concentration and exposure time; (2) cumulative lethal and non-lethal effects (% affected organisms/total organisms x 100) per concentration over 144 hours, and (3) mean lethal concentration (LC_{50}) calculated using a nonlinear regression analysis on GraphPad Prism 8.0.1.

2.4. Morphometric analysis

Morphometric analyses followed the methodology described by Ribeiro *et al.* (2020). All larvae were sourced from the experiment outlined in section 2.4. After 144 hours of exposure, larvae without visible malformations were selected, euthanized, and fixed in 4% paraformaldehyde for 4 hours. Subsequently, they were washed with PBS and stored in 70% ethanol until analysis. Fifteen larvae per group were randomly selected (five larvae per replicate), photographed using a microscope (Olympus BX41) equipped with a camera (Olympus Q-Color5), and analyzed with ImageJ software (v 1.54p). Morphometric parameters were divided into three categories: (i) sensory (eye diameter, maximum and minimum interocular distances); (ii) physiological (yolk sac, liver and pericardial areas); and (iii) skeletal structure (height, head width and depth, and larval length).

2.5. Biochemical markers of toxicity

To investigate the toxicity mechanisms induced by 2,4-DCP, we measured the enzymatic activity and levels of key biomarkers associated with: (i) antioxidant response and oxidative stress: catalase (CAT), glutathione S-transferase (GST), glutathione peroxidase (GPx) and malondialdehyde (MDA); (ii) neurotransmission: acetylcholinesterase (AChE); and (iii) metabolism: lactate dehydrogenase (LDH).

To this end, a new exposure experiment was conducted under the parameters outlined in section 2.4. Thirty zebrafish embryos (3 hpf) were exposed to two sublethal concentrations of 2,4-DCP for six days, with a control group maintained in E3 medium. After the exposure period, larvae without malformations were euthanized, collected, and placed into microtubes containing cold distilled water at a ratio of 20 µL per larva, resulting in a total larval extract volume of 600 µL.

The larvae were homogenized mechanically using a pestle and centrifuged at 10,000 ×g for 20 minutes to obtain the supernatant. The supernatant was then aliquoted for the different analyses as follows: 40 µL for total protein, 40 µL for GPx, 80 µL for LDH, 80 µL for GST, 80 µL for CAT, 80 µL for AChE, and 100 µL for MDA assays. Soluble protein content was measured using the Bradford method (1976). Adaptations of the Bradford method for protein quantification in zebrafish larval extracts were previously described by our research group (Martins *et al.*, 2024). GST and CAT activities were determined according to Domingues and Gravato (2018), while GPx activity followed the protocol of Massarsky *et al.* (2017). LDH activity was assessed as described by Domingues *et al.* (2010), and AChE activity was measured following Ellman's method (1961). MDA levels were measured using the method by Draper and Hadley (1990). Readings were performed in a 96-well microplate spectrophotometer (Thermo Scientific™ Multiskan™ GO) at specific wavelengths for each assay: total proteins (595 nm), GST, LDH, and GPx (340 nm), CAT (240 nm), AChE (414 nm), and MDA (532 nm). All analyses were performed in quadruplicate for each sample to ensure reliability.

2.6. Network toxicology and molecular docking

Network analysis and molecular docking are powerful tools for identifying molecular targets and pathways involved in toxicity (Huang *et al.*, 2023; Souza *et al.*, 2023; Martins *et al.*, 2025). PPI networks reveal key proteins and pathways in toxicity, while molecular docking simulates toxicant-target interactions (Huang *et al.*, 2023). This study

combines these methods with functional enrichment analysis to investigate 2,4-DCP-induced developmental toxicity in zebrafish, focusing on affected pathways and molecular targets. Supplementary Figure 1 illustrates the workflow of the applied methodology.

Although developmental toxicity mechanisms of 2,4-DCP are not well-defined, evidences suggests the involvement of nuclear receptor signaling, particularly through the perturbation of *ppara* (PPAR-related) and *esr2a* (estrogen-related) genes (Hu *et al.*, 2022; Tsukazawa *et al.*, 2022). The following methodology will provide a stronger mechanistic basis for these findings and help identify novel targets and toxicity pathways.

2.6.1. Identification of 2,4-DCP Targets Linked to Developmental Toxicity

The canonical SMILES of 2,4-DCP were obtained from PubChem (https://pubchem.ncbi.nlm.nih.gov) and analyzed using PharmMapper (http://www.lilab-ecust.cn/pharmmapper/) and Swiss Target Prediction (http://www.swisstargetprediction.ch) to identify potential target genes. To identify developmental toxicity-related genes, we searched the GeneCards (https://www.genecards.org/) and Online Mendelian Inheritance in Man (OMIM, http://omim.org/) databases using the keyword "developmental toxicity," restricting the search to *Homo sapiens*. The resulting targets were standardized to gene names using the UniProt database (https://www.uniprot.org/) and redundant entries were removed.

Finally, 2,4-DCP target genes and developmental toxicity-related genes were compared using the Draw Venn Diagram tool (http://bioinformatics.psb.ugent.be/webtools/Venn/). The overlapping genes were used for PPI network construction and functional enrichment analysis.

2.6.2. PPI network building

Developmental toxicity-related genes associated with 2,4-DCP were imported into the STRING database (https://string-db.org) for the construction of a protein-protein interaction (PPI) network. The network was generated using experimentally derived data, restricted to the *Homo sapiens* species, with a minimum required interaction score of 0.9 (highest confidence). Although the analysis was based on human data, its application to zebrafish studies is justified by the high genomic homology between humans and zebrafish (approximately 70%), which translates into significant biological similarities, such

embryogenesis and responses to toxicants (Howe *et al.*, 2013). Disconnected nodes were excluded from the network.

The resulting PPI network was imported into Cytoscape 3.10.0 for visualization and analysis. Central nodes were identified using the parameters *degree* and *betweenness centrality* (BC). The degree quantifies a node's connections within the network, highlighting its role in information transmission, while BC indicates a node's capacity to bridge other nodes and maintain connectivity. Then, the cytoHubba plugin was used to identify the top five hub nodes based on degree values, providing insights into the most interconnected nodes.

2.6.3. Functional genes enrichment

The intersection of 2,4-DCP and developmental toxicity-related genes was analyzed for functional enrichment using ConsensusPath DB (http://cpdb.molgen.mpg.de). Gene Ontology (GO) enrichment analysis was performed to identify associated biological processes (BP), cellular components (CC), and molecular functions (MF) of the genes. Additionally, Reactome Pathway analysis was conducted to determine the pathways linked to these genes. GO terms and Reactome Pathways with a p-value < 0.01 were considered statistically significant. All enrichment graphs were constructed using specific Python (v. 3.11.1) libraries: matplotlib (v 3.8.2; https://matplotlib.org/stable/project/citi ng.html), pandas (v 1.5.2; https://pandas.pydata.org/about/citing. html), scipy (v, 1.13.0; https://scipy.org/citing-scipy/), and numpy (v 1.24.0; https://numpy.org/citing-numpy/) (Hunter, 2007; Harris *et al.*, 2020; Virtanen *et al.*, 2020; The pandas development team, 2022).

2.6.4. Molecular docking

To investigate the potential interactions of 2,4-DCP with key network hubs, molecular docking simulations were performed. The 3D structure of 2,4-DCP was retrieved from the PubChem database (https://pubchem.ncbi.nlm.nih.gov) in SDF format. Protein crystal structures were obtained from the RCSB Protein Data Bank (https://www.rcsb.org). A positive control was designated for each protein, generally corresponding to the co-crystallized ligand from the respective PDB structure. However, in the case of NCOA2, 2,4-D, a parent compound of 2,4-DCP, was employed as an alternative. This substitution

was implemented because the co-crystallized ligand for NCOA2 was unsuitable for docking simulations due to its excessive size.

Protein structures were prepared by removing water molecules, unwanted cofactors, and ligands, followed by the addition of polar hydrogens using Discovery Studio 2021. Structural energy minimization was performed with Swiss-PdbViewer 4.1.0 (https://spdbv.unil.ch/). Docking simulations were conducted using AutoDock Vina (Trott and Olson, 2010), with a grid box size of 20 × 20 × 20 Å. The xyz grid box coordinates, PDB IDs, and resolutions of the proteins used in docking are detailed in Supplementary Table 1, while information on the molecules used as positive controls is provided in Supplementary Table 2. Docking poses with the lowest binding energy were selected for further analysis, and the results were analyzed and visualized using BIOVIA Discovery Studio 2021 visualizer (Discovery Studio Visualizer v21.1.0.20298).

2.7. Gene expression analysis (RT-qPCR)

To validate the toxicity mechanisms suggested by network analysis and molecular docking, gene expression was evaluated in zebrafish larvae exposed to 0, 50, or 500 µg/L of 2,4-DCP under the conditions described in Section 2.4. These concentrations were selected based on a previously observed disruptive level (5 mg/L), scaled down by 10- and 100-fold to assess sublethal effects. The rationale for using lower concentrations in the gene expression analysis was the pronounced disruption of morphological and biochemical markers observed at 2.5 and 5 mg/L. Typically, gene expression changes precede these effects and are highly sensitive to chemical perturbations (Hermsen *et al.*, 2011; Velki *et al.*, 2017).

For each experimental group, three pools of 15 larvae were collected and stored in RNA-Later (Sigma-Aldrich®) at −20°C. Total RNA was extracted using the PureLink® RNA Mini Kit (Thermo Fisher Scientific), with purity verified by Nanodrop 2000. cDNA was synthesized using the High-Capacity cDNA Reverse Transcription Kit (Applied Biosystems).

Gene expression was quantified via Rt-qPCR with SYBR Green PCR Master Mix (Applied Biosystems) on a StepOne Real-Time PCR system (Thermo Fisher), using the following protocol: 95°C for 10 min, 40 cycles of 95°C for 15 s and 60°C for 60 s, followed by melt curve analysis. β-actin served as the reference gene, and expression was calculated

using the 2−ΔΔCt method (Livak and Schmittgen, 2001). The samples were analyzed in technical duplicates.

Target genes were prioritized for their roles in PPAR (*ppara*, *pparb*, *pparg*), and estrogen (*esr1*) signaling pathways linked to 2,4-DCP toxicity by network toxicology analysis. Together, these genes represent key mechanisms indicated by the top five hub nodes of the PPI network and gene enrichment analysis. *akt1* (PI3K/AKT pathway) and *shha* (developmental regulation) were included to evaluate potential non-nuclear receptor mechanisms.

Primers for *akt1*, *ppara*, *esr1*, and *β-actin* were obtained from previous studies in the literature, while primers for *pparb*, *pparg*, and *shha* were designed using the Primer3Plus tool (https://www.primer3plus.com). The specificity of all primers was evaluated using the NCBI Primer-BLAST tool (https://blast.ncbi.nlm.nih.gov/Blast.cgi). Primer sequences, their respective functions, amplicon sizes, references, and the sequences used are provided in Supplementary Table 3.

2.8. Statistical Analysis

The data were analyzed using GraphPad Prism 8.0.1. First, the normality and homoscedasticity of the data were assessed using the Shapiro-Wilk and Bartlett's tests, respectively. For normally distributed data, one-way ANOVA followed by Tukey's post hoc test was applied. For non-parametric data, the Kruskal-Wallis test was used. Statistical significance was set at $p \leq 0.05$.

3. Results

3.1. Acute toxicity assay

The developmental toxicity of 2,4-DCP was evaluated in zebrafish embryos and larvae over a 144-hour exposure period at concentrations ranging from 0 (control) to 20 mg/L. Survival rates exhibited a concentration- and time-dependent decline, with the highest mortality observed at 20 and 15 mg/L (Figure 1A). Key lethality indicators, including egg coagulation, absence of heartbeat, and delayed coagulation, were observed, and the 144-hour LC_{50} was calculated to be 13.94 mg/L with a 95% confidence interval (8.332 to 24.07 mg/L).

We also identified sub-lethal effects, with greater prevalence at 10 and 15 mg/L, though occurring less frequently at 2.5 and 5 mg/L. As illustrated in Figure 1B, the effects were categorized into no effects, sub-lethal effects, and mortality, revealing a concentration-dependent increase in both sub-lethal effects and mortality. The most common sub-lethal effects included reduced yolk sac reabsorption (RYSR), pericardial edema (PE), spinal malformations (SM), and tail malformations (TM) (Figure 1C). Other observed effects, such as yolk sac edema (YSED), craniofacial malformation (CM), and delayed hatching (HD), further highlight the developmental toxicity of 2,4-DCP. Figure 2 provides dark-field photographs of larvae (144 hpf) exhibiting these malformations.

Figure 1. Overview of the acute exposure test evaluating the effects of different concentrations of 2,4-DCP on zebrafish embryos and larvae over 144 hours. (A) Survival rates across different concentrations and exposure times. (B) Cumulative lethal and sublethal effects observed after 144 hours of exposure. (C) Prevalence of sublethal effects at each tested concentration, including pericardial edema (PE), cranial malformation (CM), spinal malformation (SM), reduced yolk sac resorption (RYSR), yolk sac edema and deformity (YSED), tail malformation (TM), and hatching delay (HD). A total of 20 animals per concentration was used (triplicate). Statistically significant differences between groups are indicated by asterisks (* = $p < 0.05$, ** = $p < 0.01$, *** = $p < 0.001$, **** = $p < 0.0001$). Respective p-values of groups showing significant differences compared with control: (A) 15 mg/L (96 h: $p = 0.027$; 120 h: $p = 0.0022$; 144 h: $p = 0.0015$); 20 mg/L (72, 96, 120, and 144 h: $p < 0.0001$). (B) 10 mg/L (no effects and sublethal effects: $p = 0.0010$); 15 mg/L (no effects: $p < 0.0001$; sublethal effects: $p = 0.0008$; mortality: $p = 0.0062$); 20 mg/L (no effects: $p < 0.0001$; mortality: $p < 0.0001$). (C) PE (10 mg/L: $p = 0.0056$; 15 mg/L: $p < 0.0001$); SM (10 mg/L: $p = 0.0041$; 15 mg/L: $p = 0.0060$); RYSR (10 and 15 mg/L: $p = 0.0012$); TM (15 mg/L: $p = 0.0031$).

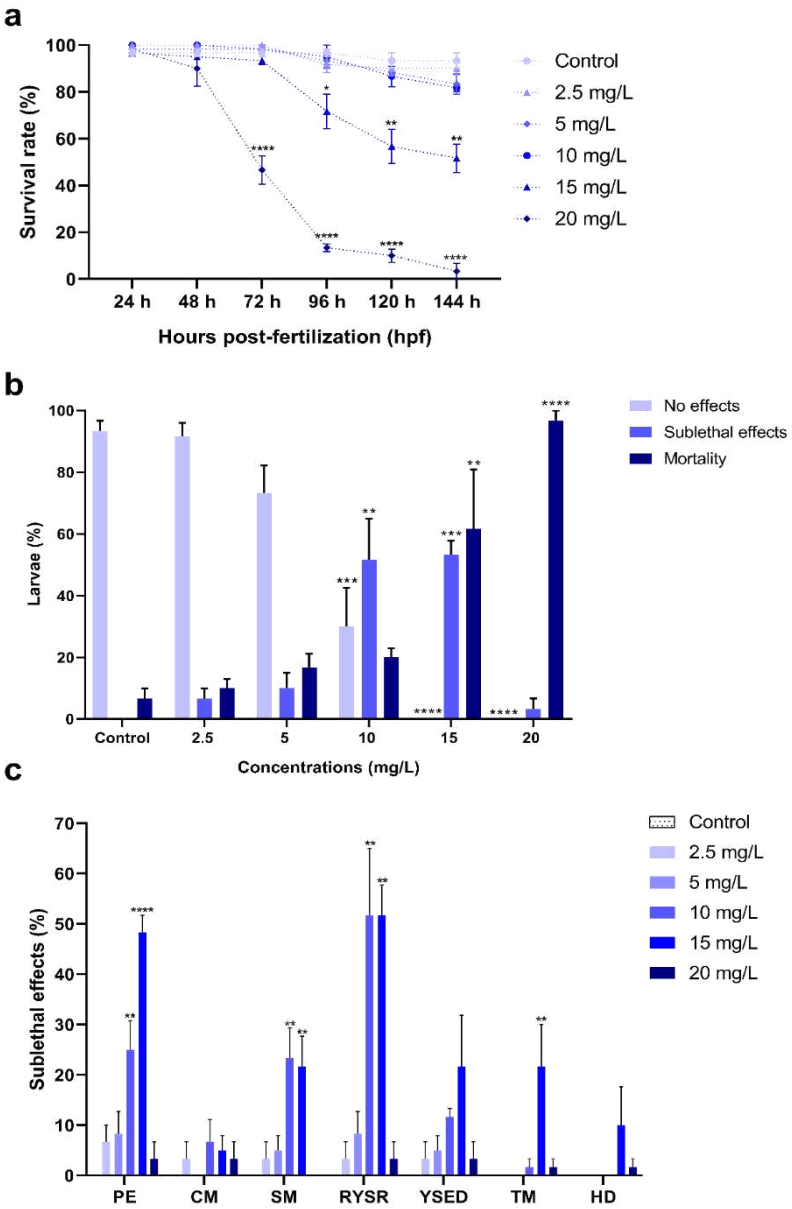

Figure 2. Sublethal effects on zebrafish larvae (144 hpf) exposed to varying concentrations of 2,4-DCP. (A) Control larva with no morphological alterations. (B and C) Larvae exposed to 2.5 and 5 mg/L of 2,4-DCP, respectively, exhibiting sublethal effects such as kyphosis (KPS), lordosis (LDS), reduced yolk sac resorption (RYSR), and tail malformation (TM). (D and E) Larvae exposed to 10 mg/L of 2,4-DCP, displaying sublethal effects including KPS, RYSR, TM, eye malformation (EM), craniofacial malformation (CM), pericardial edema (PE), and yolk sac edema (YSE). (F-H) Larvae exposed to 15 mg/L of 2,4-DCP, exhibiting sublethal effects similar to those observed at 10 mg/L but with greater severity, including pronounced yolk sac deformation (YSD). Images were captured using dark-field microscopy at a magnification of 4x.

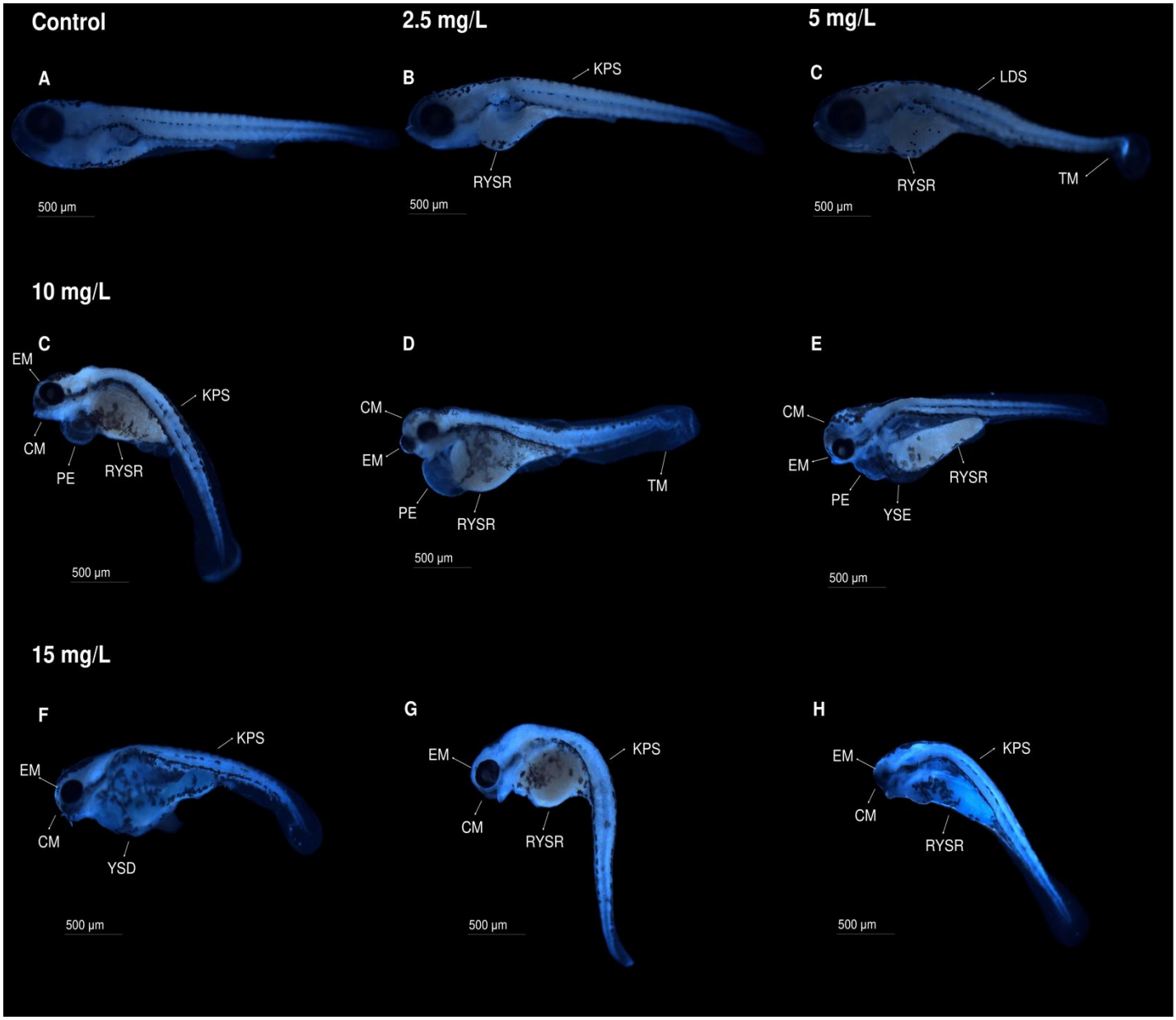

3.2. Morphometric analysis

Morphometric analyses revealed that the malformations induced by 2,4-DCP exposure extend beyond the visible abnormalities observed in the FET (Fish Embryo Acute Toxicity) test. Larvae exposed to 2.5 and 5 mg/L of 2,4-DCP, which did not exhibit apparent malformations, showed significant alterations in sensory, physiological, and skeletal structure parameters (Figure 3). A reduction in sensory parameters occurred at both concentrations, including decreased eye diameter and maximum interocular distance. Additionally, skeletal structure measurements, such as larval length, head width, and head height, showed significant reductions. Physiological parameters were also affected, with an increase in yolk sac size and a decrease in liver size. These measurements allowed for the detection of subtle alterations that were not evident in qualitative assessments alone.

Figure 3. Morphometric parameters of zebrafish larvae exposed to 2.5 and 5 mg/L of 2,4-DCP for 144 hours. n = 15 larvae per group (single replicate). Statistically significant differences between groups are indicated by different letters ($p < 0.05$). Larval length (2.5 mg/L: $p = 0.0075$; 5 mg/L: $p < 0.0001$), liver area (2.5 mg/L: $p < 0.0001$; 5 mg/L: $p = 0.0009$), yolk sac area (2.5 and 5 mg/L: $p < 0.0001$), pericardial area (2.5 mg/L: $p = 0.5712$; 5 mg/L: $p = 0.6293$), eye area (2.5 mg/L: $p = 0.0128$; 5 mg/L: $p < 0.0001$), maximum interocular distance (2.5 mg/L: $p = 0.0089$; 5 mg/L: $p = 0.0001$), minimum interocular distance (2.5 mg/L: $p = 0.4105$; 5 mg/L: $p > 0.9999$), head height (2.5 mg/L: $p = 0.0228$; 5 mg/L: $p = 0.0120$), head width (2.5 mg/L: $p = 0.0004$; 5 mg/L: $p = 0.0017$), head length (2.5 mg/L: $p = 0.9226$; 5 mg/L: $p = 0.4982$). Data for liver area, eye area, minimum interocular distance, and head width did not follow a normal distribution.

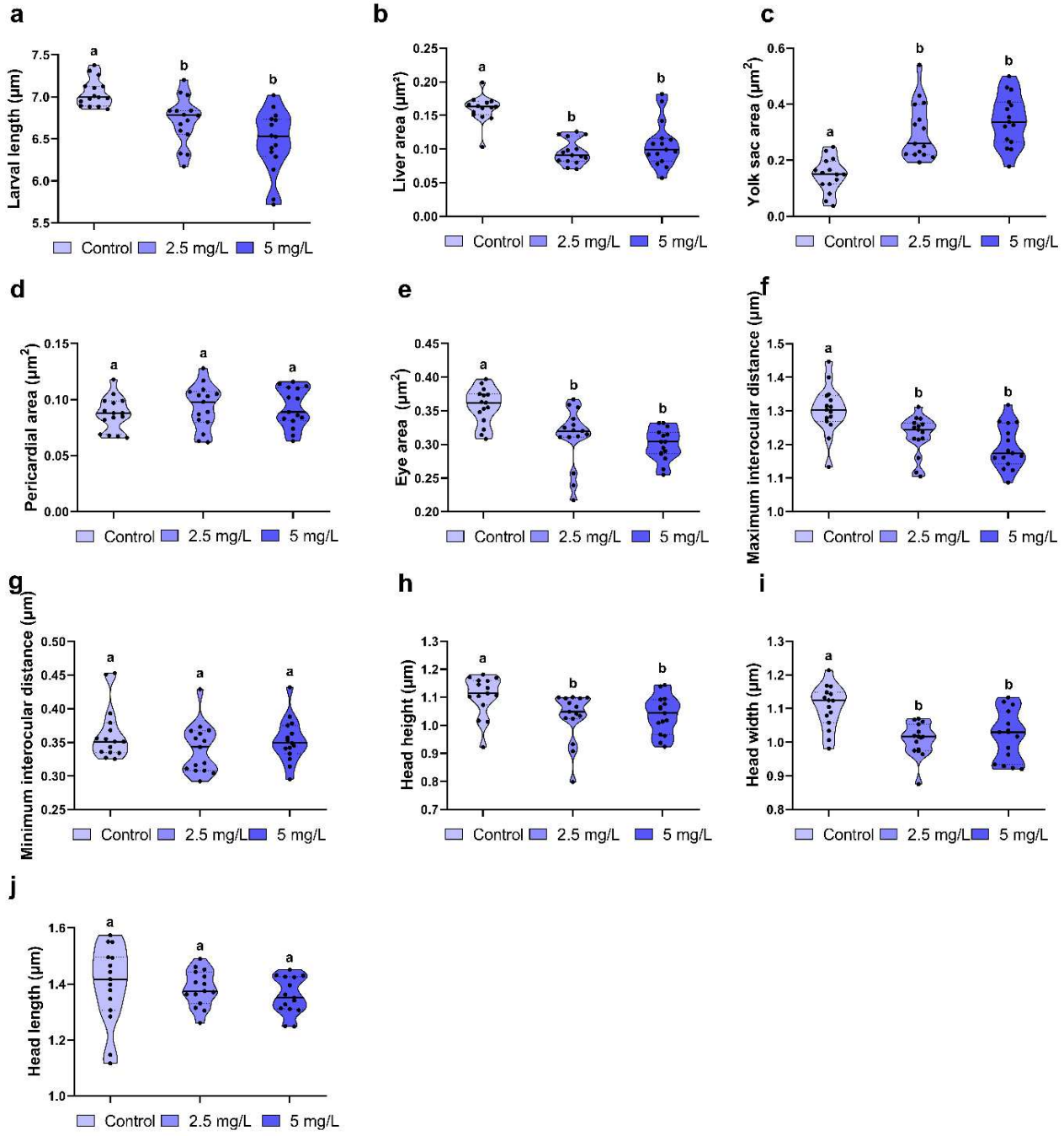

3.3. Biochemical toxicity markers

The results indicate that 2,4-DCP significantly disrupted all evaluated biomarkers (Figure 4). Activities of GST, GPx, and LDH were markedly elevated at both the lower (2.5 mg/L) and higher (5 mg/L) concentrations compared to the control group ($p < 0.05$). Specifically, GST activity increased from 103.39 ± 1.21 in the control group to 118.96 ± 1.83 and 121.63 ± 2.27 μmol/min/mg protein at 2.5 and 5 mg/L, respectively. Similarly, GPx activity rose from 5.91 ± 0.22 to 7.05 ± 0.29 and 7.04 ± 0.10 μmol/min/mg protein, while LDH activity increased from 165.25 ± 1.33 to 190.89 ± 1.94 and 247.89 ± 7.94 μmol/min/mg protein at the same concentrations.

In contrast, CAT andAChE activities exhibited significant alterations only at the higher concentration of 5 mg/L. CAT activity increased from 92.29 ± 50.42 to 155.24 ± 36.16 μmol/min/mg protein, and AChE activity rose from 293.68 ± 4.22 to 337.66 ± 15.62 μmol/min/mg protein. These findings demonstrate a concentration-dependent effect of 2,4-DCP on oxidative stress, metabolic and neurotransmission biomarkers in zebrafish, highlighting its potential to induce biochemical disruptions at these exposure levels.

Figure 4. Enzymatic activity levels of lactate dehydrogenase (LDH) (a), catalase (CAT) (b), acetylcholinesterase (AchE) (c), glutathione S-transferase (GST) (d), and glutathione peroxidase (GPx) (e), as well as malondialdehyde (MDA) (f) concentrations in zebrafish larvae exposed to increasing concentrations of 2,4-DCP for 144 hours. A total of 30 larvae per group were used to analyze all biomarkers (single replicate). Measurements were performed in technical quadruplicates. Results are presented as mean ± standard deviation. Significant differences between groups are indicated by asterisks (* = $p < 0.05$, ** = $p < 0.01$, *** = $p < 0.001$, **** = $p < 0.0001$). p-values of treated groups showing differences compared with control: LDH (2.5 and 5 mg/L: $p < 0.0001$); CAT (5 mg/L: $p = 0.0366$); AChE (5 mg/L: $p = 0.0132$); GST (2.5 and 5 mg/L: $p < 0.0001$); GPx (2.5 and 5 mg/L: $p = 0.0001$); MDA (2.5 mg/L: $p = 0.0337$; 5 mg/L: $p = 0.0132$). Only AChE data did not follow a normal distribution.

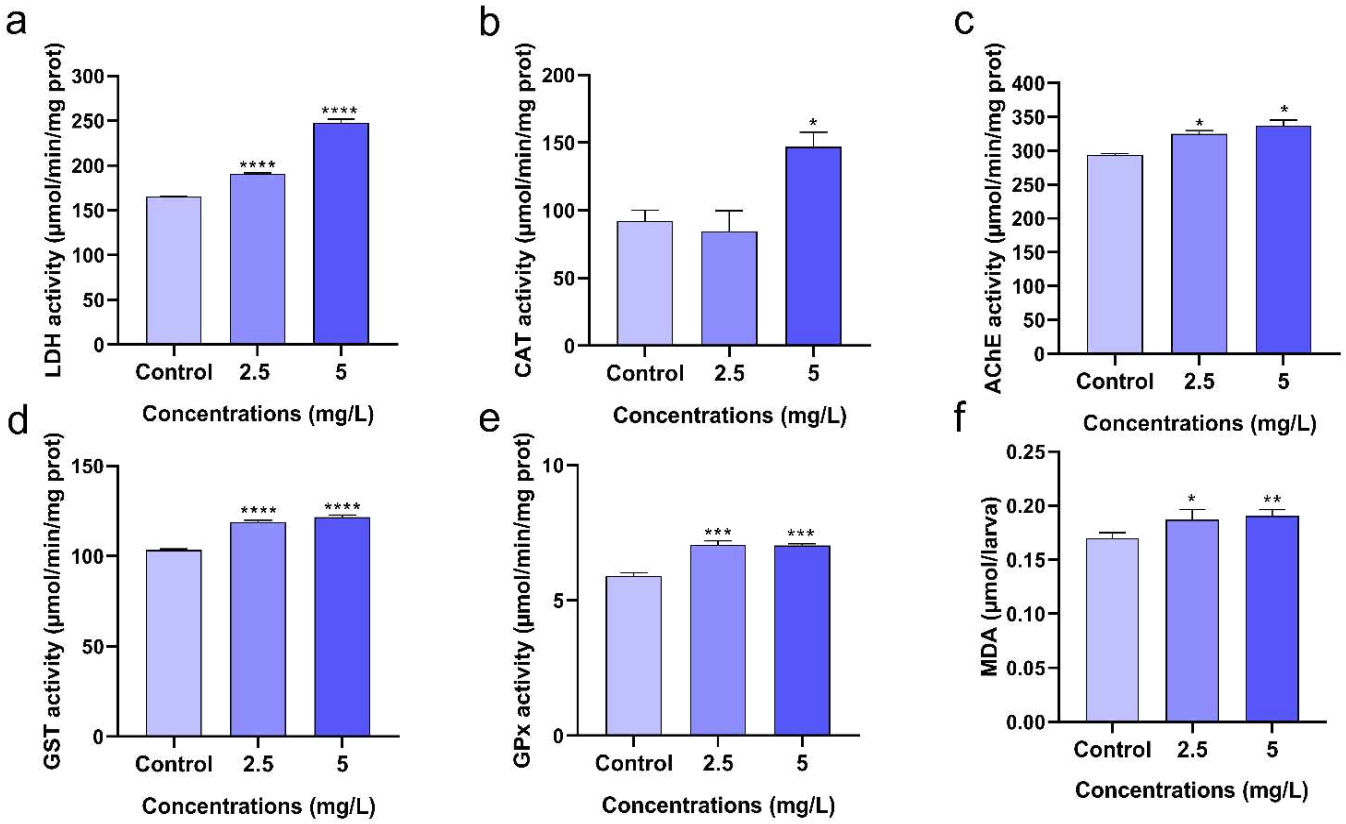

3.4. Identification of 2,4-DCP-induced developmental toxicity related genes

After standardization and removal of duplicate results, the Swiss Target Prediction and PharmMapper databases identified 187 potential targets for 2,4-DCP. In parallel, searches in GeneCards and OMIM databases returned 9,521 genes associated with developmental toxicity. Using a Venn diagram, we identified 170 targets of 2,4-DCP that are also linked to developmental toxicity (Figure 5A). These 170 genes were selected for subsequent analyses in this study.

Figure 5. (A) Venn diagram showing the overlap of target proteins related to 2,4-DCP and developmental toxicity (Dev. Tox.). (B) PPI network of targets related to 2,4-DCP-induced developmental toxicity. Nodes represent genes, and edges show interactions. Node size reflects degree and color intensity indicates BC. (C) Top five hub nodes by degree according Cytohubba plugin. Color intensity indicates high degree. (D) Heatmap of molecular docking interactions of 2,4-DCP with core targets. The y-axis lists the hub nodes, and the x-axis shows 2,4-DCP and the positive control for each protein. The color scale represents the predicted binding energy for each interaction. (E and F) Enrichment Analysis of Genes Associated with 2,4-DCP-induced developmental toxicity. (E) Top 10 GO terms for Cellular Component, Biological Process, and Molecular Function. (F) Top 15 Reactome pathways. In both panels, the x-axis shows the number of associated genes, and the color gradient from yellow to blue represents decreasing significance according FDR-values.

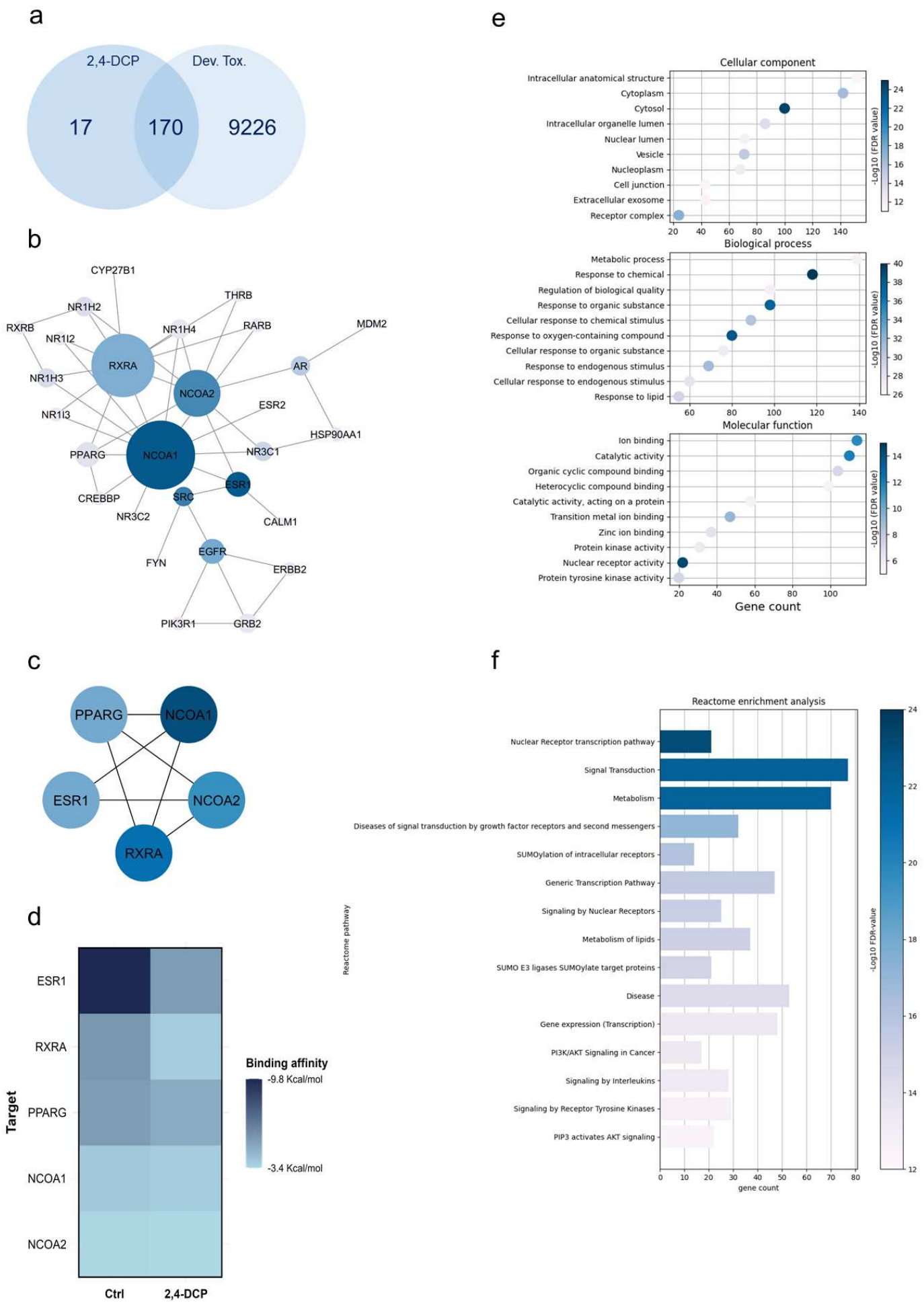
a
2,4-DCP
Dev. Tox.
17
170
9226
b
CYP27B1
THRB
NR1H2
RXRB
NR1H4
RARB
MDM2
NR1I2
RXRA
AR
NR1H3
NCOA2
ESR2
NR1I3
HSP90AA1
PPARG
NCOA1
NR3C1
ESR1
CREBBP
SRC
NR3C2
CALM1
EGFR
FYN
ERBB2
PIK3R1
GRB2
c
PPARG
NCOA1
ESR1
NCOA2
RXRA
d
Reactome pathway
ESR1
RXRA
PPARG
NCOA1
NCOA2
Target
Ctrl
2,4-DCP
Binding affinity
-9.8 Kcal/mol
-3.4 Kcal/mol
e
Cellular component
Intracellular anatomical structure
Cytoplasm
Cytosol
Intracellular organelle lumen
Nuclear lumen
Vesicle
Nucleoplasm
Cell junction
Extracellular exosome
Receptor complex
-Log10 (FDR value)
Biological process
Metabolic process
Response to chemical
Regulation of biological quality
Response to organic substance
Cellular response to chemical stimulus
Response to oxygen-containing compound
Cellular response to organic substance
Response to endogenous stimulus
Cellular response to endogenous stimulus
Response to lipid
Molecular function
Ion binding
Catalytic activity
Organic cyclic compound binding
Heterocyclic compound binding
Catalytic activity, acting on a protein
Transition metal ion binding
Zinc ion binding
Protein kinase activity
Nuclear receptor activity
Protein tyrosine kinase activity
Gene count
f
Reactome enrichment analysis
Nuclear Receptor transcription pathway
Signal Transduction
Metabolism
Diseases of signal transduction by growth factor receptors and second messengers
SUMOylation of intracellular receptors
Generic Transcription Pathway
Signaling by Nuclear Receptors
Metabolism of lipids
SUMO E3 ligases SUMOylate target proteins
Disease
Gene expression (Transcription)
PI3K/AKT Signaling in Cancer
Signaling by Interleukins
Signaling by Receptor Tyrosine Kinases
PIP3 activates AKT signaling
gene count
-Log10 FDR value

3.5. Building a PPI network

Using the 170 genes obtained from the Venn diagram, we constructed a protein-protein interaction (PPI) network using the STRING database, resulting in a network with 170 nodes and 52 edges. Subsequently, we removed disconnected nodes from the central network and imported the refined network into Cytoscape, obtaining a final network comprising 41 nodes and 52 edges.

In Cytoscape, we performed topological analyses to generate an enhanced and informative visualization, where node size is proportional to degree and color intensity reflects betweenness centrality (Figure 5B). Using the CytoHubba plugin, we identified the top five most influential nodes in the network based on degree: NCOA1, RXRA, NCOA2, PPARG, and ESR1, ranked in descending order of importance (Figure 5C). The full names of these proteins, along with their degree and betweenness centrality values, are provided in Supplementary Table 4. Notably, the top-ranking proteins are nuclear receptors, suggesting that they may represent a central mechanism underlying the developmental toxicity induced by 2,4-DCP.

3.6. Functional enrichment

We performed functional enrichment analysis of the genes using the ConsensusPathDB database. To minimize redundancy, the analysis was restricted to Gene Ontology (GO) categories at level 4. For Biological Processes (BP), Molecular Functions (MF), and Cellular Components (CC), we identified 506, 87, and 28 statistically significant results ($p < 0.01$), respectively. Figure 5E illustrates the top 10 GO terms for each category. For BP, the most relevant processes were "response to chemical," "response to organic substance," and "response to oxygen-containing compound." For CC, the top terms were "cytosol," "receptor complex," and "cytoplasm." For MF, the most significant terms were "nuclear receptor activity," "catalytic activity," and "ion binding."

Additionally, Reactome analysis returned 341 statistically significant results, with the top 15 pathways shown in Figure 5F. Among these, two pathways related to nuclear receptors were particularly notable: "Nuclear Receptor Transcription Pathways" and "Signaling by Nuclear Receptors." Other important pathways included "Signal Transduction" and "Metabolism."

.

3.7. Molecular docking

Figure 5D illustrates the binding energy of the interaction between 2,4-DCP and the top five proteins in the network, compared to their respective positive controls. The results demonstrate that 2,4-DCP interacts with all five proteins, with some binding energies being notably close to those of the positive controls, particularly for NCOA1, NCOA2, and PPARG. The specific interactions between 2,4-DCP and the amino acids of these proteins are depicted in Supplementary Figure 2. To evaluate the significance of these interactions, we conducted a literature review to assess the functional importance of the amino acids involved in 2,4-DCP binding, as well as to identify known inhibitors or activators that target the same residues.

2,4-DCP interacts with the Phe314 and Arg311 residues of NCOA1, which are critical for stabilizing interactions with transcription factors and cofactors, such as STAT6, thereby facilitating the transcriptional regulation of target genes (Russo *et al.*, 2017). 2,4-DCP also interacts with residues Tyr747 and Arg746 of NCOA2. Additionally, 2,4-DCP binds to key amino acids involved in the binding of 9-cis-retinoic acid, a metabolite of retinoic acid and an RXRA agonist (Egea *et al.*, 2000). Residues such as Ala271, Ala272, and Phe313 are essential for forming a hydrophobic pocket that stabilizes the ligand-binding domain (LBD).

Furthermore, 2,4-DCP interacts with the Phe404 residue of ESR1, which plays a crucial role in guiding and stabilizing hormonal binding within the ligand-binding domain (LBD) of the protein (Tanenbaum *et al.*, 1998). Regarding PPARG, 2,4-DCP interacts with residues Ile326, Leu330, Met329, Ala292, and Arg288. According to our docking simulations, these residues are also targeted by 4-chloro-6-fluoroisophthalamide, used as a positive control, which is an inverse agonist of PPARG (Orsi *et al.*, 2023).

It is important to note that docking was performed primarily to support the PPI network analysis and to explore potential interaction sites of 2,4-DCP. Although zebrafish possess several nuclear receptors orthologous to those in humans, ensuring functional similarity (Schaaf *et al.*, 2017), structural differences cannot be excluded and may influence binding affinity. Therefore, further modeling studies or resolution of zebrafish receptors by X-ray crystallography, followed by comparison with human structures, are required to strengthen translational relevance.

3.8. Gene expression

The results demonstrated significant alterations in the relative expression of all analyzed genes in response to exposure to both concentrations of 2,4-DCP (50 and 500 µg/L) (Figure 6). The following statistical outcomes were observed: *ppara* ($F(2,6) = 32.30$, $p = 0.006$), *pparb* ($F(2,4) = 113.8$, $p = 0.0003$), *pparg* ($F(2,6) = 42.60$, $p = 0.0003$), *esr1* ($F(2,4) = 249.4$, $p = 0.0001$), *akt1* ($F(2,5) = 11.30$, $p = 0.01$), and *shha* ($F(2,4) = 20.23$, $p = 0.008$).

Post hoc analysis revealed significant downregulation of *ppara* and *pparg* at both concentrations. Specifically, *ppara* expression decreased to 0.42-fold at 50 µg/L ($p = 0.0005$) and to 0.31-fold at 500 µg/L ($p = 0.002$), while *pparg* levels dropped to 0.53-fold at 50 µg/L ($p = 0.0003$) and to 0.49-fold at 500 µg/L ($p = 0.0005$). In contrast, *pparb* expression showed significant upregulation, increasing by 1.03-fold at 50 µg/L ($p = 0.0003$) and 0.69-fold at 500 µg/L ($p = 0.001$). Similarly, *esr1* expression increased at both concentrations, with 1.25-fold and 1.76-fold at 50 µg/L ($p = 0.001$) and 500 µg/L ($p < 0.0001$), respectively.

Notably, gene expression changes were not restricted to nuclear receptors. *akt1* was significantly downregulated at 50 µg/L (0.37-fold, $p = 0.009$), while *shha* showed reduced expression at both concentrations (50 µg/L: 0.44-fold, $p = 0.005$; 500 µg/L: 0.25-fold, $p = 0.03$).

Figure 6. Relative gene expression (Fold change) in zebrafish larvae exposed to 2,4-DCP (0, 50, and 500 µg/L) (n = 3 pools of 15 fry zebrafish per group). Mean and SEM are represented. Statistical results are expressed by ANOVA followed by Dunnett's multiple comparisons test, $p < 0.05$ *; $p < 0.01$ **; $p < 0.001$ ***; $p < 0.0001$ ****. p-values of treated groups showing differences compared with control: *ppara* (50 µg/L: p = 0.0005; 500 µg/L: p = 0.0021); *pparb* (50 µg/L: p = 0.0003; 500 µg/L: p = 0.0011); *pparg* (50 µg/L: p = 0.0003; 500 µg/L: p = 0.0005); *esr1* (50 µg/L: p = 0.0017; 500 µg/L: p < 0.0001); *akt1* (50 µg/L: p = 0.0095); *shha* (50 µg/L: p = 0.0059; 500 µg/L: p = 0.0399).

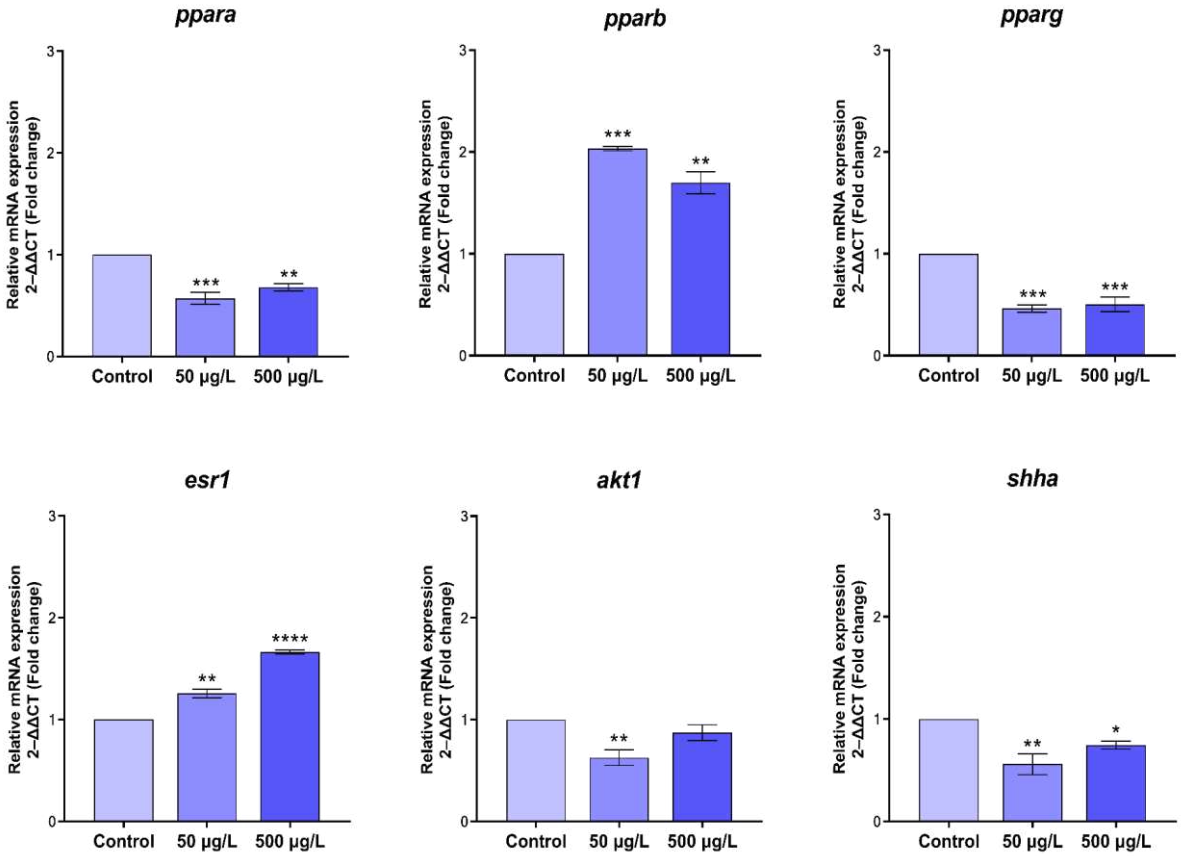

4. Discussion

Our results show that 2,4-DCP induces developmental toxicity in zebrafish embryos, causing lethality, morphological defects, biochemical and molecular disruptions. The 144 h LC_{50} was estimated at 13.94 mg/L. This value is much higher than those typically found in environmental matrices (0.01–19.96 µg/L), indicating that such concentrations are unlikely to cause significant acute toxicity (Gao *et al.*, 2008; Zhong *et al.*, 2010). However, studies using concentrations between 10 and 40 µg/L have shown that 2,4-DCP can act as an endocrine disruptor in zebrafish larvae, highlighting the need for additional toxicological assessment of environmentally relevant levels (Hu *et al.*, 2022).

Network toxicology, molecular docking and gene enrichment analyses suggest that *in vivo* effects stem from 2,4-DCP's interactions with key nuclear receptors, including NCOA1, RXRA, NCOA2, ESR1, and PPARG.

Nuclear receptors (NRs) are a superfamily of ligand-activated transcription factors that regulate gene expression and play essential roles in development and metabolism (Schaaf *et al.*, 2017). These receptors are well conserved among vertebrates. Zebrafish possess 73 NR genes, with orthologs of nearly all human NRs (Schaaf *et al.*, 2017). This conservation allows for preliminary mechanistic comparisons between species.

esr1 plays a central role in estrogen signaling, regulating processes such as reproductive development, cell differentiation, and neuroprotection (Schaaf *et al.*, 2017). *rxra* is a key receptor in retinoic acid signaling that forms heterodimers to regulate PPARs (*pparg, ppara, and pparb*) (Hernandez-Valdez *et al.*, 2023; Li *et al.*, 2021). *ncoa1* and *ncoa2*, members of the p160 coactivator family, act as broad regulators of gene expression, supporting signaling mediated by estrogen, retinoic acid, and PPARs (Sun and Xu, 2020).

Gene expression results revealed that 2,4-DCP disrupts PPAR (*ppara*, *pparb*, *pparg*) and estrogen (*esr1*) signaling, aligning with Network Toxicology predictions. To explore whether toxicity extends beyond nuclear receptor (NR) perturbation, we examined *akt1* (a PI3K/AKT pathway effector) and *shha* (a gene linked to malformations). Reactome analysis revealed PI3K/AKT-related pathways, such as PI3K/AKT signaling in cancer and PIP3 activates AKT signaling. *shha* is involved in key processes during zebrafish development, including organogenesis and the development of the nervous and skeletal systems (Male *et al.*, 2020; Wullimann and Umeasalugo, 2020; Braunstein *et al.*, 2021). Including these genes is important because, although nuclear receptors are strongly implicated by the *in sílico* analyses, additional mechanisms likely contribute to the observed malformations and biochemical alterations.

Interestingly, *akt1* was downregulated only at the lowest concentration, suggesting a potential adaptive response, while *shha* showed consistent downregulation.

Crosstalk between retinoic acid signaling and *shha* in zebrafish (Laforest *et al.*, 1998; Zhang *et al.*, 2015), as well as *shha-pparg* interactions in rat adipocytes (Yao *et al.*, 2019), suggests that *shha* dysregulation may indirectly reflect NR disruption. These findings highlight the central role of NRs in 2,4-DCP-induced developmental toxicity.

Considering that the receptors *ncoa1* and *ncoa2* play a more generalist role in supporting the expression of other nuclear receptors, this study further examines how the disruption of estrogen and PPAR signaling pathways contributes to 2,4-DCP-induced

developmental toxicity in zebrafish. The perturbation of these receptors likely disrupts critical biological pathways, providing a mechanistic basis for the observed *in vivo* effects.

4.1. Impacts on energy metabolism

Reduced yolk sac resorption, the most frequent sublethal effect observed in embryos exposed to 2,4-DCP, was evident even at lower concentrations (2.5 and 5 mg/L), where an increase in yolk sac size was noted. These alterations indicate disruptions in energy metabolism, as the yolk sac serves as the primary energy source during early development (Sant and Timme-lagary, 2018). This metabolic imbalance is further supported by increased LDH activity, suggesting a shift toward anaerobic glycolysis in response to cellular stress (Maharajan *et al.*, 2018; Muniz *et al.*, 2021).

Disruption of PPAR signaling also affects metabolic regulation. We found that both concentrations of 2,4-DCP suppressed *ppara* and *pparg* expression while upregulating *pparb*.

ppara primarily governs fatty acid oxidation, whereas *pparg* is central to adipocyte differentiation, lipid storage, and lipid homeostasis (Li *et al.*, 2024). In contrast, *pparb* is involved in fatty acid metabolism, energy metabolism, and cellular differentiation (Den Broeder *et al.*, 2015). Its upregulation may offset the suppression of other nuclear receptors, supporting metabolic balance under toxic stress

Previous studies have demonstrated the effects of 2,4-DCP on zebrafish energy metabolism. Tsukazawa *et al.* (2022) reported that embryos exposed to 2,4-DCP (2.5 mg/L) for five days exhibited lipid accumulation, coinciding with reduced expression of *ppara* and *ACO* (acyl-CoA oxidase), a key enzyme in peroxisomal fatty acid β-oxidation (Honda *et al.*, 2016). The downregulation of these genes disrupts fatty acid oxidation, ultimately promoting lipid retention in exposed embryos (Tsukazawa *et al.*, 2022). These findings are consistent with our *in vivo* observations, where impaired lipid metabolism correlated with delayed yolk sac resorption.

pparg dysfunction also has been implicated in lipid metabolism disorders and is considered a potential therapeutic target for hyperlipidemia in zebrafish larvae (Li *et al.*, 2024). Supporting this, exposure to T0070907, a *pparg* antagonist, resulted in enlarged and darkened yolk sacs in zebrafish embryos, likely due to suppressed expression of lipid transport and fatty acid oxidation genes (e.g., *apobb1*, *apoea*, *mttp*, *cpt2*), leading to lipid accumulation (Boom *et al.*, 2024). Furthermore, treatment with the *pparg* agonist rosiglitazone similarly induced yolk sac enlargement and downregulated lipid metabolism

genes (*apoea*, *mttp*) (Boom *et al.*, 2024). This suggests that yolk sac enlargement may serve as a common morphological endpoint for *pparg* disruption, irrespective of the underlying mechanism.

Estrogen signaling was also disrupted in animals exposed to 2,4-DCP. *esr1*, a key regulator of lipid metabolism, modulates critical processes such as adipogenesis, lipolysis, and hepatic lipid homeostasis (Qiu *et al.*, 2017). Impairment of *esr1* has been shown to downregulate genes involved in hepatic lipid and carbohydrate metabolism in rats (Khristi *et al.*, 2019). Similarly, zebrafish exposed to nonylphenol for 21 days exhibited reduced *esr1* expression, which correlated with disruptions in fatty acid biosynthesis (e.g., downregulation of *Srebf1* and *Fasn*) and the development of macrovesicular steatosis (Mukherjee *et al.*, 2022).

Endocrine disruption by 2,4-DCP has been well-documented in zebrafish. Larvae exposed to 2,4-DCP from 20 to 50 days post-fertilization (dpf) showed significantly decreased *esr1* expression (Zhang *et al.*, 2020). Comparable effects were observed in 5 dpf larvae following a 10-day exposure to 10 and 20 μg/L of 2,4-DCP (Hu *et al.*, 2022). Although less studied, *esr2* has also been implicated in 2,4-DCP toxicity mechanisms in zebrafish larvae, further reinforcing its role as an endocrine disruptor (Hu *et al.*, 2022).

4.2. Spine and cranial malformation

Larvae treated with 2,4-DCP exhibited various skeletal malformations, with the severity increasing at higher concentrations. These deformities included spinal abnormalities such as kyphosis and lordosis, as well as malformations of the tail and craniofacial structures. Even at lower concentrations, alterations in skeletal structure were apparent, including changes in head dimensions (width and height) and body length. Previous studies have reported similar skeletal malformations, including spinal curvatures and cranial cartilage deformities, in zebrafish larvae (120 h) exposed to a mixture of 2,4-DCP, triclosan, and 2,4,6-trichlorophenol. Our findings suggest that 2,4-DCP alone can induce skeletal malformations.

Interestingly, nuclear receptors are known to play a critical role in bone physiology, regulating processes such as osteogenesis and skeletal development (Imai *et al.*, 2013). Given this, the observed skeletal malformations may result from 2,4-DCP disrupting nuclear receptor signaling pathways, thereby interfering with bone metabolism in zebrafish larvae.

Estrogen receptors, such as ESR1, are crucial for maintaining bone health (Imai *et al.*, 2013). Alterations in the *esr1* gene have been linked to decreased bone mineral density (BMD), which contributes to increased bone turnover, reduced bone mass, and a higher risk of fractures in both men and women (Sowers *et al.*, 2004; Khosla *et al.*, 2004; Krela-Kaźmierczak *et al.*, 2019). Moreover, osteoclast-specific ER knockout female mice exhibit significant trabecular bone loss alongside high bone turnover metabolism (Imai *et al.*, 2013; Nakamura *et al.*, 2007).

The role of estrogen receptor signaling in bone metabolism has also been demonstrated in zebrafish. Larvae exposed to higher concentrations of 17-β estradiol (E2) exhibited severe craniofacial defects, whereas lower concentrations caused more subtle changes in head morphology (Pashae Ahi *et al.*, 2016). Additionally, a co-expressed gene network involved in larval head development (including *cpn1*, *dnajc3*, *lman1*, *rrbp1a*, *ssr1*, and *tram*) showed a stronger transcriptional response of *esr1*, underscoring its central role in craniofacial development (Pashae Ahi *et al.*, 2016)

Disruption of retinoic acid (RA) signaling has also been linked to skeletal malformations in zebrafish. Gray and Lovely (2024) showed that cranial neural crest cells (CNCCs) and pharyngeal endoderm cells are particularly sensitive to such disruptions, highlighting the essential role of the RXRA receptor. CNCCs are specialized embryonic stem cells derived from the neural tube border and play a critical role in craniofacial development. They migrate to the pharyngeal arches, where they condense and differentiate to form a substantial portion of the craniofacial skeleton (Depew *et al.*, 2002; Roth *et al.*, 2021). Likewise, the pharyngeal endoderm contributes to shaping the arches, giving rise to structures such as the jaw, branchial cartilages, and other craniofacial components (Hanaoka *et al.*, 2004).

It is important to note that retinoic acid signaling is also vital for the activation of other nuclear receptors, such as PPARs, whose expression was significantly altered following 2,4-DCP exposure (Schaaf *et al.*, 2017).

Studies suggest that PPARs also play critical roles in bone metabolism. In PPARα$^{-/-}$ mice, an increased bone marrow space was observed in males, indicating a role in bone marrow regulation (Wu *et al.*, 2000). Additionally, the PPARα-specific agonist bezafibrate has been shown to stimulate osteoblast differentiation and inhibit osteoclast formation *in vitro* (Takada *et al.*, 2000; Chan *et al.*, 2007). In rats, bezafibrate enhanced periosteal bone formation, increased femoral bone mineral density (BMD), and reduced bone marrow space, suggesting an anabolic effect on bones (Still *et al.*, 2008; Syversen *et al.*, 2009).

Conversely, *pparg* regulates bone marrow differentiation by promoting adipogenesis and inhibiting osteoblastogenesis. This can lead to increased bone marrow adiposity, reduced BMD, and impaired osteoblast differentiation, as observed in various *in vivo* and *in vitro* studies (Lecka-Czernik *et al.*, 2002; Ali *et al.*, 2005; Akune *et al.*, 2004; Rzonca *et al.*, 2004).

These findings suggest that disruption of estrogen, retinoic acid, and PPAR signaling pathways contributes to the skeletal abnormalities observed in zebrafish larvae. However, its important to note that other mechanisms can be envolved, such *shha* signaling inibithion. In zebrafish, it has been observed that *shha* inhibition disrupts osteoblast positioning and impairs proper skeletal branching and organization, resulting in less-branched and misaligned bones (Braunstein *et al.*, 2021). Data showing cross-talk between *shha* and nuclear receptors, including in zebrafish, suggest that these mechanisms may act concomitantly (Laforest *et al.*, 1998; Zhang *et al.*, 2015).

4.3. Sensory and neurotransmission disruptions

Larvae exposed to low concentrations of 2,4-DCP exhibited significant alterations in sensory morphometric parameters, including reduced eye diameter and maximum interocular distance. These changes may be a consequence of the craniofacial abnormalities previously described. However, 2,4-DCP also disrupted acetylcholinesterase (AChE) activity, a key enzyme in cholinergic neurotransmission (Ton *et al.*, 2006; Gaaied *et al.*, 2020). Given that AChE dysfunction can impair neuronal signaling, this disruption may negatively impact both neurological and sensory development in larvae (Ton *et al.*, 2006; Gaaied *et al.*, 2020).

Notably, in young zebrafish larvae (7–8 dpf), nearly half of their neurons are located in the eyes, which occupy approximately one-quarter of their total body volume (Zimmermann *et al.*, 2018). Thus, the observed morphometric alterations may also reflect underlying neurochemical disruptions induced by 2,4-DCP exposure.

The herbicide 2,4-D, the parent compound of 2,4-DCP, has been shown to affect the nervous system of zebrafish embryos and larvae. It increases apoptotic cells in the brain, disrupts catecholaminergic neurons, impairs cholinesterase activity, and alters swimming behavior (Ton *et al.*, 2006; Gaaied *et al.*, 2020). In addition, 2,4-D interferes with visually guided behaviors, such as prey capture, by disrupting the neural circuits involved in vision (Dehnert *et al.*, 2019).

Given that *in silico* analyses suggest overlapping toxicity mechanisms between 2,4-D and 2,4-DCP, including nuclear receptor disruption (Martins *et al.*, 2025), the evidence supports the hypothesis that 2,4-DCP may also induce neurotoxicity.

Nuclear receptor signaling pathways play a crucial role in neural development. Gray and Lovely (2024) demonstrated in zebrafish embryos that CNCCs are highly sensitive to disruptions RA signaling. During CNCC migration and morphogenesis, they observed co-expression of *rar*/*rxr* genes (encoding RA receptors such as RXRA) with sox10:eGFP, a CNCC-specific marker. These findings suggest that RA receptors are essential for CNCC development, likely regulating peripheral nervous system formation (Rocha *et al.*, 2019). Since CNCCs give rise to neurons and glia of the peripheral nervous system, 2,4-DCP-induced neurotoxicity may be linked to RA signaling disruption.

Retinoic acid signaling also regulates PPAR activity, which is crucial for neurodevelopment. 2,4-DCP is PPARα disruptor (Tsukazawa *et al.*, 2022) and *pparaa*/*pparab* are highly expressed in the developing zebrafish central nervous system. Their disruption leads to reduced proliferation of neural and glial precursor cells (Hsieh *et al.*, 2018). While *pparg* plays a neuroprotective role in humans and rodents by preventing neuroinflammation (Rijnsburger *et al.*, 2016; Pizcueta *et al.*, 2023), its function in zebrafish neurodevelopment remains poorly understood. However, our data suggest that neurotoxicity via nuclear receptor disruption is also occurring in zebrafish.

Estrogen receptor (ER) signaling is also essential for zebrafish neurodevelopment (Boueid *et al.*, 2023). Estradiol exposure reduces neural cell proliferation, as evidenced by fewer BrdU-positive cells in the thalamus, olfactory bulbs, telencephalon, and preoptic areas (Vaillant *et al.*, 2020). Furthermore, *esr2* knockout embryonic stem cells exhibit impaired neurogenesis and significant downregulation of *Hes3*, a key regulator of the Notch-Hes pathway involved in neural differentiation (Varshney *et al.*, 2017).

Notably, zebrafish larvae exposed to 2,4-DCP for 10 days show increased *esr2* expression, with docking studies confirming its interaction with the receptor (Hu *et al.*, 2022). These findings, aligned with the *esr1* disruption observed in our study, suggest that 2,4-DCP interferes with estrogen signaling, contributing to neurotoxicity.

Furthermore, reduced *shha* expression can also impair neurodevelopment. Shh/Shha signaling plays a crucial role in zebrafish neurodevelopment by regulating the proliferation and differentiation of radial glia-derived neuronal precursors, including dopaminergic, serotonergic, and GABAergic neurons (Male *et al.*, 2020). It is also essential for ventral patterning of the neural tube and proper formation of hypothalamic and basal

telencephalic structures (Wullimann and Umeasalugo, 2020). Disruption of *shha* expression impairs neurogenesis, alters neuronal migration, and compromises the organization of neural circuits (Male *et al.*, 2020; Wullimann and Umeasalugo, 2020).

4.4. Impacts on antioxidant responses

Biochemical analyses in this study indicate increased activity of the antioxidant enzymes CAT, GST, and GPx in response to 2,4-DCP exposure. CAT converts hydrogen peroxide (H_2O_2) into water and oxygen, reducing cellular oxidative stress. GST facilitates detoxification by conjugating electrophilic compounds with glutathione, while GPx neutralizes lipid peroxides and H_2O_2, protecting biomolecules from oxidative damage (Krysko *et al.*, 2010; Massarsky *et al.*, 2017).

Tsukazawa *et al.* (2022) demonstrated that zebrafish embryos exposed to 2.5 mg/L of 2,4-DCP exhibited elevated intracellular reactive oxygen species (ROS) levels, supporting our findings that increased antioxidant enzyme activity serves as an adaptive response to mitigate ROS-induced cellular damage. However, the elevated levels of malondialdehyde (MDA), a marker of lipid peroxidation (Rizzo *et al.*, 2024), suggest that this response was insufficient to fully prevent oxidative stress at both tested concentrations (2.5 and 5 mg/L), potentially leading to cellular and membrane damage. The increased activity of lactate dehydrogenase (LDH) further supports this hypothesis, as it indicates cellular and tissue injury (Arya *et al.*, 2010; Maharajan *et al.*, 2018; Martins *et al.*, 2021).

Elevated ROS levels and oxidative damage have also been linked to edema formation in zebrafish exposed to various environmental contaminants (Tanaka *et al.*, 2021; Huang *et al.*, 2022; Wang *et al.*, 2024). This may result from vascular damage, which increases tissue permeability and leads to abnormal fluid accumulation (Mittal *et al.*, 2014; Philip *et al.*, 2017), potentially explaining the pericardial and yolk sac edemas observed in this study.

Nuclear receptor disruption may further overwhelm antioxidant defenses, largely driven by lipid accumulation. Excessive fat deposition can compromises cellular antioxidant capacity through multiple pathways, including mitochondrial β-oxidation overload, upregulation of pro-oxidant enzymes, and the accumulation of toxic byproducts such as MDA (Pan *et al.*, 2018; Lan *et al.*, 2022). Supporting our founds, Tsukazawa *et al.* (2022) showed that 2,4-DCP exposure in zebrafish embryos led to increased ROS levels, reduced *ppara* expression, and lipid accumulation.

The inhibition of *ppara* impairs the expression of mitochondrial and peroxissomes β-oxidation genes, while *pparg* suppression favors pathological lipid storage. Their concurrent inhibition severely disrupts fatty acid catabolism (Fan and Evans, 2015; Todisco *et al.*, 2022), creating a cycle where lipid overload further burdens mitochondria, increases ROS production, and exacerbates cellular and tissues damages (Aqeel *et al.*, 2025). Estrogen signaling has also been associated with the inhibition of mitochondrial respiratory chain complexes, reduced ATP production, and increased ROS generation, further contributing to these mechanisms (Okoh *et al.*, 2011).

Moreover, there is evidence that nuclear receptors also regulate the antioxidant response. In mouse cardiomyocytes, retinoid signaling, together with PPARα and PGC-1α (a PPARγ coactivator), plays a crucial role in the antioxidant response to oxidative stress by regulating the transcription factor Nrf2, which controls the activation of antioxidant enzymes such as SOD and CAT (Ibarra-Lara *et al.*, 2025). There is also evidence that this correlation may occur in zebrafish. Embryos treated with perfluorooctanesulfonic acid (PFOS) exhibited an Nrf2-mediated antioxidant response with adaptive cross-talk between *ppara* and *pparg* (Sant *et al.*, 2018). These findings suggest that the suppression of *pparα* and *pparg* observed in this study may favor oxidative stress by limiting the antioxidant capacity.

Together, these findings suggest that oxidative stress induced by 2,4-DCP involves both direct ROS generation and nuclear receptor disruption. This may impair antioxidant defenses and contribute to the observed biochemical and morphological alterations. However, it is important to consider the potential involvement of other mechanisms, such as PI3K/AKT signaling. This pathway is essential for translocating the transcription factor Nrf2 to the nucleus and for maintaining adequate NADPH levels, which are critical for glutathione synthesis and the antioxidant response (Koundouros and Poulogiannis, 2018). The observed downregulation of *akt1* at 50 µg/L suggests that, under certain conditions, this mechanism may also contribute to redox imbalance and increased oxidative stress.

4.5. Considerations and future perspectives

This study provides novel mechanistic insights into 2,4-DCP toxicity in zebrafish. We characterized 2,4-DCP-induced alterations across multiple biological levels (morphological, biochemical, and molecular) and linked these effects to key systems, including energy metabolism, skeletal development, and neurotransmission. The observed correlation between molecular initiating events and multifaceted phenotypic outcomes

highlights a major advantage of the zebrafish model, which allows the assessment of a wide spectrum of toxicity endpoints during early development. Moreover, these mechanistic insights provide a robust foundation for future studies at environmentally relevant concentrations, facilitating the identification of the most sensitive pathways and endpoints under realistic exposure scenarios.

5. Conclusion

This study demonstrates that 2,4-DCP induces developmental toxicity in zebrafish, leading to increased lethality, morphological abnormalities, and both biochemical and molecular disruptions. Through network toxicology and molecular docking analyses, we identified nuclear receptors as key mediators of 2,4-DCP toxicity, with potential targets including NCOA1, NCOA2, RXRA, PPARG, and ESR1.

Gene expression results further confirm the involvement of nuclear receptors, particularly through the disruption of PPAR and estrogen signaling pathways. By integrating experimental data with existing literature, we established clear correlations between nuclear receptor activity and developmental outcomes such as skeletal malformations, impaired yolk sac absorption, and alterations in sensory function, neurotransmission, and oxidative stress responses.

These findings offer novel insights into the mechanisms underlying 2,4-DCP-induced developmental toxicity in zebrafish and contribute to a deeper understanding of its toxicological profile, supporting future efforts in toxicity assessment and mitigation strategies.

We recommend that future studies employ environmentally relevant concentrations and/or chronic experimental approachs to investigate whether the mechanisms described here are perturbed at such conditions. Identifying the most sensitive molecular, biochemical and phenotypic markers could guide the development of robust biomarkers for 2,4-DCP contamination in fish, thereby providing crucial data to inform regulatory agencies in establishing precise environmental safety guidelines for this contaminant.

CRediT authorship contribution statement

Rafael Xavier Martins: Conceptualization, Data curation, Formal analysis, Investigation, Methodology, Writing – original draft. **Romério de Oliveira Lima Filho**: Methodology, Formal analysis, Data curation. **Cleyton de Sousa Gomes**: Methodology, Formal analysis, Data curation. **Matheus Carvalho**: Methodology, Formal analysis, Data

curation. **Maria Eduarda de Souza Maia**: Methodology, Investigation. **Marcos Vinicius Porto Medeiros**: Methodology, Investigation. **Milena Pereira Arruda**: Methodology, Investigation. **Ana Julia Antunes de Magalhães**: Methodology, Investigation. **Juliana Alves da Costa Ribeiro Souza**: Methodology, Investigation. **Thaís Feitosa Guimarães**: Methodology, Investigation. **Bianca Mataribu**: Methodology, Formal analysis. **Catarina Serrão**: Methodology, Formal analysis. **Luis Fernando Marques-Santos**: Resources, Supervision, Writing – review & editing. **Ana Carolina Luchiari**: Resources. **Sílvia Regina Batistuzzo de Medeiros**: Resources. **Terezinha Souza**: Conceptualization, Writing – review & editing. **Davi Farias**: Conceptualization, Project administration, Resources, Supervision, Writing – review & editing.

Declaration of competing interest

The authors declare no conflicts of interest regarding the publication of this manuscript.

Acknowledgments

We thank the Universidade Federal do Ceara ´ (UFC, Brazil), Universidade Federal da Paraíba (UFPB, Brazil), Fundaçao ˜ de Apoio a ` Pesquisa do Estado da Paraíba (FAPESQ, Brazil), Coordenaçao ˜ de Aperfeiçoamento de Pessoal de Nível Superior (CAPES, Brazil), and Conselho Nacional de Desenvolvimento Científco e Tecnologico ´ (CNPq, Brazil) for supporting this research with grants and scholarships.

Funding

This research was funded by Public Call n. 03 Produtividade em Pesquisa PROPESQ/PRPG/ UFPB, grant number PVA13245-2020, Public Call Demanda Universal FAPESQ, grant number 3045/2021.

4.4. Artigo 4

Environmental Levels of 2,4-D Herbicide and its 2,4-DCP Metabolite Disrupt Hepatotoxicity-Related Mechanisms in Zebrafish Larvae

Rafael Xavier Martins[1,2], Marcos Vinicius Porto Medeiros[2], Catarina Serrão[3], Bianca Mataribu[3], Ana Julia Antunes de Magalhães[2], Romério de Oliveira Lima Filho[4], Wellington Lima da Silva Sobrinho[2], Kathia Beatriz Dantas de Lima[2], Micaelle Thaís Barros de Sousa[2], Josefa Gerlane da Silva[6], Rafael David Souto de Azevedo[6], Luis Fernando Marques-Santos[3], Ana Carolina Luchiari[4], Sílvia Regina Batistuzzo de Medeiros[6], Terezinha Souza[2], Davi Farias[1,2,*]

[1]Post-Graduation Program in Biochemistry, Department of Biochemistry and Molecular Biology, Building 907, Campus Pici, Federal University of Ceará, 60455-970 Fortaleza, Brazil

[2]Laboratory for Risk Assessment of Novel Technologies, Department of Molecular Biology, Federal University of Paraiba, João Pessoa, 58050-085, Brazil

[3]Laboratory of Cell and Developmental Biology, Department of Molecular Biology, Federal University of Paraiba, João Pessoa, 58050-085, Brazil

[4]FishLab, Department of Physiology & Behavior, Federal University of Rio Grande do Norte, Natal, RN, Brazil

[5]University of Pernambuco - UPE, Garanhuns Campus. 105 Captain Pedro Rodrigues Street. Garanhuns-PE, Brazil.

[6]Department of Cell Biology and Genetics, Biosciences Center, Federal University of Rio Grande do Norte, Natal, RN, Brazil

[*]Corresponding author:
Professor Davi F. Farias
E-mail: davi@dbm.ufpb.br
Phone: +55-83-32167633

Abstract

The herbicide 2,4-dichlorophenoxyacetic acid (2,4-D) and its major metabolite, 2,4-dichlorophenol (2,4-DCP), are widely detected in aquatic ecosystems. Although both compounds are known hepatotoxicants in vertebrates, their effects at environmentally relevant concentrations remain poorly understood. This study investigates the hepatotoxic potential of 2,4-D and 2,4-DCP (3–300 μg/L) in zebrafish larvae (Danio rerio) at concentrations mimicking environmental detection levels. The primary objective was to identify biological mechanisms most susceptible to disruption. To this end, 72 hpf larvae were exposed to the compounds for 72 hours, until reaching 144 hpf. Hepatic responses were evaluated using biochemical markers of hepatic damage (ALT, AST, ALP and LDH), oxidative and metabolic stress (SOD, CAT, GST, GPx, MDA and CS), lipid metabolism (TG, CT and Oil Red O), mitochondrial function (TMRE), intracellular ROS (H2DCF-DA), cell death (acridine orange), and gene expression analyses. Both compounds induced hepatotoxicity across all concentrations, mainly reflected by elevated ALT and AST activity. Overall, they disrupted antioxidant defenses, lipid metabolism, and mitochondrial function without triggering detectable cell death. Distinct mechanistic profiles were identified: (i) 2,4-D primarily impaired antioxidant defenses and increased oxidative damage, whereas (ii) 2,4-DCP caused stronger metabolic stress, characterized by enhanced lipid accumulation, suppression of pparα and pparγ and broad modulation of inflammatory and apoptotic pathways that appeared to prevent cell death. These findings demonstrate that environmentally relevant levels of 2,4-D and 2,4-DCP compromise hepatic homeostasis through compound-specific mechanisms and highlight sensitive pathways that may guide future risk assessment, inform regulatory strategies, and support toxicity mitigation efforts.

Keywords: Emerging contaminants; Biomarker analysis; Chlorophenols; Biochemical and molecular mechanisms

1. **Introduction**

Herbicides constitute the most widely sold category of agricultural inputs, accounting for approximately 47.5% of all pesticides applied to crops worldwide (Sharma *et al.*, 2019). Among them, 2,4-dichlorophenoxyacetic acid (2,4-D), a synthetic herbicide belonging to the phenoxyacetic acid class, is recognized for its high efficacy in controlling broadleaf weeds in crops such as rice, wheat, sorghum, sugarcane, and corn (Islam *et al.*, 2018; Martins *et al.*, 2024a).

Due to its widespread use, 2,4-D has become a major environmental contaminant, frequently detected in drinking water and other environmental samples. In Brazil, it has been the second most sold herbicide since 2013, with 51,872.24 tons marketed in 2023 (IBAMA, 2024). Monitoring data from 2014–2017 revealed its presence in 92% of public water supply samples from more than 2,300 municipalities. Although only two samples exceeded the Brazilian legal limit of 30 μg/L, 4,270 detections were above the European Union threshold of 0.1 μg/L (SISAGUA, 2018; Zuanazzi *et al.*, 2020). Moreover, elevated concentrations have also been reported in the country. According to the Environmental Company of the State of São Paulo (CETESB), concentrations as high as 366.6 μg/L were detected in rivers located in sugarcane-producing regions of the state (CETESB, 2018).

In the United States, 2,4-D ranked as the fifth most used herbicide in 2012, with concentrations of 0.1–12 μg/L reported in urban surface waters (Peterson *et al.*, 2016; ATSDR, 2020). Detection has also been documented in water bodies from other countries, including Spain (62–207 ng/L), Australia (3.5 ng/L), Iran (16.6 μg/L), and Greece (1.16 μg/L) (Rodil *et al.*, 2012; Yamini & Saleh, 2013; Tsaboula *et al.*, 2016; Meftaul *et al.*, 2020).

In the environment, 2,4-D undergoes biotic and abiotic degradation, yielding transformation products with distinct chemical properties (Magnoli *et al.*, 2020). 2,4-dichlorophenol (2,4-DCP), a major degradation product of 2,4-D and other organochlorines (e.g., triclosan), has been designated as a priority pollutant in China and the U.S. due to its persistence and toxicity (USEPA, 1979; Liu *et al.*, 2018; Zhang *et al.*, 2020).

In China, 2,4-DCP was detected in 51.3% of surface water samples from over 600 sites, with concentrations ranging from 0.01 to 19.96 μg/L (Gao *et al.*, 2008; Zhong *et al.*, 2010). In Brazil, a drinking water supply system in Minas Gerais showed 2,4-DCP concentrations ranging from 0.42 to 10.03 μg/L in untreated water and 2.94 to 3.33 μg/L

in treated water (Ramos *et al.*, 2021). Its presence has also reported in river waters in France (0–4.89 μg/L); surface waters in South Africa (0.1–10 μg/L) and wastewater in Australia (0.1–6.72 μg/L) (Farounbi & Ngqwala, 2020; Pan *et al.*, 2021).

The presence of 2,4-D and 2,4-DCP in the environment is a significant concern, as exposure to these compounds has been linked to hepatotoxic effects across multiple experimental models, including rodents, fish, and liver cell lines (Troudi *et al.*, 2012; Li *et al.*, 2013; Fu *et al.*, 2016; Tichati *et al.*, 2020; Martins *et al.*, 2021; Tichati *et al.*, 2021). *In vivo*, 2,4-D exposure has been associated with liver enlargement, histopathological alterations, changes in aminotransferase and alkaline phosphatase activity, oxidative stress, and decreased antioxidant defenses (Tichati *et al.*, 2020; Tichati *et al.*, 2021; Martins *et al.*, 2021). Likewise, 2,4-DCP has been shown to impair liver function by inducing histopathological damage, oxidative stress, mitochondrial dysfunction, and apoptosis, both *in vitro* and *in vivo* (Fu *et al.*, 2016; Li *et al.*, 2013).

Nevertheless, studies investigating the hepatotoxicity of this compounds at environmentally relevant concentrations remain scarce, limiting the risks assessment for real exposure scenarios. To bridge this knowledge gap, our research group previously employed an *in silico* approach, integrating network toxicology and molecular docking, which identified putative molecular targets and toxicity pathways for both compounds (Martins *et al.*, 2025).

This prior work predicted that 2,4-D and 2,4-DCP share common mechanisms, potentially disrupting key signaling cascades such as PI3K/AKT and nuclear receptors (e.g., PPARs), by interacting with critical proteins including SRC, AKT1, RXRA, HSP90AA1, and MDM2. The computational model futher predicted that such interactions could trigger key mechanisms of hepatotoxicity, including the induction of oxidative stress, dysregulation of lipid metabolism, mitochondrial dysfunction, and activation of cell death pathways (Arnesdotter *et al.*, 2021; Martins *et al.*, 2025). Building on these *in silico* predicions, the present study now aims to empirically validate these proposed mechanisms *in vivo* using a zebrafish model.

The zebrafish larvae is an effective model for assessing hepatotoxicity, given the structural and functional similarities of its liver with that of mammals, including humans (Shimizu *et al.*, 2023). By 72 hours post-fertilization (hpf), the liver is functional and perfused, allowing the measurement of key biochemical markers of hepatic injury, including alanine aminotransferase (ALT), aspartate aminotransferase (AST), and alkaline phosphatase (ALP) (Zhang *et al.*, 2017; Zhao *et al.*, 2019; Martins *et al.*, 2021).

Moreover, this model enables mechanistic investigations of hepatotoxic effects (such as oxidative stress, lipid metabolism dysregulation, mitochondrial dysfunction, and cell death) using biochemical assays, fluorescent probes, vital dyes, and RT-qPCR-based gene expression analysis (Mandal *et al.*, 2019; Smirnova *et al.*, 2021; Balamurugan *et al.*, 2022; Tsukazawa *et al.*, 2022).

This study investigates the hepatotoxic potential of environmentally relevant concentrations of 2,4-D and 2,4-DCP in zebrafish larvae, aiming to identify the biological mechanisms most susceptible to disruption. We hypothesize that such exposures will induce hepatic alterations and perturb key pathways, revealing distinct mechanistic susceptibilities between the two compounds.

2. Materials and methods

2.1. Animals

Zebrafish embryos (AB strain) were obtained from the Alternative Model Organism Production Unit (UniPOM) at the Federal University of Paraíba, João Pessoa, Brazil. Adult zebrafish (~6 months old) were housed in a recirculating aquaculture system with controlled water quality (pH, ammonia, nitrite), temperature (26 ± 1 °C), and a 14:10 h light/dark photoperiod. To induce spawning, adults were transferred to breeding tanks (male-to-female ratio 2:1). Fertilized embryos were collected the following morning and incubated in E3 embryo medium (5.0 mM NaCl, 0.17 mM KCl, 0.33 mM $CaCl_2$, 0.33 mM $MgSO_4$). Viability was assessed under stereomicroscope (Televal 31, Zeiss, Germany; 50× magnification), by selecting embryos exhibiting normal cleavage and absence of morphological abnormalities. Viable embryos were maintained in E3 medium at 28.5 ºC until 72 hours post-fertilization (hpf) for use in acute exposure experiments. All experimental procedures were conduced in accordance with ethical guidelines and were approved by the Animal Ethics Committee of the Federal University of Paraíba (Protocol No. 7468180624).

2.2. Chemicals and exposure solutions

2,4-Dichlorophenoxyacetic acid (2,4-D; CAS 94-75-7, Sigma-31518) and 2,4-Dichlorophenol (2,4-DCP; CAS 120-83-2, Sigma-105953) were purchased from Sigma-Aldrich Co. (St. Louis, MO, USA), both with a purity of 99%. For each exposure, the compounds were dissolved in E3 embryo medium to prepare a stock solution of 10 mg/L,

which was subsequently diluted to obtain the desired test concentrations of 3, 30, and 300 µg/L. The intermediate concentration (30 µg/L) corresponds to the maximum level allowed in drinking water according to Brazilian legislation (SISAGUA, 2018). The lowest concentration (3 µg/L) reflects environmentally relevant levels commonly found in waters bodies (Rodil *et al.*, 2012; Yamini & Saleh, 2013; Tsaboula *et al.*, 2016; Meftaul *et al.*, 2020), while the highest (300 µg/L) was used to assess potential concentration-dependent effects and simulate elevated contamination scenarios (CETESB, 2018). All other reagents were of analytical grade.

2.3. Acute exposure assays

Acute toxicity tests were performed following Martins *et al.* (2021), with minor modifications. Zebrafish larvae at 72 h post-fertilization (hpf) were exposed to 2,4-D and 2,4-DCP at concentrations of 3, 30, and 300 µg/L for 72 h. This exposure window was chosen because, at 72 hpf, larvae possess a functional liver and do not require exogenous feeding until 6 days post-fertilization (dpf) (Zhang *et al.*, 2017; Zhao *et al.*, 2019).

Exposures were conducted under static conditions (no medium renewal) in 96-well plates, with one larva per well in 300 µL of solution. Renewals were not conducted because the water half-lives of 2,4-D and 2,4-DCP are approximately 15 days (USEPA, 2015; Dehnert *et al.*, 2019; Gaaied *et al.*, 2020). To minimize evaporation, plates were covered with plastic wrap. A negative control (E3 medium only) was included. All plates were maintained in a climate-controlled chamber (Embryo, Scienlabor, Ribeirão Preto, Brazil) at 26 ± 1 °C under a 14:10 h light/dark cycle. The experiment was repeated for each biomarker analysis, varying only in the number of larvae and post-exposure procedures as detailed below.

2.4. Biochemical analyses

2.4.1. Assessment of hepatotoxicity markers

To assess whether the selected concentrations induce hepatic damage, we measured the activity of alanine aminotransferase (ALT), aspartate aminotransferase (AST), and alkaline phosphatase (ALP) enzymes, which are considered gold-standard biomarkers for detecting liver toxicity in larval zebrafish (Zhang *et al.*, 2017; Zhao *et al.*, 2019; Martins *et al.*, 2021). In addition, we measured lactate dehydrogenase (LDH) activity, a key indicator of cellular damage and impaired oxygen availability (Laganà *et al.*, 2019).

The methodology was based on Martins *et al.* (2021), with minor modifications on time exposure. Acute exposure to 2,4-D and 2,4-DCP was conducted using 30 larvae per treatment group. Following exposure, larvae were euthanized with clove oil (1.5 mL/L), rinsed, and pooled into microtubes containing 0.1 M phosphate buffer (pH 7.4; 20 µL per larva), then stored at −20 °C until analysis. For the tests, the samples were thawed in an ice bath and mechanically homogenized using a pestle. Then, they were centrifuged (10,000 ×g, 20 min) to obtain the supernatant, which was used for protein quantification and enzymatic activity assays. Soluble protein levels were determined using the Bradford method (1976), and enzyme activities were measured via spectrophotometric diagnostic kits (LabTest, Minas Gerais, Brazil), following the manufacturer's instructions. These methods were adapted for 96-well plates as described in our previous study (Martins *et al.*, 2024b). LDH activity followed the motodology described for Domingues and Gravato (2010). All measurements were performed in quadruplicate for each sample.

2.4.2. Triglycerides and Cholesterol quantification

The determination of total cholesterol and triglyceride levels followed the protocol described by Balamurugan *et al.* (2022), which adapted the Bligh and Dyer method for lipid extraction in zebrafish larvae. An acute exposure assay was performed as described in Section 2.3, using 30 larvae per treatment group. After exposure, the larvae were euthanized with clove oil (1.5 mL/L), rinsed, and pooled in microtubes containing 200 µL of homogenization buffer (Tris 1 mM, 20 mM EDTA). The samples were mechanically homogenized, centrifuged at 4,000 × g for 10 minutes, and the supernatant was collected. This supernatant underwent sequential extraction with metanol (95%) and chloroform (99.5%) to isolate the organic phase containing lipids, which was subsequently used for the analyses.

Total cholesterol and triglyceride concentrations were quantified using spectrophotometric diagnostic kits (LabTest, Minas Gerais, Brazil), according to the manufacturer's instructions. All measurements were performed in quadruplicate for each sample.

2.4.3. Oxidative and metabolic stress evaluation

To assess oxidative and metabolic stress, a panel of biomarkers was analyzed, including the enzymatic activities of superoxide dismutase (SOD), catalase (CAT), glutathione S-transferase (GST), glutathione peroxidase (GPx) and citrate synthase (CS) and malondialdehyde (MDA) levels. Enzyme activity measurements (SOD, CAT, GST, GPx, and CS) were conducted following acute exposure, as described in section 2.3, using 40 larvae per treatment. After exposure, larvae were euthanized, stored, and processed as detailed in section 2.4. For MDA quantification, a separate acute exposure was carried out under identical conditions, using 30 larvae per treatment. Larvae were euthanized with clove oil, rinsed and pooled in groups, each homogenized in 200 µL of 50 mM Tris-HCl buffer (pH 7.4), and stored at −20 °C. Samples were then mechanically homogenized using a pestle, centrifuged at 3,000 × g for 10 minutes, and the supernatants collected for subsequent analysis.

Spectrophotometric assays were performed using the obtained supernatants. Soluble protein content was determined using the Bradford method (1976). CAT and GST activities were measured following the protocols of Domingues and Gravato (2018), GPx activity was assessed as described by Massarsky *et al.* (2017), and MDA levels were determined according to the method of Draper and Hadley (1990). CS activity was assessed as described by Azevedo *et al.* (2024). All biomarker measurements were performed in quadruplicate for each sample.

2.5 ROS detection via H_2DCFH-DA

Intracellular ROS production was assessed using the fluorescent probe 2′,7′-dichlorodihydrofluorescein diacetate (H_2DCFH-DA), following the methodology described by Thorstensen (2014) and adapted by Maia *et al.* (2025). After pesticide exposure, groups of 15 larvae per treatment were washed with E3 medium and incubated in 24-well plates containing 2 mL of 1 µM H_2DCFH-DA solution for 1 h at 26 °C in the dark. Larvae were then rinsed, anesthetized with clove oil, and embedded in 1% agarose on glass slides. Fluorescence was detected using an Olympus BX41 microscope (excitation: 488 nm), and images captured with an Olympus Q-Color 5™ camera. Mean fluorescence intensity (MFI) was quantified in ImageJ software by measuring green fluorescence across the whole body of each larva.

2.6 Mitochondrial membrane potential analyses via TMRE

Mitochondrial membrane potential was evaluated using tetramethylrhodamine ethyl ester (TMRE) according to Mandal *et al.* (2018), with modifications to probe concentration and larval number. After exposure, groups of 15 larvae per treatment were incubated in 2 mL of 5 µM TMRE solution under the same conditions as above (1 h at 26 °C, in the dark), followed by washing, anesthesia, and mounting as described. Fluorescence was analyzed using the red channel (excitation: 549 nm; emission: 575 nm), and MFI was calculated in ImageJ.

2.7. Cell death detection via acridine orange (AO)

Apoptosis was assessed using AO, a DNA-intercalating fluorescent dye, based on the protocol by Smirnova *et al.* (2021). Groups of 15 larvae per treatment were incubated in 2 mL of dye solution for 30 min at 26 °C in the dark. After washing and anesthesia, larvae were mounted on slides as previously described. Fluorescence was detected using the green channel (excitation: 485 nm; emission: 535 nm), and quantified using ImageJ.

2.8. Lipid accummulation analysis via oil red O (ORO) staining

ORO staining was performed according to the protocol described by Balamurugan *et al.* (2022). Briefly, an acute exposure assay was conducted using 12 larvae per treatment. Larvae were euthanized, rinsed, and fixed in 4% paraformaldehyde overnight (12–16 h) at 4 °C. After fixation, samples were washed with 0.1 M PBS (pH 7.4) and incubated in 60% isopropanol for 30 minutes.

The isopropanol was then removed, and larvae were incubated with the working ORO solution (7.3 mM) for 3 hours under gentle agitation. Samples were centrifuged (500 × g), washed three times with 60% isopropanol to remove nonspecific staining, and then rinsed twice with PBS. Stained larvae were imaged under an inverted light microscope using a câmera (Moticam 5+, Motic, Canada) at 4× magnification to assess neutral lipid accumulation.

2.9. Gene expression analysis

To better understand the mechanisms affected by environmentally relevant concentrations of 2,4-D and 2,4-DCP, we performed a reverse transcription quantitative PCR (RT-qPCR) analysis. For each experimental group, three pools of 15 larvae were

collected and stored in RNAlater (Sigma-Aldrich®) at −20 °C. Total RNA was extracted using the PureLink® RNA Mini Kit (Thermo Fisher Scientific), and its purity was assessed with a Nanodrop 2000 spectrophotometer. Complementary DNA (cDNA) was synthesized from 1 µg of total RNA using the High-Capacity cDNA Reverse Transcription Kit (Applied Biosystems).

Gene expression was quantified using SYBR Green PCR Master Mix (Applied Biosystems) on a StepOne Real-Time PCR System (Thermo Fisher Scientific). The thermal cycling conditions were as follows: 95 °C for 10 min, followed by 40 cycles of 95 °C for 15 s and 60 °C for 60 s, ending with a melt curve analysis to confirm amplification specificity. β-actin was used as the reference gene, and relative expression levels were calculated using the 2^−ΔΔCt method.

Target genes were selected based on an *in silico* study conducted by our research group (Martins *et al.*, 2025), which suggested potential hepatotoxicity mechanisms of the pesticide and its metabolite. The genes analyzed included those related to nuclear receptors and PPAR signaling (*ppara*, *pparg*), PI3K/AKT signaling (*akt1*), apoptosis (*bax*, *bcl2*, *tp53*, *casp3*), inflammation (*tnf-α*), and antioxidant response (*nrf2*). Primer sequences are listed in Supplementary Table 1.

2.10. Statistic analysis

Data were analyzed using GraphPad Prism 8.0.1. Normality and homogeneity of variances were tested with Shapiro-Wilk and Bartlett's tests, respectively. One-way ANOVA followed by Dunnett's multiple comparisons test was used for parametric data, while non-parametric data were analyzed using the Kruskal-Wallis test followed by Dunn's multiple comparisons test. Statistical significance was set at $p \leq 0.05$.

3. Results

3.1. Hepatotoxicity biomarkers

Hepatic enzyme biomarkers confirmed the hepatotocixity of both 2,4-D and 2,4-DCP at the tested concentrations (Figure 1). ALT activity was significantly elevated across all treatment groups compared to the control ($p < 0.0001$). AST activity also increased signicantly in most groups, including 2,4-D at 30 and 300 µg/L and 2,4-DCP at 3 µg/L (all $p < 0.0001$), as well as 2,4-DCP at 30 µg/L ($p = 0.0048$) and 300 µg/L ($p = 0.0483$). In contrast, no change was observed for 2,4-D at 3 µg/L. ALP activity exhibeited

a more variable pattern: it was signicantly reduced by 2,4-D at 3 µg/L ($p = 0.003$) and by 2,4-DCP at 30 µg/L ($p=0.0003$), but markedly increased following exposure to 2,4-D at 30 µg/L ($p < 0.0001$). 2,4-D decreased LDH activity at 300 µg/L ($p < 0.0001$), whereas 2,4-DCP increased it at all tested concentrations ($p < 0.0001$).

Figure 1. Enzymatic activity of alanine aminotransferase (ALT) (a), aspartate aminotransferase (AST) (b), alkaline phosphatase (ALP) (c) and lactate dehydrogenase (LDH) (d) in zebrafish larvae exposed to different concentrations of 2,4-D and 2,4-DCP for 72 h. Values are presented as mean ± standard deviation. Statistical differences between groups were determined by one-way ANOVA followed by Dunnett's post-hoc test. Asterisks indicate significant differences compared with the control (* $p < 0.05$, ** $p < 0.01$, *** $p < 0.001$, **** $p < 0.0001$).

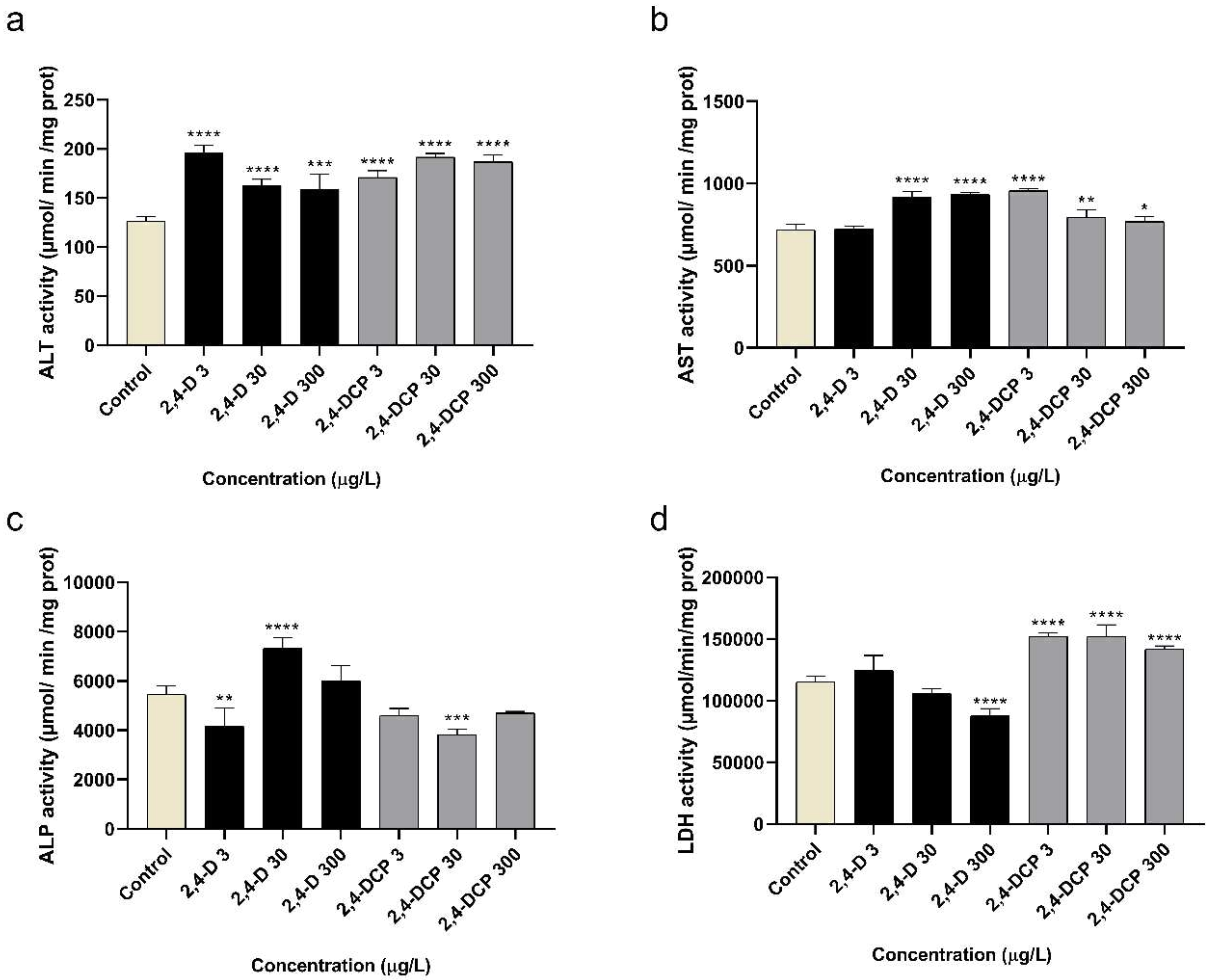

3.2. Oxidative and metabolic stress

The results indicate that both 2,4-D and 2,4-DCP disrupted oxidative stress and metabolic markers, but with distinct profiles (Figure 2). SOD activity was significantly increased in all treatments with both compounds compared to the control (2,4-D: 3 µg/L, $p = 0.0031$; 30 µg/L, $p = 0.0007$; 300 µg/L, $p = 0.0003$; 2,4-DCP: 3 µg/L, $p = 0.0061$; 30 µg/L, $p = 0.0008$; 300 µg/L, $p < 0.0001$).

Exposure to 2,4-D significantly increased CAT activity at 300 µg/L ($p = 0.0006$). Additionally, GST activity was significantly suppressed at all tested concentrations (3 µg/L, $p = 0.01$; 30 µg/L, $p < 0.0001$; 300 µg/L, $p = 0.0017$), while MDA levels were elevated (3 and 30 µg/L, $p = 0.0002$; 300 µg/L, $p = 0.0127$). No significant changes were observed in GPx activity. In contrast, 2,4-DCP significantly increased CAT activity at 3 µg/L ($p = 0.0002$), and elevated MDA levels at 30 µg/L ($p = 0.0014$). No significant effects were detected on GST or GPx activities. No significant change in CS activity was observed for 2,4-D. In contrast, 2,4-DCP reduced CS activity at 3 µg/L ($p = 0.0211$) and increased it at 30 and 300 µg/L ($p = 0.004$ and $p = 0.0374$, respectively).

Figure 2. Enzymatic activity of SOD (a), CAT (b), GPx (c), GST (d), MDA levels (e) and CS (f) in zebrafish larvae exposed to different concentrations of 2,4-D and 2,4-DCP for 72 h. Values are presented as mean ± standard deviation. For SOD, data are expressed as the mean area under the curve ± standard deviation. Statistical differences between groups were determined by one-way ANOVA followed by Dunnett's post-hoc test. Asterisks indicate significant differences compared with the control (* $p < 0.05$, ** $p < 0.01$, *** $p < 0.001$, **** $p < 0.0001$).

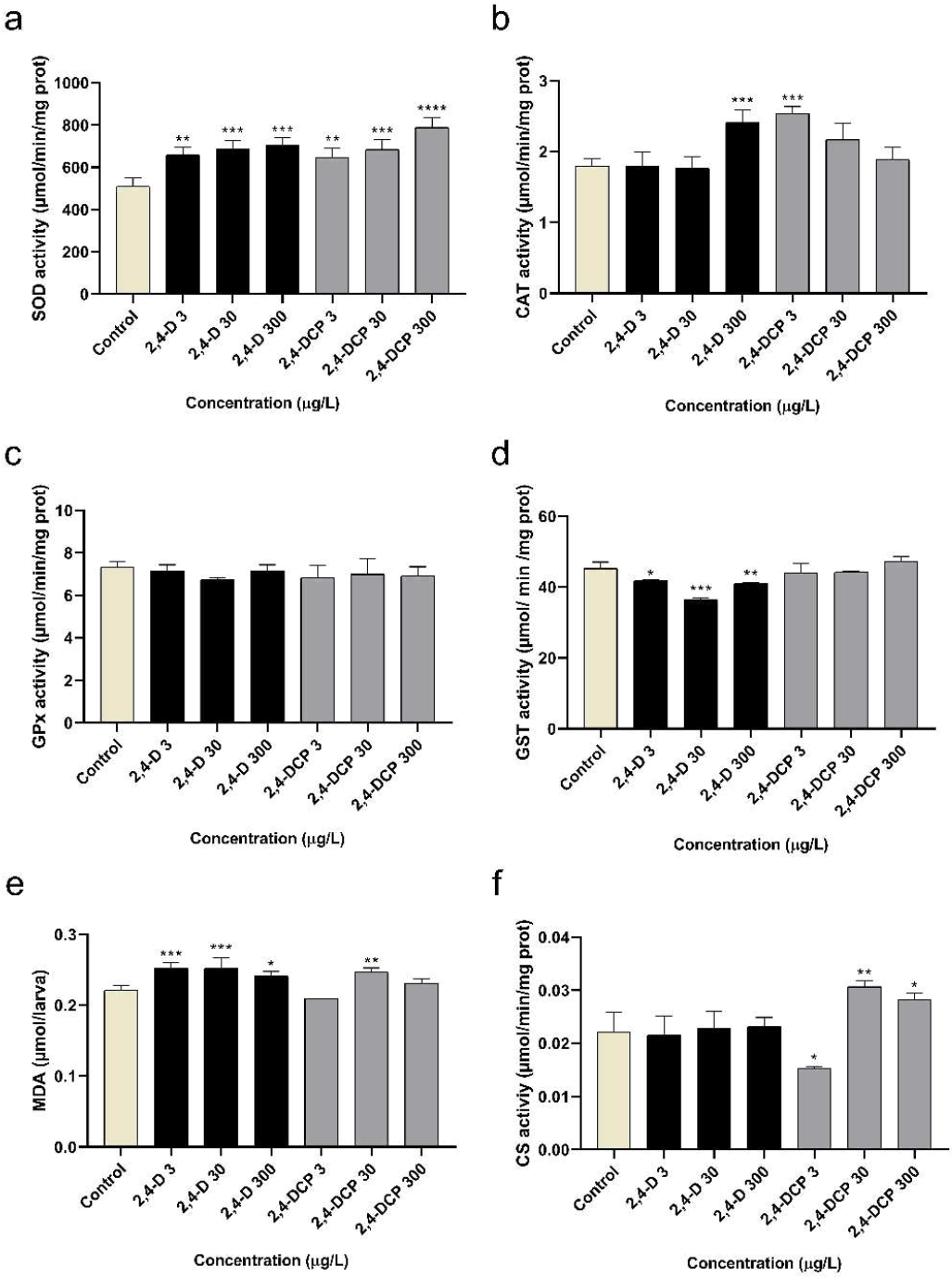

3.3. Total tryglicerides, cholesterol mensuration and ORO staining

Exposure to 2,4-D and 2,4-DCP resulted in increased accumulation of total triglycerides and cholesterol in zebrafish larvae (Figure 3). In the 2,4-D-treated groups, triglyceride levels were significantly elevated at 30 and 300 µg/L ($p = 0.0215$ and $p = 0.0188$, respectively), while total cholesterol levels showed a significant increase at 300 µg/L ($p = 0.0188$). In contrast, 2,4-DCP exposure led to a significant rise in triglyceride content at 3 µg/L ($p = 0.0471$) and in total cholesterol levels at 3, 30 and 300 µg/L ($p = 0.0116$, $p = 0.0403$ and $p = 0.0201$, respectively).

Oil Red O (ORO) staining corroborated the biochemical analyses, revealing the accumulation of neutral lipids in zebrafish larvae, predominantly in the head, liver, and yolk sac regions (Figure 3). In larvae exposed to 2,4-D, increased staining intensity was most apparent at 30 µg/L. However, lipid accumulation was more pronounced in the 2,4-DCP-treated groups, particularly at 3 and 300 µg/L.

Figure 3. Lipid profile of zebrafish larvae exposed to different concentrations of 2,4-D and 2,4-DCP for 72 h. Triglyceride levels (a) and cholesterol levels (b) are presented as mean ± standard deviation. Statistical differences between groups were determined by one-way ANOVA followed by Dunnett's post-hoc test. Asterisks indicate significant differences (* $p < 0.05$, ** $p < 0.01$, *** $p < 0.001$, **** $p < 0.0001$). (c) Negative control larva stained with Oil Red O (ORO); (d–f) larvae exposed to 3, 30, and 300 µg/L of 2,4-D, respectively; (g–i) larvae exposed to 3, 30, and 300 µg/L of 2,4-DCP, respectively. In ORO-stained larvae, the liver area is highlighted.

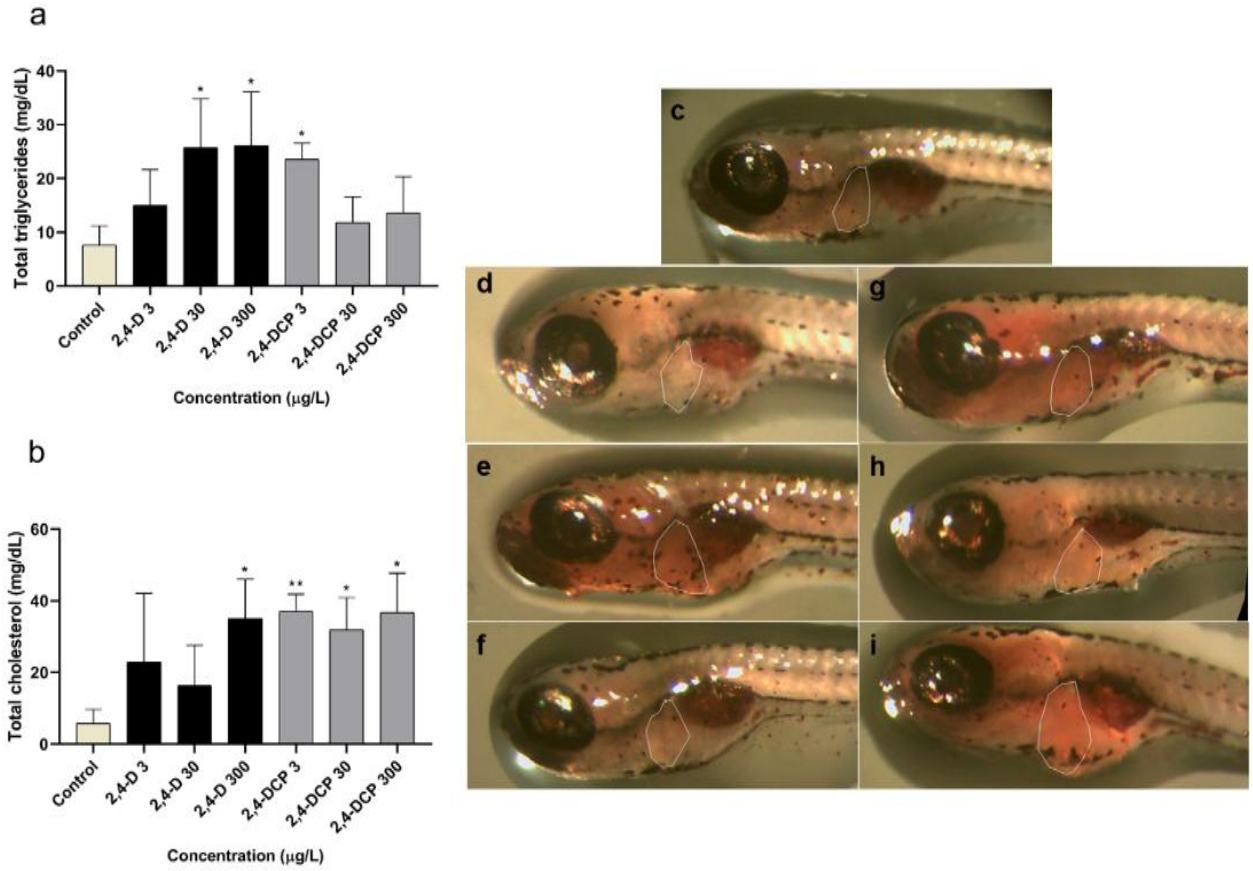

3.4 Fluorescent probes

In the TMRE assay (Figure 4), all treatments with 2,4-D and 2,4-DCP (except 2,4-DCP at 30 µg/L) showed statistically significant differences compared with the control. Exposure to 2,4-D at 3 µg/L increased fluorescence intensity, whereas 30 and 300 µg/L caused a significant decrease ($p < 0.0001$). Similarly, 2,4-DCP at 3 and 300 µg/L also reduced fluorescence intensity ($p < 0.0001$). In the H_2DCFDA assay (Figure 5), fluorescence intensity increased only at 300 µg/L, for 2,4-D ($p = 0.0215$) and 2,4-DCP ($p < 0.0001$). In contrast, Acridine Orange staining (Figure 6) revealed no statistically significant differences among groups.

Figure 4. Zebrafish larvae exposed to different concentrations of 2,4-D and 2,4-DCP and subsequently stained with the fluorescent probe TMRE. (a) Negative control larva; (b–d) larvae exposed to 3, 30, and 300 µg/L of 2,4-D, respectively; (e–g) larvae exposed to 3, 30, and 300 µg/L of 2,4-DCP, respectively. Asterisks indicate significant differences (* $p < 0.05$, ** $p < 0.01$, *** $p < 0.001$, **** $p < 0.0001$).

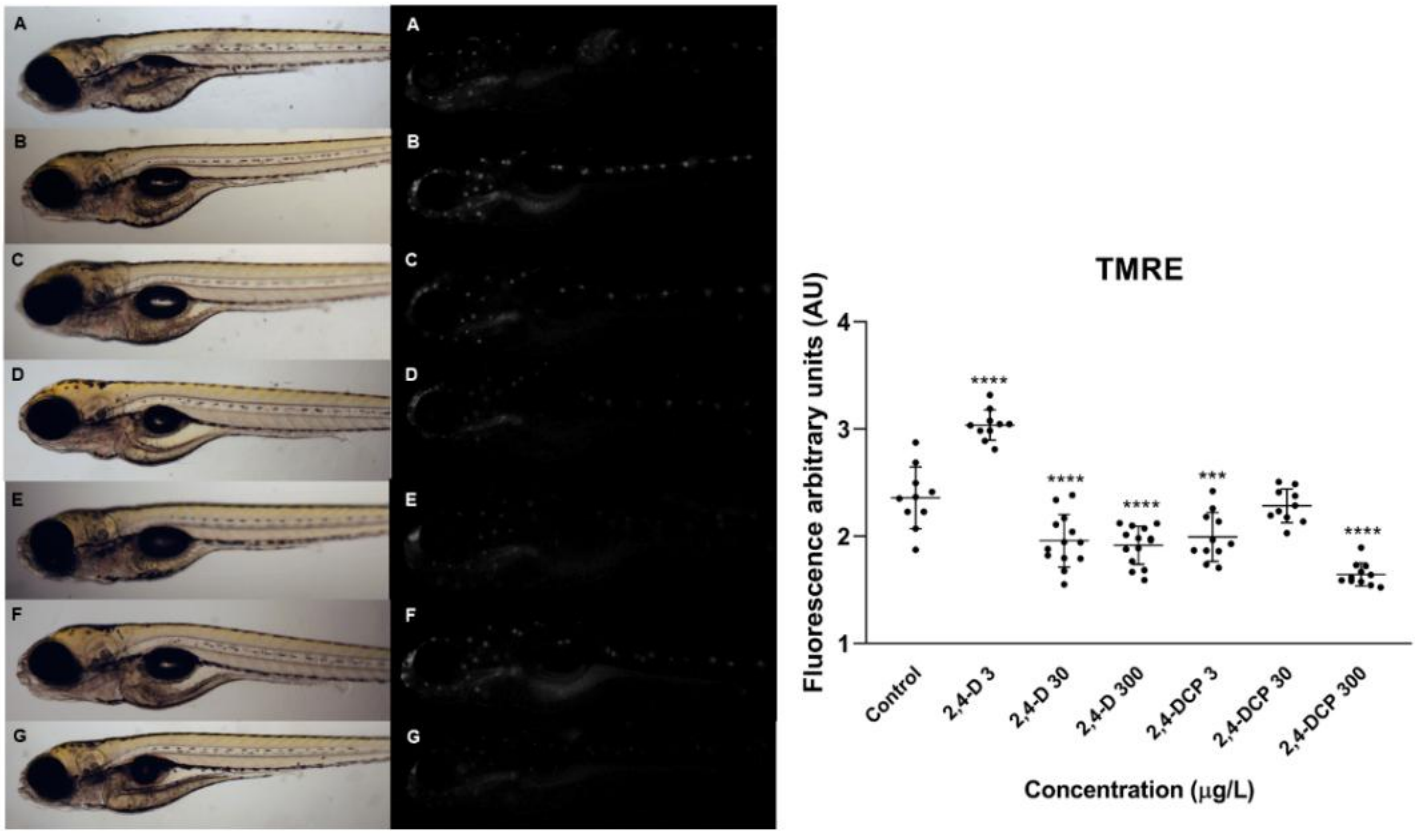

Figure 5. Zebrafish larvae exposed to different concentrations of 2,4-D and 2,4-DCP and subsequently stained with the fluorescent probe H2DCFDA. (a) Negative control larva; (b–d) larvae exposed to 3, 30, and 300 µg/L of 2,4-D, respectively; (e–g) larvae exposed to 3, 30, and 300 µg/L of 2,4-DCP, respectively. Asterisks indicate significant differences (* $p < 0.05$, ** $p < 0.01$, *** $p < 0.001$, **** $p < 0.0001$).

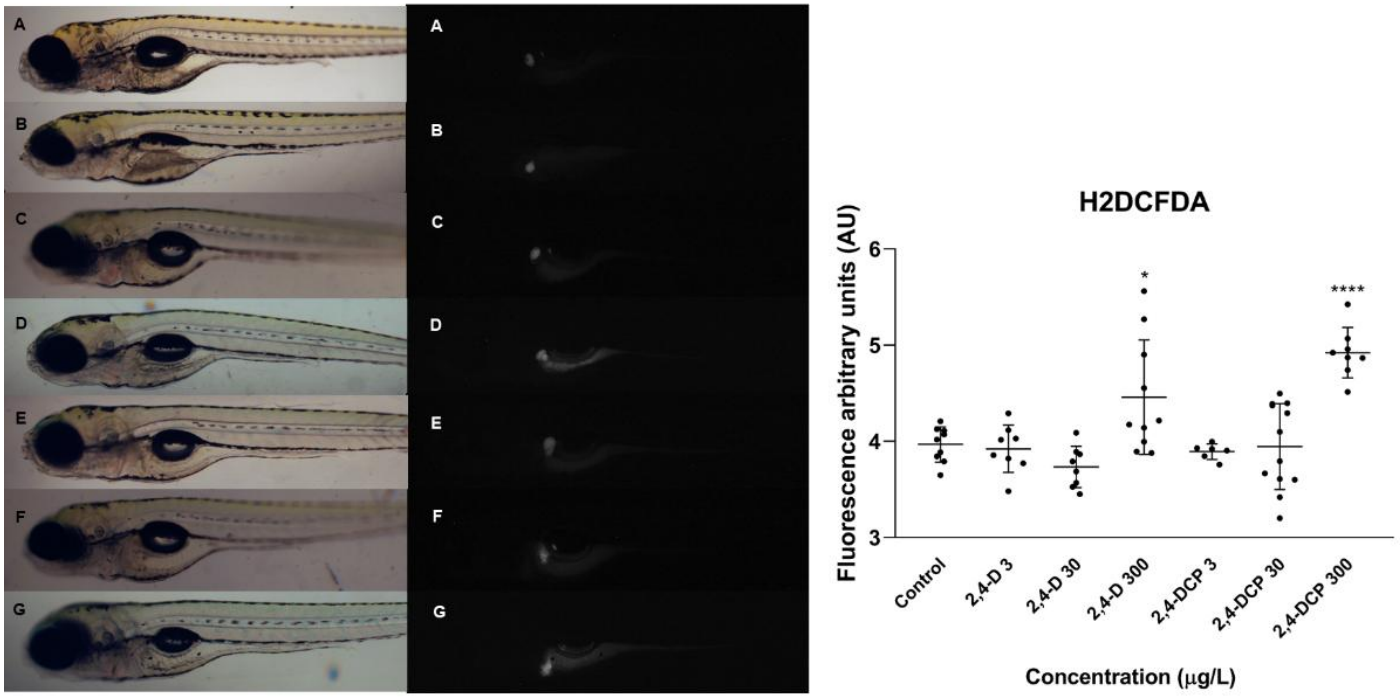

Figure 6. Zebrafish larvae exposed to different concentrations of 2,4-D and 2,4-DCP and subsequently stained with the fluorescent probe Acridine Orange. (a) Negative control larva; (b–d) larvae exposed to 3, 30, and 300 µg/L of 2,4-D, respectively; (e–g) larvae exposed to 3, 30, and 300 µg/L of 2,4-DCP, respectively. Asterisks indicate significant differences (* $p < 0.05$, ** $p < 0.01$, *** $p < 0.001$, **** $p < 0.0001$).

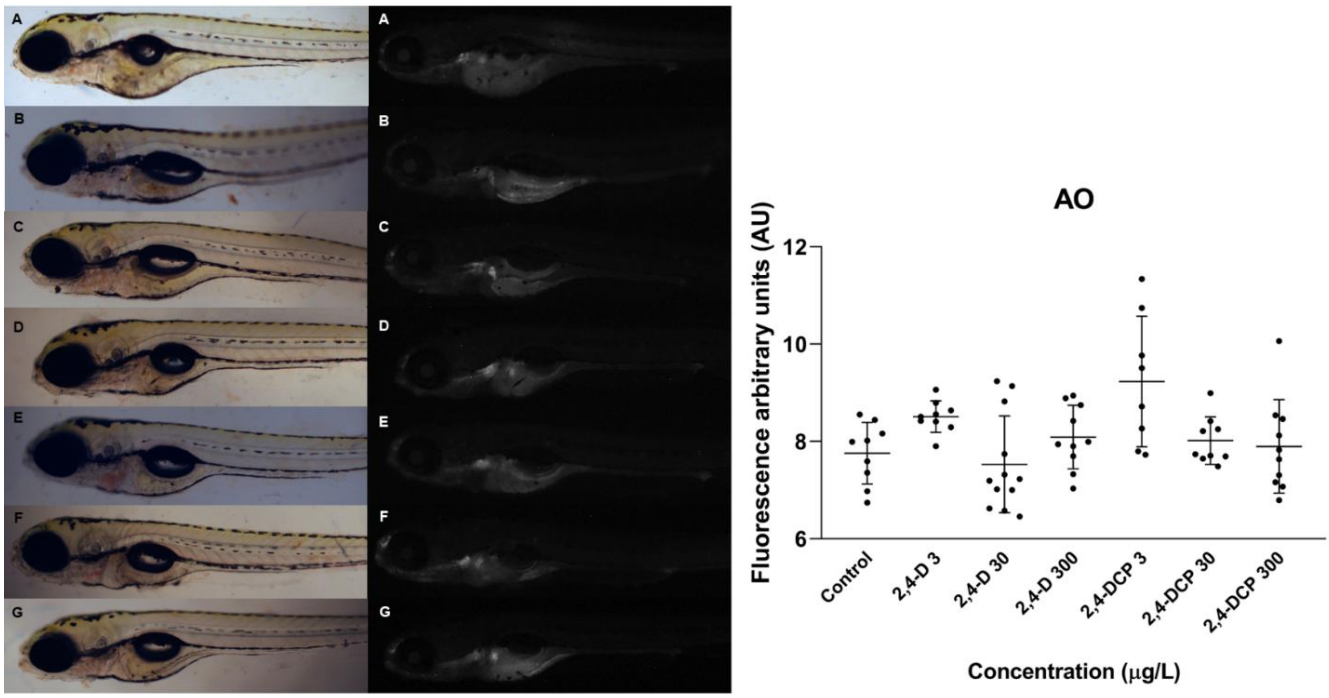

3.5. Gene expression analyses

Gene expression analysis revealed significant alterations in the relative mRNA levels of multiple genes following exposure to both 2,4-D and 2,4-DCP (Figure 7). Statistically significant differences were observed for *ppara* ($F = 21.02$, *p* < 0.0001), *pparg* ($F = 38.15$, $p < 0.0001$), *tp53* ($F = 9.949$, $p = 0.0003$), *bax* ($F = 41.18$, $p < 0.0001$), *casp3* ($F = 15.63$, $p < 0.0001$), *tnfa* ($F = 7.177$, *p* = 0.0036), and *nrf2* ($F = 9.567$, $p = 0.0012$).

Post hoc analysis indicated that 2,4-D significantly suppressed *pparg* expression at 30 µg/L ($p = 0.002$), while upregulating *tp53* and *nrf2* at 3 µg/L ($p = 0.048$ and $p = 0.0444$, respectively). Additionally, *tnfa* expression was downregulated at 30 and 300 µg/L ($p = 0.0089$ and $p = 0.0088$, respectively).

In contrast, 2,4-DCP demonstrated a more pronounced effect on gene expression disruption. All tested concentrations significantly suppressed the expression of *ppara* (3 µg/L, $p = 0.0007$; 30 µg/L, $p = 0.0004$; 300 µg/L, $p = 0.0009$), *pparg* ($p < 0.0001$), *bax* ($p < 0.0001$), *casp3* (3 µg/L, $p = 0.0003$; 30 µg/L, $p = 0.0002$; 300 µg/L, $p = 0.0005$), and *tnfa* (3 µg/L, $p = 0.0371$; 30 µg/L, $p = 0.0146$; 300 µg/L, $p = 0.0316$). Furthermore, *tp53* expression was downregulated at 30 µg/L ($p = 0.0042$), whereas *nrf2* expression was upregulated at 300 µg/L ($p = 0.0007$).

No significant changes were observed in the expression of *bcl2* and *akt1* following exposure to either compound at any concentration tested.

Figure 7. Relative gene expression (Fold change) in zebrafish larvae exposed to 2,4-D and 2,4-DCP (0, 3, 30 and 300 µg/L) (n = 3 pools of 15 fry zebrafish per group). Mean and SEM are represented. Statistical results are expressed by ANOVA followed by Dunnett's multiple comparisons test, * $p < 0.05$, ** $p < 0.01$, *** $p < 0.001$, **** $p < 0.0001$.

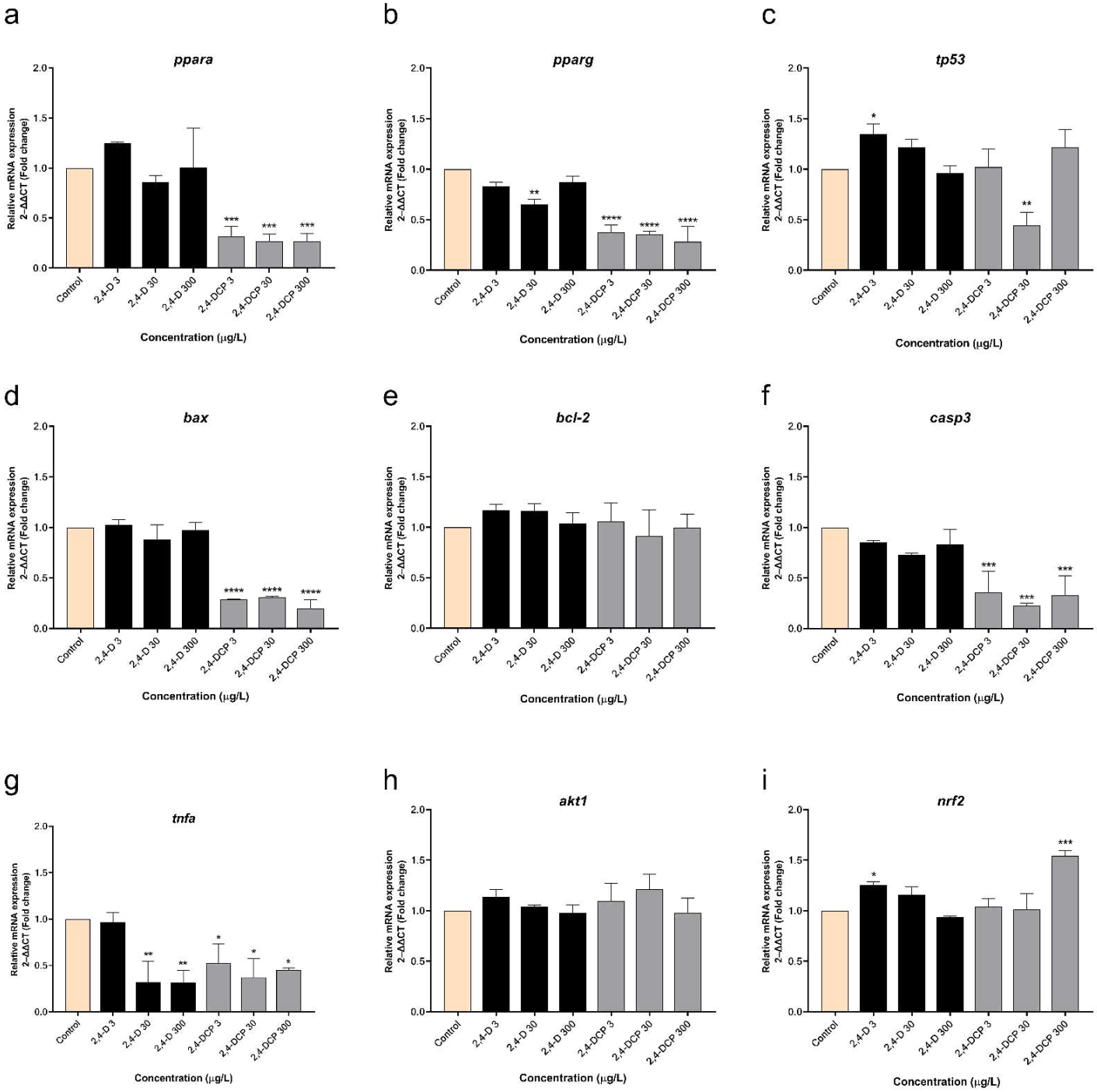

4. Discussion

The results demonstrate that all tested concentrations of 2,4-D and 2,4-DCP induced hepatotoxicity in zebrafish larvae, as evidenced by the consistent increase in ALT and AST activity. The ALT/AST ratio is a well-established marker of liver health in both clinical and experimental settings, including zebrafish larvae models (Sookoian *et al.*, 2015; MC Guill, 2016; Li *et al.*, 2020; Martins *et al.*, 2024a; Martins *et al.*, 2024b). Both enzymes are predominantly localized in hepatocytes, and their release into the extracellular environment following membrane damage leads to elevated activity, making them sensitive biomarkers of liver injury (Giannini *et al.*, 2005; Sookoian *et al.*, 2015; Martins *et al.*, 2024a).

Furthermore, ALP activities were altered at specific concentrations of 2,4-D and 2,4-DCP. Exposure to 2,4-D reduced ALP activity at 3 µg/L and increased it at 30 µg/L, whereas 2,4-DCP reduced ALP activity at 30 µg/L. Since ALP is located in the membranes of biliary canaliculi, changes in its activity may reflect impaired bile flow, commonly associated with liver injury and hepatobiliary disorders (Giannini *et al.*, 2005; Fernandes *et al.*, 201; Martins *et al.*, 2024a).

Regarding LDH, which is involved in anaerobic energy metabolism, increased activity is often linked to oxygen deficiency and tissue damage (Lagana *et al.*, 2019). Although LDH is not a specific marker of hepatotoxicity, elevated levels are frequently associated with liver disorders (Wang *et al.*, 2012; Martins *et al.*, 2021; Martins *et al.*, 2024b). In this study, 2,4-DCP increased LDH activity at all tested concentrations, suggesting a more diffuse pattern of metabolic stress. Conversely, 2,4-D reduced LDH only at the highest concentration, which may reflect severe injury sufficient to compromise enzyme production and/or impair function under this condition.

Collectively, alterations in these four biochemical markers (ALT, AST, ALP and LDH) demonstrate that environmentally relevant concentrations of 2,4-D and 2,4-DCP can induce hepatotoxicity in zebrafish larvae. However, subsequent results suggest that these compounds exhibit distinct features in their hepatotoxic mechanisms. The following discussion will therefore examine how each chemical disrupts key metabolic processes, including oxidative stress, lipid metabolism, mitochondrial function, and cell death, to elucidate their hepatotoxic profiles.

Redox homeostasis disruption emerged as a pivotal mechanism underlying the hepatotoxicity induced by both compounds. However, 2,4-D demonstrated a more

pronounced impact than 2,4-DCP. The antioxidant defense system was particularly altered by 2,4-D, which elevated SOD activity at all concentrations and CAT activity only at 300 µg/L. Concurrently, it reduced GST activity and induced a consistent increase in MDA levels across all tested concentrations. This suggests that the compensatory upregulation of other enzymes was ineffective in preventing oxidative damage.

This is relevant because GST not only helps maintain redox balance but also plays a key role in detoxification through glutathione conjugation, removing electrophilic products of lipid peroxidation such as lipid hydroperoxides, 4-HNE, and MDA (Bhattacharjee *et al.*, 2007; Singhal *et al.*, 2015; Massarsky *et al.*, 2017). Its diminution likely reduced detoxification capacity, directly promoting MDA accumulation, which can damage cellular structures and contribute to the progression of liver disease (Zelber-Sagi *et al.*, 2020).

In contrast, 2,4-DCP caused a milder disruption of the redox system and oxidative damage. SOD activity increased at all concentrations, CAT was elevated only at 3 µg/L, and MDA accumulation occurred only at 30 µg/L, indicating a more subtle and transient oxidative imbalance compared to 2,4-D. Although intracellular ROS detected by the H_2DCFDA probe were significant only at the highest concentration for both compounds, molecular analyses revealed distinct patterns of antioxidant regulation. Expression of *nrf2*, a key transcriptional regulator of oxidative stress responses, was upregulated at the lowest concentration of 2,4-D, whereas for 2,4-DCP this response appeared only at the highest concentration (Ngo and Duennwald, 2022). These findings suggest that 2,4-D elicits an earlier antioxidant response, reflecting the greater susceptibility of the antioxidant system to this compound.

ROS accumulation was detected by H_2DCFDA only at the highest concentrations, likely because SOD and CAT effectively neutralized ROS at lower levels. At the highest concentration, ROS production may have exceeded antioxidant capacity, leading to accumulation. Notably, CAT activity in 2,4-DCP-treated samples was elevated at 3 µg/L, possibly as an early response to increased ROS, but this effect was lost at higher concentrations, suggesting enzyme depletion. These findings underscore the role of oxidative stress in the toxicity of these compounds.

Previous work from our group suggested that oxidative stress induced by 2,4-D and 2,4-DCP could be associated with impairment of the PI3K/AKT pathway (Martins *et al.*, 2025). However, no changes in *akt1* expression were observed in the present study,

indicating that, under the conditions tested, modulation of this pathway is not a primary mechanism of toxicity.

Lipid accumulation was also a mechanism induced by both 2,4-D and 2,4-:DCP, with 2,4-DCP having a stronger effect. Biochemical analyses showed increased cholesterol at all 2,4-DCP concentrations and elevated triglycerides at 3 µg/L. ORO staining confirmed lipid accumulation, showing intense reddish coloration in the larvae. Gene expression analyses suggest that these effects may be partly driven by the suppression of the nuclear receptors *pparα* and *pparγ*, key regulators of lipid metabolism, which were markedly downregulated at all 2,4-DCP concentrations (Schaaf *et al.*, 2017; Den Broeder *et al.*, 2015).

pparα is a key regulator of hepatic fatty acid β-oxidation, promoting lipid degradation, whereas *pparγ* controls adipogenesis and lipid storage in adipose tissue (Den Broeder *et al.*, 2015; Wang *et al.*, 2020; Li *et al.*, 2024). Suppression of these receptors impairs both processes, reducing lipid oxidation and compromising appropriate lipid storage, thereby favoring pathological lipid accumulation (Wang *et al.*, 2020; Hu *et al.*, 2023). Our results are consistent with previous findings, as zebrafish embryos exposed to 2,4-DCP have also shown lipid accumulation associated with the suppression of *pparα* and ACO (acyl-CoA oxidase), a key enzyme in peroxisomal fatty acid β-oxidation (Honda *et al.*, 2016).

In contrast, 2,4-D induced a less pronounced lipid accumulation than its metabolite. At 30 µg/L, a reduction in *pparγ* expression was observed, accompanied by elevated triglyceride levels and intense ORO staining in zebrafish larvae. Interestingly, *pparγ* plays a complex and essential role in protecting the liver against inflammation, oxidative stress, and fatty liver disease, and has been proposed as a therapeutic target through different agonists to mitigate hepatic disorders (Wu *et al.*, 2020). Therefore, the suppression of *pparγ* by 2,4-D likely contributes significantly to lipid accumulation and hepatotoxicity. Moreover, these results support our previous findings, which hypothesized that PPAR deregulation underlies the lipid metabolism disturbances induced by 2,4-D and 2,4-DCP (Martins *et al.*, 2025).

In addition to PPAR suppression, alterations in CS activity provide further evidence of the greater potential of 2,4-DCP to promote lipid accumulation. Treatment with 2,4-DCP decreased CS activity at 3 µg/L but increased it at 30 and 300 µg/L, whereas 2,4-D caused no changes. CS is a key mitochondrial matrix enzyme of the tricarboxylic

acid (TCA) cycle that catalyzes the condensation of acetyl-CoA and oxaloacetate to form citrate (Mycielska *et al.*, 2009; Zhao *et al.*, 2022).

Elevated CS activity increases mitochondrial citrate levels, which can be exported to the cytoplasm via the mitochondrial citrate carrier (mCiC) and converted by ATP citrate lyase (ACLY) into acetyl-CoA, a major precursor for fatty acid and cholesterol biosynthesis, thereby favoring hepatic lipid accumulation (Mycielska *et al.*, 2009; Zhao *et al.*, 2022). Furthermore, enhanced CS activity intensifies citrate flux through the TCA cycle, boosting oxidative metabolism, which may contribute to increased reactive oxygen species (ROS) generation and oxidative stress (Convertini *et al.*, 2016). Conversely, reduced CS activity, as observed at 3 µg/L, can also be detrimental by limiting oxidative phosphorylation and ATP production, while simultaneously promoting ROS formation and mitochondrial dysfunction (Li *et al.*, 2012; Xu *et al.*, 2022).

Lipid metabolism disorders are strongly associated with mitochondrial dysfunction (Aqeel *et al.*, 2025). In this study, mitochondrial membrane potential (ΔΨm) was assessed using TMRE staining. Exposure to 2,4-DCP induced a reduction in ΔΨm at 3 and 300 µg/L, indicating mitochondrial depolarization (McGlothen *et al.*, 2024). This depolarization reflects proton leakage through the respiratory chain, which compromises key functions such as β-oxidation and contributes directly to lipid accumulation (Guerra *et al.*, 2022; Li *et al.*, 2025). This metabolic disruption was reinforced by the suppression of both *pparα* and *pparγ*. The inhibition of *pparα* impairs the expression of mitochondrial and peroxissomes β-oxidation genes, while *pparγ* suppression favors lipid storage. Their concurrent inhibition severely disrupts fatty acid catabolism (Fan and Evans, 2015; Todisco *et al.*, 2022), creating a cycle where lipid overload further burdens mitochondria, increases ROS production, and exacerbates dysfunction (Aqeel *et al.*, 2025).

In contrast, 2,4-D elicited a biphasic response. A low concentration (3 µg/L) increased ΔΨm, suggesting mitochondrial hyperpolarization and enhanced oxidative phosphorylation (McGlothen *et al.*, 2024). However, at higher concentrations (30 and 300 µg/L), ΔΨm decreased, indicating depolarization likely caused by intense mitochondrial stress, electron leakage, and impaired ATP synthesis (McGlothen *et al.*, 2024). Notably, at 3 µg/L, antioxidant metabolism was significantly disrupted without concurrent lipid accumulation. This indicates that the initial dysfunction induced by 2,4-D is primarily linked to redox imbalance, a conclusion reinforced by the observed hyperpolarization. The lipid accumulation seen at higher concentrations is therefore a secondary effect,

likely resulting from impaired β-oxidation exacerbated by mitochondrial dysfunction and *pparγ* suppression, particularly evident at 30 µg/L.

In summary, both compounds ultimately cause mitochondrial dysfunction and lipid accumulation, but their mechanisms differ. 2,4-DCP acts through the early disruption of lipid metabolic pathways, whereas 2,4-D primarily triggers oxidative stress initially.

Despite the perturbations described above, no cell death was detected for either compound according to AO staining. However, molecular analyses revealed distinct strategies by which 2,4-D and 2,4-DCP maintain cell viability.

Exposure to 2,4-D at 3 µg/L increased *tp53* expression, indicative of a cellular damage response. Under normal conditions, *tp53* promotes apoptosis by activating pro-apoptotic genes (e.g., *bax*), repressing anti-apoptotic genes (e.g., *bcl-2*), and initiating caspase cascades (Aubrey *et al.*, 2016). In this study, no changes were observed in *bax*, *bcl-2*, or *casp3*, suggesting that apoptosis was not initiated. This apparent resistance to apoptosis is likely mediated by compensatory defense mechanisms. Consistently, *nrf2* was upregulated at the same concentration. Because *nrf2* activation is triggered by elevated ROS levels, this indicates a metabolic adaptation aimed at protecting cells from oxidative stress, a key inducer of apoptosis (Rojo de la Vega *et al.*, 2018; Jenkins *et al.*, 2021).

At higher concentrations (30 and 300 µg/L), *tnf-α* expression was suppressed. Given the central role of *tnf-α* in the extrinsic apoptotic pathway and in hepatic inflammation, this downregulation likely represents an additional protective mechanism that mitigates inflammatory and apoptotic signaling (Alvarez *et al.*, 2011; Del Campo *et al.*, 2018). Collectively, these findings indicate that 2,4-D exposure elicits an adaptive response that counteracts oxidative and inflammatory stress, thereby preventing apoptosis.

In contrast, 2,4-DCP required broader modulation of cell death pathways to maintain viability, reflecting a higher degree of metabolic stress. Across all concentrations, 2,4-DCP caused more severe metabolic perturbations than 2,4-D, as evidenced by increased LDH activity, disrupted CS activity, suppression of *pparα* and *pparγ*, and enhanced lipid accumulation. Elevated LDH activity increases lactate production, compromising energy homeostasis and promoting inflammatory processes, which contribute to liver disease progression (Yao *et al.*, 2024). Similarly, lipid accumulation is a hallmark of liver disorders such as non-alcoholic fatty liver disease

(NAFLD), where it is associated with oxidative stress and inflammation (Delli *et al.*, 2021). These findings suggest that larvae exposed to 2,4-DCP experience heightened metabolic stress and require multiple protective mechanisms to prevent apoptosis.

At the molecular level, 2,4-DCP downregulated *tp53* at 30 µg/L, while all concentrations suppressed the expression of pro-apoptotic genes (*bax* and *casp3*) and the inflammatory gene *tnf-α* (Aubrey *et al.*, 2016). This broad suppression reflects a greater reliance on apoptosis evasion compared with 2,4-D throug direct inhibition of apoptotic and inflammatory pathways.

Although these mechanisms were effective in preventing cell death under the present conditions, apoptosis evasion is a well-established hallmark of carcinogenesis (Tian *et al.*, 2024). Epidemiological studies in China have associated 2,4-DCP exposure with an increased risk of thyroid cancer, although further studies are needed to establish causality (Yang *et al.*, 2021).

5. Conclusions

This study showed that environmentally relevant concentrations of 2,4-D and 2,4-DCP are hepatotoxic to zebrafish larvae, affecting antioxidant defenses, inducing lipid accumulation, and causing mitochondrial dysfunction, without significant cell death. Notably, 2,4-D had a stronger impact on the antioxidant system and oxidative damage, whereas 2,4-DCP imposed greater metabolic stress, promoting lipid accumulation, marked suppression of *pparα* and *pparγ*, mitochondrial depolarization even at low concentrations, and broad modulation of genes related to cell death to prevent apoptosis. These findings inform regulatory agencies and future research, highlighting that environmental levels of these compounds can elicit toxic effects and identifying sensitive mechanisms that may be targeted for toxicity mitigation.

4.5. Artigo 5

Long-term exposure to the herbicide 2,4-D and its metabolite 2,4-DCP promotes hepatic morphological alterations in adult zebrafish

Rafael Xavier Martins[1,2], Maria Eduarda Maia[1,2], Cleyton de Sousa Gomes[2], Matheus Alves[2], Marcos Vinicius Porto Medeiros[2], Ana Julia Antunes de Magalhães[2], Juliana Alves da Costa Ribeiro Souza[2], Patricia Mirela da Silva[3], Terezinha Souza[2], Davi Farias[1,2,*]

[1]Post-Graduation Program in Biochemistry, Department of Biochemistry and Molecular Biology, Building 907, Campus Pici, Federal University of Ceará, 60455-970 Fortaleza, Brazil

[2]Laboratory for Risk Assessment of Novel Technologies, Department of Molecular Biology, Federal University of Paraiba, João Pessoa, 58050-085, Brazil

[3]Laboratory of Immunology and Pathology of Invertebrates (LABIPI), Department of Molecular Biology, Federal University of Paraiba, João Pessoa, Brazil.

[*]Corresponding author:
Professor Davi F. Farias
E-mail: davi@dbm.ufpb.br
Phone: +55-83-32167633

Abstract

The herbicide 2,4-Dichlorophenoxyacetic acid (2,4-D) and its major environmental metabolite, 2,4-Dichlorophenol (2,4-DCP), are frequently detected in surface and drinking waters. Both compounds are hepatotoxic to vertebrates, but most studies focus on acute exposures, limiting knowledge of their chronic effects. Here, we evaluated the effects of long-term exposure to 2,4-D (30 and 3000 μg/L) and 2,4-DCP (30 and 300 μg/L) in adult zebrafish (*Danio rerio*) over 21 days. Following exposure, fish were euthanized, and livers were harvested for biochemical (AST, ALP, LDH, GST and GPx) and histopathological analyses. Enzymatic activities remained largely unchanged, except for a reduction in ALP in the low 2,4-DCP group. In contrast, histopathology revealed pronounced cellular and tissue alterations. Low concentrations of 2,4-D induced microvesicular steatosis and cell death, as indicated by pyknotic nuclei and karyorrhexis, whereas high concentrations aggravated these lesions, leading to macrovesicular steatosis and hepatic parenchymal disorganization. These changes are indicative of non-alcoholic steatohepatitis (NASH), a severe form of non-alcoholic fatty liver disease (NAFLD). Exposure to 2,4-DCP caused milder steatosis compared to 2,4-D, but high 2,4-DCP exposure induced hepatocyte degeneration, tissue disorganization, and vascular congestion. These findings show that long-term exposure to 2,4-D and its metabolite induces liver toxicity with fat accumulation in zebrafish, raising concerns about the safety of the legally permitted 2,4-D level in Brazilian drinking water (30 μg/L).

Keywords: 2,4-Dichlorophenol; 2,4-Dichlorophenoxyacetic; aquatic toxicology; morfological markers; non-alcoholic steatohepatitis; pesticides.

1. Introduction

The herbicide 2,4-dichlorophenoxyacetic acid (2,4-D) and its major environmental metabolite 2,4-dichlorophenol (2,4-DCP) are significant emerging contaminants (USEPA, 1979; Liu *et al.*, 2018; Zhang *et al.*, 2020). 2,4-D is widely applied to crops such as rice, wheat, maize, and sugarcane, and its extensive use is reflected in frequent environmental detections (Islam *et al.*, 2018; Martins *et al.*, 2024).

In Brazil, 2,4-D has been the second most sold herbicide since 2013, with 51,872.24 tons marketed in 2023. Monitoring conducted between 2014 and 2017 detected its presence in 92% of public water supply samples collected from more than 2,300 municipalities. Although only two samples exceeded the Brazilian legal limit of 30 µg/L, 4,270 detections surpassed the European Union threshold of 0.1 µg/L (SISAGUA, 2018; Zuanazzi *et al.*, 2020). Elevated concentrations of 2,4-D have also been reported, reaching 366.6 µg/L in rivers in sugarcane-producing regions of São Paulo State (CETESB, 2018). This herbicide has similarly been detected worldwide, including the USA (0.1–12 µg/L), Spain (62–207 ng/L), Australia (3.5 ng/L), Iran (16.6 µg/L), and Greece (1.16 µg/L) (Rodil *et al.*, 2012; Yamini & Saleh, 2013; Peterson *et al.*, 2016; Tsaboula *et al.*, 2016; Meftaul *et al.*, 2020; ATSDR, 2020).

2,4-DCP is also frequently detected and may originate from sources other than 2,4-D, such as the degradation of other organochlorines, including triclosan. In Brazil, drinking water systems in Minas Gerais showed 2,4-DCP concentrations ranging from 0.42 to 10.03 µg/L in untreated water and 2.94 to 3.33 µg/L in treated water (Ramos *et al.*, 2021). Its occurrence has also been reported in river waters in France (0–4.89 µg/L) and China (0.01–19.96 µg/L), in surface waters in South Africa (0.1–10 µg/L), and in wastewater in Australia (0.1–6.72 µg/L) (Gao *et al.*, 2008; Zhong *et al.*, 2010; Farounbi & Ngqwala, 2020; Pan *et al.*, 2021).

These compounds raise environmental concern due to their association with hepatotoxicity in non-target organisms. *In vivo* exposure to 2,4-D has been linked to liver enlargement, histopathological alterations, changes in aminotransferase and alkaline phosphatase activity, oxidative stress, and decreased antioxidant defenses (Tichati *et al.*, 2020; Martins *et al.*, 2021; Tichati *et al.*, 2021;). Likewise, 2,4-DCP has been shown to impair liver function through histopathological damage, oxidative stress, mitochondrial dysfunction, and apoptosis, both *in vitro* and *in vivo* (Fu *et al.*, 2016; Li *et al.*, 2013).

However, most studies have employed acute exposures at high concentrations, which may not reflect the long-term effects of repeated low-level exposure. A chronic study reported that oral administration of 2 mg/kg/day for six months exacerbated non-alcoholic fatty liver disease (NAFLD), increasing inflammation and fibrosis in rats (Romualdo *et al.*, 2023). Although informative, such doses are far above environmentally encountered levels. In Brazil, the maximum permitted concentration of 2,4-D in drinking water remains substantially higher than the more conservative limits adopted by the European Union, and no environmental threshold has yet been established for 2,4-DCP (SISAGUA, 2018; Zuanazzi *et al.*, 2020).

Given this regulatory discrepancy and the lack of chronic data at low to moderate exposure levels, studies addressing concentrations close to or above current safety thresholds are essential to determine whether these values indeed ensure protection for non-target organisms. Zebrafish (Danio rerio) provide a suitable model for such investigations due to the structural, functional, and regenerative similarities between their liver and that of humans (Shimizu *et al.*, 2023). Moreover, this species enables an integrated evaluation of biochemical, histological, and morphological endpoints indicative of hepatotoxicity (Zhang *et al.*, 2017; Zhao *et al.*, 2019; Martins *et al.*, 2021).

Accordingly, this study aimed to investigate the potential long-term hepatotoxic effects of 2,4-D and 2,4-DCP in zebrafish, using a range of concentrations that include the Brazilian maximum permitted value (30 μg/L) for 2,4-D in drinking water. This concentration represents the current regulatory benchmark considered safe for human exposure but may not necessarily protect aquatic organisms under chronic conditions. Higher concentrations were also evaluated to reflect potential contamination peaks and to identify dose-dependent responses. We hypothesize that the current Brazilian limit is not protective enough and that more conservative thresholds, such as those adopted by the European Union, may be warranted.

2. Materials and Methods

2.1. Definition of test concentrations for 2,4-D and 2,4-DCP

The lowest concentrations tested for 2,4-D and 2,4-DCP were defined based on the Brazilian maximum permissible value (MPV) for 2,4-D in drinking water (30 μg/L), representing a regulatory exposure scenario. To capture possible subchronic effects beyond this limit, higher concentrations were selected according to previous acute

toxicity assays in zebrafish larvae. For 2,4-D, 3000 µg/L was chosen since no morphological alterations were observed at this level (Martins *et al.*, 2021). For 2,4-DCP, the upper concentration was set at 300 µg/L, below the range that induced overt toxicity (unpublished data). This gradient allowed us to assess both the safety margin of the current regulatory limit and the progression of hepatic effects under increasing exposure levels.

2.2. Chemicals

2,4-D (CAS 94-75-7) and 2,4-DCP (CAS 120-83-2) were purchased from Sigma-Aldrich Co. (St. Louis, MO, USA) with purities of 99%. For the exposure assays, 100 mg/L stock solutions (500 mL) of each compound were prepared at each renewal and subsequently diluted to achieve the final concentrations used in the experiments: (i) 30 and 3000 µg/L for 2,4-D, and (ii) 30 and 300 µg/L for 2,4-DCP. All other reagents used were of analytical grade.

2.3. Animals husbandry

Sixty adult zebrafish (3–4 months old, AB strain) were obtained from the Unit for the Production of Non-Conventional Model Organisms (UniPOM), Department of Molecular Biology, Federal University of Paraíba (UFPB, João Pessoa, Brazil). Fish were housed in 20 L polypropylene tanks containing filtered, dechlorinated water at a density of 1 fish/L. Each tank was equipped with an external filter providing physical, chemical, and biological filtration. Animals were kept under controlled conditions of temperature (26 ± 1 °C) and photoperiod (14 h light/10 h dark), and water quality parameters (pH, ammonia and nitrite) were monitored daily. Fish were fed twice daily with commercial feed (ColorBits, Tetra, Melle, Germany) and supplemented with Artemia nauplii three times per week.

All procedures were conducted in accordance with the Brazilian National Council for the Control of Animal Experimentation (CONCEA), Normative Resolution No. 61 (May 2, 2023), and approved by the Ethics Committee on Animal Use of the Federal University of Paraíba (CEUA-UFPB; protocol 7468180624).

2.4. Chronic exposition

2.4.1. Animals adaptation to experimental conditions

Prior to long-term exposure to 2,4-D and 2,4-DCP, fish underwent a two-week acclimation period under the same experimental conditions. Animals were randomly assigned to five treatment groups: negative control (recirculating system water only), 2,4-D low (30 µg/L) and high (3000 µg/L), and 2,4-DCP low (30 µg/L) and high (300 µg/L). Each treatment was conducted in duplicate, with 10 fish per 8-L glass tank (n = 20 fish per treatment), under continuous aeration.

Water used during both the acclimation and exposure periods was supplied from a 500-L closed recirculation system, maintaining proper quality parameters and a well-established microbiota. The macro- and microenvironmental conditions, as well as water quality, were maintained as described in the previous section. Complete water renewal was performed every three days to maintain safe levels of ammonia and nitrite. This renewal frequency was not expected to interfere with the nominal exposure concentrations of 2,4-D and 2,4-DCP, given their reported water half-lives of approximately 15 days (USEPA, 2015; Dehnert *et al.*, 2019; Gaaied *et al.*, 2020).

2.4.2. Long-term exposure

Long-term exposures were conducted based on adaptations of the methodologies described by Peng *et al.* (2019) and Cao *et al.* (2019). At the end of the acclimation period, aliquots of the stock solution were added to system water to achieve the desired final concentrations: 2,4-D and 2,4-DCP at 30 µg/L (2.4 mL in 7.9976 L), 2,4-D at 3000 µg/L (240 mL in 7.760 L), and 2,4-DCP at 300 µg/L (24 mL in 7.976 L). The exposure lasted for three weeks (21 days). Temperature and photoperiod conditions, water quality parameters (pH, ammonia, and nitrite), feeding, and exposure solution renewals were performed as described in section 2.4.1. Additionally, daily monitoring was conducted to detect mortality and potential behavioral alterations, such as abnormal swimming.

At the end of the exposure period, fish were euthanized using clove oil (1.5 mL/L), and livers were dissected. Sample preparation and storage followed protocols specific to each type of analysis. For biochemical analyses, livers from five fish per concentration were individually placed in 1.5 mL cryotubes and frozen at –20 °C. For histopathological analyses, livers from three fish per concentration were fixed in 4% formaldehyde for 24 h and then transferred to 70% ethanol for storage until analysis. In total, livers from eight fish per concentration were used for these analyses, while the remaining 12 per group were preserved for future analyses.

2.5 Enzimatic biomarkers analysis

Enzymatic activities associated with hepatotoxicity, including aspartate aminotransferase (AST) and alkaline phosphatase (ALP), as well as those related to oxidative and metabolic stress, namely lactate dehydrogenase (LDH), glutathione S-transferase (GST), and glutathione peroxidase (GPx), were evaluated. After thawing on ice, each liver was individually homogenized in 600 µL of ice-cold 0.1 M phosphate buffer (pH 7.4) using a pestle. The homogenate was centrifuged at 10,000 rpm for 20 min, and the resulting supernatant was used for the analyses.

Aliquots of the supernatant were allocated as follows for each assay: total protein (40 µL), AST (40 µL), ALP (20 µL), LDH (80 µL), GST (80 µL) and GPx (40 µL). Soluble protein levels were determined using the Bradford method (1976). Enzymatic activities were determined according to established methods. Specifically, LDH was measured following Domingues *et al.* (2010); GST following Domingues and Gravato (2018); and GPx according to Massarsky *et al.* (2017). The activities of AST, and ALP were assessed using commercial spectrophotometric kits (Labtest, Brazil) as described by Martins *et al.* (2021) and following the manufacturer's instructions. All measurements were performed in technical quadruplicates.

2.6. Histopatological analysis

Zebrafish livers were fixed in 4% formaldehyde for 24 h and processed following standard histological procedures: (1) dehydration through a graded ethanol series (70% for 24 h, followed by 80%, 96% [two baths], and 100% [two baths], each for 1 h); (2) clearing in xylene, first with an absolute ethanol–xylene solution (1:1) for 1 h, followed by two successive baths in 100% xylene for 1 h each; and (3) embedding in liquid paraffin (~50 °C) in two successive baths of 1 h each, followed by embedding in fresh paraffin blocks. Sections (5 µm) were stained with Harris hematoxylin and eosin and examined under a light microscope (Olympus BX41, Japan). Livers from three animals per group were evaluated for cellular and tissue alterations.

2.7. Statistical analysis

Data were analyzed using GraphPad Prism 8 software and are presented as mean ± standard deviation. Normality and homogeneity of variances were assessed using the Shapiro–Wilk and Barttleys tests, respectively. Data with a normal distribution were

analyzed by one-way ANOVA followed by Tukey's post hoc test ($p < 0.05$), while non-normally distributed data were analyzed using the Kruskal–Wallis test ($p < 0.05$).

3. Results

3.1. Enzimatic biomarkers

No significant differences in enzymatic activity were observed between treated and control groups for most of the biomarkers evaluated. However, the group exposed to 30 μg/L of 2,4-DCP showed a significant reduction in ALP activity, from 18.25 to 5.4 μmol/min/mg protein ($p = 0.019$).

Figure 1. Enzymatic activity levels of AST (a), ALP (b), LDH (c), GST (d), and GPx (e) in the livers of adult zebrafish exposed to 2,4-D (low: 3 µg/L; high: 3000 µg/L) and 2,4-DCP (low: 3 µg/L; high: 300 µg/L) for 21 days. Five individual livers per group were analyzed for all biomarkers and measurements were performed in technical quadruplicates. Data are presented as mean ± standard deviation. Significant differences between groups are indicated by asterisks (*, $p < 0.05$).

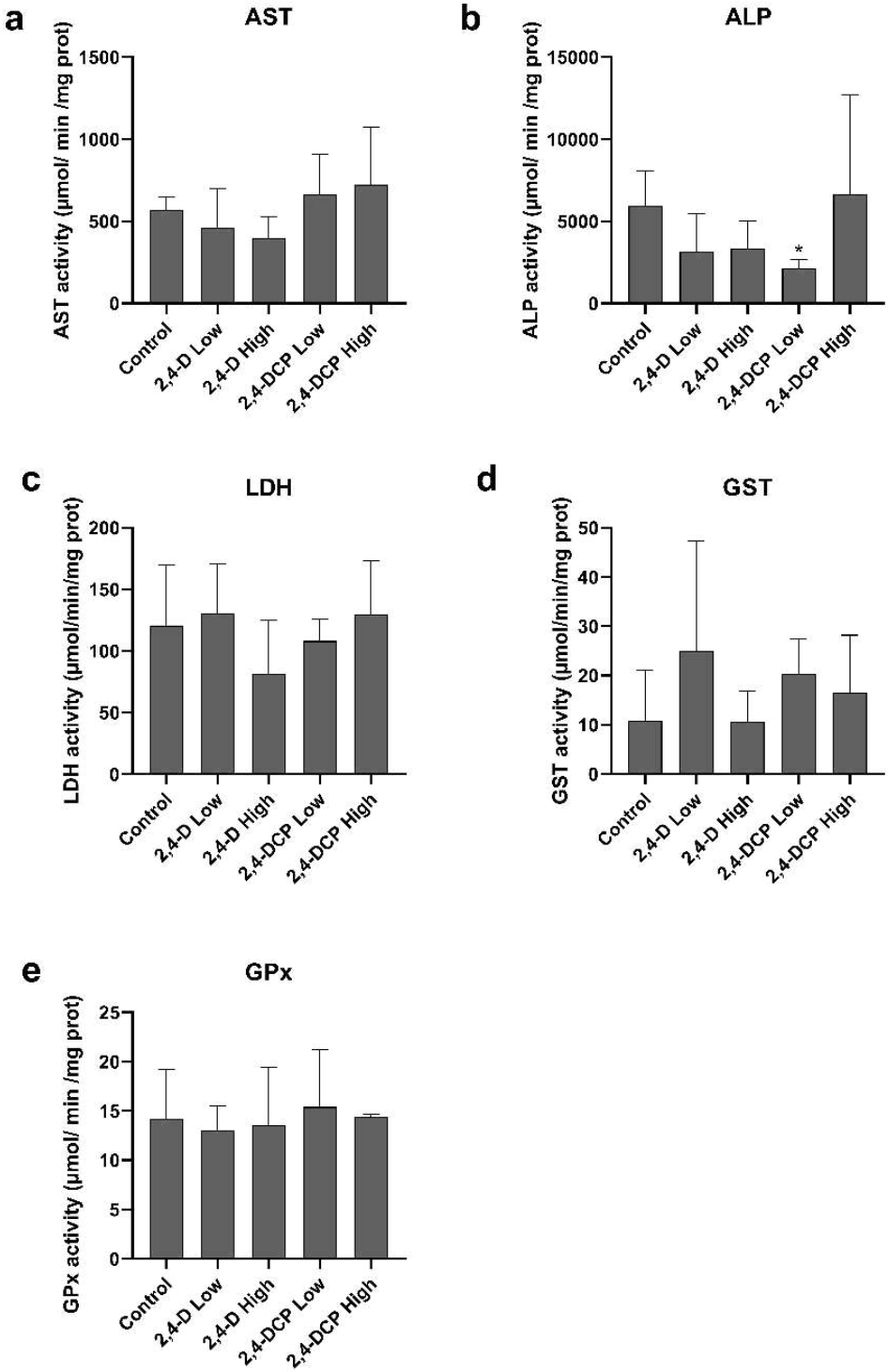

3.2. Histopatological analysis

In contrast to the biochemical analyses, histopathological evaluation revealed distinct cellular and tissue alterations in the liver of zebrafish exposed to 2,4-D and 2,4-DCP (Figures 2 and 3). Livers from control animals displayed characteristics of a morphologically healthy organ, including preserved architecture, well-defined hepatocytes, and centrally located nuclei.

Exposure to 30 μg/L of 2,4-D induced cytoplasmic vacuolization with lipid droplet accumulation, indicative of microvesicular steatosis (Cast *et al.*, 2019; Israelsen *et al.*, 2024). Hepatic parenchymal disorganization was also evident, characterized by loss of cell boundaries and nuclear alterations, including shrunken, condensed, and hyperchromatic nuclei consistent with pyknosis, as well as fragmented chromatin, indicative of karyorrhexis (Taatjes *et al.*, 2008; Li *et al.*, 2022). At 3000 μg/L, similar alterations were observed, but with additional large vacuoles and eccentric nuclei, features characteristic of macrovesicular steatosis, together with areas of necrosis (Cast *et al.*, 2019).

In the 2,4-DCP low group, hepatocytes displayed multiple cytoplasmic vacuoles with accumulation of small lipid droplets, indicative of microvesicular steatosis (Cast *et al.*, 2019). In the 2,4-DCP high group, in addition to this effect, further cellular alterations were observed, including vascular congestion, increased eosinophilic content, hepatic parenchymal disorganization, and loss of cellular architecture.

Figure 2. Histological sections of zebrafish liver exposed to different concentrations of 2,4-D. (A–C) Liver from control animals showing healthy hepatocytes with preserved architecture. (D–F) Liver from animals exposed to 30 µg/L of 2,4-D displaying early cellular alterations. (G–I) Liver from animals exposed to 3000 µg/L of 2,4-D exhibiting more pronounced cellular alterations. Arrowheads indicate pyknotic nuclei; arrows, karyorrhexis; asterisks, cytoplasmic vacuolization indicative of steatosis; triangles, large intracellular vacuoles with eccentric nuclei, consistent with macrovesicular steatosis. N, necrosis; circles, degenerated hepatocytes.

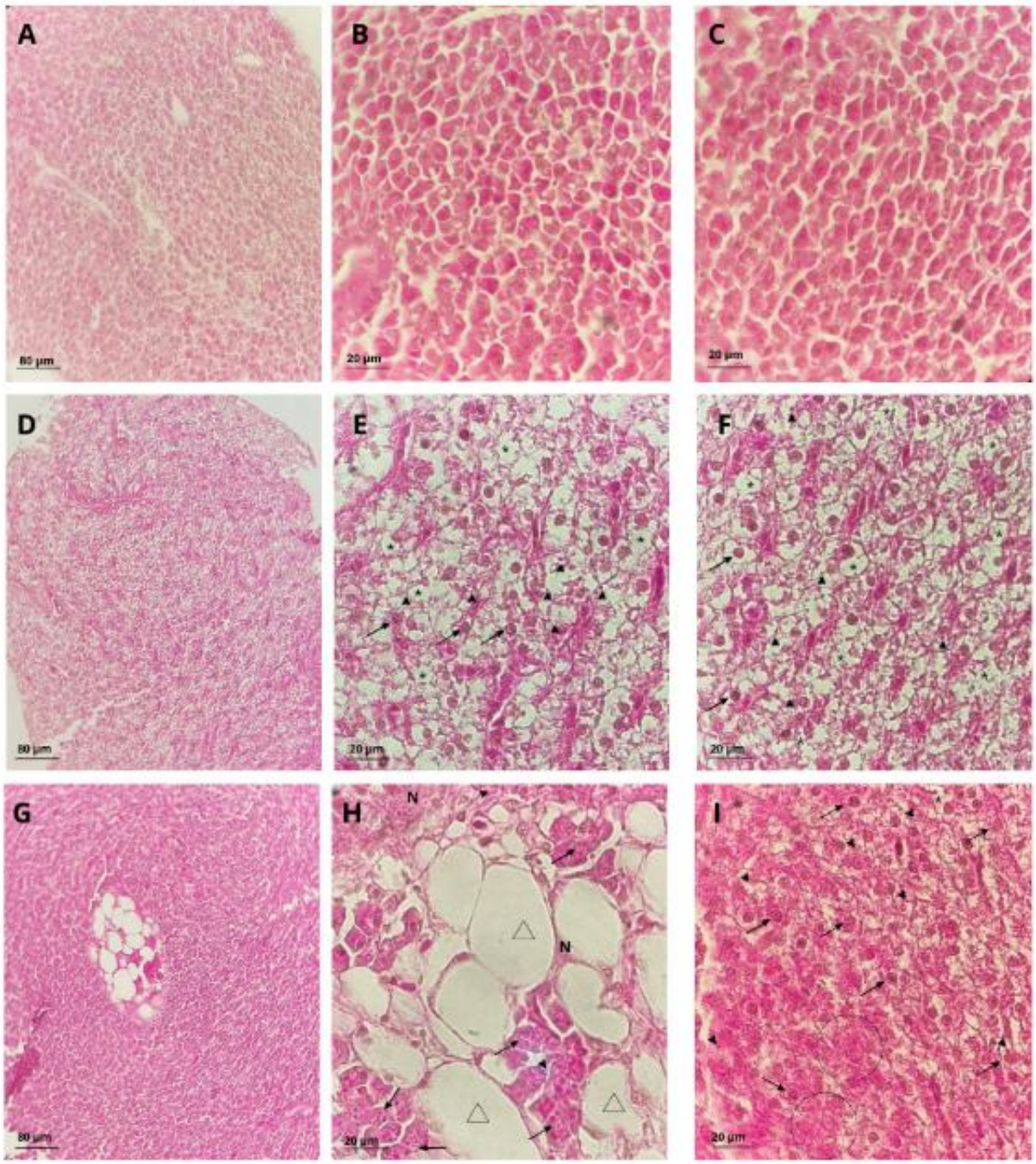

Figure 3. Histological sections of zebrafish liver exposed to different concentrations of 2,4-DCP. (A–C) Liver from control animals showing healthy hepatocytes with preserved architecture. (D–F) Liver from animals exposed to 30 µg/L of 2,4-DCP displaying cellular alterations. Arrowheads indicate cytoplasmic vacuolization consistent with lipid accumulation and microvesicular steatosis. (G–I) Liver from animals exposed to 300 µg/L of 2,4-DCP showing more pronounced cellular alterations. Arrowheads indicate extensive cytoplasmic vacuolization and steatosis; "C" denotes vascular congestion; circles highlight degenerating hepatocytes.

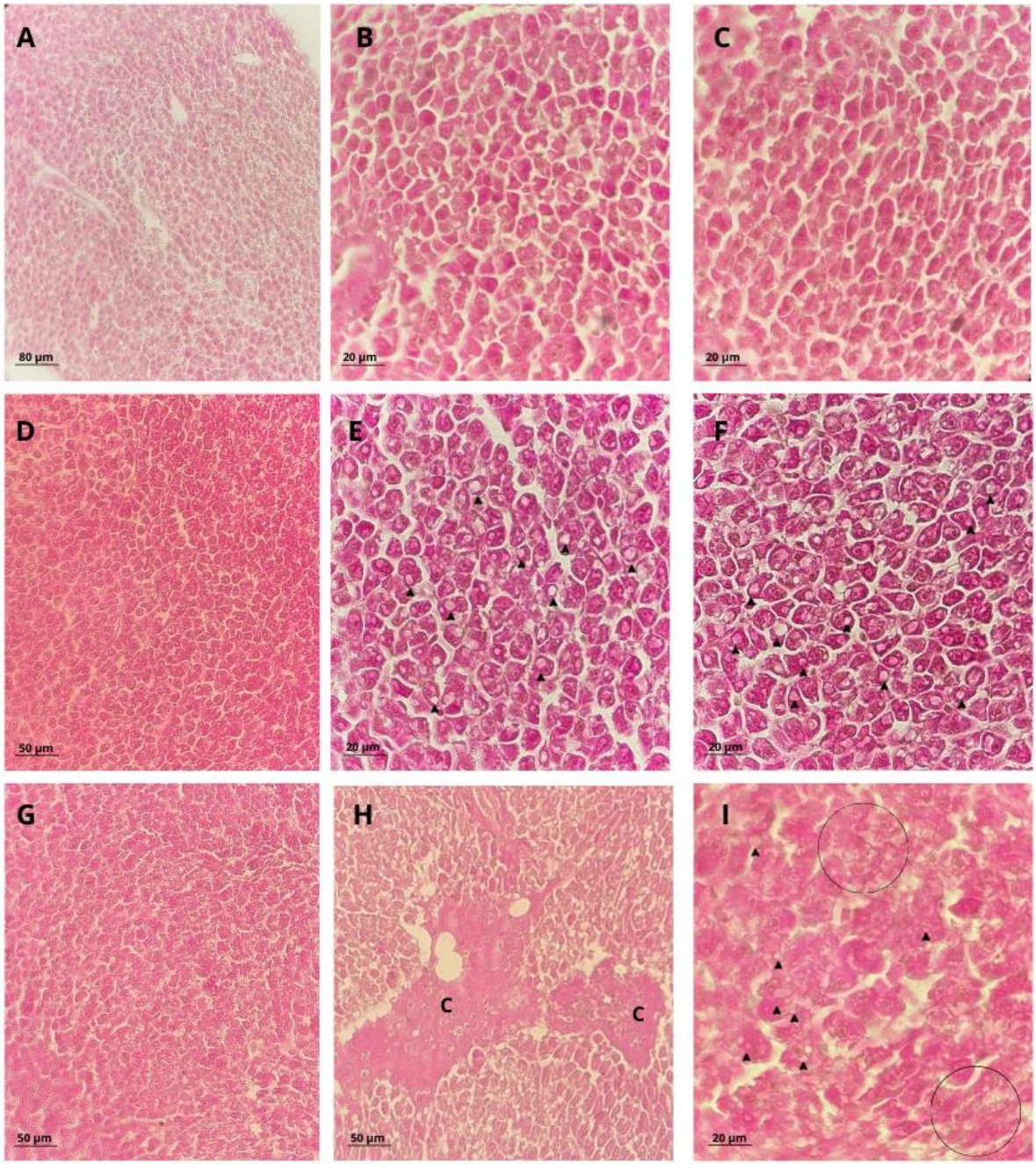

4. Discussion

This study demonstrated that 2,4-D and 2,4-DCP induced hepatotoxicity in zebrafish at the tested concentrations, as evidenced by the cellular and tissue alterations observed in the histopathological analysis. A prominent effect of 2,4-D exposure was the presence of cytoplasmic vacuolizations, indicative of lipid accumulation (Chang *et al.*, 2023; Israelsen *et al.*, 2024). These findings suggest that 2,4-D exposure leads to hepatic steatosis, closely resembling the pathology of non-alcoholic fatty liver disease (NAFLD) (Chang *et al.*, 2023).

Furthermore, the observation of pyknotic nuclei and karyorrhexis indicated cell death, such as apoptosis and necrosis (Taatjes *et al.*, 2008). Together, these alterations demonstrate that both low and high 2,4-D exposures promoted the development of an advanced stage of NAFLD, non-alcoholic steatohepatitis (NASH), which is characterized not only by steatosis but also by inflammation and hepatocellular injury (Lai *et al.*, 2021; Chang *et al.*, 2023).

Supporting these findings, a study in mice by Romualdo *et al.* (2023) showed that chronic exposure to 2 mg/kg/day of 2,4-D exacerbated Western diet-induced NAFLD by enhancing pro-inflammatory parameters and fibrosis. Our data demonstrate that 2,4-D alone, even at a concentration of 30 µg/L, was able to induce a NASH-like phenotype in zebrafish after 21 days of exposure (Lai *et al.*, 2021). This is particularly concerning since this concentration corresponds to the maximum permitted limit in Brazilian drinking water (SISAGUA, 2018).

Interestingly, exposure to 30 µg/L of 2,4-DCP also resulted in lipid droplet accumulation in zebrafish hepatocytes, although to a lesser extent. At this concentration, no evidence of cell death was observed. More severe effects were only detected in the 300 µg/L group, which included hepatocyte degeneration, increased eosinophilic content, disruption of tissue architecture, and lipid accumulation.

Our findings align with Tsukazawa *et al.* (2022), who reported that acute exposure to 2.5 mg/L of 2,4-DCP induced lipid accumulation in zebrafish larvae. Our data suggest this is a common mechanism, also triggered under chronic exposure and at significantly lower concentrations.

Previous work from our group demonstrated that 2,4-D and its metabolite share hepatotoxic mechanisms, including oxidative stress, mitochondrial dysfunction, lipid accumulation, and cell death (Martins *et al.*, 2025). In addition, key pathways have been

identified, such as nuclear receptor signaling, which plays a central role in lipid metabolism processes including biosynthesis, storage, and β-oxidation (Den Broeder *et al.*, 2015; Martins *et al.*, 2025).

Supporting this, lipid accumulation induced by 2,4-DCP in zebrafish was accompanied by reduced expression of the nuclear receptor *ppara*, which stimulates the transcription of genes involved in mitochondrial and peroxisomal β-oxidation (Fan and Evans, 2015; Todisco *et al.*, 2022). Histopathological analysis further confirmed that chronic exposure to both compounds promote lipid accumulation and cellular damage. However, at 30 μg/L, these effects were more pronounced in zebrafish exposed to 2,4-D compared to 2,4-DCP.

This discrepancy may be explained by their distinct mechanisms. *In silico* curation identified 216 protein targets related to hepatotoxicity for 2,4-D, compared to 113 for 2,4-DCP (Martins *et al.*, 2025), suggesting a broader range of toxic actions for the parent compound. Furthermore, molecular docking with common target proteins (e.g., RXRA, SRC, HSP90AA1, MDM2, ESR1) showed more negative binding energies for 2,4-D, indicating a higher potential for interaction and disruption of biological pathways (Martins *et al.*, 2025).

Despite evidence of morphological alterations in the histopathological analysis, no significant disruption was observed in the enzymatic activity of most biochemical markers examined. GST, GPx, and LDH activities were measured to assess oxidative and metabolic stress. GST and GPx are antioxidant enzymes involved in glutathione metabolism, which is essential for neutralizing free radicals and detoxifying endogenous and exogenous compounds (Massarsky *et al.*, 2017). LDH serves as a marker of anaerobic metabolism and is generally elevated under hypoxic conditions or tissue injury (Lagana *et al.*, 2019). AST and ALP are well-established indicators of hepatic health and hepatobiliary disorders, respectively (Martins *et al.*, 2024). Although ALP activity was reduced in the group treated with 30 μg/L of 2,4-DCP, more pronounced biochemical changes were expected based on the histopathological results.

One possible explanation for the lack of statistical significance in the biochemical data is the high genetic variability of zebrafish, even among laboratory strains (Parichy *et al.*, 2015). Since all five animals per treatment were analyzed individually rather than as pooled samples, this variability likely contributed to substantial data dispersion. Similarly, Ye *et al.* (2022) reported high variability in GPx, SOD, and CAT activities in

the livers of zebrafish exposed to polychlorinated diphenyl ethers, even using 10 animals per treatment, indicating that such dispersion is typical in individual-based analyses.

Therefore, a more efficient approach for future studies may be to increase the sample size (n) per treatment and utilize pooled samples. This strategy is commonly employed for the determination of biochemical and molecular markers in zebrafish larvae and would better represent a mean value for the treatment group (Wei *et al.*, 2023).

5. Conclusion

This study demonstrates that chronic exposure to 2,4-D and its metabolite 2,4-DCP induces hepatotoxicity in adult zebrafish. Liver damage was marked mainly by lipid accumulation, with 2,4-D showing features consistent with NASH disease. Importantly, these effects occurred at concentrations equivalent to the permissible limit for 2,4-D in Brazilian drinking water, raising concerns about the adequacy of current regulations for protecting aquatic vertebrates. The findings also underscore the need to monitor environmental levels of 2,4-DCP, for which detection data in Brazil remain scarce. Future studies should aim to clarify the mechanistic basis of chronic hepatotoxicity by identifying the molecular pathways and targets involved. This knowledge is crucial for guiding damage mitigation strategies and for identifying biomarkers of intoxication by the herbicide and its metabolite.

5. CONSIDERAÇÕES FINAIS

Os resultados obtidos nesta tese de doutorado ampliam de forma significativa o conhecimento sobre a hepatotoxicidade induzida pelo herbicida 2,4-D e seu metabólito 2,4-DCP. Uma das principais lacunas preenchidas refere-se à identificação dos potenciais alvos moleculares e vias de sinalização envolvidos nesses efeitos tóxicos. Por meio de abordagens integradas de toxicologia de redes e simulações de docking molecular, foram identificadas proteínas-chave associadas ao dano hepático, como SRC, RXRA, ESR1 e AKT1, além da participação de vias críticas como sinalização de receptores nucleares e a via PI3K/AKT. Os resultados demonstram ainda que grande parte desses alvos e vias são compartilhados entre o 2,4-D e o 2,4-DCP, sugerindo um mecanismo hepatotóxico convergente entre o composto original e seu metabólito ambiental.

Outra lacuna importante preenchida por esta tese refere-se à hepatotoxicidade em concentrações ambientalmente relevantes desses compostos. Demonstramos que a exposição aguda às concentrações de 3, 30 e 300 μg/L de 2,4-D e 2,4-DCP (níveis compatíveis com aqueles detectados em ambientes aquáticos contaminados) induz hepatotoxicidade em larvas de peixe-zebra. A partir da análise de marcadores bioquímicos e moleculares de toxicidade, esses efeitos foram associados a mecanismos cruciais envolvidos na progressão de doenças hepáticas, incluindo estresse oxidativo, perda do potencial de membrana mitocondrial e acúmulo lipídico. Além disso, esses achados experimentais corroboraram os resultados das análises *in silico*, revelando que a disrupção desses mecanismos, em parte, está associada à alteração da expressão de receptores nucleares, como *ppara* e *pparg*.

Observou-se ainda que, embora ambos os compostos acionem vias de toxicidade semelhantes, os padrões de resposta foram distintos: o 2,4-D promoveu principalmente estresse oxidativo, enquanto o 2,4-DCP afetou de forma mais intensa o metabolismo lipídico. Esses resultados sugerem que, apesar de compartilharem mecanismos moleculares, existem diferenças mecanísticas entre os compostos, possivelmente relacionadas à afinidade diferencial por alvos moleculares, concentração e tempo de exposição.

Além disso, esta tese também preencheu uma lacuna crítica relacionada à hepatotoxicidade crônica desses contaminantes. Em peixes-zebra adultos expostos por 21 dias ao 2,4-D ou 2,4-DCP, foram observadas alterações histopatológicas hepáticas significativas, incluindo acúmulo de lipídios, sinais de morte celular e desorganização da arquitetura tecidual. Diferentemente do observado na exposição aguda, na exposição

crônica o 2,4-D induziu maior acúmulo de gordura hepática em comparação ao 2,4-DCP, resultando em um quadro compatível com doença hepática gordurosa não alcoólica (NAFLD). Um achado particularmente preocupante, já que essas alterações ocorreram inclusive na concentração equivalente ao VMP de 2,4-D em água potável no Brasil.

Os resultados desta tese questionam a segurança do VMP de 30 μg/L de 2,4-D em água potável, atualmente adotado no Brasil. Demonstramos efeitos tóxicos em peixe-zebra mesmo em concentrações consideradas seguras pela legislação, indicando que o valor vigente pode subestimar riscos ambientais e à saúde pública. Assim, reforçamos a necessidade de reavaliação regulatória desse limite, bem como a realização de novos estudos **(**eco)toxicológicos com concentrações ambientais em diferentes modelos biológicos, a fim de gerar evidências para processos de revisão normativa.

Além disso, evidenciamos que o 2,4-DCP deve ser considerado um contaminante emergente prioritário, uma vez que demonstrou toxicidade em baixas concentrações e permanece pouco monitorado e negligenciado em políticas ambientais no Brasil. Por ser metabólito comum de diversos organoclorados, destacamos a urgência de programas de monitoramento e avaliações adicionais sobre sua toxicidade em níveis consistentes com a exposição humana e ambiental.

Por fim, este trabalho propôs uma abordagem metodológica integrada, alinhada aos princípios dos 3Rs da experimentação animal. O uso de estratégias *in silico* orientou a seleção de alvos moleculares em etapas que, na toxicologia tradicional, demandariam o uso extensivo de animais, contribuindo diretamente para o princípio de *Reduction*. A adoção do peixe-zebra como modelo experimental, sobretudo em estágios embrionários e larvais, permitiu a obtenção de dados mecanísticos, ao mesmo tempo em que minimizou o sofrimento animal e reduziu o número de vertebrados utilizados, em consonância com o princípio de *Refinement*. Abordagens integradas como esta são eficientes em estudos mecanísticos de toxicidade, fornecendo informações relevantes e promovendo avanços éticos na experimentação animal.

REFERÊNCIAS

ABDELLATIF, A. G.; PRÉAT, V.; VAMECQ, J.; NILSSON, R.; ROBERFROID, M. Peroxissome proliferation and modulation of rat liver carcinogenesis by 2,4-dichlorophenoxyacetic acid, 2,4,5-trichlorophenoxyacetic acid, perfluorooctanoic acid and nafenopin. **Carcinogenesis**, v. 11, n. 11, p. 1899–1902, 1990.

ACKERS, J. T.; JOHNSTON, M. F.; HAASCH, M. L. Immunodetection of hepatic peroxisomal PMP70 as an indicator of peroxisomal proliferation in the mummichog, *Fundulus heteroclitus*. **Marine Environmental Research**, v. 50, n. 1–5, p. 361–365, 2000. https://doi.org/10.1016/S0141-1136(00)00061-1.

ADEVA-ANDANY, M. M.; CALVO-CASTRO, I.; FERNÁNDEZ-FERNÁNDEZ, C.; DONAPETRY-GARCÍA, C.; PEDRE-PIÑEIRO, A. M. Significance of L-carnitine for human health. **IUBMB Life**, v. 69, n. 8, p. 578–594, 2017. https://doi.org/10.1002/iub.1646.

AGÊNCIA NACIONAL DE VIGILÂNCIA SANITÁRIA (ANVISA). Índice monográfico: 2,4-D. Brasília, 2021. Disponível em: https://www.gov.br/anvisa/ptbr/setorregulado/regularizacao/agrotoxicos/monografias/monografias-autorizadas/d/4285json-file-1. Acesso em: 8 out. 2025.

AGENCY FOR TOXIC SUBSTANCES AND DISEASE REGISTRY (ATSDR). Toxicological profile for 2,4-dichlorophenoxyacetic acid. Atlanta, 2020. Disponível em: https://www.atsdr.cdc.gov/ToxProfiles/tp.asp?id=1481&tid=288. Acesso em: 18 dec. 2023.

AKUNE, T. *et al.* PPARγ insufficiency enhances osteogenesis through osteoblast formation from bone marrow progenitors. **Journal of Clinical Investigation**, v. 113, n. 6, p. 846–855, 2004. https://doi.org/10.1172/JCI200419900.

AL-BAROUDI, D. A.; ARAFAT, R.; EL-KHOLY, T. Hepatoprotective effect of chamomile capitula extract against 2,4-dichlorophenoxyacetic acid-induced hepatotoxicity in rats. **Life Science Journal**, v. 11, n. 8, p. 34–40, 2014.

ALI, A. A. *et al.* Rosiglitazone causes bone loss in mice by suppressing osteoblast differentiation and bone formation. **Endocrinology**, v. 146, n. 3, p. 1226–1235, 2005. https://doi.org/10.1210/en.2004-0735.

ALLAMEH, A. *et al.* Oxidative stress in liver pathophysiology and disease. **Antioxidants**, v. 12, n. 9, p. 1653, 2023. https://doi.org/10.3390/antiox12091653.

ALMAZROO, O. A.; MIAH, M. K.; VENKATARAMANAN, R. Drug metabolism in the liver. **Clinics in Liver Disease**, v. 21, n. 1, p. 1–20, 2017. https://doi.org/10.1016/j.cld.2016.08.001.

APARECIDA, M.; CAMPOS VENTURA-CAMARGO, B. D.; MIYUKI, M. Toxicity of herbicides: impact on aquatic and soil biota and human health. In: PRICE, A. (ed.). **Herbicides—current research and case studies in use**. Rijeka: InTech, 2013. https://doi.org/10.5772/55851.

SATAPATHY, A.; RAO, M. V. Protective effect of curcumin on 2,4-dichlorophenoxyacetic acid exerted hepatotoxicity in mice. **Research Journal of Pharmacy and Technology**, v. 11, n. 2, p. 637–642, 2018. https://doi.org/10.5958/0974-360X.2018.00119.1.

AQEEL, A. *et al.* Mechanistic insights into impaired β-oxidation and its role in mitochondrial dysfunction: a comprehensive review. **Diabetes Research and Clinical Practice**, v. 223, p. 112129, 2025. https://doi.org/10.1016/j.diabres.2025.112129.

ARNESDOTTER, E. *et al.* Derivation, characterisation and analysis of an adverse outcome pathway network for human hepatotoxicity. **Toxicology**, v. 459, p. 152856, 2021. https://doi.org/10.1016/j.tox.2021.152856.

ARROYAVE-OSPINA, J. C. *et al.* Role of oxidative stress in the pathogenesis of non-alcoholic fatty liver disease: implications for prevention and therapy. **Antioxidants**, v. 10, n. 2, p. 174, 2021. https://doi.org/10.3390/antiox10020174.

ARYA, D. S. *et al.* Effect of *Piper betle* on cardiac function, marker enzymes and oxidative stress in isoproterenol-induced cardiotoxicity in rats. **Toxicology Mechanisms and Methods**, v. 20, n. 9, p. 564–571, 2010. https://doi.org/10.3109/15376516.2010.514962.

AUBREY, B. J.; STRASSER, A.; KELLY, G. L. Tumor-suppressor functions of the TP53 pathway. **Cold Spring Harbor Perspectives in Medicine**, v. 6, n. 5, p. a026062, 2016. https://doi.org/10.1101/cshperspect.a026062.

AYDIN, H. *et al.* Effects of 2,4-dichlorophenoxyacetic acid (2,4-D) treatment on the epididymal spermatozoa, blood serum transaminases and its accumulation in liver of rats. [Dados incompletos].

AZEVEDO, R. D. S. *et al.* The tissue-specific nature of physiological zebrafish mitochondrial bioenergetics. **Mitochondrion**, v. 77, p. 101901, 2024. https://doi.org/10.1016/j.mito.2024.101901.

BADAWI, A. F.; CAVALIERI, E. L.; ROGAN, E. G. Effect of chlorinated hydrocarbons on expression of cytochrome P450 1A1, 1A2 and 1B1 and 2- and 4-hydroxylation of 17β-estradiol in female Sprague–Dawley rats. [Dados incompletos].

BALAMURUGAN, K. *et al.* Protocol to evaluate hyperlipidemia in zebrafish larvae. **STAR Protocols**, v. 3, n. 4, p. 101819, 2022. https://doi.org/10.1016/j.xpro.2022.101819.

BAMBINO, K.; CHU, J.; MORRISON, J. Hepatotoxicity in zebrafish larvae. **Methods in Molecular Biology**, v. 1965, p. 129–138, 2019. https://doi.org/10.1007/978-1-4939-9182-2_9.

BHARADWAJ, L. *et al.* Altered gene expression in human hepatoma HepG2 cells exposed to low-level 2,4-dichlorophenoxyacetic acid and potassium nitrate. **Toxicology in Vitro**, v. 19, n. 5, p. 603–619, 2005. https://doi.org/10.1016/j.tiv.2005.03.011.

BHATTACHARJEE, S.; RANA, T.; SENGUPTA, A. Inhibition of lipid peroxidation and enhancement of GST activity by cardamom and cinnamon during chemically induced colon carcinogenesis in Swiss albino mice. **Asian Pacific Journal of Cancer Prevention**, v. 8, n. 4, p. 578–582, 2007.

BIOVIA; DASSAULT SYSTÈMES. Discovery Studio Visualizer, v21.1.0.20298. San Diego, 2021. Disponível em: https://discover.3ds.com/discovery-studio-visualizer-download. Acesso em: dez. 2024.

BONFIM, D. J. P. *et al.* Hepatic, renal and pancreatic damage associated with chronic exposure to oral and inhaled 2,4-dichlorophenoxyacetic acid (2,4-D): an environmental exposure model in rats. **Comparative Clinical Pathology**, v. 29, n. 5, p. 1001–1010, 2020. https://doi.org/10.1007/s00580-020-03150-8.

BOUEID, M. J. *et al.* Zebrafish as an emerging model to study estrogen receptors in neural development. **Frontiers in Endocrinology**, v. 14, p. 1240018, 2023. https://doi.org/10.3389/fendo.2023.1240018.

BRADFORD, M. M. A rapid and sensitive method for the quantitation of microgram quantities of protein utilizing the principle of protein-dye binding. **Analytical Biochemistry**, v. 72, p. 248–254, 1976. https://doi.org/10.1016/0003-2697(76)90527-3.

BRAUNBECK, T. *et al.* Towards an alternative for the acute fish LC(50) test in chemical assessment: the fish embryo toxicity test goes multi-species—an update. **ALTEX**, v. 22, n. 2, p. 87–102, 2005.

BRAUNSTEIN, J. A. *et al.* Basal epidermis collective migration and local Sonic hedgehog signaling promote skeletal branching morphogenesis in zebrafish fins. **Developmental Biology**, v. 477, p. 177–190, 2021. https://doi.org/10.1016/j.ydbio.2021.04.010.

BUENO FRANCO SALLA, G. *et al.* Kinetics of the metabolic effects, distribution spaces and lipid-bilayer affinities of the organochlorinated herbicides 2,4-D and picloram in the liver. **Toxicology Letters**, v. 313, p. 137–149, 2019. https://doi.org/10.1016/j.toxlet.2019.06.008.

CANOSA, P. *et al.* Aquatic degradation of triclosan and formation of toxic chlorophenols in presence of low concentrations of free chlorine. **Analytical and Bioanalytical Chemistry**, v. 383, n. 7–8, p. 1119–1126, 2005. https://doi.org/10.1007/s00216-005-0116-4.

CASIMERO, M. *et al.* Herbicide use history and weed management in Southeast Asia. **Advances in Weed Science**, v. 40, p. e020220054, 2022. https://doi.org/10.51694/AdvWeedSci/2022;40:seventy-five013.

CASSAR, S. *et al.* Use of zebrafish in drug discovery toxicology. **Chemical Research in Toxicology**, v. 33, n. 1, p. 95–118, 2020. https://doi.org/10.1021/acs.chemrestox.9b00335.

CATTANEO, R. *et al.* Metabolic and histological parameters of silver catfish (*Rhamdia quelen*) exposed to commercial formulation of 2,4-dichlorophenoxyacetic acid (2,4-D) herbicide. **Pesticide Biochemistry and Physiology**, v. 92, n. 3, p. 133–137, 2008. https://doi.org/10.1016/j.pestbp.2008.07.004.

CELIK, I.; TULUCE, Y.; ISIK, I. Influence of subacute treatment of some plant growth regulators on serum marker enzymes and erythrocyte and tissue antioxidant defense and lipid peroxidation in rats. **Journal of Biochemical and Molecular Toxicology**, v. 20, n. 4, p. 174–182, 2006. https://doi.org/10.1002/jbt.20134.

CHAN, B. Y. *et al.* PPAR agonists modulate human osteoclast formation and activity in vitro. **Bone**, v. 40, n. 1, p. 149–159, 2007. https://doi.org/10.1016/j.bone.2006.06.022.

CHANG, J. Y. L. Liver physiology: metabolism and detoxification. In: MCMANUS, L. M.; MITCHELL, R. N. (ed.). **Pathophysiology of human disease**. Elsevier, 2014. p. 1770–1782. https://doi.org/10.1016/B978-0-12-386456-7.04202-7.

CHATURVEDI, A. K.; KUNTZ, D. J.; RAO, N. G. S. Metabolic aspects of the toxicology of mixtures of parathion, toxaphene and/or 2,4-D in mice. **Journal of Applied Toxicology**, v. 11, n. 4, p. 245–251, 1991. https://doi.org/10.1002/jat.2550110404.

CHEN, Z. *et al.* Role of oxidative stress in the pathogenesis of nonalcoholic fatty liver disease. **Free Radical Biology and Medicine**, v. 152, p. 116–141, 2020. https://doi.org/10.1016/j.freeradbiomed.2020.02.025.

CHENG, M. L. *et al.* The immune niche of the liver. **Clinical Science**, v. 135, n. 20, p. 2445–2466, 2021. https://doi.org/10.1042/CS20190654.

CHUA, F. Z. *et al.* Sexual dimorphism in zebrafish aggression and metabolism under acute ammonia stress. **Comparative Biochemistry and Physiology Part C: Toxicology & Pharmacology**, v. 290, p. 110131, 2025. https://doi.org/10.1016/j.cbpc.2025.110131.

CICHOŻ-LACH, H. Oxidative stress as a crucial factor in liver diseases. **World Journal of Gastroenterology**, v. 20, n. 25, p. 8082, 2014. https://doi.org/10.3748/wjg.v20.i25.8082.

COCK, T. A. *et al.* Enhanced bone formation in lipodystrophic PPARγ(hyp/hyp) mice relocates haematopoiesis to the spleen. **EMBO Reports**, v. 5, n. 10, p. 1007–1012, 2004. https://doi.org/10.1038/sj.embor.7400259.

COMPANHIA AMBIENTAL DO ESTADO DE SÃO PAULO (CETESB). Qualidade das águas interiores no Estado de São Paulo: relatório 2017. São Paulo: CETESB, 2018. Disponível em: https://cetesb.sp.gov.br/aguas-interiores/wp-content/uploads/sites/12/2018/06/Relat%C3%B3rio-de-Qualidade-das-%C3%81guas-Interiores-no-Estado-de-S%C3%A3o-Paulo-2017.pdf. Acesso em: 8 out. 2025.

CONVERTINI, P. *et al.* The contribution of the citrate pathway to oxidative stress in Down syndrome. **Immunology**, v. 149, n. 4, p. 423–431, 2016. https://doi.org/10.1111/imm.12659.

COTTERILL, J. V. *et al.* Predicting estrogen receptor binding of chemicals using a suite of in silico methods: complementary approaches of (Q)SAR, molecular docking and molecular dynamics. **Toxicology and Applied Pharmacology**, v. 378, p. 114630, 2019. https://doi.org/10.1016/j.taap.2019.114630.

CURI, L. M. *et al.* Acute toxicity and sublethal effects caused by a commercial herbicide formulated with 2,4-D on *Physalaemus albonotatus* tadpoles. **Water, Air, & Soil Pollution**, v. 230, n. 1, p. 22, 2019. https://doi.org/10.1007/s11270-018-4073-x.

DA FONSECA, M. B. *et al.* The 2,4-D herbicide effects on acetylcholinesterase activity and metabolic parameters of piava freshwater fish (*Leporinus obtusidens*). **Ecotoxicology and Environmental Safety**, v. 69, n. 3, p. 416–420, 2008. https://doi.org/10.1016/j.ecoenv.2007.08.006.

DA SILVA, A. P. *et al.* Does exposure to environmental 2,4-dichlorophenoxyacetic acid concentrations increase mortality rate in animals? A meta-analytic review. **Environmental Pollution**, v. 303, p. 119179, 2022. https://doi.org/10.1016/j.envpol.2022.119179.

DAI, X. *et al.* 2,4-DCP compromises the fertilization capacity of mouse oocytes. **Journal of Cellular Physiology**, v. 236, n. 11, p. 7605–7611, 2021. https://doi.org/10.1002/jcp.30403.

DAKHAKHNI, T. H.; RAOUF, G. A.; QUSTI, S. Y. Evaluation of the toxic effect of the herbicide 2,4-D on rat hepatocytes: an FT-IR spectroscopic study. **European Biophysics Journal**, v. 45, n. 4, p. 311–320, 2016. https://doi.org/10.1007/s00249-015-1097-7.

DALMOLIN, S. P.; DREON, D. B.; THIESEN, F. V.; DALLEGRAVE, E. Biomarkers of occupational exposure to pesticides: systematic review of insecticides. **Environmental Toxicology and Pharmacology**, v. 75, p. 103304, 2020. https://doi.org/10.1016/j.etap.2019.103304.

DATTA, S. *et al.* A high-throughput screen for mitochondrial function reveals known and novel mitochondrial toxicants in a library of environmental agents. **Mitochondrion**, v. 31, p. 79–83, 2016. https://doi.org/10.1016/j.mito.2016.10.001.

DE OLIVEIRA, A. Á. S. *et al.* Integrating morphological, biochemical, behavioural and molecular approaches to investigate developmental toxicity triggered by tebuthiuron in zebrafish (*Danio rerio*). **Chemosphere**, v. 340, p. 139894, 2023. https://doi.org/10.1016/j.chemosphere.2023.139894.

DEHNERT, G. K.; KARASOV, W. H.; WOLMAN, M. A. 2,4-dichlorophenoxyacetic acid containing herbicide impairs essential visually guided behaviors of larval fish. **Aquatic Toxicology**, v. 209, p. 1–12, 2019. https://doi.org/10.1016/j.aquatox.2019.01.015.

DELGADO-COELLO, B. Liver regeneration observed across the different classes of vertebrates from an evolutionary perspective. **Heliyon**, v. 7, n. 3, e06449, 2021. https://doi.org/10.1016/j.heliyon.2021.e06449.

DELLI BOVI, A. P. *et al.* Oxidative stress in non-alcoholic fatty liver disease: an updated mini review. **Frontiers in Medicine**, v. 8, p. 595371, 2021. https://doi.org/10.3389/fmed.2021.595371.

DELMAR, J. A.; GALLEGO, P.; GRANDE, L. Role of inflammatory response in liver diseases: therapeutic strategies. **World Journal of Hepatology**, v. 10, n. 1, p. 1–7, 2018. https://doi.org/10.4254/wjh.v10.i1.1.

DEN BROEDER, M. J. *et al.* Zebrafish as a model to study the role of peroxisome proliferating-activated receptors in adipogenesis and obesity. **PPAR Research**, 2015, 358029, 2015. https://doi.org/10.1155/2015/358029.

DI PAOLO, O.; DE DUFFARD, A. M. E.; DUFFARD, R. In vivo and in vitro binding of 2,4-dichlorophenoxyacetic acid to a rat liver mitochondrial protein. **Chemico-Biological Interactions**, v. 137, n. 3, p. 229–241, 2001. https://doi.org/10.1016/S0009-2797(01)00255-1.

DIERICKX, P. J. Interaction of chlorophenoxyalkyl acid herbicides with rat-liver glutathione S-transferases. **Food and Chemical Toxicology**, v. 21, n. 5, p. 575–579, 1983. https://doi.org/10.1016/0278-6915(83)90143-6.

DIERICKX, P. J. Hepatic glutathione S-transferases in rainbow trout and their interaction with 2,4-dichlorophenoxyacetic acid and 1,4-benzoquinone. **Comparative Biochemistry and Physiology Part C**, v. 82, n. 2, p. 495–500, 1985. https://doi.org/10.1016/0742-8413(85)90199-9.

DIERICKX, P. J. Interaction of 1,4-benzoquinone and 2,4-dichlorophenoxyacetic acid with microsomal glutathione transferase from rat liver. **Archives Internationales de Physiologie et de Biochimie**, v. 96, n. 1, p. 1–5, 1988. https://doi.org/10.3109/13813458809079619.

DING, H. R.; WANG, J. L.; REN, H. Z.; SHI, X. L. Lipometabolism and glycometabolism in liver diseases. **BioMed Research International**, 2018, 1287127, 2018. https://doi.org/10.1155/2018/1287127.

DIXON, A.; OSTERLOH, J.; BECKER, C. Inhibition of palmitoyl co-enzyme A hydrolase in mitochondria and microsomes by pharmaceutical organic anions. **Journal of Pharmaceutical Sciences**, v. 79, n. 2, p. 103–105, 1990. https://doi.org/10.1002/jps.2600790205.

DOMINGUES, I.; GRAVATO, C. Oxidative stress assessment in zebrafish larvae. In: **Methods in Molecular Biology**. New York: Humana Press, 2018. p. 477–486. https://doi.org/10.1007/978-1-4939-7883-0_26.

DOMINGUES, I. *et al.* Biomarkers as a tool to assess effects of chromium (VI): comparison of responses in zebrafish early life stages and adults. **Comparative**

Biochemistry and Physiology Part C, v. 152, n. 3, p. 338–345, 2010. https://doi.org/10.1016/j.cbpc.2010.05.010.

DRAPER, H. H.; HADLEY, M. Malondialdehyde determination as index of lipid peroxidation. **Methods in Enzymology**, v. 186, p. 421–431, 1990. https://doi.org/10.1016/0076-6879(90)86135-I.

EGEA, P. F. *et al.* Crystal structure of the human RXRα ligand-binding domain bound to its natural ligand: 9-cis retinoic acid. **EMBO Journal**, v. 19, n. 11, p. 2592–2601, 2000. https://doi.org/10.1093/emboj/19.11.2592.

ELIA, A. C. *et al.* Association of glutathione peroxidase activity with an acidic glutathione S-transferase in carp liver. **Italian Journal of Zoology**, v. 67, n. 1, p. 39–43, 2000. https://doi.org/10.1080/11250000009356292.

ELLMAN, G. L. *et al.* A new and rapid colorimetric determination of acetylcholinesterase activity. **Biochemical Pharmacology**, v. 7, n. 2, p. 88–95, 1961. https://doi.org/10.1016/0006-2952(61)90145-9.

ELUFIOYE, T. O.; HABTEMARIAM, S. Hepatoprotective effects of rosmarinic acid: insight into its mechanisms of action. **Biomedicine & Pharmacotherapy**, v. 112, p. 108600, 2019. https://doi.org/10.1016/j.biopha.2019.108600.

ENSMINGER, M. P. *et al.* Pesticide occurrence and aquatic benchmark exceedances in urban surface waters and sediments in three urban areas of California, USA, 2008–2011. **Environmental Monitoring and Assessment**, v. 185, n. 5, p. 3697–3710, 2013. https://doi.org/10.1007/s10661-012-2821-8.

ENVIRONMENTAL PROTECTION AGENCY (EPA). Persistent organic pollutants: a global issue, a global response. 2014. Disponível em: https://www.epa.gov/international-cooperation/persistent-organic-pollutants-global-issue-global-response. Acesso em: [inserir data].

ENVIRONMENTAL PROTECTION AGENCY (EPA). Reregistration eligibility decision for 2,4-D. Washington, DC, 2005.

EVANGELISTA DE DUFFARD, A. *et al.* Effects of 2,4-dichlorophenoxyacetic acid butyl ester on chick liver. **Archives of Environmental Contamination and Toxicology**, v. 25, n. 2, 1993. https://doi.org/10.1007/BF00212131.

FAN, W.; EVANS, R. PPARs and ERRs: molecular mediators of mitochondrial metabolism. **Current Opinion in Cell Biology**, v. 33, p. 49–54, 2015. https://doi.org/10.1016/j.ceb.2014.11.002.

FAROUNBI, A. I.; NGQWALA, N. P. Occurrence of selected endocrine disrupting compounds in the Eastern Cape Province of South Africa. **Environmental Science and Pollution Research**, v. 27, n. 14, p. 17268–17279, 2020. https://doi.org/10.1007/s11356-020-08082-y.

FERNANDES, M. S. *et al.* Alkaline phosphatase activity in plasma and liver of rats submitted to chronic exposure to fluoride. **Brazilian Archives of Biology and Technology**, v. 54, n. 6, p. 1187–1192, 2011. https://doi.org/10.1590/S1516-89132011000600014.

FERREIRA-GUEDES, S.; MENDES, B.; LEITÃO, A. L. Degradation of 2,4-dichlorophenoxyacetic acid by a halotolerant strain of *Penicillium chrysogenum*: antibiotic production. **Environmental Technology**, v. 33, p. 677–686, 2012. https://doi.org/10.1080/09593330.2011.588251.

FORBES, S. J.; NEWSOME, P. N. Liver regeneration: mechanisms and models to clinical application. **Nature Reviews Gastroenterology & Hepatology**, v. 13, n. 8, p. 473–485, 2016. https://doi.org/10.1038/nrgastro.2016.97.

FORTNER, A. *et al.* Apoptosis regulation by the tyrosine-protein kinase CSK. **Frontiers in Cell and Developmental Biology**, v. 10, p. 1078180, 2022. https://doi.org/10.3389/fcell.2022.1078180.

FRANSEN, M.; LISMONT, C.; WALTON, P. The peroxisome-mitochondria connection: how and why? **International Journal of Molecular Sciences**, v. 18, n. 6, p. 1126, 2017. https://doi.org/10.3390/ijms18061126.

FREISTHLER, M. S. *et al.* Association between increasing agricultural use of 2,4-D and population biomarkers of exposure: findings from the National Health and Nutrition Examination Survey, 2001–2014. **Environmental Health**, v. 21, n. 1, p. 23, 2022. https://doi.org/10.1186/s12940-021-00815-x.

FREITAS, L. *et al.* Animal models in the neurotoxicology of 2,4-D. *Human &* **Experimental Toxicology**, v. 38, n. 10, p. 1178–1182, 2019. https://doi.org/10.1177/0960327119860172.

FROMENTY, B.; RODEN, M. Mitochondrial alterations in fatty liver diseases. **Journal of Hepatology**, v. 78, n. 2, p. 415–429, 2023. https://doi.org/10.1016/j.jhep.2022.09.020.

FU, J. *et al.* Endoplasmic reticulum stress is involved in 2,4-dichlorophenol-induced hepatotoxicity. **Journal of Toxicological Sciences**, v. 41, n. 6, p. 745–756, 2016. https://doi.org/10.2131/jts.41.745.

GAAIED, S. *et al.* 2,4-Dichlorophenoxyacetic acid herbicide effects on zebrafish larvae: development, neurotransmission and behavior as sensitive endpoints. **Environmental Science and Pollution Research**, v. 27, n. 4, p. 3686–3696, 2020. https://doi.org/10.1007/s11356-019-04488-5.

GAAIED, S. *et al.* Gene expression patterns and related enzymatic activities of detoxification and oxidative stress systems in zebrafish larvae exposed to the 2,4-dichlorophenoxyacetic acid herbicide. **Chemosphere**, v. 224, p. 289–297, 2019. https://doi.org/10.1016/j.chemosphere.2019.02.125.

GALLAGHER, E.; DIGIULIO, R. Effects of 2,4-dichlorophenoxyacetic acid and picloram on biotransformation, peroxisomal and serum enzyme activities in channel catfish (*Ictalurus punctatus*). **Toxicology Letters**, v. 57, n. 1, p. 65–72, 1991. https://doi.org/10.1016/0378-4274(91)90120-U.

GAO, J. *et al.* Levels and spatial distribution of chlorophenols – 2,4-dichlorophenol, 2,4,6-trichlorophenol, and pentachlorophenol in surface water of China. **Chemosphere**, v. 71, n. 6, p. 1181–1187, 2008. https://doi.org/10.1016/j.chemosphere.2007.10.018.

GAUDET, P. *et al.* Primer on the Gene Ontology. **Methods in Molecular Biology**, v. 1446, p. 25–37, 2017. https://doi.org/10.1007/978-1-4939-3743-1_3.

GE, R. *et al.* Effect of peroxisome proliferators on the methylation and protein level of the c-myc protooncogene in B6C3F1 mice liver. **Journal of Biochemical and Molecular Toxicology**, v. 16, n. 1, p. 41–47, 2002. https://doi.org/10.1002/jbt.10019.

GIANNINI, E. G.; TESTA, R.; SAVARINO, V. Liver enzyme alteration: a guide for clinicians. **Canadian Medical Association Journal**, v. 172, n. 3, p. 367–379, 2005. https://doi.org/10.1503/cmaj.1040752.

GIBB, S. Toxicity testing in the 21st century: a vision and a strategy. **Reproductive Toxicology**, v. 25, n. 1, p. 136–138, 2008. https://doi.org/10.1016/j.reprotox.2007.10.013.

GOESSLING, W.; SADLER, K. C. Zebrafish: an important tool for liver disease research. **Gastroenterology**, v. 149, n. 6, p. 1361–1377, 2015. https://doi.org/10.1053/j.gastro.2015.08.034.

GONG, L. *et al.* Hepatoprotective effect of forsythiaside A against acetaminophen-induced liver injury in zebrafish: coupling network pharmacology with biochemical pharmacology. **Journal of Ethnopharmacology**, v. 271, p. 113890, 2021. https://doi.org/10.1016/j.jep.2021.113890.

GONZÁLEZ-FRAGA, J.; DIPP-ALVAREZ, V.; BARDULLAS, U. Quantification of spontaneous tail movement in zebrafish embryos using a novel open-source MATLAB application. **Zebrafish**, v. 16, n. 2, p. 214–216, 2019. https://doi.org/10.1089/zeb.2018.1688.

GORZINSKI, S. Acute, pharmacokinetic, and subchronic toxicological studies of 2,4-dichlorophenoxyacetic acid. **Fundamental and Applied Toxicology**, v. 9, n. 3, p. 423–435, 1987. https://doi.org/10.1016/0272-0590(87)90025-X.

GRAY, R.; LOVELY, C. B. Redefining retinoic acid receptor expression in zebrafish embryos using hybridization chain reaction. **Differentiation**, v. 140, p. 100822, 2024. https://doi.org/10.1016/j.diff.2024.100822.

GUERRA, I. M. S. *et al.* Mitochondrial fatty acid β-oxidation disorders: from disease to lipidomic studies – a critical review. **International Journal of Molecular Sciences**, v. 23, n. 22, p. 13933, 2022. https://doi.org/10.3390/ijms232213933.

GULATI, K.; RESHI, M. R.; RAI, N.; RAY, A. Hepatotoxicity: its mechanisms, experimental evaluation and protective strategies. **American Journal of Pharmacology**, v. 1, n. 1, p. 1004, 2018. https://doi.org/10.29328/journal.ajp.1001004.

HAN, K.-H. Relationships among alcoholic liver disease, antioxidants, and antioxidant enzymes. **World Journal of Gastroenterology**, v. 22, n. 1, p. 37, 2016. https://doi.org/10.3748/wjg.v22.i1.37.

HANAOKA, R. *et al.* Zebrafish gcmb is required for pharyngeal cartilage formation. **Mechanisms of Development**, v. 121, n. 10, p. 1235–1247, 2004. https://doi.org/10.1016/j.mod.2004.05.011.

HARRIS, C. R. *et al.* Array programming with NumPy. **Nature**, v. 585, n. 7825, p. 357–362, 2020. https://doi.org/10.1038/s41586-020-2649-2.

HENNEQUIN, L. F. *et al.* N-(5-chloro-1,3-benzodioxol-4-yl)-7-[2-(4-methylpiperazin-1-yl)ethoxy]-5-(tetrahydro-2H-pyran-4-yloxy)quinazolin-4-amine, a novel dual-specific c-Src/Abl kinase inhibitor. **Journal of Medicinal Chemistry**, v. 49, n. 22, p. 6465–6488, 2006. https://doi.org/10.1021/jm060434q.

HERMSEN, S. A. *et al.* Chemical class-specific gene expression changes in the zebrafish embryo after exposure to glycol ether alkoxy acids and 1,2,4-triazole antifungals. **Reproductive Toxicology**, v. 32, n. 2, p. 245–252, 2011. https://doi.org/10.1016/j.reprotox.2011.05.010.

HERNÁNDEZ-VALDEZ, J.; VELÁZQUEZ-ZEPEDA, A.; SÁNCHEZ-MEZA, J. C. Effect of pesticides on peroxisome proliferator-activated receptors (PPARs) and their association with obesity and diabetes. **PPAR Research**, 2023, 1743289, 2023. https://doi.org/10.1155/2023/1743289.

HIETANEN, E.; LINNAINMAA, K.; VAINIO, H. Effects of phenoxyherbicides and glyphosate on the hepatic and intestinal biotransformation activities in the rat. *Acta* **Pharmacologica et Toxicologica**, v. 53, n. 2, p. 103–112, 1983. https://doi.org/10.1111/j.1600-0773.1983.tb01876.x.

HIETANEN, E. *et al.* Enhanced peroxisomal β-oxidation of fatty acids and glutathione metabolism in rats exposed to phenoxyacetic acid. **Toxicology**, v. 34, p. 103–111, 1985.

HONDA, K. *et al.* Role of peroxisome proliferator-activated receptor alpha in the expression of hepatic fatty acid oxidation-related genes in chickens. **Animal Science Journal**, v. 87, n. 1, p. 61–66, 2016. https://doi.org/10.1111/asj.12392.

HOWE, K. *et al.* The zebrafish reference genome sequence and its relationship to the human genome. **Nature**, v. 496, n. 7446, p. 498–503, 2013. https://doi.org/10.1038/nature12111.

HSIEH, Y. C. *et al.* PPARα deficiency inhibits the proliferation of neuronal and glial precursors in the zebrafish central nervous system. **Developmental Dynamics**, v. 247, n. 12, p. 1264–1275, 2018. https://doi.org/10.1002/dvdy.24683.

HU, P. *et al.* Nuclear receptor PPARα as a therapeutic target in diseases associated with lipid metabolism disorders. **Nutrient***s*, v. 15, n. 22, p. 4772, 2023. https://doi.org/10.3390/nu15224772.

HU, Y. *et al.* 2,4-dichlorophenol increases primordial germ cell numbers via ESR2a-dependent pathway in zebrafish larvae. **Environmental Science & Technology**, v. 56, n. 19, p. 13878–13887, 2022. https://doi.org/10.1021/acs.est.2c05212.

HUANG, S. Efficient analysis of toxicity and mechanisms of environmental pollutants with network toxicology and molecular docking strategy: acetyl tributyl citrate as an example. **Science of the Total Environment**, v. 905, p. 167904, 2023. https://doi.org/10.1016/j.scitotenv.2023.167904.

HUANG, X. *et al.* The PI3K/AKT pathway in obesity and type 2 diabetes. **International Journal of Biological Sciences**, v. 14, n. 11, p. 1483–1496, 2018. https://doi.org/10.7150/ijbs.27173.

HUANG, Y. *et al.* Carboxin can induce cardiotoxicity in zebrafish embryos. **Ecotoxicology and Environmental Safety**, v. 233, p. 113318, 2022. https://doi.org/10.1016/j.ecoenv.2022.113318.

HUNTER, J. D. Matplotlib: a 2D graphics environment. **Computing in Science & Engineering**, v. 9, n. 3, p. 90–95, 2007. https://doi.org/10.1109/MCSE.2007.55.

INSTITUTO BRASILEIRO DO MEIO AMBIENTE E DOS RECURSOS NATURAIS RENOVÁVEIS (IBAMA). Relatórios de comercialização de agrotóxicos. Brasília, 2024. Disponível em: http://www.ibama.gov.br/agrotoxicos/. Acesso em: 12 maio 2024.

IBAMA. Pesticide commercialization reports. Brasília, 2022. Disponível em: https://www.gov.br/ibama/en-us/topics/chemicals-and-biology/pesticides/pesticide-commercialization-reports. Acesso em: 15 fev. 2023.

ISLAM, F. *et al.* Potential impact of the herbicide 2,4-dichlorophenoxyacetic acid on human and ecosystems. **Environment International**, v. 111, p. 332–351, 2018. https://doi.org/10.1016/j.envint.2017.10.020.

ISLAM, M. A. *et al.* Behavioural, developmental and biochemical effects in zebrafish caused by ibuprofen, irgarol and terbuthylazine. **Chemosphere**, v. 344, p. 140373, 2023. https://doi.org/10.1016/j.chemosphere.2023.140373.

ITOH, K. *et al.* 2,4-dichlorophenoxyacetic acid (2,4-D)- and 2,4,5-trichlorophenoxyacetic acid (2,4,5-T)-degrading gene cluster in *Bradyrhizobium elkanii* USDA94. **Microbiological Research**, v. 188–189, p. 62–71, 2016. https://doi.org/10.1016/j.micres.2016.04.014.

JAESCHKE, H.; MCGILL, M. R.; RAMACHANDRAN, A. Oxidant stress, mitochondria, and cell death mechanisms in drug-induced liver injury: lessons learned from acetaminophen hepatotoxicity. **Drug Metabolism Reviews**, v. 44, n. 1, p. 88–106, 2012. https://doi.org/10.3109/03602532.2011.602688.

JAN, R.; CHAUDHRY, G. E. Understanding apoptosis and apoptotic pathways targeted cancer therapeutics. **Advanced Pharmaceutical Bulletin**, v. 9, n. 2, p. 205–218, 2019. https://doi.org/10.15171/apb.2019.024.

JENKINS, T.; GOUGE, J. Nrf2 in cancer, detoxifying enzymes and cell death programs. **Antioxidants**, v. 10, n. 7, p. 1030, 2021. https://doi.org/10.3390/antiox10071030.

JONES, J. G. Hepatic glucose and lipid metabolism. **Diabetologia**, v. 59, n. 6, p. 1098–1103, 2016. https://doi.org/10.1007/s00125-016-3940-5.

JU, Z. *et al.* Combined toxicity of 2,4-dichlorophenoxyacetic acid and its metabolites 2,4-dichlorophenol (2,4-DCP) on two nontarget organisms. **ACS Omega**, v. 4, n. 1, p. 1669–1677, 2019. https://doi.org/10.1021/acsomega.8b02282.

JUAN-GARCÍA, A.; BIND, M. A.; ENGERT, F. Larval zebrafish as an in vitro model for evaluating toxicological effects of mycotoxins. **Ecotoxicology and Environmental Safety**, v. 202, p. 110909, 2020. https://doi.org/10.1016/j.ecoenv.2020.110909.

LI, J. *et al.* Ameliorative potential of ellagic acid via PPARγ against hyperlipidemia: insights from mice and zebrafish. **Food Bioscience**, v. 62, p. 105582, 2024. https://doi.org/10.1016/j.fbio.2024.105582.

KALIPCI, E.; OZDEMIR, C.; OZTAS, H. Assessing eco-toxicological effects of industrial 2,4-D acid iso-octylester herbicide on rat pancreas and liver. **Biotechnic & Histochemistry**, v. 88, n. 3–4, p. 202–207, 2013. https://doi.org/10.3109/10520295.2012.758312.

KAMBUROV, A. *et al.* ConsensusPathDB—a database for integrating human functional interaction networks. **Nucleic Acids Research**, v. 37, p. D623–D628, 2009. https://doi.org/10.1093/nar/gkn698.

KARKUCINSKA-WIECKOWSKA, A. *et al.* Mitochondria, oxidative stress and nonalcoholic fatty liver disease: a complex relationship. **European Journal of Clinical Investigation**, v. 52, n. 3, e13622, 2022. https://doi.org/10.1111/eci.13622.

KATOH, H. *et al.* Induction of rat hepatic long-chain acyl-CoA hydrolases by various peroxisome proliferators. **Biochemical Pharmacology**, v. 33, n. 7, p. 1081–1085, 1984. https://doi.org/10.1016/0006-2952(84)90517-3.

KAWASHIMA, Y. *et al.* Effects of 2,4-dichlorophenoxyacetic acid and 2,4,5-trichlorophenoxyacetic acid on peroxisomal enzymes in rat liver. **Biochemical Pharmacology**, v. 33, n. 2, p. 241–245, 1984. https://doi.org/10.1016/0006-2952(84)90481-7.

KAYA, I. *et al.* The effects of carbaryl and 2,4-dichlorophenoxyacetic acid on oxidative stress index in *Capoeta capoeta*. **Pakistan Journal of Zoology**, v. 51, n. 1, 2019. https://doi.org/10.17582/journal.pjz/2019.51.1.189.193.

KENNEPOHL, E.; MUNRO, I. Phenoxy herbicides (2,4-D). In: KRIEGER, R. (ed.). **Handbook of pesticide toxicology**. 2. ed. San Diego: Academic Press, 2001. p. 1623–1638.

KHOSLA, S. *et al.* Relationship of estrogen receptor genotypes to bone mineral density and to rates of bone loss in men. **Journal of Clinical Endocrinology & Metabolism**, v. 89, n. 4, p. 1808–1816, 2004. https://doi.org/10.1210/jc.2003-031703.

KHRISTI, V. *et al.* Liver transcriptome data of Esr1 knockout male rats reveals altered expression of genes involved in carbohydrate and lipid metabolism. **Data in Brief**, v. 22, p. 771–780, 2019. https://doi.org/10.1016/j.dib.2018.12.089.

KIM, K.-H.; KABIR, E.; JAHAN, S. A. Exposure to pesticides and the associated human health effects. **Science of the Total Environment**, v. 575, p. 525–535, 2017. https://doi.org/10.1016/j.scitotenv.2016.09.009.

KLEIBOEKER, B.; LODHI, I. J. Peroxisomal regulation of energy homeostasis: effect on obesity and related metabolic disorders. **Molecular Metabolism**, v. 65, p. 101577, 2022. https://doi.org/10.1016/j.molmet.2022.101577.

KNOPP, D.; SCHILLER, F. Oral and dermal application of 2,4-dichlorophenoxyacetic acid sodium and dimethylamine salts to male rats. **Archives of Toxicology**, v. 66, n. 3, p. 170–174, 1992. https://doi.org/10.1007/BF01974010.

KOUNDOUROS, N.; POULOGIANNIS, G. Phosphoinositide 3-kinase/Akt signaling and redox metabolism in cancer. **Frontiers in Oncology**, v. 8, p. 160, 2018. https://doi.org/10.3389/fonc.2018.00160.

KOZUKA, H. *et al.* Characteristics of induction of peroxisomal fatty acid oxidation-related enzymes in rat liver by drugs: relationships between structure and inducing activity. **Biochemical Pharmacology**, v. 41, p. 617–623, 1991.

KRELA-KAŹMIERCZAK, I. *et al.* ESR1 gene variants are predictive of osteoporosis in female patients with Crohn's disease. **Journal of Clinical Medicine**, v. 8, n. 9, p. 1306, 2019. https://doi.org/10.3390/jcm8091306.

KUNTZ, D. J. *et al.* Toxicity of mixtures of parathion, toxaphene and/or 2,4-D in mice. **Journal of Applied Toxicology**, v. 10, n. 4, p. 257–266, 1990. https://doi.org/10.1002/jat.2550100406.

LAFOREST, L. *et al.* Involvement of the sonic hedgehog, patched 1 and bmp2 genes in patterning of the zebrafish dermal fin rays. **Development**, v. 125, n. 21, p. 4175–4184, 1998. https://doi.org/10.1242/dev.125.21.4175.

LAGANA, G. *et al.* Lactate dehydrogenase inhibition: biochemical relevance and therapeutical potential. **Current Medicinal Chemistry**, v. 26, n. 18, p. 3242–3252, 2019. https://doi.org/10.2174/0929867324666170209103444.

LAN, Y. *et al.* Dietary sea buckthorn polysaccharide reduced lipid accumulation, alleviated inflammation and oxidative stress, and normalized imbalance of intestinal

microbiota induced by high-fat diet in zebrafish (*Danio rerio*). **Fish Physiology and Biochemistry**, v. 48, n. 6, p. 1717–1735, 2022. https://doi.org/10.1007/s10695-022-01105-0.

LECKA-CZERNIK, B. *et al.* Divergent effects of selective peroxisome proliferator-activated receptor-gamma 2 ligands on adipocyte versus osteoblast differentiation. **Endocrinology**, v. 143, n. 6, p. 2376–2384, 2002. https://doi.org/10.1210/endo.143.6.8834.

LI, B.; CAI, S.-Y.; BOYER, J. L. The role of the retinoid receptor, RAR/RXR heterodimer, in liver physiology. **Biochimica et Biophysica Acta – Molecular Basis of Disease**, v. 1867, n. 5, p. 166085, 2021. https://doi.org/10.1016/j.bbadis.2021.166085.

LI, C.; GRILLO, M. P.; BENET, L. Z. In vitro studies on the chemical reactivity of 2,4-dichlorophenoxyacetyl-S-acyl-CoA thioester. **Toxicology and Applied Pharmacology**, v. 187, n. 2, p. 101–109, 2003. https://doi.org/10.1016/S0041-008X(02)00043-1.

LI, H. *et al.* 2,4-dichlorophenol induces apoptosis in primary hepatocytes of grass carp (*Ctenopharyngodon idella*) through mitochondrial pathway. **Aquatic Toxicology**, v. 140–141, p. 117–122, 2013. https://doi.org/10.1016/j.aquatox.2013.05.015.

LI, K. *et al.* Developmental toxicity of 2,4-dichlorophenoxyacetic acid in zebrafish embryos. **Chemosphere**, v. 171, p. 40–48, 2017. https://doi.org/10.1016/j.chemosphere.2016.12.032.

LI, S. *et al.* Tebuconazole induced oxidative stress related hepatotoxicity in adult and larval zebrafish (*Danio rerio*). **Chemosphere**, v. 241, p. 125129, 2020. https://doi.org/10.1016/j.chemosphere.2019.125129.

LI, X. *et al.* Mitochondrial dysfunction as a pathogenesis and therapeutic strategy for metabolic-dysfunction-associated steatotic liver disease. **International Journal of Molecular Sciences**, v. 26, n. 9, p. 4256, 2025. https://doi.org/10.3390/ijms26094256.

LI, Y. *et al.* Peroxisome proliferator-activated receptors: a key link between lipid metabolism and cancer progression. **Clinical Nutrition**, v. 43, n. 2, p. 332–345, 2024. https://doi.org/10.1016/j.clnu.2023.12.005.

LIEBSCH, M. *et al.* Alternatives to animal testing: current status and future perspectives. **Archives of Toxicology**, v. 85, n. 8, p. 841–858, 2011. https://doi.org/10.1007/s00204-011-0718-x.

LIN, C. C. *et al.* Loss of the respiratory enzyme citrate synthase directly links the Warburg effect to tumor malignancy. **Scientific Reports**, v. 2, p. 785, 2012. https://doi.org/10.1038/srep00785.

LIPPA, B. *et al.* Synthesis and structure based optimization of novel Akt inhibitors. **Bioorganic & Medicinal Chemistry Letters**, v. 18, n. 11, p. 3359–3363, 2008. https://doi.org/10.1016/j.bmcl.2008.04.034.

LIU, D. D. *et al.* Effects of inhibiting PI3K-Akt-mTOR pathway on lipid metabolism homeostasis in goose primary hepatocytes. **Animal**, v. 10, n. 8, p. 1319–1327, 2016. https://doi.org/10.1017/S1751731116000380.

LIU, J. *et al.* Response mechanisms to joint exposure of triclosan and its chlorinated derivatives on zebrafish (*Danio rerio*) behavior. **Chemosphere**, v. 193, p. 820–832, 2018. https://doi.org/10.1016/j.chemosphere.2017.11.106.

LIU, W. *et al.* Formation and contamination of PCDD/Fs, PCBs, PeCBz, HxCBz and polychlorophenols in the production of 2,4-D products. **Chemosphere**, v. 92, n. 3, p. 304–308, 2013. https://doi.org/10.1016/j.chemosphere.2013.03.031.

LIVAK, K. J.; SCHMITTGEN, T. D. Analysis of relative gene expression data using real-time quantitative PCR and the 2(-Delta Delta C(T)) method. **Methods**, v. 25, n. 4, p. 402–408, 2001. https://doi.org/10.1006/meth.2001.1262.

LUNDGREN, B.; MEIJER, J.; DEPIERRE, J. W. Induction of cytosolic and microsomal epoxide hydrolases and proliferation of peroxisomes and mitochondria in mouse liver after dietary exposure to phenoxyacetic acids. **Biochemical Pharmacology**, v. 36, n. 6, p. 815–821, 1987. https://doi.org/10.1016/0006-2952(87)90169-9.

LUO, Y. *et al.* Electron paramagnetic resonance investigation of in vivo free radical formation and oxidative stress induced by 2,4-dichlorophenol in the freshwater fish *Carassius auratus*. **Environmental Toxicology and Chemistry**, v. 24, n. 9, p. 2145–2153, 2005. https://doi.org/10.1897/04-640R.1.

LUSHCHAK, V. I. *et al.* Pesticide toxicity: a mechanistic approach. **EXCLI Journal**, v. 17, p. 1101–1136, 2018. https://doi.org/10.17179/EXCLI2018-1710.

MA, Y. *et al.* Disruption of endocrine function in in vitro H295R cell-based and in vivo assay in zebrafish by 2,4-dichlorophenol. **Aquatic Toxicology**, v. 106–107, p. 173–181, 2012. https://doi.org/10.1016/j.aquatox.2011.11.006.

MAGNOLI, K. *et al.* Herbicides based on 2,4-D: its behavior in agricultural environments and microbial biodegradation aspects – a review. **Environmental Science and Pollution Research**, v. 27, n. 31, p. 38501–38512, 2020. https://doi.org/10.1007/s11356-020-10370-6.

MAHARAJAN, K. *et al.* Toxicity assessment of pyriproxyfen in vertebrate model zebrafish embryos (*Danio rerio*): a multi biomarker study. **Aquatic Toxicology**, v. 196, p. 132–145, 2018. https://doi.org/10.1016/j.aquatox.2018.01.010.

MAIA, M. E. *et al.* Effects of atrazine, diuron and glyphosate mixtures on zebrafish embryos: acute toxicity and oxidative stress responses. **Ecotoxicology**, v. 34, p. 304–316, 2025. https://doi.org/10.1007/s10646-024-02839-8.

MALE, I. *et al.* Hedgehog signaling regulates neurogenesis in the larval and adult zebrafish hypothalamus. **eNeuro**, v. 7, n. 6, 2020. https://doi.org/10.1523/eneuro.0226-20.2020.

MANDAL, A.; PINTER, K.; DRERUP, C. M. Analyzing neuronal mitochondria in vivo using fluorescent reporters in zebrafish. **Frontiers in Cell and Developmental Biology**, v. 6, p. 144, 2018. https://doi.org/10.3389/fcell.2018.00144.

MANSOURI, A.; GATTOLLIAT, C.-H.; ASSELAH, T. Mitochondrial dysfunction and signaling in chronic liver diseases. **Gastroenterology**, v. 155, n. 3, p. 629–647, 2018. https://doi.org/10.1053/j.gastro.2018.06.083.

MARTINS, R. X. *et al.* Biochemical markers for liver injury in zebrafish larvae. **Methods in Molecular Biology**, v. 2753, p. 469–482, 2024. https://doi.org/10.1007/978-1-0716-3625-1_29.

MARTINS, R. X. *et al.* 2,4-D herbicide-induced hepatotoxicity: unveiling disrupted liver functions and associated biomarkers. **Toxics**, v. 12, n. 1, p. 35, 2024. https://doi.org/10.3390/toxics12010035.

MARTINS, R. X. *et al.* A network toxicology and molecular docking-based approach revealed shared hepatotoxic mechanisms and targets between the herbicide 2,4-D and its metabolite 2,4-DCP. **Toxicology**, v. 513, p. 154086, 2025. https://doi.org/10.1016/j.tox.2025.154086.

MARTINS, R. X. *et al.* Exposure to 2,4-D herbicide induces hepatotoxicity in zebrafish larvae. **Comparative Biochemistry and Physiology Part C: Toxicology & Pharmacology**, v. 248, p. 109110, 2021. https://doi.org/10.1016/j.cbpc.2021.109110.

MASSARSKY, A.; KOZAL, J. S.; DI GIULIO, R. T. Glutathione and zebrafish: old assays to address a current issue. **Chemosphere**, v. 168, p. 707–715, 2017. https://doi.org/10.1016/j.chemosphere.2016.11.004.

MATVIISHYN, T. M. *et al.* Tissue-specific induction of oxidative stress in goldfish by 2,4-dichlorophenoxyacetic acid. **Environmental Toxicology and Pharmacology**, v. 37, n. 2, p. 861–869, 2014. https://doi.org/10.1016/j.etap.2014.02.007.

MAWARDI, M. *et al.* Cholestatic liver disease: practice guidelines from the Saudi Association for the Study of Liver Diseases and Transplantation. **Saudi Journal of Gastroenterology**, v. 27, Suppl. 1, p. S1–S26, 2021. https://doi.org/10.4103/sjg.sjg_112_21.

MAZHAR, F. M. *et al.* Fetotoxicity of 2,4-dichlorophenoxyacetic acid in rats and the protective role of vitamin E. **Toxicology and Industrial Health**, v. 30, n. 5, p. 480–488, 2014. https://doi.org/10.1177/0748233712459915.

MCGILL, M. R. The past and present of serum aminotransferases and the future of liver injury biomarkers. **EXCLI Journal**, v. 15, p. 817–828, 2016. https://doi.org/10.17179/excli2016-800.

MCGLOTHEN, K. I. *et al.* Outward depolarization of the microglia mitochondrial membrane potential following lipopolysaccharide exposure. *Frontiers in Cellular Neuroscience*, v. 18, p. 1430448, 2024. https://doi.org/10.3389/fncel.2024.1430448.

MEFTAUL, I. M. *et al.* Movement and fate of 2,4-D in urban soils: a potential environmental health concern. **ACS Omega**, v. 5, n. 22, p. 13287–13295, 2020. https://doi.org/10.1021/acsomega.0c01330.

MENEZES, C. *et al.* Commercial formulation containing 2,4-D affects biochemical parameters of silver catfish. **Fish Physiology and Biochemistry**, v. 41, n. 2, p. 323–330, 2015. https://doi.org/10.1007/s10695-014-9985-9.

MESNAGE, R.; ANTONIOU, M. N. Ignoring adjuvant toxicity falsifies the safety profile of commercial pesticides. **Frontiers in Public Health**, v. 5, p. 361, 2018. https://doi.org/10.3389/fpubh.2017.00361.

MILACIC, M. *et al.* The Reactome pathway knowledgebase 2024. **Nucleic Acids** *Research*, v. 52, D1, p. D672–D678, 2024. https://doi.org/10.1093/nar/gkad1025.

MIRANDA, S. *et al.* Overexpression of mdr2 gene by peroxisome proliferators in the mouse liver. [s.d.].

MITTAL, M. *et al.* Reactive oxygen species in inflammation and tissue injury. **Antioxidants & Redox Signaling**, v. 20, n. 7, p. 1126–1167, 2014. https://doi.org/10.1089/ars.2012.5149.

MIYARES, R. L.; DE REZENDE, V. B.; FARBER, S. A. Zebrafish yolk lipid processing. **Disease Models & Mechanisms**, v. 7, n. 7, p. 915–927, 2014. https://doi.org/10.1242/dmm.015800.

MUNIZ, M. S. *et al.* Moxidectin toxicity to zebrafish embryos. **Environmental Pollution**, v. 283, p. 117096, 2021. https://doi.org/10.1016/j.envpol.2021.117096.

MURSHID, A.; EGUCHI, T.; CALDERWOOD, S. K. Stress proteins in aging and life span. **International Journal of Hyperthermia**, v. 29, n. 5, p. 442–447, 2013. https://doi.org/10.3109/02656736.2013.798873.

MUSTONEN, R. *et al.* Effects of phenoxyacetic acids on hepatic peroxisome proliferation. **Archives of Toxicology**, v. 63, n. 3, p. 203–208, 1989. https://doi.org/10.1007/BF00316369.

MYCIELSKA, M. E. *et al.* Citrate transport and metabolism in mammalian cells. **BioEssays**, v. 31, n. 1, p. 10–20, 2009. https://doi.org/10.1002/bies.080137.

NAKAMURA, T. *et al.* Estrogen prevents bone loss via estrogen receptor alpha and induction of Fas ligand in osteoclasts. **Cell**, v. 130, n. 5, p. 811–823, 2007. https://doi.org/10.1016/j.cell.2007.07.025.

NAKBI, A. *et al.* Hypolipidemic and antioxidant activities of virgin olive oil in 2,4-dichlorophenoxyacetic acid–treated rats. **Nutrition**, v. 28, n. 1, p. 81–91, 2012. https://doi.org/10.1016/j.nut.2011.02.009.

NAKBI, A. *et al.* Effects of olive oil on oxidative stress in 2,4-dichlorophenoxyacetic acid-treated rats. **Nutrition & Metabolism**, v. 7, p. 80, 2010. https://doi.org/10.1186/1743-7075-7-80.

NAULT, M. E. *et al.* Efficacy and selectivity following a whole-lake 2,4-D application. **Lake and Reservoir Management**, v. 30, n. 1, p. 1–10, 2014. https://doi.org/10.1080/10402381.2013.862586.

NECHALIOTI, P.-M. *et al.* Evaluation of perinatal exposure of glyphosate and its mixture with 2,4-D and dicamba on liver redox status. **Environmental Research**, v. 228, p. 115906, 2023. https://doi.org/10.1016/j.envres.2023.115906.

NESKOVIĆ, N. *et al.* Toxic effects of 2,4-D herbicide on fish. **Journal of Environmental Science and Health, Part B**, v. 29, n. 2, p. 265–279, 1994. https://doi.org/10.1080/03601239409372879.

NGO, V.; DUENNWALD, M. L. Nrf2 and oxidative stress: mechanisms and implications in human disease. **Antioxidants**, v. 11, n. 12, p. 2345, 2022. https://doi.org/10.3390/antiox11122345.

OAKES, D. J.; POLLAK, J. K. Effects of Tordon 75D® on mitochondrial oxidative functions. **Toxicology**, v. 136, n. 1, p. 41–52, 1999. https://doi.org/10.1016/S0300-483X(99)00055-4.

OECD. *Test No. 236: Fish Embryo Acute Toxicity (FET) Test*. Paris: OECD Publishing, 2013. https://doi.org/10.1787/9789264203709-en.

OKOH, V.; DEORAJ, A.; ROY, D. Estrogen-induced reactive oxygen species-mediated signaling contributes to breast cancer. **Biochimica et Biophysica Acta – Reviews on Cance***r*, v. 1815, n. 1, p. 115–133, 2011. https://doi.org/10.1016/j.bbcan.2010.10.005.

OKUMOTO, K. *et al.* Peroxisome: metabolic functions and biogenesis. In: LIZARD, G. (ed.). **Peroxisome biology**. Cham: Springer, 2020. p. 3–17. https://doi.org/10.1007/978-3-030-60204-8_1.

OLSON, R. J.; TRUMBLE, T. E.; GAMBLE, W. Alterations in cholesterol biosynthesis by aryloxy acids. **Biochemical Journal**, v. 142, n. 2, p. 445–448, 1974. https://doi.org/10.1042/bj1420445.

ORE, A.; AKINLOYE, O. Oxidative stress and antioxidant biomarkers in non-alcoholic fatty liver disease. **Medicina**, v. 55, n. 2, p. 26, 2019. https://doi.org/10.3390/medicina55020026.

ORSI, D. L. *et al.* Discovery of orally bioavailable PPARG inverse-agonists. **Bioorganic & Medicinal Chemistry**, v. 78, p. 117130, 2023. https://doi.org/10.1016/j.bmc.2022.117130.

ORUÇ, E. Ö.; ÜNER, N. Combined effects of 2,4-D and azinphosmethyl in liver of *Oreochromis niloticus*. **Comparative Biochemistry and Physiology Part C**, v. 127, n. 3, p. 291–296, 2000. https://doi.org/10.1016/S0742-8413(00)00159-6.

OZAKI, K. *et al.* Unique renal tubule changes induced by 2,4-D in rats and mice. **Toxicologic Pathology**, v. 29, n. 4, p. 440–450, 2001. https://doi.org/10.1080/01926230152499791.

ÖZASLAN, M. S. *et al.* Inhibition effects of pesticides on glutathione-S-transferase activity. **Journal of Biochemical and Molecular Toxicology**, v. 32, n. 9, e22196, 2018. https://doi.org/10.1002/jbt.22196.

ÖZCAN ORUÇ, E.; ÜNER, N. Marker enzyme assessment in *Cyprinus carpio* exposed to 2,4-D. **Journal of Biochemical and Molecular Toxicology**, v. 16, n. 4, p. 182–188, 2002. https://doi.org/10.1002/jbt.10040.

PALMEIRA, C. M.; MORENO, A. J.; MADEIRA, V. M. Interactions of herbicides 2,4-D and dinoseb with liver mitochondrial bioenergetics. **Toxicology and Applied Pharmacology**, v. 127, n. 1, p. 50–57, 1994. https://doi.org/10.1006/taap.1994.1138.

PALMEIRA, C. M.; MORENO, A. J.; MADEIRA, V. M. C. Thiols metabolism altered by herbicides. **Toxicology Letters**, v. 81, n. 2–3, p. 115–123, 1995. https://doi.org/10.1016/0378-4274(95)03414-5.

PAN, Y. *et al.* Oxidative stress and mitochondrial dysfunction mediate Cd-induced hepatic lipid accumulation in zebrafish (*Danio rerio*). **Aquatic Toxicology**, v. 199, p. 12–20, 2018. https://doi.org/10.1016/j.aquatox.2018.03.017.

PAN, X. *et al.* Products distribution and contribution of reactions to 2,4-dichlorophenol removal. **Water Research**, v. 194, p. 116916, 2021. https://doi.org/10.1016/j.watres.2021.116916.

PANDAS DEVELOPMENT TEAM. *pandas-dev/pandas: pandas (v1.5.2)*. Zenodo, 2022. https://doi.org/10.5281/zenodo.7344967.

PARADIES, G. Oxidative stress, cardiolipin and mitochondrial dysfunction in NAFLD. **World Journal of Gastroenterology**, v. 20, n. 39, p. 14205, 2014. https://doi.org/10.3748/wjg.v20.i39.14205.

PARICHY, D. M. Advancing biology through zebrafish ecology and evolution. *eLife*, v. 4, e05635, 2015. https://doi.org/10.7554/eLife.05635.

PARK, H.; KIM, K. Urinary concentrations of dichlorophenols in Korean adults. **International Journal of Environmental Research and Public Health**, v. 15, n. 4, p. 589, 2018. https://doi.org/10.3390/ijerph15040589.

PASHAY AHI, E. *et al.* Effects of estrogen on skeletal gene expression in zebrafish. **PeerJ**, v. 4, e1878, 2016. https://doi.org/10.7717/peerj.1878.

PAULINO, C. A. *et al.* Acute, subchronic and chronic 2,4-dichlorophenoxyacetic acid intoxication in rats. **Veterinary and Human Toxicology**, v. 38, n. 5, p. 348–352, 1996.

PENG, C. *et al.* HSP90 mediates the connection of multiple programmed cell death in diseases. **Cell Death & Disease**, v. 13, n. 11, p. 929, 2022. https://doi.org/10.1038/s41419-022-05373-9.

PENG, X. *et al.* Chronic exposure to environmental concentrations of phenanthrene impairs zebrafish reproduction. **Ecotoxicology and Environmental Safety**, v. 182, p. 109376, 2019. https://doi.org/10.1016/j.ecoenv.2019.109376.

PEREIRA, L. F.; CAMPELLO, A. P.; SILVEIRA, O. Effect of tordon 2,4-D 64/240 triethanolamine BR on the energy metabolism of rat liver mitochondria. **Journal of Applied Toxicology**, v. 14, n. 1, p. 21–26, 1994. DOI: https://doi.org/10.1002/jat.2550140105.

PETERSON, M. A.; MCMASTER, S. A.; RIECHERS, D. E.; SKELTON, J.; STAHLMan, P. W. 2,4-D past, present, and future: a review. **Weed Technology**, v. 30, n. 2, p. 303–345, 2016. DOI: https://doi.org/10.1614/wt-d-15-00131.1.

PHILIP, A. M. *et al.* Development of a zebrafish sepsis model for high-throughput drug discovery. **Molecular Medicine**, v. 23, p. 134–148, 2017. DOI: https://doi.org/10.2119/molmed.2016.00188.

PIZCUETA, P. *et al.* Development of PPARγ agonists for the treatment of neuroinflammatory and neurodegenerative diseases: leriglitazone as a promising candidate. **International Journal of Molecular Sciences**, v. 24, n. 4, p. 3201, 2023. DOI: https://doi.org/10.3390/ijms24043201.

QIU, S. *et al.* Hepatic estrogen receptor α is critical for regulation of gluconeogenesis and lipid metabolism in males. **Scientific Reports**, v. 7, p. 1661, 2017. DOI: https://doi.org/10.1038/s41598-017-01937-4.

QIU, Y.-Y.; ZHANG, J.; ZENG, F.-Y.; ZHU, Y. Z. Roles of the peroxisome proliferator-activated receptors (PPARs) in the pathogenesis of nonalcoholic fatty liver disease (NAFLD). **Pharmacological Research**, v. 192, p. 106786, 2023. DOI: https://doi.org/10.1016/j.phrs.2023.106786.

RAMANATHAN, R.; ALI, A. H.; IBDAH, J. A. Mitochondrial dysfunction plays central role in nonalcoholic fatty liver disease. **International Journal of Molecular Sciences**, v. 23, n. 13, p. 7280, 2022. DOI: https://doi.org/10.3390/ijms23137280.

RAMOS, L. C. S. *et al.* Occurrence and human health risk assessment of phenolic compounds in drinking water from Brazil. **Science of the Total Environment**, v. 785, p. 147379, 2021. DOI: https://doi.org/10.1016/j.scitotenv.2021.147379.

REBELO, R.; CALDAS, E. Avaliação de risco ambiental de ambientes aquáticos afetados pelo uso de agrotóxicos. **Química Nova**, v. 37, p. 1199–1208, 2014. DOI: https://doi.org/10.5935/0100-4042.20140165.

RIBEIRO, R. X. *et al.* Ecotoxicological assessment of effluents from Brazilian wastewater treatment plants using zebrafish embryotoxicity test: a multi-biomarker

approach. **Science of the Total Environment**, v. 735, p. 139036, 2020. DOI: https://doi.org/10.1016/j.scitotenv.2020.139036.

RIZZO, M. Measurement of malondialdehyde as a biomarker of lipid oxidation in fish. **American Journal of Analytical Chemistry**, v. 15, p. 303–332, 2024. DOI: https://doi.org/10.4236/ajac.2024.159020.

ROCHA, M. *et al.* Neural crest development: insights from the zebrafish. **Developmental Dynamics**, v. 249, n. 1, p. 88–111, 2020. DOI: https://doi.org/10.1002/dvdy.122.

RODIL, R. *et al.* Emerging pollutants in sewage, surface and drinking water in Galicia (NW Spain). **Chemosphere**, v. 86, n. 10, p. 1040–1049, 2012. DOI: https://doi.org/10.1016/j.chemosphere.2011.11.053.

ROJO DE LA VEGA, M.; CHAPMAN, E.; ZHANG, D. D. NRF2 and the hallmarks of cancer. **Cancer Cell**, v. 34, n. 1, p. 21–43, 2018. DOI: https://doi.org/10.1016/j.ccell.2018.03.022.

ROMUALDO, G. R. *et al.* Modifying effects of 2,4-D and glyphosate exposures on gut-liver-adipose tissue axis of diet-induced non-alcoholic fatty liver disease in mice. **Ecotoxicology and Environmental Safety**, v. 268, p. 115688, 2023. DOI: https://doi.org/10.1016/j.ecoenv.2023.115688.

ROTH, D. M.; BAYONA, F.; BADDAM, P.; GRAF, D. Craniofacial development: neural crest in molecular embryology. **Head and Neck Pathology**, v. 15, n. 1, p. 1–15, 2021. DOI: https://doi.org/10.1007/s12105-020-01224-1.

RUIZ DE ARCAUTE, C.; SOLONESKI, S.; LARRAMENDY, M. L. Toxic and genotoxic effects of the 2,4-dichlorophenoxyacetic acid (2,4-D)-based herbicide on the Neotropical fish *Cnesterodon decemmaculatus*. **Ecotoxicology and Environmental Safety**, v. 128, p. 222–229, 2016. DOI: https://doi.org/10.1016/j.ecoenv.2016.02.027.

RUSSO, L. *et al.* Insight into the molecular recognition mechanism of the coactivator NCoA1 by STAT6. **Scientific Reports**, v. 7, p. 16845, 2017. DOI: https://doi.org/10.1038/s41598-017-17088-5.

RZONCA, S. O. *et al.* Bone is a target for the antidiabetic compound rosiglitazone. **Endocrinology**, v. 145, n. 1, p. 401–406, 2004. DOI: https://doi.org/10.1210/en.2003-0746.

SALVO, L. M. *et al.* Toxicity assessment of 2,4-D and MCPA herbicides in primary culture of fish hepatic cells. **Journal of Environmental Science and Health, Part B**, v. 50, n. 7, p. 449–455, 2015. DOI: https://doi.org/10.1080/03601234.2015.1018754.

SANT, K. E.; TIMME-LARAGY, A. R. Zebrafish as a model for toxicological perturbation of yolk and nutrition in the early embryo. **Current Environmental Health Reports**, v. 5, n. 1, p. 125–133, 2018. DOI: https://doi.org/10.1007/s40572-018-0183-2.

SANT, K. E. *et al.* Nrf2a modulates the embryonic antioxidant response to perfluorooctanesulfonic acid (PFOS) in the zebrafish, *Danio rerio*. **Aquatic Toxicology,** v. 198, p. 92–102, 2018. DOI: https://doi.org/10.1016/j.aquatox.2018.02.010.

SANTAGOSTINO, A. *et al.* Effects of phenoxyacetic acid herbicides on chicken embryo liver drug metabolizing enzymes. **Pharmacology & Toxicology**, v. 68, n. 2, p. 110–114, 1991. DOI: https://doi.org/10.1111/j.1600-0773.1991.tb02046.x.

SAVOVA, M. S. *et al.* Targeting PI3K/AKT signaling pathway in obesity. **Biomedicine & Pharmacotherapy**, v. 159, p. 114244, 2023. DOI: https://doi.org/10.1016/j.biopha.2023.114244.

SCHAAF, M. J. M. Nuclear receptor research in zebrafish. **Journal of Molecular Endocrinology**, v. 59, n. 1, p. R65–R76, 2017. DOI: https://doi.org/10.1530/JME-17-0031.

SCHNEIDER, C. A.; RASBAND, W. S.; ELICEIRI, K. W. NIH Image to ImageJ: 25 years of image analysis. **Nature Methods**, v. 9, n. 7, p. 671–675, 2012. DOI: https://doi.org/10.1038/nmeth.2089.

SHAFEEQ, S.; MAHBOOB, T. Magnesium supplementation ameliorates toxic effects of 2,4-dichlorophenoxyacetic acid in rat model. **Human & Experimental Toxicology**, v. 39, n. 1, p. 47–58, 2020. DOI: https://doi.org/10.1177/0960327119874428.

SHAFEEQ, S.; MAHBOOB, T. 2,4-Dichlorophenoxyacetic acid induced hepatic and renal toxicological perturbations in rat model: attenuation by selenium supplementation. **Toxicology and Industrial Health**, v. 37, n. 3, p. 152–163, 2021. DOI: https://doi.org/10.1177/0748233720983167.

SHANNON, P. *et al.* Cytoscape: a software environment for integrated models of biomolecular interaction networks. **Genome Research**, v. 13, n. 11, p. 2498–2504, 2003. DOI: https://doi.org/10.1101/gr.1239303.

SHANNON, R. D. *et al.* Mitochondrial response to chlorophenols as a short-term toxicity assay. **Environmental Toxicology and Chemistry**, v. 10, n. 1, p. 57–66, 1991. DOI: https://doi.org/10.1002/etc.5620100107.

SHARMA, A. *et al.* Worldwide pesticide usage and its impacts on ecosystem. *SN* **Applied Sciences**, v. 1, n. 11, p. 1446, 2019. DOI: https://doi.org/10.1007/s42452-019-1485-1.

SHIMIZU, N.; SHIRAISHI, H.; HANADA, T. Zebrafish as a useful model system for human liver disease. **Cells**, v. 12, n. 18, p. 2246, 2023. DOI: https://doi.org/10.3390/cells12182246.

SINGH, S. Inhibition of human glutathione S-transferases by 2,4-dichlorophenoxyacetate (2,4-D) and 2,4,5-trichlorophenoxyacetate (2,4,5-T). **Toxicology and Applied Pharmacology**, v. 81, n. 2, p. 328–336, 1985. DOI: https://doi.org/10.1016/0041-008X(85)90170-X.

SINGHAL, S. S. *et al.* Antioxidant role of glutathione S-transferases: 4-hydroxynonenal, a key molecule in stress-mediated signaling. **Toxicology and Applied Pharmacology**, v. 289, n. 3, p. 361–370, 2015. DOI: https://doi.org/10.1016/j.taap.2015.10.006.

SINHA, K.; DAS, J.; PAL, P. B.; SIL, P. C. Oxidative stress: the mitochondria-dependent and mitochondria-independent pathways of apoptosis. **Archives of Toxicology**, v. 87, n. 7, p. 1157–1180, 2013. DOI: https://doi.org/10.1007/s00204-013-1034-4.

SISAGUA. Detection and concentration of pesticides from 2014 to 2017 in human drinking water. Brasília: Ministry of Health, 2018. Disponível em: http://www.vigilanciasanitaria.sc.gov.br/index.php/saude-ambiental/sisagua. Acesso em: 10 abr. 2023.

SMIRNOVA, A. *et al.* Increased apoptosis, reduced Wnt/β-catenin signaling, and altered tail development in zebrafish embryos exposed to a human-relevant chemical mixture. **Chemosphere**, v. 264, pt. 1, p. 128467, 2021. DOI: https://doi.org/10.1016/j.chemosphere.2020.128467.

SOLONESKI, S.; NIKOLOFF, N.; LARRAMENDY, M. L. Analysis of possible genotoxicity of the herbicide flurochloridone and its commercial formulations: Endo III and Fpg alkaline comet assays in Chinese hamster ovary (CHO-K1) cells. **Mutation Research/Genetic Toxicology and Environmental Mutagenesis**, v. 797, p. 46–52, 2016. DOI: https://doi.org/10.1016/j.mrgentox.2016.01.004.

SONG, M. *et al.* Carnitine acetyltransferase deficiency mediates mitochondrial dysfunction-induced cellular senescence in dermal fibroblasts. **Aging Cell**, 2023. DOI: https://doi.org/10.1111/acel.14000.

SOOKOIAN, S.; PIROLA, C. J. Liver enzymes, metabolomics and genome-wide association studies: from systems biology to the personalized medicine. **World Journal of Gastroenterology**, v. 21, n. 3, p. 711–725, 2015. DOI: https://doi.org/10.3748/wjg.v21.i3.711.

SOUZA, J. A. D. C. R. *et al.* Network toxicology and molecular docking to investigate the non-AChE mechanisms of organophosphate-induced neurodevelopmental toxicity. **Toxics**, v. 11, n. 8, p. 710, 2023. DOI: https://doi.org/10.3390/toxics11080710.

SOWERS, M. *et al.* Estrogen receptor genotypes and their association with the 10-year changes in bone mineral density and osteocalcin concentrations. **Journal of Clinical Endocrinology & Metabolism**, v. 89, n. 2, p. 733–739, 2004. DOI: https://doi.org/10.1210/jc.2003-030606.

STILL, K. *et al.* The peroxisome proliferator activator receptor alpha/delta agonists linoleic acid and bezafibrate upregulate osteoblast differentiation and induce periosteal bone formation in vivo. **Calcified Tissue International**, v. 83, n. 4, p. 285–292, 2008. DOI: https://doi.org/10.1007/s00223-008-9174-x.

SUBHASREE, N. *et al.* The MDM2-p53 pathway revisited. **The Journal of Biomedical Research**, v. 27, n. 4, p. 254, 2013. DOI: https://doi.org/10.7555/JBR.27.20130030.

SULE, R. O.; CONDON, L.; GOMES, A. V. A common feature of pesticides: oxidative stress—the role of oxidative stress in pesticide-induced toxicity. **Oxidative Medicine and Cellular Longevity**, v. 2022, p. 1–31, 2022. DOI: https://doi.org/10.1155/2022/5563759.

SUN, H. *et al.* Exposure to 2,4-dichlorophenoxyacetic acid induced PPARβ-dependent disruption of glucose metabolism in HepG2 cells. **Environmental Science and Pollution Research**, v. 25, n. 17, p. 17050–17057, 2018. DOI: https://doi.org/10.1007/s11356-018-1921-6.

SUN, Z.; XU, Y. Nuclear receptor coactivators (NCOAs) and corepressors (NCORs) in the brain. **Endocrinology**, v. 161, n. 8, p. bqaa083, 2020. DOI: https://doi.org/10.1210/endocr/bqaa083.

ŚWIDERSKA, E. *et al.* Role of PI3K/AKT pathway in insulin-mediated glucose uptake. In: SZABLEWSKI, L. (ed.). **Blood Glucose Levels**. London: IntechOpen, 2020. DOI: https://doi.org/10.5772/intechopen.80402.

SYVERSEN, U. *et al.* Different skeletal effects of the peroxisome proliferator activated receptor (PPAR)α agonist fenofibrate and the PPARγ agonist pioglitazone. *BMC* **Endocrine Disorders**, v. 9, p. 10, 2009. DOI: https://doi.org/10.1186/1472-6823-9-10.

TAHRI-JOUTEY, M. *et al.* Mechanisms mediating the regulation of peroxisomal fatty acid beta-oxidation by PPARα. **International Journal of Molecular Sciences**, v. 22, n. 16, p. 8969, 2021. DOI: https://doi.org/10.3390/ijms22168969.

TAKADA, I. *et al.* Alteration of a single amino acid in peroxisome proliferator-activated receptor-α (PPARα) generates a PPARδ phenotype. **Molecular Endocrinology**, v. 14, n. 5, p. 733–740, 2000. DOI: https://doi.org/10.1210/mend.14.5.0463.

TANAKA, K. *et al.* Oxidative stress inducers potentiate 2,3,7,8-tetrachlorodibenzo-p-dioxin-mediated pre-cardiac edema in larval zebrafish. **Journal of Veterinary Medical Science,** v. 83, n. 7, p. 1050–1058, 2021. DOI: https://doi.org/10.1292/jvms.21-0081.

TANENBAUM, D. M. *et al.* Crystallographic comparison of the estrogen and progesterone receptor's ligand binding domains. **Proceedings of the National Academy of Sciences**, v. 95, n. 11, p. 5998–6003, 1998. DOI: https://doi.org/10.1073/pnas.95.11.5998.

TAYEB, W. *et al.* Alteration of lipid status and lipid metabolism, induction of oxidative stress and lipid peroxidation by 2,4-dichlorophenoxyacetic herbicide in rat liver. **Toxicology Mechanisms and Methods**, v. 23, n. 6, p. 449–458, 2013. DOI: https://doi.org/10.3109/15376516.2013.780275.

TAYEB, W. *et al.* Hepatotoxicity induced by sub-acute exposure of rats to 2,4-dichlorophenoxyacetic acid based herbicide "Désormone lourd". **Journal of Hazardous Materials**, v. 180, n. 1–3, p. 225–233, 2010. DOI: https://doi.org/10.1016/j.jhazmat.2010.04.018.

THORSTENSEN, K. L. *Pesticides induce oxidative stress in zebrafish embryo*. 2014. Dissertação (Master's thesis) – The University of Bergen, Bergen, 2014.

TIAN, X. *et al.* Targeting apoptotic pathways for cancer therapy. **Journal of Clinical Investigation**, v. 134, n. 14, p. e179570, 2024. DOI: https://doi.org/10.1172/JCI179570.

TICHATI, L.; TREA, F.; OUALI, K. Potential role of selenium against hepatotoxicity induced by 2,4-dichlorophenoxyacetic acid in albino Wistar rats. **Biological Trace Element Research**, v. 194, n. 1, p. 228–236, 2020. DOI: https://doi.org/10.1007/s12011-019-01773-9.

TICHATI, L.; TREA, F.; OUALI, K. The antioxidant study proprieties of *Thymus munbyanus* aqueous extract and its beneficial effect on 2,4-dichlorophenoxyacetic acid-induced hepatic oxidative stress in albino Wistar rats. **Toxicology Mechanisms and Methods**, v. 31, n. 3, p. 212–223, 2021. DOI: https://doi.org/10.1080/15376516.2020.1870183.

TIRICHEN, H.; YAIGOUB, H.; XU, W.; WU, C.; LI, R.; LI, Y. Mitochondrial reactive oxygen species and their contribution in chronic kidney disease progression through oxidative stress. **Frontiers in Physiology**, v. 12, p. 627837, 2021. DOI: https://doi.org/10.3389/fphys.2021.627837.

TODISCO, S.; SANTARSIERO, A.; CONVERTINI, P.; DE STEFANO, G.; GILIO, M.; IACOBAZZI, V.; INFANTINO, V. PPAR alpha as a metabolic modulator of the liver: role in the pathogenesis of nonalcoholic steatohepatitis (NASH). **Biology,** v. 11, n. 5, p. 792, 2022. DOI: https://doi.org/10.3390/biology11050792.

TON, C.; LIN, Y.; WILLETT, C. Zebrafish as a model for developmental neurotoxicity testing. *Birth Defects Research Part A:* **Clinical and Molecular Teratology**, v. 76, n. 7, p. 553–567, 2006. DOI: https://doi.org/10.1002/bdra.20281.

TOU, W. I.; CHEN, C. Y.-C. In silico investigation of potential Src kinase ligands from traditional Chinese medicine. **PLoS ONE**, v. 7, n. 3, e33728, 2012. DOI: https://doi.org/10.1371/journal.pone.0033728.

TROTT, O.; OLSON, A. J. AutoDock Vina: improving the speed and accuracy of docking with a new scoring function, efficient optimization, and multithreading. **Journal of Computational Chemistry**, v. 31, n. 2, p. 455–461, 2010. DOI: https://doi.org/10.1002/jcc.21334.

TROUDI, A.; BEN AMARA, I.; SAMET, A. M.; ZEGHAL, N. Oxidative stress induced by 2,4-phenoxyacetic acid in liver of female rats and their progeny: biochemical and histopathological studies. **Environmental Toxicology**, v. 27, n. 3, p. 137–145, 2012. DOI: https://doi.org/10.1002/tox.20624.

TSABOULA, A.; PAPADAKIS, E.-N.; VRYZAS, Z.; KOTOPOULOU, A.; KINTZIKOGLOU, K.; PAPADOPOULOU-MOURKIDOU, E. Environmental and human risk hierarchy of pesticides: a prioritization method, based on monitoring, hazard assessment and environmental fate. **Environment International**, v. 91, p. 78–93, 2016. DOI: https://doi.org/10.1016/j.envint.2016.02.008.

TSUKAZAWA, K. S.; LI, L.; TSE, W. K. F. 2,4-dichlorophenol exposure induces lipid accumulation and reactive oxygen species formation in zebrafish embryos. **Ecotoxicology and Environmental Safety**, v. 230, p. 113133, 2022. DOI: https://doi.org/10.1016/j.ecoenv.2021.113133.

TUSCHL, H.; SCHWAB, C. Cytotoxic effects of the herbicide 2,4-dichlorophenoxyacetic acid in HepG2 cells. **Food and Chemical Toxicology**, v. 41, n. 3, p. 385–393, 2003. DOI: https://doi.org/10.1016/S0278-6915(02)00238-7.

TUSCHL, H.; SCHWAB, C. E. Flow cytometric methods used as screening tests for basal toxicity of chemicals. **Toxicology in Vitro**, v. 18, n. 4, p. 483–491, 2004. DOI: https://doi.org/10.1016/j.tiv.2003.12.004.

UNITED STATES. Agency for Toxic Substances and Disease Registry (ATSDR). *Toxicological profile for 2,4-dichlorophenoxyacetic acid*. Atlanta, 2020. Disponível em: https://www.atsdr.cdc.gov/ToxProfiles/tp.asp?id=1481&tid=288. Acesso em: 15 fev. 2026.

UNITED STATES. Environmental Protection Agency (USEPA). *Water-related environmental fate of 129 priority pollutants*. Washington, DC, 1979. v. 2, p. 412–432.

UNITED STATES. Environmental Protection Agency (USEPA). *Update of human health ambient water quality criteria: 2,4-dichlorophenol (120-83-2)*. EPA 820-R-15-084. Washington, DC: Office of Water, Office of Science and Technology, 2015. Disponível em: https://www.epa.gov/sites/default/files/2015-10/documents/final-2-4-dichlorophenol.pdf. Acesso em: 15 fev. 2026.

UNITED STATES. Department of Agriculture (USDA). *World agricultural production*. Circular series. Washington, DC, 2017.

UNITED STATES. Department of Agriculture (USDA). *Dow AgroSciences petitions (09-233-01p, 09-349-01p, and 11-234-01p) for determinations of nonregulated status for 2,4-D-resistant corn and soybean varieties: draft environmental impact statement*. Washington, DC, 2014. Disponível em: http://www.aphis.usda.gov/brs/aphisdocs/24d_deis.pdf. Acesso em: 15 fev. 2026.

VAILLANT, C. *et al.* Neurodevelopmental effects of natural and synthetic ligands of estrogen and progesterone receptors in zebrafish eleutheroembryos. **General and Comparative Endocrinology**, v. 288, p. 113345, 2020. DOI: https://doi.org/10.1016/j.ygcen.2019.113345.

VAINIO, H.; LINNAINMAA, K.; KÄHÖNEN, M.; NICKELS, J.; HIETANEN, E.; MARNIEMI, J.; PELTONEN, P. Hypolipidemia and peroxisome proliferation induced

by phenoxyacetic acid herbicides in rats. **Biochemical Pharmacology**, v. 32, n. 18, p. 2775–2779, 1983. DOI: https://doi.org/10.1016/0006-2952(83)90091-6.

VAINIO, H.; NICKELS, J.; LINNAINMAA, K. Phenoxy acid herbicides cause peroxisome proliferation in Chinese hamsters. **Scandinavian Journal of Work, Environment & Health**, v. 8, n. 1, p. 70–73, 1982. DOI: https://doi.org/10.5271/sjweh.2494.

VAN METER, R. J.; GLINSKI, D. A.; PURUCKER, S. T.; HENDERSON, W. M. Influence of exposure to pesticide mixtures on the metabolomic profile in post-metamorphic green frogs (*Lithobates clamitans*). **Science of the Total Environment**, v. 624, p. 1348–1359, 2018. DOI: https://doi.org/10.1016/j.scitotenv.2017.12.175.

VARSHNEY, M. K. *et al.* Role of estrogen receptor beta in neural differentiation of mouse embryonic stem cells. **Proceedings of the National Academy of Sciences**, v. 114, n. 41, p. E10428–E10437, 2017. DOI: https://doi.org/10.1073/pnas.1714094114.

VASSILEV, L. T. *et al.* In vivo activation of the p53 pathway by small-molecule antagonists of MDM2. **Science**, v. 303, n. 5659, p. 844–848, 2004. DOI: https://doi.org/10.1126/science.1092472.

VEITH, A.; MOORTHY, B. Role of cytochrome P450s in the generation and metabolism of reactive oxygen species. **Current Opinion in Toxicology**, v. 7, p. 44–51, 2018. DOI: https://doi.org/10.1016/j.cotox.2017.10.003

VELKI, M.; MEYER-ALERT, H.; SEILER, T. B.; HOLLERT, H. Enzymatic activity and gene expression changes in zebrafish embryos and larvae exposed to pesticides diazinon and diuron. **Aquatic Toxicology**, v. 193, p. 187–200, 2017. DOI: https://doi.org/10.1016/j.aquatox.2017.10.019.

VENUGOPAL, D.; JAYANTHI, P.; RAVICHANDRAN, B. Biomonitoring and biomarkers of pesticide exposure and human health risk assessment. In: SINGH, P.; SINGH, S.; SILLANPÄÄ, M. (eds.). **Pesticides in the Natural Environment**. Amsterdam: Elsevier, 2022. p. 563–584. DOI: https://doi.org/10.1016/B978-0-323-90489-6.00021-5.

VESSEY, D. A.; BOYER, T. D. Differential activation and inhibition of different forms of rat liver glutathione S-transferase by the herbicides 2,4-dichlorophenoxyacetate (2,4-D) and 2,4,5-trichlorophenoxyacetate (2,4,5-T). **Toxicology and Applied Pharmacology**, v. 73, n. 3, p. 492–499, 1984. DOI: https://doi.org/10.1016/0041-008X(84)90101-7.

VIEIRA, L. V. DA S.; REIS, J. F.; LEITÃO, E. L.; FRANÇA, B. N. DE A.; GOMES, M. B. V.; SALVADOR, S. D.; SILVA, R. O. DE S. Análise do acesso ao transplante de fígado nas diferentes regiões brasileiras de 2018 a 2022: um estudo transversal. **Brazilian Journal of Transplantation**, v. 26, n. 1, 2023. DOI: https://doi.org/10.5935/bjt.2023.01.06.

VIGÁRIO, A. F.; SABÓIA-MORAIS, S. M. T. Effects of the 2,4-D herbicide on gills epithelia and liver of the fish *Poecilia vivipara*. **Pesquisa Veterinária Brasileira**, v. 34, n. 6, p. 523–528, 2014. DOI: https://doi.org/10.1590/S0100-736X2014000600005.

VIRTANEN, P. *et al.* SciPy 1.0: fundamental algorithms for scientific computing in Python. ***Nature Methods***, v. 17, n. 3, p. 261–272, 2020. DOI: https://doi.org/10.1038/s41592-019-0686-2.

VON HELLFELD, R.; BROTZMANN, K.; BAUMANN, L.; STRECKER, R.; BRAUNBECK, T. Adverse effects in the fish embryo acute toxicity (FET) test: a catalogue of unspecific morphological changes versus more specific effects in zebrafish (*Danio rerio*) embryos. ***Environmental Sciences Europe***, v. 32, p. 122, 2020. DOI: https://doi.org/10.1186/s12302-020-00398-3.

WANG, C.; YOULE, R. J. The role of mitochondria in apoptosis. *Annual Review of* **Genetics**, v. 43, n. 1, p. 95–118, 2009. DOI: https://doi.org/10.1146/annurev-genet-102108-134850.

WANG, W. *et al.* Involvement of fatty acid metabolism in the hepatotoxicity induced by divalproex sodium. **Human & Experimental Toxicology**, v. 31, n. 11, p. 1092–1101, 2012. DOI: https://doi.org/10.1177/0960327112444477.

WANG, W. *et al.* Induction of oxidative stress and cardiac developmental toxicity in zebrafish embryos by arsenate at environmentally relevant concentrations. **Ecotoxicology and Environmental Safety**, v. 280, p. 116529, 2024. DOI: https://doi.org/10.1016/j.ecoenv.2024.116529.

WANG, Y.; NAKAJIMA, T.; GONZALEZ, F. J.; TANAKA, N. PPARs as metabolic regulators in the liver: lessons from liver-specific PPAR-null mice. **International Journal of Molecular Sciences**, v. 21, n. 6, p. 2061, 2020. DOI: https://doi.org/10.3390/ijms21062061.

WARNER, J. *et al.* Soluble epoxide hydrolase inhibition in liver diseases: a review of current research and knowledge gaps. **Biology**, v. 9, n. 6, p. 124, 2020. DOI: https://doi.org/10.3390/biology9060124.

WHITFIELD, J. B. Gamma glutamyl transferase. **Critical Reviews in Clinical Laboratory Sciences**, v. 38, n. 4, p. 263–355, 2001. DOI: https://doi.org/10.1080/20014091084227.

WRIGHT, L. *et al.* Structure-activity relationships in purine-based inhibitor binding to HSP90 isoforms. **Chemistry & Biology**, v. 11, n. 6, p. 775–785, 2004. DOI: https://doi.org/10.1016/j.chembiol.2004.03.033.

WU, L.; GUO, C.; WU, J. Therapeutic potential of PPARγ natural agonists in liver diseases. **Journal of Cellular and Molecular Medicine**, v. 24, n. 5, p. 2736–2748, 2020. DOI: https://doi.org/10.1111/jcmm.15028.

WU, X. *et al.* Frequency of stromal lineage colony forming units in bone marrow of peroxisome proliferator-activated receptor-alpha-null mice. **Bone**, v. 26, n. 1, p. 21–26, 2000. DOI: https://doi.org/10.1016/S8756-3282(99)00247-0.

WULLIMANN, M. F.; UMEASALUGO, K. E. Sonic hedgehog expression in zebrafish forebrain identifies the teleostean pallidal signaling center and shows preglomerular complex and posterior tubercular dopamine cells to arise from shh cells. **Journal of Comparative Neurology**, v. 528, n. 8, p. 1321–1348, 2020. DOI: https://doi.org/10.1002/cne.24825.

XIN, J. *et al.* Unraveling DINCH-induced hepatotoxicity mechanisms via network toxicology and molecular docking with experimental validation. *Ecotoxicology and* **Environmental Safety**, v. 299, p. 118305, 2025. DOI: https://doi.org/10.1016/j.ecoenv.2025.118305.

XU, X. *et al.* Effect of downregulated citrate synthase on oxidative phosphorylation signaling pathway in HEI-OC1 cells. **Proteome Science**, v. 20, n. 1, p. 14, 2022. DOI: https://doi.org/10.1186/s12953-022-00196-0.

YAKOVENKO, B. V.; TRETYAK, O. P.; MEKHED, O. B.; ISKEVYCH, O. V. Effect of herbicides and surfactants on enzymes of energy metabolism in European carp. **Ukrainian Journal of Ecology**, v. 8, n. 1, p. 948–952, 2018. DOI: https://doi.org/10.15421/2018_297.

YAMINI, Y.; SALEH, A. Ultrasound-assisted emulsification microextraction combined with injection-port derivatization for the determination of some chlorophenoxyacetic acids in water samples. **Journal of Separation Science**, v. 36, n. 14, p. 2330–2338, 2013. DOI: https://doi.org/10.1002/jssc.201300340.

YANG, M. *et al.* Integrated network toxicology, transcriptomics and gut microbiomics reveals hepatotoxicity mechanism induced by benzo[a]pyrene exposure in mice. **Toxicology and Applied Pharmacology**, v. 491, p. 117050, 2024. DOI: https://doi.org/10.1016/j.taap.2024.117050.

YANG, Q.; GONZALEZ, F. J. Peroxisome proliferator-activated receptor alpha regulates B lymphocyte development via an indirect pathway in mice. *Biochemical* **Pharmacology**, v. 68, n. 11, p. 2143–2150, 2004. DOI: https://doi.org/10.1016/j.bcp.2004.07.016.

YANG, W. J. *et al.* Exposure to 2,4-dichlorophenol, 2,4,6-trichlorophenol, pentachlorophenol and risk of thyroid cancer: a case-control study in China. **Environmental Science and Pollution Research**, v. 28, n. 43, p. 61329–61343, 2021. DOI: https://doi.org/10.1007/s11356-021-14898-z.

YAO, Q. *et al.* Sonic hedgehog signaling instigates high-fat diet-induced insulin resistance by targeting PPARγ stability. **Journal of Biological Chemistry**, v. 294, n. 9, p. 3284–3293, 2019. DOI: https://doi.org/10.1074/jbc.RA118.004411.

YAO, S. *et al.* Role of lactate and lactate metabolism in liver diseases (review). **International Journal of Molecular Medicine**, v. 54, n. 1, p. 59, 2024. DOI: https://doi.org/10.3892/ijmm.2024.5383.

YILMAZ, H. R.; YUKSEL, E. Effect of 2,4-dichlorophenoxyacetic acid on the activities of some metabolic enzymes for generating pyridine nucleotide pool of cells from mouse liver. **Toxicology and Industrial Health**, v. 21, n. 7–8, p. 231–237, 2005. DOI: https://doi.org/10.1191/0748233705th231oa.

ZAFFARONI, N. P.; ZAVANELLA, T.; CATTANEO, A.; ARIAS, E. The toxicity of 2,4-dichlorophenoxyacetic acid to the adult crested newt. **Environmental Research**, v. 41, n. 1, p. 79–87, 1986. DOI: https://doi.org/10.1016/S0013-9351(86)80169-4.

ZBINDEN, G. Predictive value of animal studies in toxicology. **Regulatory Toxicology and Pharmacology**, v. 14, n. 2, p. 167–177, 1991. DOI: https://doi.org/10.1016/0273-2300(91)90004-F.

ZELBER-SAGI, S. *et al.* Serum malondialdehyde is associated with non-alcoholic fatty liver and related liver damage differentially in men and women. **Antioxidants**, v. 9, n. 7, p. 578, 2020. DOI: https://doi.org/10.3390/antiox9070578.

ZHANG, C.; ANDERSON, A.; COLE, G. J. Analysis of crosstalk between retinoic acid and sonic hedgehog pathways following ethanol exposure in embryonic zebrafish. **Birth Defects Research Part A: Clinical and Molecular Teratology**, v. 103, n. 12, p. 1046–1057, 2015. DOI: https://doi.org/10.1002/bdra.23460.

ZHANG, C. *et al.* 2,4-Dichlorophenol induces feminization of zebrafish (*Danio rerio*) via DNA methylation. **Science of the Total Environment**, v. 708, p. 135084, 2020. DOI: https://doi.org/10.1016/j.scitotenv.2019.135084.

ZHANG, Y. *et al.* Combined toxicity of triclosan, 2,4-dichlorophenol and 2,4,6-trichlorophenol to zebrafish (*Danio rerio*). **Environmental Toxicology and Pharmacology**, v. 57, p. 9–18, 2018. DOI: https://doi.org/10.1016/j.etap.2017.11.006.

ZHAO, C. *et al.* Hepatotoxicity evaluation of *Euphorbia kansui* on zebrafish larvae in vivo. **Phytomedicine**, v. 62, p. 152959, 2019. DOI: https://doi.org/10.1016/j.phymed.2019.152959.

ZHAO, S.; IYENGAR, R. Systems pharmacology: network analysis to identify multiscale mechanisms of drug action. **Annual Review of Pharmacology and Toxicology**, v. 52, n. 1, p. 505–521, 2012. DOI: https://doi.org/10.1146/annurev-pharmtox-010611-134520.

ZHAO, Y. *et al.* Citrate promotes excessive lipid biosynthesis and senescence in tumor cells for tumor therapy. **Advanced Science**, v. 9, n. 1, e2101553, 2022. DOI: https://doi.org/10.1002/advs.202101553.

ZHONG, W. *et al.* Screening level ecological risk assessment for phenols in surface water of the Taihu Lake. **Chemosphere**, v. 80, n. 9, p. 998–1005, 2010. DOI: https://doi.org/10.1016/j.chemosphere.2010.05.036.

ZIMMERMANN, M. J. Y. *et al.* Zebrafish differentially process color across visual space to match natural scenes. **Current Biology**, v. 28, n. 13, p. 2018–2032.e5, 2018. DOI: https://doi.org/10.1016/j.cub.2018.04.075.

ZUANAZZI, N. R.; GHISI, N. D. C.; OLIVEIRA, E. C. Analysis of global trends and gaps for studies about 2,4-D herbicide toxicity: a scientometric review. **Chemosphere**, v. 241, p. 125016, 2020. DOI: https://doi.org/10.1016/j.chemosphere.2019.125016.

ZYCHLINSKI, L.; ZOLNIEROWICZ, S. Comparison of uncoupling activities of chlorophenoxy herbicides in rat liver mitochondria. **Toxicology Letters**, v. 52, n. 1, p. 25–34, 1990. DOI: https://doi.org/10.1016/0378-4274(90)90162-F.

APÊNDICE A - BIOCHEMICAL MARKERS FOR LIVER INJURY IN ZEBRAFISH LARVAE

Rafael Xavier Martins[a,b], Juliana Alves Costa Ribeiro Souza[b,c], Maria Eduarda Maia[a,b], Matheus Carvalho[a], Terezinha Souza[a], Davi Farias[a,b,c,*]

[a]Post-Graduation Program in Biochemistry, Department of Biochemistry and Molecular Biology, Federal University of Ceará, 60455-970, Fortaleza, Brazil

[b]Department of Molecular Biology, Federal University of Paraíba, 58051-900, João Pessoa, Brazil

[c]Post-Graduation Program in Natural and Synthetic Bioactive Products, Health Sciences Centre, Federal University of Paraíba, 58051-900, João Pessoa, Brazil

[*] Corresponding author:

Professor Davi F. Farias

E-mail: davi@dbm.ufpb.br

Phone: +55-83-32167633

Abstract

The liver plays a crucial role in detoxification processes and metabolism of xenobiotics, and, therefore, it is a target organ of toxicity of different classes of chemicals. In this context, some key enzymes present in liver are considered to be good biochemical markers of hepatic damage and can have their activities determined via spectrophotometry. Aspartate and alanine aminotransferases, alkaline phosphatase, lactate dehydrogenase and glutathione peroxidase are enzymes that have activities often changed in response to hepatotoxic compounds, and can be accessed through the larval period of zebrafish (*Danio rerio*). In this work, we described methodologies for analyses of these five biomarkers in pooled zebrafish larvae through spectrophotometry.

Keywords: Hepatic diseases, liver failure, drug induced liver injury, biochemical markers.

Introduction

The liver is the main organ responsible for metabolization of xenobiotics in organisms. Consequently, hepatic damages are a common side effect as a result of the exposure to toxic chemicals (as drugs and pesticides) and represent a worrisome factor for study areas such as Toxicology and Ecotoxicology [11]. In this regard, zebrafish (*Danio rerio*) larvae have been showing to be an efficient model system for the evaluation of the hepatotoxic potential of substances. Besides the low maintenance cost and feasibility of use in laboratory, the zebrafish liver shares high structural, metabolic and functional similarity with those of mammals, including humans [9]. This similarity allows classical biochemical markers of liver damage (*e.g.* alanine aminotransferase) to be accessed in zebrafish larvae ≥ 72 hours post-fertilization (hpf), when liver is perfused with blood and functional [18].

In this work we describe the determination of five enzymatic markers for assessment of hepatotoxicity in zebrafish larvae via spectrophotometry: aspartate aminotransferase (AST), alanine aminotransferase (ALT), alkaline phosphatase (ALP), lactate dehydrogenase (LDH) and glutathione peroxidase (GPx). AST and ALT are transaminase enzymes present in high quantities in liver and are released into the circulation by damaged hepatocytes, being the AST/ALT ratio one of the most robust markers of liver damage [13]. In turn, ALP is located in the epithelial cells of intrahepatic bile ducts, and an increase in its levels is related to hepatobiliary disorders [8,7]. LDH participates in the energy production via anaerobic metabolism, and an elevation in its activity indicates cell injury and/or low oxygen availability [12]. Finally, GPx is an abundant liver enzyme that displays antioxidant activity, controlling the excessive production of reactive oxygen species (ROS) and protecting cell structures from oxidative damage [17].

Methodologies for determination of AST, ALT and ALP activities here described are based on enzyme reactions according to Keiding *et al.* [10]. Reactions were optimized for use in spectrophotometric diagnosis kit (Doles, Goiás, Brazil), already adapted for use in zebrafish larvae by Martins *et al.* [14]. In the case of the employed methodologies for determination of LDH and GPx, they were performed according to the procedures described by Domingues *et al.* [6] and Massarsky *et al.* [15], respectively, with modifications. Here are listed the enzimatic principles for determination of AST, ALT, ALP, LDH and GPx activitys:

- AST

$$\text{Aspartate + 2-Oxaglutarate} \xrightarrow{\text{AST}} \text{Oxalacetate + Glutamate}$$

$$\text{Oxalacetate + NADH + H}^{+} \xrightarrow{\text{MDH}} \text{Malate + NAD}^{+}$$

- ALT

$$\text{Alanine + 2-Oxaglutarate} \xrightarrow{\text{ALT}} \text{Pyruvate + Glutamate}$$

$$\text{Pyruvate+ NADH + H}^{+} \xrightarrow{\text{LDH}} \text{Lactate + NAD}^{+}$$

- ALP

$$\textit{p}\text{-Nitrophenylphosphate} \xrightarrow{\text{ALP}} \textit{p}\text{-Nitrophenol + phosphate}$$

- LDH

$$\text{Pyruvate + NADH + H}^{+} \xrightarrow{\text{LDH}} \text{Lactate + NAD}^{+}$$

- GPx

$$\text{2GSH + H}_2\text{O}_2 \xrightarrow{\text{GPx}} \text{2 H}_2\text{O + GSSH}$$

$$\text{GSSG + NADPH + H}^{+} \xrightarrow{\text{GR}} \text{2 GSH + NADP}^{+}$$

Oxidation of NADH to NAD+ is directly proportional to ALT and AST activities. Thus, both enzyme activities are calculated through decrease of absorbance of NADH solution at 340 nm. ALP catalyzes p-Nitrophenylphosphate hydrolysis, releasing p-Nitrophenol, which has yellow color. ALP activity is proportional to intensity of the solution color. Therefore, ALP activity is determined by the quantity of p-Nitrophenol formed, measured at 405 nm. LDH catalyzes conversion of pyruvate to lactate in the presence of NADH. Absorbance decrease at 340 nm due to oxidation of NADH to NAD+

is proportional to LDH activity in the sample. GPx catalyzes the oxidation reaction of (2) GSH to GSSG, utilizing H2O2 as substrate. GR catalyzes the regeneration reaction of GSH in the presence of NADPH. Oxidation of NADPH to NADP+ is proportional to GPx activity. Therefore, enzyme activity is calculated by the reduction of absorbance of NADPH solution at 340 nm.

Materials

2.1 Equipment

1. Centrifuge capable of rotating at 10,000 x RCF (g) and cooling at 4 ºC;
2. A microplate spectrophotometer able to detect the following wavelength: 340, 405 and 595 nm;
3. pHmeter;
4. Vortex mixer;
5. Magnetic stirrer;
6. Multichannel pipette with capacity range between 20 and 250 µL.
7. Semi-automatic micropipette with volume range between 1 and 1000 µL.

2.2 Sample processing

1. 1.5 mL microcentrifuge tubes (microtubes);
2. Polypropylene pestle for grinding samples in microtubes;
3. Distilled water.
4. Coolbox with ice.

2.3 Protein determination

1. Bradford Reagent: Weigh 26.32 mg of Coomassie Brilliant Blue G-250 and dissolve it in 12.5 mL of ethanol 95 % (v/v). Leave the solution under constant stirring for 1 h, protected from light (dark room and covered with aluminum foil).

Transfer the solution to a 250 mL volumetric flask, add 25 mL of 85% (v/v) orthophosphoric acid and fill the volumetric flask to the mark with distilled water. Filter the solution twice through a filter paper and store it at room temperature protected from light (in a bottle covered with aluminum foil). In these conditions, Bradford reagent is valid for a month.

2. Bovine serum albumin (BSA) solution: Weigh 25 mg of BSA and dissolve it in 25 mL of distilled water to make a 1 mg/mL BSA stock solution (SS).
3. Bovine serum albumin (BSA) standards: In 1.5 mL microtubes, prepare 10 solutions with increasing BSA concentrations by diluting the stock solution in distilled water (DW), according to table 1. Microtubes must be kept frozen (-20 ºC) until usage. Under these conditions, the solutions are usually usable for up to three months.

Table 1 – Instructions for dilution of stock solution (SS) in distilled water (DW) for preparation of the standard curve with BSA in mg/mL.

Concentration (mg/mL)	**SS (µL)**	**DW (µL)**
0.5	50	950
1	100	900
1.5	150	850
2	200	800
2.5	250	750
3	300	700
3.5	350	650
4	400	600
4.5	450	550
5	500	500

2.4 Aspartate aminotransferase determination

1. Solution A (121 mmol/L Tris; 362 mmol/L L-aspartate; ≥ 950 U/L Malate dehydrogenase and ≥ 900 U/L Lactate dehydrogenase buffer; pH 7.8) (*see* **Note 1**): Weigh 0.23 g of tris(hydroxymethyl)aminomethane, 0.77 g of L-aspartic acid and dissolve them in 10 mL of distilled water. Add small quantities of NaOH or HCl (both at 1 M) to the solution in order to adjust the pH to 7.8. Add 6.3 µL of a stock solution of malate dehydrogenase commercially available (from pig heart, 5,000 U, Sigma M1567-5KU) to the Tris and Aspartic acid solution (*see* **Note 2**). Add to the previous solution 1 µL of a lactate dehydrogenase stock solution, commercially available (from rabbit muscle, 10,000 U, Sigma L2500-10KU). Subsequently, make up for the final volume of 16 mL in a graduated cylinder with distilled water. Store the container at 4 ºC, protected from light with aluminum foil. In these conditions, it is recommended that solution A be stored for up to one month.
2. Solution B (1.3 mmol/L NADH and 75 mmol/L 2-Oxoglutarate): Weigh 3.4 mg of NADH and 43.8 mg of 2-oxoglutarate and dissolve them in 4 mL of distilled water. Store the container at 4 ºC protected from light with aluminum foil. In these conditions, it is recommended that the solution be stored for up to one month.
3. Assay Solution: Make the assay solution mixing 4 mL of solution A with 1 mL of solution B. Homogenize the mixture in a vortex mixer and keep the bottle/container protected from light at 4 ºC. In these conditions, the assay solution will remain stable for up to fourteen days after manufacture.
4. 96 well clear flat bottom UV-transparent microplates.

2.5 Alanine aminotransferase determination

1. Solution A (150 mmol/L Tris; 750 mmol/L L-alanine; and >1000U/L Lactate dehydrogenase; pH 7.3) (*see* **Note 1**): Weigh 0.290 g of tris(hydroxymethyl)aminomethane, 1.06 g of L-alanine and dissolve it in 8 mL of distilled water. Adjust the pH to 7.3 using small quantities of NaOH or HCl (both at 1 M). Add 1 µL of a lactate dehydrogenase stock solution, commercially available (from rabbit muscle, 10,000 U, Sigma L2500-10KU) (see **Note 2**). Subsequently, make up for the final volume of 16 mL with distilled water. Store the container/bottle at 4 ºC, protected from light with aluminum foil. In these conditions, it is recommended that the solution can be used for up to one month.
2. Solution B (1.3 mmol/L NADH and 75 mmol/L 2-Oxoglutarate): the same from topic 2.3.
3. Assay Solution: the same from topic 2.3.
4. 96 well clear flat bottom UV-transparent microplates.

2.6 Alcaline phosfatase determination

1. Buffer solution (1.25 mmol/L diethanolamine and 0.1%) sodium azide (see **Note 3**): Weigh 2.1 mg of diethanolamine and 16 mg of sodium azide (NaN3) and dissolve them in 10 mL of distilled water Adjust the pH to 9.8 with small amounts of NaOH or HCl, both at 1 M. Make up for the final volume of 16 mL with distilled water. Store the container/bottle at 4 ºC, protected from light with aluminum foil. In these conditions, it is recommended that the solution can be used for up to one month.
2. Substrate (50 mmol/L p-nitrophenyl phosphate; 0.1 % (m/v) sodium azide): Weigh 43.8 mg of p-nitrophenyl phosphate and 4 mg of sodium azide (NaN3) and dissolve them in 4 mL of distilled water.

3. Assay solution: Prepare the assay solution by transferring the substrate to the container with the buffer solution and homogenize it by shaking the bottle upside down several times. Should a smaller volume be necessary for the tests, the assay solution might also be obtained by mixing 4 parts buffer solution and 1 part substrate (4:1). This solution remains stable for 30 days when stored at 4 ºC.
4. 96 well clear flat bottom UV-transparent microplates.

2.7 Lactate dehydrogenase determination

1. 0.1 M Tris-NaCl buffer solution (pH 7.2): weigh 3.025 g of Tris reagent and 2.19 g of NaCl, and dissolve them in 200 mL of distilled water. Adjust the pH to 7.2 with HCl or NaOH (both at 1 M) and add distilled water to bring the volume to 250 mL in a volumetric flask. This solution should be kept at 4 ºC until the moment of use and lasts for one month in these conditions.
2. 0.24 mM NADH: weigh 1 mg of NADH and dissolve it in 5.882 mL of Tris-NaCl buffer (0.1 M, pH 7.2). This solution must be prepared on the day of use and must be kept refrigerated (4 ºC) or in ice bath until the moment of use.
3. 10 mM pyruvate solution: weigh 5.502 mg of pyruvate and dissolve it in 5 mL of 0.1 M Tris-NaCl buffer (pH 7.2). This solution must be made on the day of use and must be kept at 4 ºC or in ice bath until the moment of use.
4. All solutions must be at room temperature (20-25 ºC) at the moment of the assay.
5. 96 well clear flat bottom UV-transparent microplates.

2.8 Glutathione peroxidase determination

1. 1000 mM Monobasic potassium phosphate (KH_2PO_4) solution: weigh 2.4 g of KH_2PO_4 and dissolve it in 15 mL of distilled water.

2. 1000 mM Dibasic potassium phosphate (K_2HPO_4) solution: weigh 1.95 g of K_2HPO_4 and dissolve it in 5 mL of distilled water.
3. 134 mM EDTA solution: weigh 0.25 g of EDTA disodium salt and dissolve it in 5 mL of distilled water.
4. Potassium phosphate buffer solution (KPB-50): mix 800 µL of KH_2PO_4 solution with 1.5 mL of K_2HPO_4 solution and 180 µL of EDTA solution. Make up for the final volume of 50 mL with distilled water, adjusting the pH to 7.
5. Potassium phosphate buffer solution (KPB-100): mix 0.4 mL of KH2PO4 solution with 0.6 mL of K2HPO4 solution and 82 µL of EDTA solution. Make up for the final volume of 10 mL with distilled water, adjusting the pH to 7.
6. 2 U/mL Glutathione Reductase (GR) solution: mix 5 µL of a commercial solution of GR (from *Saccharomyces cerevisae*, 100 U, Sigma G3664) in 500 µL of KPB-100 buffer.
7. Reaction solution (5 mM NaN_3, 18 mM GSH and 0.9 U /mL of GR): weigh 7.8 mg of sodium azide (NaN_3), 138.3 mg of reduced glutathione (GSH) and dissolve it in 20 mL of KPB-50 buffer. Afterwards, add 177 µL of a GR stock solution and make up for the final volume of 25 mL with distilled water. This solution must be prepared on the day of use and kept refrigerated (4 ºC) or in ice bath until the moment of use.
8. 6 mM NADPH: weigh 5 mg of NADPH and dissolve it in 1 mL of KPB-50 buffer. Keep the solution protected from light and in ice bath or cooled (4 ºC). In these conditions, this solution lasts for three days.
9. 0.016 % (v/v) Hydrogen peroxide (H_2O_2): dilute 0.55 µL of a commercial solution of H_2O_2 (30%) in 1 mL of distilled water. Prepare the solution on the day

of the assay and keep it in ice bath or cooled (4 ºC) and protected from light until its use.

10. 96 well clear flat bottom UV-transparent microplates.

Methods

3.1 Sample processing

1. Evaluation of hepatic markers is possible in zebrafish larvae ≥ 3dpf (days post-fertilization), once they display their liver perfused with blood and totally functional in this stage of life. Exposure to the test-substance is based on FET test (Fish Embryo Acute Toxicity test), OECD's protocol N°. 236 (2013) [16], modified by Martins *et al.* [14], and it can take place until 7 dpf without the need of feeding the animals. Due to the great amount of larvae necessary for the assessment of the biomarkers, it is recommended the use of Petri dish as a container for the assay. After assay, a pool of 100 zebrafish larvae must be collected, rinsed with distilled water and deposited in 1.5 mL microtubes containing 700 µL of cold distilled water. The sample must be kept frozen (- 20 ºC) until the moment of the analyses.
2. Samples must be thawed in ice bath and kept this way during processing and analyses.
3. Macerate larvae mechanically with the aid of a polypropylene pestle until the microtube content shows a dark-gray color (*see* **Note 4).**
4. Subsequently, centrifuge samples at 10,000 x g during 20 min at 4 °C for the extraction of post-mitochondrial supernatant (PMS).
5. Divide the PMS content in 6 different microtubes (*see* **Note 5**), being:
   - 100 µL for total protein determination;
   - 100 µL for AST
   - 100 for ALT
   - 100 µL for ALP
   - 100 µL for GPx
   - 200 µL for LDH
6. Microtubes might be kept frozen at – 20 ºC until the moment of the analyses.

3.2 Protein determination

1. Thaw the 10 BSA solutions (0.5 – 5 mg/mL) and the microtubes containing the samples in ice bath.
2. Pipette 10 µL of BSA solutions in different columns of the plate in triplicates as shown in **figure 1**.
3. Pipette 10 µL of distilled water in the first column in triplicate (blank).

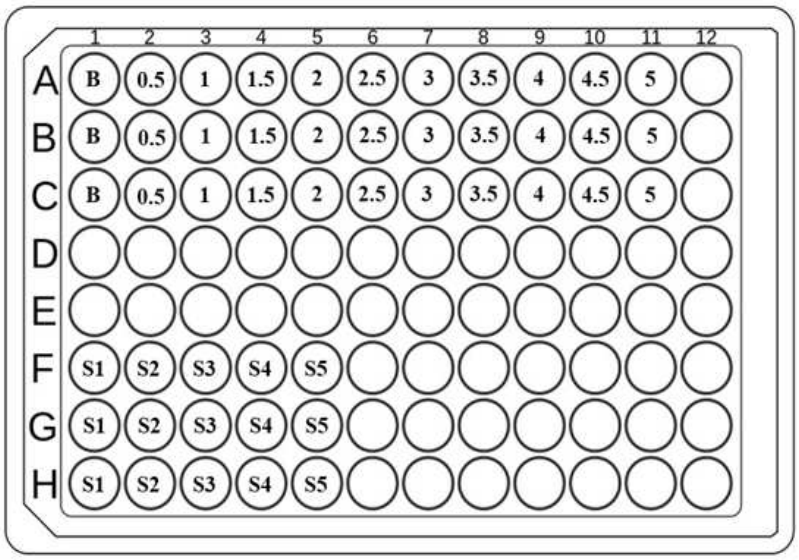

Figure 1. Schematic representation of the plate utilized for the determination of protein concentrations. B – blank, BSA (0.5 – 5 mg/mL) – standard curve, **S** (1 – 5) – samples.

4. Pipette 10 µL of samples, in triplicates, in the columns of your choice.
5. It is important that the content of each microtube (BSA and samples) be homogenized in a vortex mixer before being added to the plate, for a better standardization of results.
6. With a multichannel pipette, add 250 µL of Bradford reagent in each well of the plate (blank, samples and BSA).
7. Afterwards, wrap the microplate with an aluminum foil sheet in order to protect it from light, and wait for 10 min until reading.
8. Perform absorbance reading at 595 nm;
9. Obtain the mean of absorbances of each group (BSA and samples) and subtract them from the mean of blank absorbance.

10. In order to calculate protein concentration from the standard curve, one must consider that x = protein concentration, in mg/mL and y = absorbance. The construction of a graph relating each concentration of the BSA solution to its respective absorbance makes a linear equation (y = ax + b), where it is possible to obtain a factor from the inverse of a (factor = 1/a). In this way, multiply in a direct way the absorbance of each sample by the factor, which will result in the concentration of soluble protein in mg/mL.
11. Due to the high zebrafish larval mass utilized, perhaps the protein level of the samples will be superior to those ones determined with the BSA standard curve. In this case, it is necessary to dilute the samples until the protein levels fit in the detection limit of the assay (*see* **Note 6**). The number of dilutions must be included in the calculation of the proteins: *mean of absorbances x factor x number of dilutions*

3.3 Determination of aminotransferases (ALT and AST)

1. Thaw the samples intended for ALT and AST determinations in ice bath.
2. With a multichannel micropipette, pipette 100 µL of the reaction solution in each well of the 96 well clear flat bottom UV-transparent microplate (quadruplicate) and keep them at room temperature during 5 minutes.
3. In the first column, add 10 µL of distilled water to each well (blank).
4. Pipette 10 µL of each sample in each well of the other columns.
5. Homogenize the content in the wells by gently patting the plate on one of its sides, or placing the plate in a shaker, waiting for 1 minute until reading.
6. Do the reading at 340 nm, in 1 minute interval during 10 minutes.

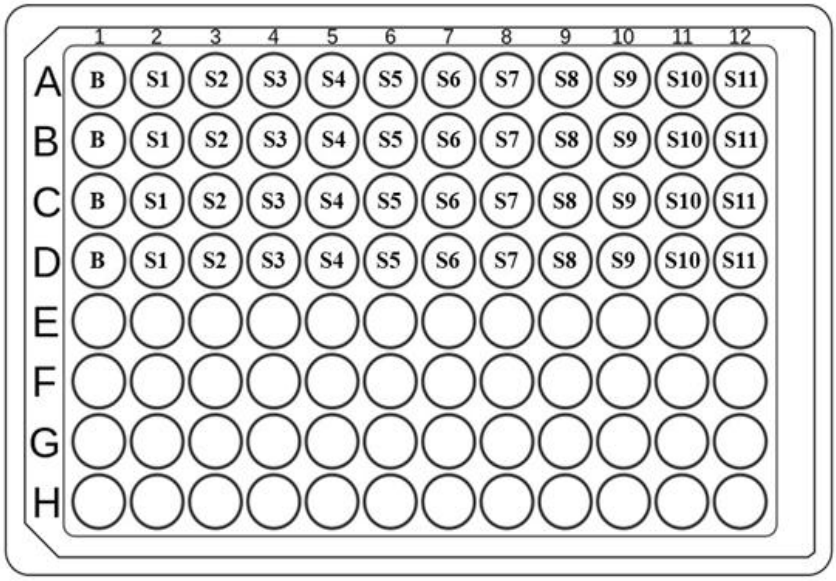

Figure 2 – Schematic representation of the plate utilized for determination of activity of biomarkers of liver damage. B – blank, S (1 – 11) – samples.

7. Calculate the variation of absorbance per minute during reading time with the following formula:

$$\Delta\text{ABS} = \frac{x - y}{10\ min}$$

- Initial reading: x
- Final reading: y

8. Afterwards, use this value to calculate ALT and AST activities in µmoL/min/mg of protein utilizing the following equation:

$$\text{Activity} = \frac{\left(\Delta\text{ABS}_{\text{sample}} - \Delta\text{ABS}_{\text{blank}}\right) * \text{Vt/Vs}}{\text{Prot} * \varepsilon * \text{d}} * 1000$$

Where:

- $\Delta\text{ABS}_{\text{sample}}$ is the variation of absorbance of samples per minute during reading time;

- ΔABS_{blank} is the variation of absorbance of blank per minute during reading time;
- Vt/Vs (Total volume/volume of samples) is the dilution factor of samples in the well content (here, 110 µL/ 10 µL);
- Pro tis the total protein content in samples in mg/mL;
- ε is NADH molar extinction coefficient (6.22 mM/cm) at 340 nm;
- d is the length that light covered (path length, in this case ≈ 0.33 cm).
- 1000 is used to convert mM in µmoL and it can express enzyme activity in µmoL/min/mg of protein.

3.4 Alcaline phosphatase (ALP) determination

1. Thaw samples directed to ALP determination in ice bath
2. In a 96 well clear flat bottom UV-transparent microplate:
3. With a multichannel micropipette, pipette 250 µL of the reaction solution in each well (quadruplicate) and keep them at room temperature during 5 minutes.
4. In the first column, add 5 µL of distilled water to each well (blank).
5. Pipette 5 µL of each sample in each well of the other columns.
6. Homogenize the content in the wells by gently patting the plate on one of its sides, or placing the plate in a shaker, waiting for 1 minute until reading.
7. Do the reading at 405 nm, in 2.5 minutes interval during 10 minutes.
8. Calculate variation of absorbance per minute according to item 5 of topic 3.3.
9. Calculate ALP activity in µmoL/min/mg according to item 6 of topic 3.3, making the following modifications: Vt/Vs (255 µL/ 5 µL); ε is *p*-Nitrophenol molar extinction coefficient (18,45 mM/ cm) at 405 nm; d (≈ 0.76 cm).

3.5 Lactate dehydrogenase determination

1. Thaw samples intended for LDH determination in ice bath.
2. In a 96 well clear flat bottom UV-transparent microplate:
3. In the first column, add 24.2 µL of distilled water to each well (blank).
4. In the other columns, pipette 24.2 µL of each sample in each well of these columns in quadruplicate.
5. With a multichannel pipette, add 24.2 µL of the pyruvate solution in all wells (blank and samples).

6. Add 151.5 µL of the NADH solution in all wells and send the microplate for reading
7. Perform the reading at 340 nm, in 20 s intervals during 5 minutes;
8. Calculate variation of absorbance per minute according to item 5 of topic 3.3 (reading time: 5 min).
9. Calculate LDH activity in µmoL/min/mg according to item 6 of topic 3.3, making the following changes: Vt/Vs (200 µL/ 24.2 µL); ε is NADH molar extinction coefficient (6.22 mM/cm^{-1}) at 340 nm; d (≈ 0.6 cm).

3.6 Glutathione peroxidase determination

1. Thaw samples destined for GPx determination in ice bath.
2. In a 96 well clear flat bottom UV-transparent microplate:
3. In the first column, pipette 10 µL of distilled water in each well (blank).
4. Pipette10 µL of sample at the bottom of each well, in quadruplicate.
5. Using a multichannel pipette, add 200 µL of the assay solution to each well.
6. Homogenize the content in the wells by gently patting the plate on one of its sides, or placing the plate in a shaker, at room temperature, during 5 minutes.
7. Add 10 µL of the NADPH solution in all wells. Perform the first kinetic reading at 340 nm until the absorbance curve is stabilized (approximately 5 min).
8. Remove the plate from the reader and add 10 µL of the hydrogen peroxide (H2O2) solution to each well (see Note 7).
9. Do the second kinetic reading at 340 nm, in 30 s intervals during 10 minutes.
10. Calculate the variation of absorbance per minute according to item 5 of topic 3.3.
11. Calculate GPx activity in µmoL/min/mg according to item 6 of topic 3.3, making the following modifications: Vt/Vs (230 µL/10 µL); ε is NADPH molar extinction coefficient (6.22 mM/cm) at 340 nm (d ≈ 0.7 cm).

Notes

1. The solutions of this assay are in accordance with the instructions of spectrophotometry diagnosis kit (Doles, Goiás, Brazil), which is based on the method described by Keiding *et al.* [10]. Kit instructions point to the following adaptations in relation to the original methodology: difference in the methodology of manufacture of solutions, change in the concentration of reagents and absence of EDTA in the buffer.

2. The method described by Keiding *et al.* [10] uses malate dehydrogenase (1,100 U/mg) and desidrogenase (500 U/mg) from pig heart and muscle, respectively. In this work, we suggest the use of more concentrated stock solutions in order to facilitate the dilution process. Other commercial solutions might be used, however the calculations must be adjusted in order to ensure the necessary concentration of the enzymes in the reaction solution.
3. In the method described by Keiding *et al.* [10], the diethanolamine buffer contains 0.5 mmol/L $MgCl_2$. However, this chemical compound is not described in the instructions of the spectrophotometry diagnosis kit, and, therefore, is not listed in this work.
4. Maceration should take place until the amount of larvae debris suspended in the solution is as small as possible (at least 2 minutes per microtube). Moreover, after maceration of each sample, the pestles must be replaced or cleansed with distilled water and dried with paper towel.
5. The cited volumes are higher than those needed in order to perform the essays in quadruplicates. This was thought in case there is the need to repeat the reading due to any technical error.
6. If it is necessary to dilute the samples in order to determine the protein levels, transfer an aliquot of the original microtube and make the dilution in another microtube.
7. Addition of NADH and H_2O_2 to the microplate wells will initiate the reaction. Thus, for a better standardization of reading it is recommended that these reagents be added with the smallest interval time possible in the technical replicates. The microplate must be sent to the microplate reader as soon as possible.

Acknowledgments

We thank to Universidade Federal da Paraíba (UFPB, Brazil), Fundação de Apoio à Pesquisa do Estado da Paraíba (FAPESQ, Brazil), Coordenação de Aperfeiçoamento de Pessoal de Nível Superior (CAPES, Brazil) and Conselho Nacional de Desenvolvimento Científico e Tecnológico (CNPq, Brazil) for supporting this research with grants and scholarships.

Funding

This work was supported by the Public Call n. 03 Produtividade em Pesquisa PROPESQ/PRPG/UFPB, João Pessoa, Brazil [grant number PVA13245-2020]; and the Public Call Demanda Universal FAPESQ, Campina Grande, Brazil [grant number 3045/2021].

APÊNDICE B - MATERIAL SUPLEMENTAR REFERENTE AO ARTIGO 2

Supplementary figure 1. 2D representation of the interactions between 2,4-D and amino acid residues of potential target proteins.

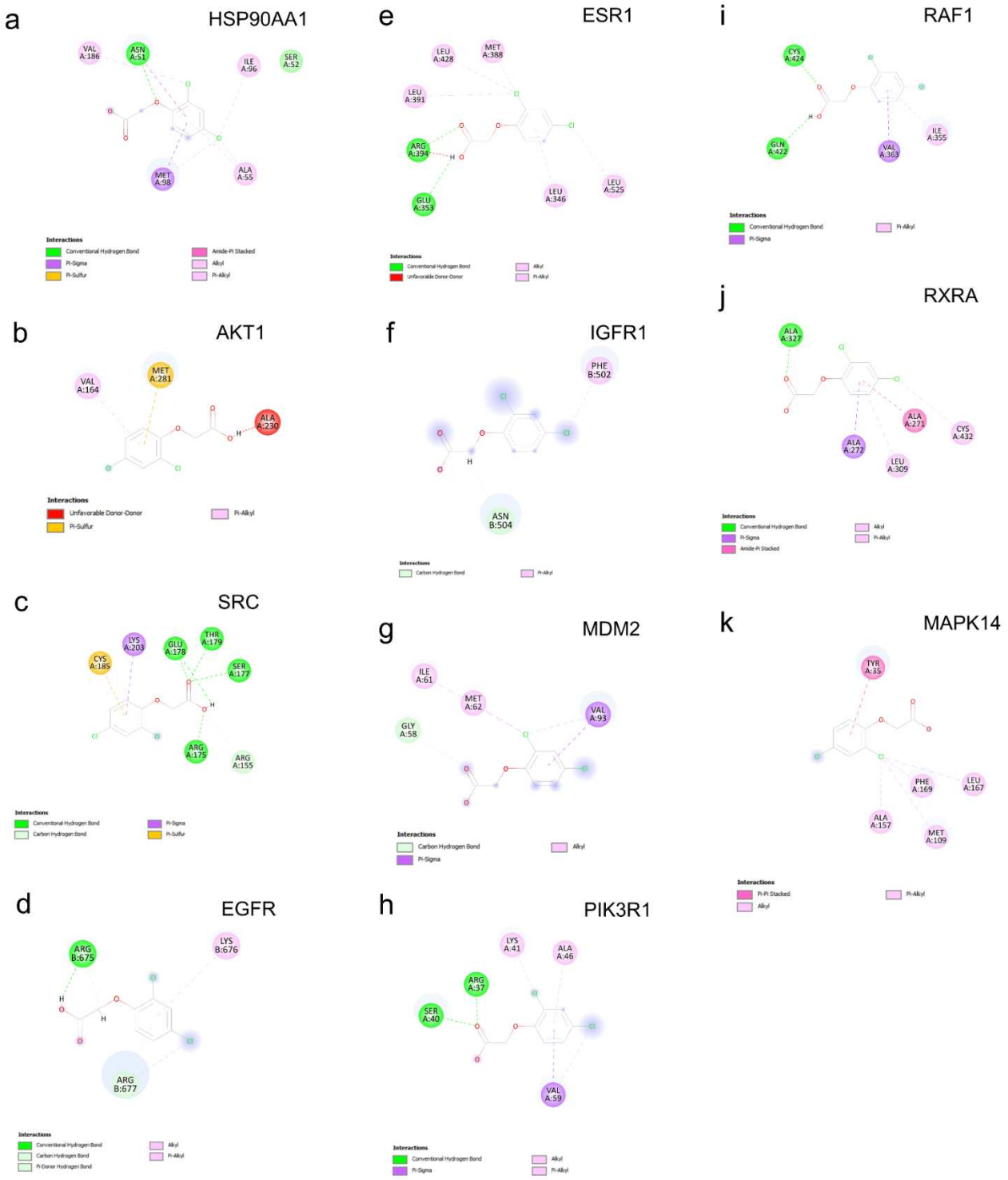

Supplementary figure 2. 2D representation of the interactions between 2,4-DCP and amino acid residues of potential target proteins.

Supplementary figure 3. 2D representation of the interactions between the proteins and their respective positive control ligands, highlighting the amino acid residues.

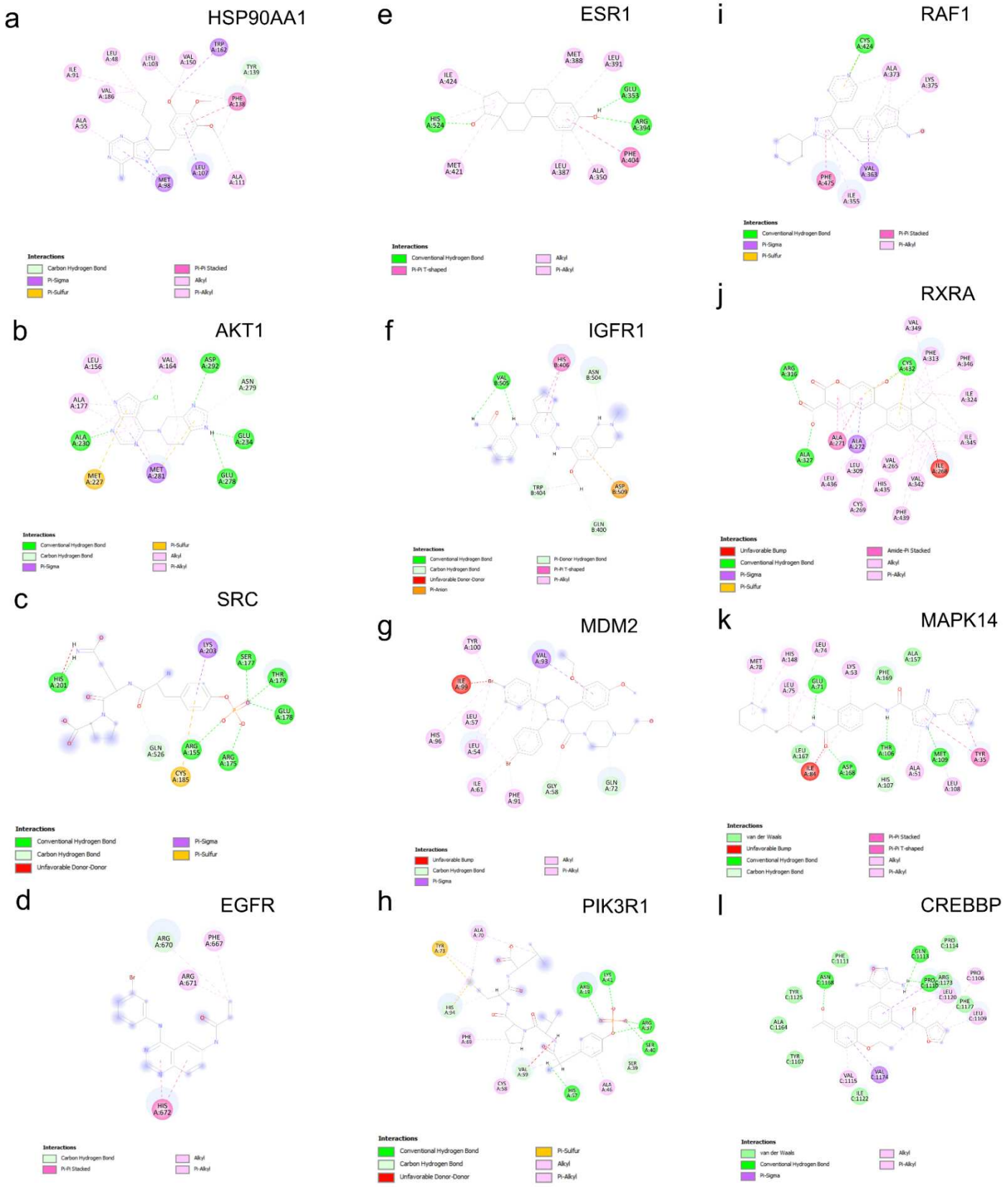

Supplementary Table 1. PDB IDs, resolutions, and organisms of proteins used in molecular docking analysis.

Target protein	Ligand (IUPAC name)	Abbreviation	PubChem CID	Function
HSP90AA1	9-butyl-8-[(3,4,5-trimethoxyphenyl)methyl]purin-6-amine	PU3	448965	Antagonist
RXRA	7-hydroxy-2-oxo-6-(3,5,5,8,8-pentamethyl-6,7-dihydronaphthalen-2-yl)chromene-3-carboxylic acid	WY5	131750108	-
EGFR	4-[(3-Bromophenyl)amino]-6-acrylamidoquinazoline	PD168393	4708	Antagonist
SRC	N-(5-chloro-1,3-benzodioxol-4-yl)-7-[2-(4-methylpiperazin-1-yl)ethoxy]-5-(oxan-4-yloxy)quinazolin-4-amine	H8H	10302451	Antagonist
AKT1	5-chloro-4-(3,4,6,7-tetrahydroimidazo[4,5-c]pyridin-5-yl)-7H-pyrrolo[2,3-d]pyrimidine	CQW	24798742	Antagonist
PIK3R1	Phosphopeptide from beta-platelet-derived growth factor receptor	PGFRB	472408796	Agonist
ESR1	(8R,9S,13S,14S,17S)-13-methyl-6,7,8,9,11,12,14,15,16,17-decahydrocyclopenta[a]phenanthrene-3,17-diol	EST	5757	Agonist
RAF1	(NE)-N-[5-(1-piperidin-4-yl-3-pyridin-4-ylpyrazol-4-yl)-2,3-dihydroinden-1-ylidene]hydroxylamine	SM5	11653652	Antagonist
IGF1R	2-fluoro-6-[[2-[(6-methoxy-2-methyl-3,4-dihydro-1H-isoquinolin-7-yl)amino]-7H-pyrrolo[2,3-d]pyrimidin-4-yl]amino]benzamide	-	59442083	Antagonist
MDM2	[(4S,5R)-4,5-bis(4-bromophenyl)-2-(2-ethoxy-4-methoxyphenyl)-4,5-dihydroimidazol-1-yl]-[4-(2-hydroxyethyl)piperazin-1-yl]methanone	IMZ	5288631	Antagonist
MAPK14	5-amino-N-[[4-(3-cyclohexylpropylcarbamoyl)phenyl]methyl]-1-phenylpyrazole-4-carboxamide	SR-318	139030333	Antagonist
CREBBP	N-[3-(5-acetyl-2-ethoxyphenyl)-5-(3-amino-5-methyl-1,2-oxazol-4-yl)phenyl]furan-2-carboxamide	JGK	145997892	-

Supplementary Table 2. Information on ligands used as positive controls in docking analysis.

Target	PDB ID	Resolution	Organism
HSP90AA1	1UY6	1.90 Å	*Homo sapiens*
RXRA	6JNR	2.30 Å	*Homo sapiens*
EGFR	2M0B	NMR (model 1)	*Homo sapiens*
SRC	2H8H	2.20 Å	*Homo sapiens*
AKT1	3CQW	2.00 Å	*Homo sapiens*
PIK3R1	1H9O	1.79 Å	*Homo sapiens*
ESR1	1A52	2.80 Å	*Homo sapiens*
RAF1	3OMV	4.00 Å	*Homo sapiens*
IGF1R	7V3P	3.60 Å	*Homo sapiens*
MDM2	1RV1	2.30 Å	*Homo sapiens*
MAPK14	6SFO	1.75 Å	*Homo sapiens*
CREBBP	6QST	2.10 Å	*Homo sapiens*

Suplementary table 3. Gridbox xyz coordinates for molecular docking of 2,4-D and 2,4-DCP with core targets from the PPI network.

	Center Grid Box (xyz Coordinates)		
Target proteins	X	Y	Z
HSP90AA1	13.40	11.18	24.85
RXRA	28.31	18.53	-4.80
EGFR	-0.71	-23.43	-10.53
SRC	29.51	47.29	87.71
CREBBP	19.07	40.08	-20.17
AKT1	5.99	3.01	17.34
PIK3R1	14.85	9.57	20.78
ESR1	106.73	15.02	96.62
RAF1	7.19	16.79	32.93
IGF1R	155.89	190.23	174.45
MDM2	9.80	7.53	13.11
MAPK14	1.32	1.11	-18.53

Supplementary Table 4. Potential targets of 2,4-D and 2,4-DCP linked to hepatotoxicity

2,4-D targets

Target	Protein name
SOD2	Superoxide Dismutase 2
FGFR1	Fibroblast Growth Factor Receptor 1
MET	MET Proto-Oncogene, Receptor Tyrosine Kinase
HNMT	Histamine N-Methyltransferase
ELANE	Elastase, Neutrophil Expressed
TEK	TEK Receptor Tyrosine Kinase
MAOA	Monoamine Oxidase A
GRB2	Growth Factor Receptor Bound Protein 2
SHBG	Sex Hormone Binding Globulin
RARB	Retinoic Acid Receptor Beta
GSTP1	Glutathione S-Transferase Pi 1
AURKA	Aurora Kinase A
NR1I3	Nuclear Receptor Subfamily 1 Group I Member 3
GC	GC Vitamin D Binding Protein
FYN	FYN Proto-Oncogene, Src Family Tyrosine Kinase
KIT	KIT Proto-Oncogene, Receptor Tyrosine Kinase
TACR2	Tachykinin Receptor 2
JAK2	Janus Kinase 2
F2	Coagulation Factor II, Thrombin
CYP2C9	Cytochrome P450 Family 2 Subfamily C Member 9
CA5A	Carbonic Anhydrase 5A
ESR1	Estrogen Receptor 1
TYMS	Thymidylate Synthetase
ITK	IL2 Inducible T Cell Kinase
CCNA2	Cyclin A2
GSK3B	Glycogen Synthase Kinase 3 Beta
PPARD	Peroxisome Proliferator Activated Receptor Delta
MMP3	Matrix Metallopeptidase 3
MAPK1	Mitogen-Activated Protein Kinase 1
MDM2	Murine double minute 2
AKT2	AKT Serine/Threonine Kinase 2
EGFR	Epidermal Growth Factor Receptor
PDE5A	Phosphodiesterase 5A
MAPK8	Mitogen-Activated Protein Kinase 8
F10	Coagulation Factor X
MTAP	Methylthioadenosine Phosphorylase
AKR1B1	Aldo-Keto Reductase Family 1 Member B
HSP90AB1	Heat Shock Protein 90 Alpha Family Class B Member 1
SRC	SRC Proto-Oncogene, Non-Receptor Tyrosine Kinase
CDK2	Cyclin Dependent Kinase 2
PGR	Progesterone Receptor
SEC14L2	SEC14 Like Lipid Binding 2
THRA	Thyroid Hormone Receptor Alpha

CA3	Carbonic Anhydrase 3
PIK3R1	Phosphoinositide-3-Kinase Regulatory Subunit 1
ALB	Albumin
YARS1	Tyrosyl-TRNA Synthetase 1
ESR2	Estrogen Receptor 2
BRAF	B-Raf Proto-Oncogene, Serine/Threonine Kinase
EPHB4	EPH Receptor B4
ERBB4	Erb-B2 Receptor Tyrosine Kinase 4
SLC6A2	Solute Carrier Family 6 Member 2
GSTA1	Glutathione S-Transferase Alpha 1
MMP13	Matrix Metallopeptidase 13
RXRA	Retinoid X Receptor Alpha
NR1H3	Nuclear Receptor Subfamily 1 Group H Member 3
DPP4	Dipeptidyl Peptidase 4
PLA2G2A	Phospholipase A2 Group IIA
PPARG	Peroxisome Proliferator Activated Receptor Gamma
NR3C1	Nuclear Receptor Subfamily 3 Group C Member 1
MAPK14	Mitogen-Activated Protein Kinase 14
LCK	LCK Proto-Oncogene, Src Family Tyrosine Kinase
NR1H2	Nuclear Receptor Subfamily 1 Group H Member 2
TBXAS1	Thromboxane A Synthase 1
SULT2A1	Sulfotransferase Family 2A Member 1
PPIA	Peptidylprolyl Isomerase A
CASP7	Caspase 7
ACHE	Acetylcholinesterase
CASP3	Caspase 3
HSP90AA1	Heat Shock Protein 90 Alpha Family Class A Member 1
CA7	Carbonic Anhydrase 7
PARP1	Poly(ADP-Ribose) Polymerase 1
VDR	Vitamin D Receptor
KDR	Kinase Insert Domain Receptor
PTPN1	Protein Tyrosine Phosphatase Non-Receptor Type 1
RORA	RAR Related Orphan Receptor A
TTR	Transthyretin
MAOB	Monoamine Oxidase B
BACE1	Beta-Secretase 1
RBP4	Retinol Binding Protein 4
ADK	Adenosine Kinase
CA2	Carbonic Anhydrase 2
NR1H4	Nuclear Receptor Subfamily 1 Group H Member 4
RARG	Retinoic Acid Receptor Gamma
MIF	Macrophage Migration Inhibitory Factor
MAP2K1	Mitogen-Activated Protein Kinase Kinase 1
HSD11B1	Hydroxysteroid 11-Beta Dehydrogenase 1
NR1I2	Nuclear Receptor Subfamily 1 Group I Member 2
TTPA	Alpha Tocopherol Transfer Protein
AR	Androgen Receptor
IGF1	Insulin Like Growth Factor 1
MMP7	Matrix Metallopeptidase 7

NOS2	Nitric Oxide Synthase 2
NMNAT1	Nicotinamide Nucleotide Adenylyltransferase 1
BHMT	Betaine--Homocysteine S-Methyltransferase
GMPR	Guanosine Monophosphate Reductase
ADH5	Alcohol Dehydrogenase 5 (Class III), Chi Polypeptide
BCHE	Butyrylcholinesterase
MMP16	Matrix Metallopeptidase 16
GCK	Glucokinase
ALAD	Aminolevulinate Dehydratase
F7	Coagulation Factor VII
CAPN1	Calpain 1
MAPK10	Mitogen-Activated Protein Kinase 10
HSPA8	Heat Shock Protein Family A (Hsp70) Member 8
DHFR	Dihydrofolate Reductase
BTK	Bruton Tyrosine Kinase
CTSB	Cathepsin B
PFKFB1	6-Phosphofructo-2-Kinase/Fructose-2,6-Biphosphatase 1
RAB5A	RAB5A, Member RAS Oncogene Family
CASP1	Caspase 1
HCAR2	Hydroxycarboxylic Acid Receptor 2
XIAP	X-Linked Inhibitor Of Apoptosis
PTGS2	Prostaglandin-Endoperoxide Synthase 2
CBS	Cystathionine Beta-Synthase
ADH1C	Alcohol Dehydrogenase 1C (Class I), Gamma Polypeptide
CSNK2A2	Casein Kinase 2 Alpha 2
HRAS	HRas Proto-Oncogene, GTPase
ITGB2	Integrin Subunit Beta 2
APEX1	Apurinic/Apyrimidinic Endodeoxyribonuclease 1
ARSA	Arylsulfatase A
CHIT1	Chitinase 1
FOXO1	Forkhead Box O1
MMP1	Matrix Metallopeptidase 1
STAT1	Signal Transducer And Activator Of Transcription 1
MMP12	Matrix Metallopeptidase 12
HMGCR	3-Hydroxy-3-Methylglutaryl-CoA Reductase
GSR	Glutathione-Disulfide Reductase
EIF2AK2	Eukaryotic Translation Initiation Factor 2 Alpha Kinase 2
HMOX1	Heme Oxygenase 1
GLO1	Glyoxalase I
ACADM	Acyl-CoA Dehydrogenase Medium Chain
LGALS7	Galectin 7
MMP8	Matrix Metallopeptidase 8
CTNNA1	Catenin Alpha 1
GSTM1	Glutathione S-Transferase Mu 1
CAPN2	Calpain 2
CREB1	CAMP Responsive Element Binding Protein 1
LGALS3	Galectin 3
KYAT1	Kynurenine Aminotransferase 1
BCAT2	Branched Chain Amino Acid Transaminase 2

GPR35	G Protein-Coupled Receptor 35
DPEP1	Dipeptidase 1
FABP6	Fatty Acid Binding Protein 6
MAN1B1	Mannosidase Alpha Class 1B Member 1
FECH	Ferrochelatase
ARG2	Arginase 2
PRKCQ	Protein Kinase C Theta
ADAM17	ADAM Metallopeptidase Domain 17
OTC	Ornithine Transcarbamylase
REN	Renin
AGXT	Alanine--Glyoxylate Aminotransferase
AKR1A1	Aldo-Keto Reductase Family 1 Member A1
FABP2	Fatty Acid Binding Protein 2
CSNK2A1	Casein Kinase 2 Alpha 1
ITGAL	Integrin Subunit Alpha L
ALPL	Alkaline Phosphatase, Biomineralization Associated
TGFB2	Transforming Growth Factor Beta 2
PLAU	Plasminogen Activator, Urokinase
RAC1	Rac Family Small GTPase 1
SLC6A4	Solute Carrier Family 6 Member 4
EPHA2	EPH Receptor A2
CHEK1	Checkpoint Kinase 1
TAP1	Transporter 1, ATP Binding Cassette Subfamily B Member
NOTUM	Notum, Palmitoleoyl-Protein Carboxylesterase
SERPINA1	Serpin Family A Member 1
AHCY	Adenosylhomocysteinase
SELE	Selectin E
CPB2	Carboxypeptidase B2
F11	Coagulation Factor XI
CSK	C-Terminal Src Kinase
RAF1	Raf-1 Proto-Oncogene, Serine/Threonine Kinase
CCR2	C-C Motif Chemokine Receptor 2
SULT1A1	Sulfotransferase Family 1A Member 1
APAF1	Apoptotic Peptidase Activating Factor 1
ARG1	Arginase 1
PCK1	Phosphoenolpyruvate Carboxykinase 1
TGFBR1	Transforming Growth Factor Beta Receptor 1
CDC42	Cell Division Cycle 42
HSPA1A	Heat Shock Protein Family A (Hsp70) Member 1A
EPHX2	Epoxide Hydrolase 2
CLK1	CDC Like Kinase 1
ACE	Angiotensin I Converting Enzyme
RARA	Retinoic Acid Receptor Alpha
PPARA	Peroxisome Proliferator Activated Receptor Alpha
CTSG	Cathepsin G
PYGL	Glycogen Phosphorylase L
FABP1	Fatty Acid Binding Protein 1
RNASE3	Ribonuclease A Family Member 3
PIK3CG	Phosphatidylinositol-4,5-Bisphosphate 3-Kinase Catalytic Subunit Gamma

NQO1	NAD(P)H Quinone Dehydrogenase 1
CYP3A7	Cytochrome P450 Family 3 Subfamily A Member 7
KDM4C	Lysine Demethylase 4C
IL2	Interleukin 2
HADH	Hydroxyacyl-CoA Dehydrogenase
IGF1R	Insulin Like Growth Factor 1 Receptor
ICAM1	Intercellular Adhesion Molecule 1
BCL2L1	BCL2 Like 1
HPRT1	Hypoxanthine Phosphoribosyltransferase 1
LTF	Lactotransferrin
SORD	Sorbitol Dehydrogenase
NOS3	Nitric Oxide Synthase 3
CYP2C8	Cytochrome P450 Family 2 Subfamily C Member 8
INSR	Insulin Receptor
ADH1B	Alcohol Dehydrogenase 1B (Class I), Beta Polypeptide
FABP4	Fatty Acid Binding Protein 4
AKT1	AKT Serine/Threonine Kinase 1
LCN2	Lipocalin 2
PTGS1	Prostaglandin-Endoperoxide Synthase 1
F3	Coagulation Factor III, Tissue Factor
ATIC	5-Aminoimidazole-4-Carboxamide Ribonucleotide Formyltransferase/IMP Cyclohydrolase
AMD1	Adenosylmethionine Decarboxylase 1
PAH	Phenylalanine Hydroxylase
S100A9	S100 Calcium Binding Protein A9
PMS2	PMS1 Homolog 2, Mismatch Repair System Component
MMP9	Matrix Metallopeptidase 9

2,4-DCP targets

Target	Protein name
SOD2	Superoxide Dismutase 2
FGFR1	Fibroblast Growth Factor Receptor 1
MET	MET Proto-Oncogene, Receptor Tyrosine Kinase
HNMT	Histamine N-Methyltransferase
ELANE	Elastase, Neutrophil Expressed
TEK	TEK Receptor Tyrosine Kinase
MAOA	Monoamine Oxidase A
GRB2	Growth Factor Receptor Bound Protein 2
SHBG	Sex Hormone Binding Globulin
RARB	Retinoic Acid Receptor Beta
GSTP1	Glutathione S-Transferase Pi 1
AURKA	Aurora Kinase A
NR1I3	Nuclear Receptor Subfamily 1 Group I Member 3
GC	GC Vitamin D Binding Protein
FYN	FYN Proto-Oncogene, Src Family Tyrosine Kinase
KIT	KIT Proto-Oncogene, Receptor Tyrosine Kinase

TACR2	Tachykinin Receptor 2
JAK2	Janus Kinase 2
F2	Coagulation Factor II, Thrombin
CYP2C9	Cytochrome P450 Family 2 Subfamily C Member 9
CA5A	Carbonic Anhydrase 5A
ESR1	Estrogen Receptor 1
TYMS	Thymidylate Synthetase
ITK	IL2 Inducible T Cell Kinase
CCNA2	Cyclin A2
GSK3B	Glycogen Synthase Kinase 3 Beta
PPARD	Peroxisome Proliferator Activated Receptor Delta
MMP3	Matrix Metallopeptidase 3
MAPK1	Mitogen-Activated Protein Kinase 1
MDM2	Murine double minute 2
AKT2	AKT Serine/Threonine Kinase 2
EGFR	Epidermal Growth Factor Receptor
PDE5A	Phosphodiesterase 5A
MAPK8	Mitogen-Activated Protein Kinase 8
F10	Coagulation Factor X
MTAP	Methylthioadenosine Phosphorylase
AKR1B1	Aldo-Keto Reductase Family 1 Member B
HSP90AB1	Heat Shock Protein 90 Alpha Family Class B Member 1
SRC	SRC Proto-Oncogene, Non-Receptor Tyrosine Kinase
CDK2	Cyclin Dependent Kinase 2
PGR	Progesterone Receptor
SEC14L2	SEC14 Like Lipid Binding 2
THRA	Thyroid Hormone Receptor Alpha
CA3	Carbonic Anhydrase 3
PIK3R1	Phosphoinositide-3-Kinase Regulatory Subunit 1
ALB	Albumin
YARS1	Tyrosyl-TRNA Synthetase 1
ESR2	Estrogen Receptor 2
BRAF	B-Raf Proto-Oncogene, Serine/Threonine Kinase
EPHB4	EPH Receptor B4
ERBB4	Erb-B2 Receptor Tyrosine Kinase 4
SLC6A2	Solute Carrier Family 6 Member 2
GSTA1	Glutathione S-Transferase Alpha 1
MMP13	Matrix Metallopeptidase 13
RXRA	Retinoid X Receptor Alpha
NR1H3	Nuclear Receptor Subfamily 1 Group H Member 3
DPP4	Dipeptidyl Peptidase 4
PLA2G2A	Phospholipase A2 Group IIA
PPARG	Peroxisome Proliferator Activated Receptor Gamma
NR3C1	Nuclear Receptor Subfamily 3 Group C Member 1
MAPK14	Mitogen-Activated Protein Kinase 14
LCK	LCK Proto-Oncogene, Src Family Tyrosine Kinase
NR1H2	Nuclear Receptor Subfamily 1 Group H Member 2
TBXAS1	Thromboxane A Synthase 1
SULT2A1	Sulfotransferase Family 2A Member 1

PPIA	Peptidylprolyl Isomerase A
CASP7	Caspase 7
ACHE	Acetylcholinesterase
CASP3	Caspase 3
HSP90AA1	Heat Shock Protein 90 Alpha Family Class A Member 1
CA7	Carbonic Anhydrase 7
PARP1	Poly(ADP-Ribose) Polymerase 1
VDR	Vitamin D Receptor
KDR	Kinase Insert Domain Receptor
PTPN1	Protein Tyrosine Phosphatase Non-Receptor Type 1
RORA	RAR Related Orphan Receptor A
TTR	Transthyretin
MAOB	Monoamine Oxidase B
BACE1	Beta-Secretase 1
RBP4	Retinol Binding Protein 4
ADK	Adenosine Kinase
CA2	Carbonic Anhydrase 2
NR1H4	Nuclear Receptor Subfamily 1 Group H Member 4
RARG	Retinoic Acid Receptor Gamma
MIF	Macrophage Migration Inhibitory Factor
MAP2K1	Mitogen-Activated Protein Kinase Kinase 1
HSD11B1	Hydroxysteroid 11-Beta Dehydrogenase 1
NR1I2	Nuclear Receptor Subfamily 1 Group I Member 2
TTPA	Alpha Tocopherol Transfer Protein
AR	Androgen Receptor
SLC22A2	Solute Carrier Family 22 Member 2
PTPN22	Protein Tyrosine Phosphatase Non-Receptor Type 22
AHR	Aryl Hydrocarbon Receptor
CREBBP	CREB Binding Protein
PSMB8	Proteasome 20S Subunit Beta 8
IDO1	Indoleamine 2,3-Dioxygenase 1
FLT1	Fms Related Receptor Tyrosine Kinase 1
ALOX12	Arachidonate 12-Lipoxygenase, 12S Type
ERBB2	Erb-B2 Receptor Tyrosine Kinase 2
DRD4	Dopamine Receptor D4
TYR	Tyrosinase
SLC6A3	Solute Carrier Family 6 Member 3
RNASEH1	Ribonuclease H1
ALOX5	Arachidonate 5-Lipoxygenase
ADORA2A	Adenosine A2a Receptor
SLC47A1	Solute Carrier Family 47 Member 1
DRD2	Dopamine Receptor D2
HDAC2	Histone Deacetylase 2
OPRM1	Opioid Receptor Mu 1
TLR9	Toll Like Receptor 9
ERN1	Endoplasmic Reticulum To Nucleus Signaling 1
CES1	Carboxylesterase 1
HDAC6	Histone Deacetylase 6

Supplementary Table 5. Topological Measurements of PPI Network Nodes Based on Degree and Betweenness Centrality

Compound target	Node	Protein	Degree	Betweenness centrality
Both	HSP90AA1	Heat Shock Protein 90 Alpha Family Class A Member 1	15	0.308
Both	RXRA	Retinoid X Receptor Alpha	13	0.293
Both	EGFR	Epidermal growth factor receptor	14	0.126
Both	SRC	Proto-oncogene tyrosine kinase SRC	11	0.158
2,4-DCP	CREBBP	CREB Binding Protein	10	0.328
2,4-D	AKT1	AKT Serine/Threonine Kinase 1	9	0.214
Both	PIK3R1	Phosphatidylinositol 3-kinase regulatory subunit alpha	10	0.069
Both	ESR1	Estrogen Receptor 1	10	0.180
2,4-D	RAF1	Raf-1 Proto-Oncogene, Serine/Threonine Kinase	8	0.095
2,4-D	IGF1R	Insulin Like Growth Factor 1 Receptor	6	0.045
Both	MDM2	E3 ubiquitin-protein ligase Mdm2	5	0.087
Both	MAPK14	Mitogen-activated protein kinase 14	3	0.086
2,4-DCP	ADORA2A	Adenosine receptor A2a	1	0
2,4-DCP	DRD2	Dopamine D2 receptor	1	0
Both	F10	Coagulation factor X	1	0
Both	F2	Prothrombin	1	0
2,4-D	F3	Tissue factor	1	0

2,4-D	F7	Coagulation factor VII	1	0
2,4-D	ICAM1	Intercellular adhesion molecule 1	1	0
2,4-D	ITGAL	Integrin alpha-L	1	0
2,4-D	ITGB2	Integrin beta-2	1	0
Both	RBP4	Retinol-binding protein 4	1	0
Both	TTR	Transthyretin	1	0
Both	AR	Androgen receptor	4	0.050
2,4-D	HSPA8	Heat shock cognate 71 kDa protein 8	4	0.003
Both	NR3C1	Glucocorticoid receptor	2	0.022
2,4-DCP	ERBB2	Receptor tyrosine-protein kinase erbB-2	6	0.019
2,4-DCP	AHR	Aryl hydrocarbon receptor	3	0.001
2,4-D	FOXO1	Forkhead box protein O1	2	0.077
2,4-D	STAT1	Signal transducer and activator of transcription 1-alpha/beta	3	0.028
Both	CYP27B1	25-hydroxyvitamin D-1 alpha hydroxylase, mitochondrial	2	0.066
Both	HSP90AB1	Heat shock protein HSP 90-beta	6	0.0177
Both	PTPN1	Tyrosine-protein phosphatase non-receptor type 1	5	0.012
2,4-D	NOS3	Nitric oxide synthase 3	2	0.0
Both	BRAF	Serine/threonine-protein kinase B-raf	5	0.030
Both	FGFR1	Fibroblast growth factor receptor 1	2	0.010
2,4-DCP	HDAC6	Histone deacetylase 6	2	0.0
Both	JAK2	Tyrosine-protein kinase JAK2	3	0.001

2,4-D	CSK	Tyrosine-protein kinase CSK	3	0.028
2,4-D	CSNK2A1	Casein kinase II subunit alpha	3	0.056
Both	FYN	Tyrosine-protein kinase Fyn	2	0.0
Both	PPARG	Peroxisome proliferator-activated receptor gamma	2	0.0
Both	PGR	Progesterone receptor	1	0.0
Both	ESR2	Estrogen receptor beta	1	0.0
Both	GRB2	Growth factor receptor-bound protein 2	6	0.008
2,4-D	XIAP	E3 ubiquitin-protein ligase XIAP	4	0.046
Both	KDR	Vascular endothelial growth factor receptor 2	1	0.0
Both	CDK2	Cyclin-dependent kinase 2	2	0.028
2,4-D	CREB1	Cyclic AMP-responsive element-binding protein 1	1	0.0
Both	CASP3	Caspase-3	4	0.055
Both	ERBB4	Receptor tyrosine-protein kinase erbB-4	3	0.0
Both	GSK3B	Glycogen synthase kinase-3 beta	1	0.0
Both	AKT2	RAC-beta serine/threonine-protein kinase	1	0.0
Both	MET	Hepatocyte growth factor receptor	2	0.0
2,4-D	INSR	Insulin receptor	4	0.003
Both	MAPK1	Mitogen-activated protein kinase 1	3	0.005
Both	KIT	Mast/stem cell growth factor receptor Kit	2	0.0
Both	MAP2K1	Dual specificity mitogen-activated protein kinase kinase 1	3	0.0
2,4-D	IGF1	Insulin-like growth factor I	2	0.0

2,4-D	HRAS	GTPase HRas	3	0.028
2,4-D	RARA	Retinoic acid receptor alpha	3	0.028
Both	RARB	Retinoic acid receptor beta	2	0.0
Both	NR1H3	Oxysterols receptor LXR-alpha	2	0.0
2,4-D	PPARA	Peroxisome proliferator-activated receptor alpha	2	0.0
Both	NR1H2	Oxysterols receptor LXR-beta	1	0.0
Both	NR1H4	Bile acid receptor	1	0.0
Both	NR1I2	Nuclear receptor subfamily 1 group I member 2	1	0.0
Both	NR1I3	Nuclear receptor subfamily 1 group I member 3	1	0.0
Both	PPARD	Peroxisome proliferator-activated receptor delta	1	0.0
Both	THRA	Thyroid hormone receptor alpha	1	0.0
2,4-DCP	PTPN22	Tyrosine-protein phosphatase non-receptor type 22	1	0.0
2,4-DCP	HDAC2	Histone deacetylase 2	1	0.0
2,4-D	CSNK2A2	Casein kinase II subunit alpha'	1	0.0
Both	CASP7	Caspase-7	2	0.004
Both	DUSP16	Dual specificity protein phosphatase 16	2	0.056
Both	CCNA2	Cyclin-A2	1	0.0
Both	PARP1	Poly [ADP-ribose] polymerase 1	2	0.001
2,4-D	APAF1	Apoptotic protease-activating factor 1	1	0.0
2,4-D	PIK3CG	Phosphatidylinositol 4,5-bisphosphate 3-	1	0.0

		kinase catalytic subunit gamma isoform		
Both	RARG	Retinoic acid receptor gamma	1	0.0
Both	MAPK8	Mitogen-activated protein kinase 8	2	0.028
Both	GSTP1	Glutathione S-transferase P	1	0.0

Supplementary Table 6. Moldock and Rerank scores for proteins docked with 2,4-D, 2,4-DCP, and positive controls

Target proteins	Moldock score	Rerank score	Moldock score	Rerank score	Moldock score	Rerank score
HSP90AA1	-132,763	-110.191	-53,606	-45,201	-40,794	-35,548
RXRA	-149.974	-57.329	-78,734	-65,479	-58,023	-48,371
EGFR	-123.126	-97.785	-75,955	-60,531	-56,180	-46,169
SRC	-110.580	-81.140	-85,813	-72,217	-53,111	-45,195
CREBBP	-164.484	-137.488	-	-	-40,940	-34,748
AKT1	-105.415	-87.145	-63,422	-55,335	-	-
PIK3R1	-115.817	-77.277	-69,217	-57,024	-44,868	-38,370
ESR1	-102.457	-86.904	-61,294	-53,132	-47,411	-41,197
RAF1	-124.922	-92.759	-71,322	-57,255	-	-
IGF1R	-128.888	-74.714	-19,873	-16,755	-	-
MDM2	-137.335	-95.586	-38,404	-32,456	-25,292	-22,043
MAPK14	-172.344	-127.440	-72,146	-61,594	-55,489	-46,503

APÊNDICE C - MATERIAL SUPLEMENTAR REFERENTE AO ARTIGO 3

Supplementary figure 1. *In silico* workflow for identification of targets related to developmental toxicity and 2,4-DCP

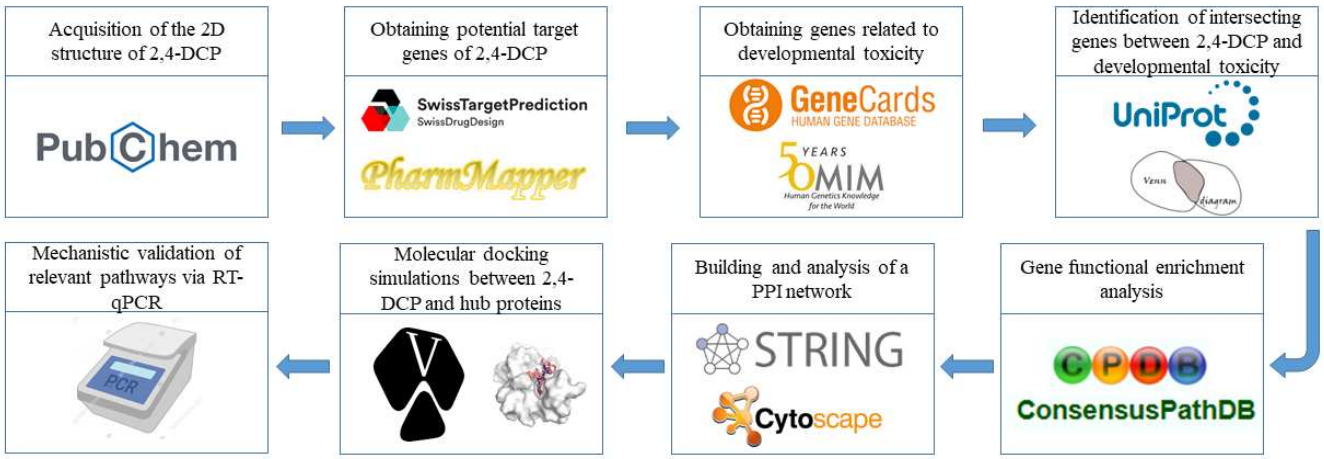

Supplementary Figure 2. 3D and 2D representations of molecular docking simulations between 2,4-DCP and potential target proteins.

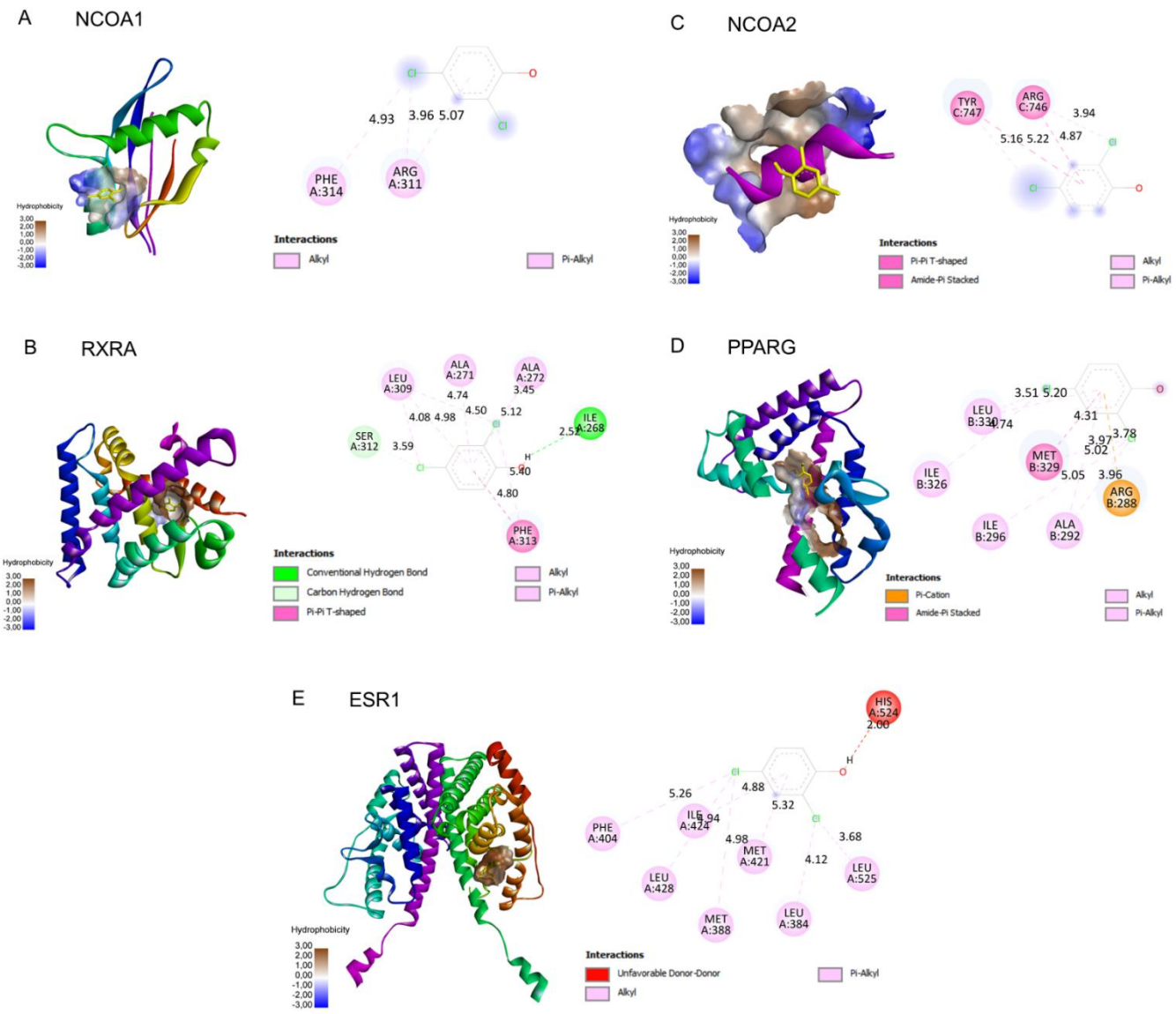

Supplementary table 1. Summary of structural characteristics of the proteins used in molecular docking analyses, including PDB ID, crystallographic resolution, source organism, and spatial (XYZ) coordinates.

Gene	Gene name	PDB ID	Resolution	Organism	Coordinates		
					X	Y	Z
NCOA1	Nuclear Receptor Coactivator 1	5NWX	2.51 Å	*Mus musculus*	-16.75	15.94	-5.48
RXRA	Retinoid X Receptor Alpha	6SJM	2.52 Å	*Homo sapiens*	18,37	3.96	23.03
NCOA2	Nuclear Receptor Coactivator 2	3GN8	2.50 Å	*Homo sapiens*	-28.01	-28.20	-21.88
ESR1	Estrogen Receptor 1	1A52	2.80 Å	*Homo sapiens*	106.25	17.46	97.95
PPARG	Peroxisome Proliferator Activated Receptor Gamma	8B8Y	2.00 Å	*Homo sapiens*	-0,20	19,80	37,91

Supplementary Table 2. Information about positive controls used in docking analysis.

Target	Control	Abbreviation	PubChem CID	Function
NCOA1	Signal transducer and activator of transcription 6 (peptide)	STAT6	-	Coactivator
RXRA	2-[4-[3,5-bis(trifluoromethyl)phenyl]phenyl]acetic acid	LFZ	23005221	Agonist
NCOA2	2-(2,4-dichlorophenoxy)acetic acid	2,4-D	1486	-
ESR1	(8R,9S,13S,14S,17S)-13-methyl-6,7,8,9,11,12,14,15,16,17-decahydrocyclopenta[a]phenanthrene-3,17-diol	EST	5757	Agonist
PPARG	1-N-benzyl-4,5-dichloro-3-N-phenylbenzene-1,3-dicarboxamide	-	166175736	Inverse agonist

Suplementary Table 3. Gene functions and primers details

Gene	Function	Primer Sequence (5' – 3') Forward (F) and Reverse (R)	Amplicon size	Reference or Gene sequence
akt1	Regulates cell cycle, apoptosis, metabolism, and stress response.	F: AAGAAGTTGGTTCCTCCGTTCAAG R: ATGTGGTCGTCTCTCGCTGTC	150	10.1016/j.bcp.2025.116752
esr1	Estrogen receptor regulating gene expression and reproductive functions.	F: GGCTGGAGGTGTTGATGATT R: CGCATTCTCCTTCACTCCTATC	105	10.1002/etc.5732
ppara	Regulation of fatty acid oxidation and lipid metabolism.	F: ACATGGAGACTCTTCAGCTGGC R: AGTCGAGGTTTGAGAATCCGGG	183	10.1016/j.scitotenv.2024.175525
pparb	Regulation of lipid metabolism, inflammation, and cell differentiation.	F: TGGAGTACGAGCGATGTGAG R: TAGTCCAGCCACCAGCTTCT	164	XM_068222866.1
pparg	Involved in adipocyte differentiation, lipid metabolism, and glucose homeostasis.	F: GTAGATGGGCTCGTGTGTCC R: CCTTCTCCACGCTCGACTAC	149	NM_131467.1
shha	Organ development, chordate embryonic development, and neurogenesis.	F: TTCGGTTGCTGCGAAATCTGG R: CGTCGCGTCGTGGAGTCTC	183	XM_068222866.1
b-actin	Predicted to be a structural constituent of the postsynaptic actin cytoskeleton.	F: CTGTTCCAGCCATCCTTCTT R: TGTTGGCATACAGGTCCTTAC	109	doi.org/10.1016/j.etap.2023.104164

Supplementary table 4. Topological measurements of core nodes in the PPI networks identified by degree and betweenness centrality (BC).

Node	Protein name	Degree	BC
NCOA1	Nuclear receptor coativator 1	12	0.422
RXRA	Retinoid X Receptor Alpha	11	0.193
NCOA2	Nuclear receptor coativator 2	8	0.300
ESR1	Estrogen Receptor 1	4	0.420
PPARG	Peroxissome proliferator-activated receptor gamma	4	0.0197